Trafficking motifs in potassium channels

Rucha Karnik

Submitted in accordance with the requirements for the degree of

Doctor of Philosophy

The University of Leeds

Multi-disciplinary Cardiovascular Research Centre

&

Institute of Membrane Systems and Biology

October 2010

The candidate confirms that the work submitted is her own, except where work which has formed part of jointly-authored publications has been included. The contribution of the candidate and the other authors to this work has been explicitly indicated below. The candidate confirms that appropriate credit has been given within the thesis where reference has been made to the work of others."

ACKNOWLEDGMENTS

ABSTRACT

The pancreatic ATP-sensitive potassium (K_{ATP}) channels couple glucose metabolism to excitability of the pancreatic β-cells to regulate insulin secretion. The channel subunits, Kir6.2 and SUR1, are encoded by the *KCNJ11* and *ABCC8* genes respectively. Genetic polymorphisms in these genes, which reduce channel activity, cause congenital hyperinsulinism (CHI) characterized by insulin hyper-secretion and hypoglycemia. The hERG (human *ether-a-go-go* related gene) potassium channels, encoded by the *KCNH2* gene, contribute to the rapidly activating delayed rectifier K^+ current (IKr), which is responsible for rapid repolarisation of the cardiac action potential. Decreased hERG channel function causes the Long QT syndrome 2 (LQTS2) and life threatening cardiac arrhythmias. Several mutations in these two clinically important potassium ion channels alter their surface density leading to disease. Therefore, it is of fundamental importance to investigate the trafficking mechanisms that regulate the surface density of these channels.

Techniques in cell biology, molecular biology and biochemistry were employed to identify the molecular basis of Sar1-GTPase dependent ER exit of the K_{ATP} and hERG channels in COPII vesicles. Blocking the cargo binding sites on the Sec24 protein of the COPII coat with membrane-permeable synthetic peptides prevented ER exit of both these channels. While the diacidic $^{280}DLE^{282}$ sequence on the Kir6.2 subunit of K_{ATP} channels was found to be the ER exit motif required for entry of the channels into COPII vesicles at the ER exit sites, such a motif was found to be absent on hERG C-terminus. Further, endocytic trafficking mechanism of hERG channels was studied in recombinant (HEK MSRII and HeLa) and native (neonatal rat cardiac myocytes) systems using cell biological and pharmacological tools. hERG channels were found to be internalised by a dynamin-independent, raft-mediated, and ARF6-dependent pathway. A prolonged block of this pathway revealed that the channels could also undergo internalisation by an alternate dynamin-mediated pathway. Internalised hERG channels were found to recycle back to the cell surface and undergo lysosomal degradation. Degradation of the channels was enhanced when Rab11a-GTPase function was disrupted leading to reduced surface density indicating that recycling is crucial to maintain cell surface density of the channels. Thus this study investigated and compared the previously unknown mechanisms of biosynthetic and endosomal trafficking of the K_{ATP} and hERG potassium channels with a conclusion that these processes play an important role in maintaining surface density and thereby in the function of these channels in physiological and patho-physiological conditions.

TABLE OF CONTENTS

LIST OF FIGURES

LIST OF TABLES

ABBREVIATIONS

ADP   Adenosine diphosphate

AlF   Aluminium fluoride

AP1   Adaptor protein 1

ARF6   ADP-ribosylation factor 6

ATP   Adenosine triphosphate

Ca^{2+} Calcium ion

Cav1   Caveolin1

CCV   Clathrin coated vesicle

CDC42   Cell division control protein 42 homolog

CDE   Clathrin-Dependent Internalisation

cDNA   Complementary DNA

CFTR   Cystic fibrosis transmembrane regulator

CHI   Congenital hyperinsulinism

CIE   Clathrin Independent Internalisation

CME   Clathrin mediated endocytosis

Cs^{+} Caesium ion

CT-B   Cholera toxin B subunit

Ctrl   Control

Cy3   Cyanine-3

DAPI   4',6-diamidino-2-phenylindole

DMEM   Dulbecco's Modified Eagle's Medium

DMSO   Dimethyl sulfoxide

DN   Dominant negative

DRM   Detergent resistant membranes

Dyn1/2   Dynamin1/2

EEA1   Early endosomal antigen 1

ER   Endoplasmic Reticulum

ERAD   ER associated degradation pathway

ERC   Endocytic recycling compartment

ERG   *ether-a-go-go related gene* potassium channel

FITC   Fluorescein isothiocyanate

GDP   Guanosine-5'-diphosphate

GFP   Green Fluorescent Protein

GPI-AP   Gycosylphosphatidylinositol anchored protein

GSIS   Glucose stimulated insulin secretion

GTP   Guanosine-5'-triphosphate

HA   Haemagglutinin A

HEK-MSRII   Human Embryonic Kidney (HEK293) cell line expressing the human
Macrophage Scavenger Receptor II

HEPES   4-(2-hydroxyethyl)-1-piperazineethanesulfonic

hERG   human *ether-a-go-go related gene* potassium channel

HRP   Horse Radish Peroxidase

K^+ Potassium ion

K_{ATP} ATP sensitive potassium channel

Kir   Inwardly rectifying potassium channel

Kv   Voltage-gated potassium channel

K_v	Voltage-gated potassium channel
LAMP-1	Lysosome-associated membrane protein 1
LE	Late endosomes
Li^+	Lithium ion
LQTS2	Long QT syndrome 2
Mg^{2+}	Magnesium ion
MHCI	Major Histocompatibility Complex Class I
MHCII	Major Histocompatibility Complex Class II
MW	Molecular weight
MβCD	methyl-β-cyclodextrin,
n	number of repeats
NA	Numerical aperture
Na^+	Sodium ion
NBD	Nucleotide binding domain
NRVCM	Neonatal Rat Ventricular Myocytes
PCR	Polymerase chain reaction
PHHI	persistent hyperinsulinemic hypoglycemia of infancy
PIPs	Phosphatidylinositol phosphates
PKA	Protein kinase-A
PKC	Protein kinase-C
PKD	Protein kinase-D
PMA	4-phorbol 12-myristate 13-acetate
PNDM	permanent neonatal diabetes mellitus
Rb^+	Rubidium ion

RE	Recycling endosomes
RhoA	Ras homolog gene family, member A
s.e.m	standard error of mean
SE	Sorting endosomes
SNARE	Soluble NSF attachment protein receptor
SUR	Sulphonylurea receptor
SUR1	Sulphonylurea Receptor Isoform1
t½	Half-life
Tfn	Transferrin
TfR	Transferrin receptor
TGN	*Trans*-Golgi network
TM	Transmembrane helix
TMD	Transmembrane domain
V	Voltage
αCD	Alpha cyclodextrin

AMINO ACIDS

Amino acid	Three letter code	Single letter code
Alanine	Ala	A
Arginine	Arg	R
Asparigine	Asn	N
Aspartic acid	Asp	D
Cysteine	Cys	C
Glutamine	Gln	Q
Glutamic acid	Glu	E
Glycine	Gly	G
Histidine	His	H
Isoleucine	Ile	I
Leucine	Leu	L
Lysine	Lys	K
Methionine	Met	M
Phenylalanine	Phe	F
Proline	Pro	P
Serine	Ser	S
Threonine	Thr	T
Tryptophan	Trp	W
Tyrosine	Tyr	Y
Valine	Val	V

CHAPTER 1

General Introduction

1.1 Ion Channels in Health and Disease

1.1.1 Ion channels - a general introduction

Ion channels are transmembrane proteins that are crucial components of living cells which facilitate and regulate passage of specific ions such as potassium (K^+), sodium (Na^+), calcium (Ca^{2+}) and chloride (Cl^-) across cellular and organelle membranes. Ion channels, like enzymes, are highly substrate specific and are stringently regulated. For example, K^+ channels are 100–1,000 times more permeable to K^+ than Na^+, although the Na^+ ion are smaller (Hille, 2001). The opening or closing of ion channels alters the electrical potential across the plasma membrane, which is critical for several physiological processes of the cell such as nerve and muscle excitation, hormone secretion, cell proliferation, sensory transduction, learning and memory, regulation of blood pressure, salt and water balance, fertilisation and cell death (Ashcroft, 2006a). More than 300 types of ion channels have been identified in living cells which differ from each other in their gating (opening or closing of pores) and selectivity (in terms of which ions they allow to pass through) giving them the ability to carry out diverse physiological roles. Ion channels can be classified depending on their functional properties or structure. Classification of ion channels based on the ions that they conduct and their properties is as follows (Hille, 2001):

- Chloride channels - involved in regulation of pH, volume homeostasis, organic solute transport, cell migration, cell proliferation and differentiation.
- Sodium channels - include voltage-gated (Nav) channels which are involved in the firing of action potential in myocytes and neurons and non-neuronal epithelial ligand-gated sodium channels (ENaC).
- Calcium channels - include both voltage-gated (Cav) and ligand-gated channels involved in diverse physiological functions.
- Potassium channels - have diverse functions and tissue distribution. Can be classified as: voltage gated (Kv), inward-rectifier (Kir), calcium activated (KCa) two-pore domain (K2P).
- Proton channels - are voltage-gated and sensitive to pH, known to function in phagocytes.
- Non-selective ion channels – for example TRP channels, which allow many types of cations, mainly Na^+, K^+ and Ca^{2+} to pass through and the cyclic nucleotide- gated (CNG) channels which conduct Na^+, K^+, Mg^{2+} and Ca^{2+} ions.

1.1.2 Ion channels and disease

Basic ion channel structure includes one or more α-subunits that form the ion conducting pore with the selectivity filter. Some channels have one or more accessory subunits also called as the β-subunits. Ion channel function depends on the number of channels in the membrane, the fraction of time they remain open (the open probability) and the conductance of the single channel and therefore alteration of any of these could disrupt channel function (Hille, 2001).

Both genetic mutations and pharmacological compounds can alter channel function leading to disease; for example the delta F508 mutation that causes retention of the chloride channel, Cystic Fibrosis Transmembrane Conductance Regulator (CFTR), in the ER causes cystic fibrosis (Cheng et al., 1990); several drugs bind to and inhibit the cardiac voltage-gated potassium channels Kv11.1 and produce the acquired long QT syndrome (LQTS). This disease can also be caused due to mutations that alter channel function and trafficking (Sanguinetti et al., 1995). Loss-of-channel function can occur due to mutations that lead to decrease in channel density by preventing channel protein synthesis or correct membrane targeting or due to drugs that may block the channels. Similarly mutations and drugs can also cause gain-of-function in ion channels leading to disease. For example, gain-of-function and loss-of-function mutations in the pancreatic ATP-sensitive potassium channels can produce distinct clinical disorders: neonatal diabetes (due to too little insulin secretion) and hyperinsulinemia (Ashcroft, 2005, Ashcroft, 2006a). Thus absence or mutation of one or more of the contributing channel subunits can result in channelopathies (defined as, diseases that result from impaired channel function). Table 1.1, adapted from (Ashcroft, 2006a), lists some of the channelopathies.

Table 1.1 Channelopathies caused due to mutations in ion channel genes

Protein	Mutation type	Channelopathies
Kir1.1 (ROMK)	*KCNJ11* (loss of function)	Bartter's syndrome
Kir 2.1	*KCNJ2* (loss of function)	Andersen's syndrome
SUR2 (cardiac K_{ATP} β subunit)	*SUR1* (loss of function)	Dilated cardiomyopathy
Kv1.1, neuronal α-subunit	*KCNA1* (loss of function)	Neuromuotonia
KVLQT1	KCNQ1 (loss of function) (gain of function)	LQTS1, Atrial fibrillation Short QT syndrome
MinK, cardiac β-subunit	*KCNE1* (loss of function)	LQTS5
TRPP2	*TRPP2*	Autosomal dominant polycystic kidney disease
TRPC6	*TRPC6* (gain of function)	Defective Mg^{2+} reabsorbtion
BK channel α-subunit (KCa)	*KCMNA1* (gain of function)	Generalised epilepsy
Nav1.1, neuronal α-subunit	*SCN1A* (gain of function) (loss of function)	Generalised epilepsy Severe myoclonic epilepsy of infancy
Nav cardiac muscle α-subunit.	*SCN5A* (gain of function)	LQTS2, Brugada syndrome, congenital heart block

Protein	Mutation type	Channelopathies
Nav, skeletal muscle α-subunit.	*SCN4A* (loss of function)	Hypokalemic periodic paralysis
CLC5 (Cl⁻ transporter in kidney)	*CLCN5* (loss of function)	Dent's disease
CLC7, (Cl⁻ transporter)	*CLC7* (loss of function)	Osteopetrosis (dense bones), blindness
GABA$_A$ receptor neuronal α1-subunit.	*GABRA1* (loss of function)	Juvenile myoclonic epilepsy
AChR skeletal muscle α1-subunit	*CHRNA1* (gain of function)	Congenital myasthenia
CFTR (epithelial Cl⁻ channel)	*CFTR* (loss of function)	Cystic fibrosis
Epithelial Na+ channel (ENaC) β- and γ-subunit	*SCNN1B* and SCNN1G (gain of function)	Hypertension (Liddle's syndrome)

1.1.3 Ion channels as drug targets

Since ion channels control a wide range of physiological functions and alteration in channel function causes disease, they have been identified as important drug targets. Over the years several compounds that modulate the activity of ion channels have been discovered and commercialised. However, early ion channel drug discovery was based on screening for drugs that cured disease in simulated animal models where nature of the molecular target was unclear. Modern age drug research is directed towards development of drugs that have ion channels as targets (Garcia and Kaczorowski, 2005, Kaczorowski et al., 2008). For example, human genetics and gene ablation studies in rodents have identified a number of new ion channel targets including Nav1.7, Nav1.4, Cav2.2, KCNMA1, Kir1.1, Kir6.2-SUR2 and KCNQ (Lifton et al., 2001, Ashcroft and Gribble, 2000b, Yu and Catterall, 2004, Gribkoff, 2008, Garcia

and Kaczorowski, 2005). Apart from the traditional pharmacological drugs, new therapeutic agents that could be the future of medicine include modulation of channel expression by regulation of promoter activity, siRNA technology, or the employment of dominant-negative interference strategies as well as small peptides. For example a peptide which is a synthetic analogue of peptides contained in the cone snail venom is being developed clinically as a treatment for acute pain. The peptide is a potent blocker of the neuronal voltage-gated calcium channel, Cav2.2 (Miljanich, 2004). Similarly, the spider toxin peptide GxTX that targets the pancreatic β-cell delayed rectifying potassium channel, Kv2.1 (KCNB1), is a potential candidate for enhancing glucose-dependent insulin secretion (GSIS), and thus for the treatment of type II diabetes (Herrington et al., 2006).

Drug discovery and development is a costly and time consuming process which meets with limited success. For example, toxicity due to interaction with unrelated channels such as the cardiac Kv11.1 which leads to life threatening arrhythmias (Witchel, 2010), is a major cause of drug failure. Success in development of new therapeutic approaches that target ion channels depends on the knowledge about how the ion channels function with respect to their ion conductance as well as trafficking of the channels in the cells. Also, understanding of the molecular mechanism underlying diseases caused by mutations in ion channels would help in the design of therapy.

1.2 Potassium Ion Channels

1.2.1 Potassium channels - a general introduction

K^+ channels regulate movement of the K^+ ions down the electrochemical gradient and maintain the cellular membrane potential. These channels are critical for membrane potential dependent functions of the cell such as regulation of cardiac action potential, regulation of insulin secretion and neural signal transduction (Aidley, 2008). K^+ is one of the predominant monovalent cation in mammalian cells, and extracellular K^+ concentrations are low. Opening of K^+ channels favours an outward flow of these positively charged ions which shifts the voltage across the cell membrane towards the equilibrium reversal potential where the tendency for K^+ ions to move outwardly (down their concentration gradient) is balanced by their tendency to move inward (down their electrical gradient). By this mechanism open K^+ channels mediate recovery after activity in excitable tissue and stabilize cellular potential (Hille, 2001).

1.2.2 Basic structure of potassium ion channels

Potassium channels are made of pore-forming subunits (α-subunit) and may be associated with auxiliary subunits (denoted as β-subunit or γ-subunit) which could be involved in channel regulation or trafficking (Pongs, 1999). The α-subunits have transmembrane α-helices with a membrane re-entering pore (P) loop. The pore-loop structure lines the top of the pore that is responsible for potassium selective permeability through the selectivity filter. K^+ channels display high selectivity towards K^+ (1.33 Å) and exclude smaller alkali metal cations Li^+ (radius 0.60 Å) and Na^+ (0.95 Å) but allow permeation of the larger ions such as rubidium Rb^+ (1.48 Å) and Cs^+ (1.69 Å) (Hille, 2001, Doyle et al., 1998). Ion selectivity occurs at the narrowest part of the channel pore due to the presence of the selectivity filter located in the P-loop of the channel which consists of a highly conserved sequence (TVGYG). Prior to entry into the selectivity filter, K^+ ion is dehydrated and this loss is compensated by the backbone carbonyls of the VGYG residues that contribute to the four oxygen rings. The ion moves through the filter by slipping from one binding site to the next in a single file at a very high rate of about 10^7-10^8 ions per second (MacKinnon, 2003). Since the carbonyl oxygen atoms in the channel pore are too far apart to enable them to interact intimately with dehydrated Na^+ ions, Na^+ is effectively excluded from the selectivity filter (Doyle et

al., 1998, Hille, 2001). Thus the selective passage of K^+ ions is also highly efficient as only one Na^+ ion passage error for every 10,000 events may occur (Yellen, 1984). The K^+ channel pore is generally coupled to the sensing domain that responds to factors such as voltage, pH, ATP or specific ligands that affect the opening or closing of the intrinsic pore gates (Pongs, 1999). The pore domains (α–subunits) of the potassium channels can be classified based on their structural organization as follows:

```
              ┌─────────────────┐
              │   α- Subunit    │
              │  (K+ channel)   │
              └─────────────────┘
         ┌─────────┬─────────────┐
  ┌────────────┐ ┌──────────┐ ┌──────────┐
  │            │ │   4TM    │ │   6TM    │
  │    2-TM    │ │(2-TM+2-TM)│ │(2-TM+4-TM)│
  └────────────┘ └──────────┘ └──────────┘
```
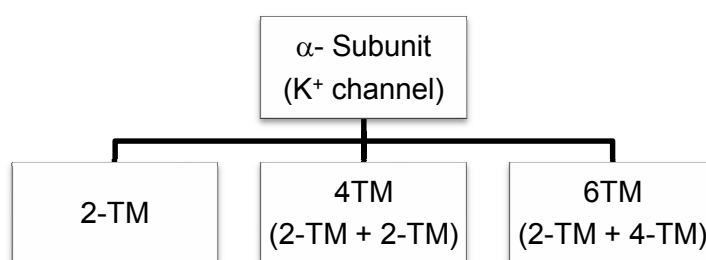
The 2-TM (trans-membrane) channels are tetramers, each subunit is typically made of two hydrophobic transmembrane segments M1, and M2 that are connected to each other by the P-loop (Figure 1.1.A). The inward rectifying potassium channels Kir are members of this family.

The 4-TM domain channels also referred to as tandem or two-pore (2P) channels are dimers. They consist of 4-TM domains (M1–M4) and two P-loops one located between M1 and M2 domains and the other located between M3 and M4 domains.

The 6-TM domain channels are tetramers, each subunit comprising of 6-TM domains and a single pore domain (Figure 1.1.C). The voltage-gated (Kv) channels are examples of channels having 6-TM α-subunits. The TM segments are designated as S1-S6. The membrane re-entrant P-loop is situated between S5 and S6. The S5 and S6 segments and the P-loop assemble in the tetramer to form the channel pore. The segments S1 to S4 form the voltage sensing (VS) domain of the Kv channels (Jiang et al., 2003, Long et al., 2005a, Long et al., 2007).
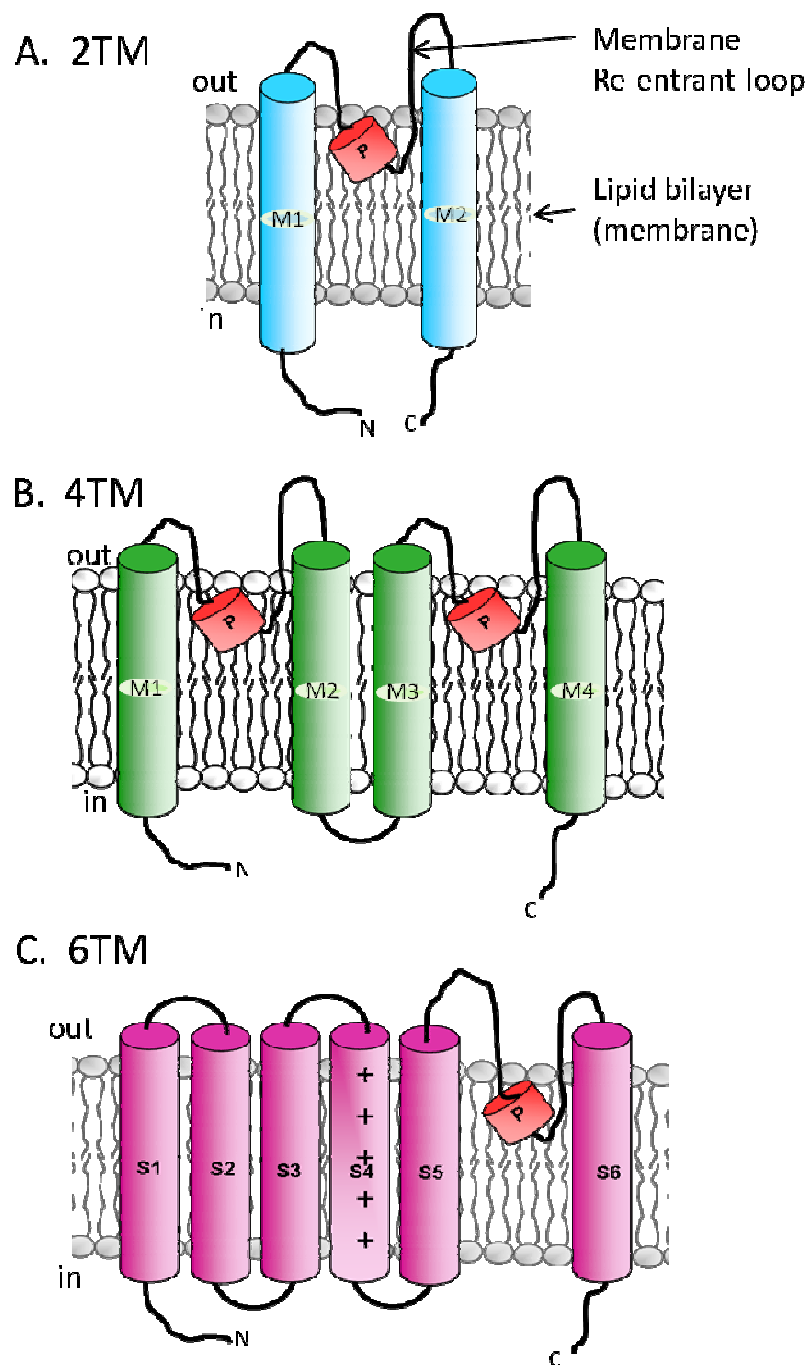
Figure 1.1 Schematic of membrane topology of pore forming subunits of different classes of K⁺ channels. Transmembrane regions of the channels are shown using cylinders along with their respective names. (A) Channels having two TM domains, (B) the two-pore domain channels, (C) channels with six TM domains including the S4 domain for voltage sensing. N, amino-terminus; C, carboxyl-terminus; P, P-helix.

1.2.3 Inwardly rectifying potassium ion channels

Introduction

Inwardly rectifying potassium channels (Kir) are an important class of K^+ channels that have been shown to regulate membrane excitability, heart rate, vascular tone, insulin release and salt flow across epithelia (for a comprehensive review see (Bichet et al., 2003). They can conduct higher inward K^+ currents at membrane voltages negative to the K^+ equilibrium potential than outward currents, even when K^+ concentrations on both sides of the membrane become equal.

The analysis of amino acid sequences of the transmembrane domains (M1 and M2) of the Kir channels suggested that these domains are equivalent to the S5 and S6 transmembrane domains of the Kv channels (MacKinnon, 1991). In light of the structural information available for the voltage-gated ion channels, it was considered that the membrane re-entrant loop between M1 and M2 formed the ion channel conduction pore (Heginbotham et al., 1994). The selectivity filter in the Kir channels is lined by residues TXGYGFR and a pair of highly conserved cysteine residues flanks the pore region of the channel. The elucidation of the chicken Kir2.2 crystal structure (Tao et al., 2009) has provided a better understanding of the biophysical basis of inward rectification. Inward rectification is attributed to the selective interaction of the channels with cytoplasmic Mg^{2+} ions and polyamines that block K^+ efflux at membrane potentials more positive than the reversal potential (Isomoto et al., 1997, Hille and Schwarz, 1978, Lu, 2004). The degree or strength of inward rectification within the Kir family depends on the binding affinity of the channel for blocking cations such as polyamines and Mg^{2+}, which plug the conduction pathway upon depolarisation and impede the outward flow of K^+ (Horie and Irisawa, 1987, Lopatin et al., 1994). Other regulators of Kir channels include extracellular K^+ concentration, the membrane anchored phospholipid, phosphatidylinositol 4,5-bisphosphate (PIP_2), ATP and protein-protein interactions (see Figure 1.2.A adapted from Tao et al., 2009 , and Figure 1.2.B adapted from Hibino et al., 2010).
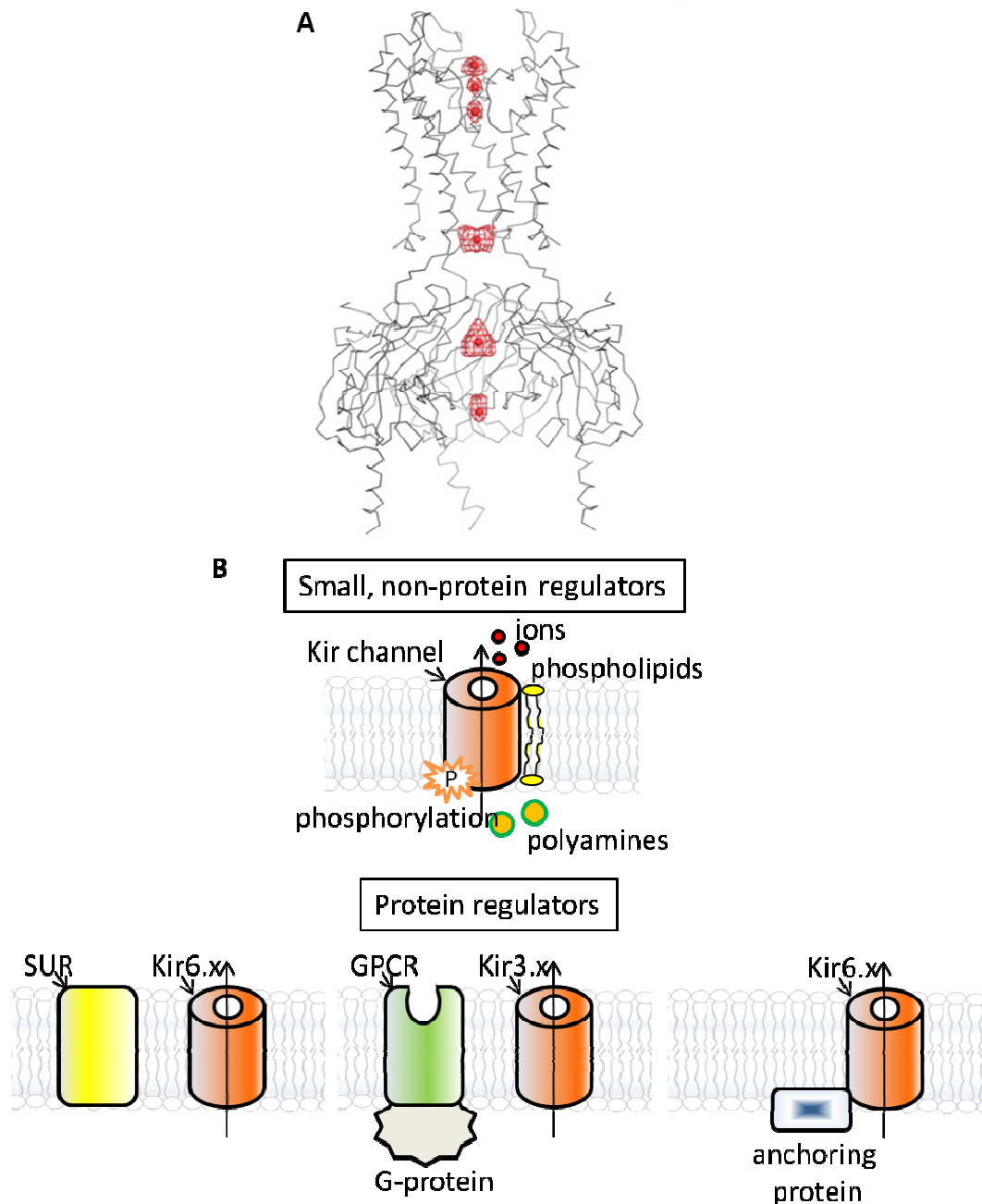
Figure 1.2 Regulators of Kir channel function. (A) Crystal structure of Kir2.2 showing the transmembrane domain, cytoplasmic domain (in grey) and ion binding sites for Rb^+. The ions are shown as spheres and coloured red, image taken from (Tao et al., 2009). (B) Kir channels can be regulated by small substances such as H^+, Mg^{2+}, Na^+; polyamines, phosphorylation and membrane phospholipids. Interactions with proteins such as the sulfonylurea receptor (SUR), G-protein coupled receptor (GPCR) and anchoring protein can also play a critical role in Kir channel regulation (Hibino et al., 2010).

Classification

About fifteen Kir subunit genes have been identified and the channels are divided into seven distinct subfamilies (Kir1-7) that exhibit variations in strength of rectification and response to cellular signals (Isomoto et al., 1997, Doring et al., 1998). These seven families of the Kir channels are functionally classified into four groups (Ashcroft et al., 1987, Krapivinsky et al., 1998, Hille, 2001, Hibino et al., 2010) as follows:

- Classical Kir channels (Kir2.x) that are constitutively active
- G-protein gated Kir channels (Kir3.x) that are regulated by G protein-coupled receptors (GPCRs)
- ATP-sensitive K^+ channels (Kir6.x) are tightly linked to cellular metabolism
- K^+ transport channels (Kir1.x, Kir4.x, Kir5.x, and Kir7.x)

Kir channels are found in multiple cell types, including macrophages, cardiac and kidney cells, leukocytes, neurons, pancreatic β-cells and endothelial cells where they have varying physiological functions. For example, in endothelial cells, Kir (Kir2.x) channels are involved in regulation of nitric oxide synthase while in kidneys Kir channels export surplus potassium into collecting tubules for removal in the urine (Chilton and Loutzenhiser, 2001). In cardiac tissue, G-protein activated Kir channels (Kir3.1 + Kir3.4) are important for heart rate modulation (Corey et al., 1998) and in pancreatic β-cells, the ATP-regulated Kir channels (K_{ATP}) are involved in glucose regulated insulin release (Ashcroft et al., 1984, Ashcroft et al., 1987).

Cloning and identification

The ATP-dependent Kir channels ROMK1/Kir1.1 (Ho et al., 1993) and the IRK1/Kir2.1 (Kubo et al., 1993) were the first Kir channels to be isolated and cloned in 1993. Architecture of the transmembrane domain of Kir channels was determined from the crystal structure of a bacterial homolog KirBac1.1 (Kuo et al., 2003). These studies showed that structurally, Kir channels are tetramers, each subunit having two transmembrane segments (TM1 and TM2), which are linked by an extracellular pore loop (P) and cytoplasmic amino (NH_2) and carboxyl (COOH) terminal domains (Figure 1.B). Since the channels lack the S4 voltage sensor region found in voltage-gated channels, the Kir channels are insensitive to membrane voltage. The Kir channel subunits are capable of both homomeric and heteromeric combinations to form functional Kir channels which display distinct properties. Heteromerisation generally occurs between members of the same subfamily, for example Kir2.1 can associate with

Kir2.2, Kir2.3, or Kir2.4 and Kir3.1 forms heteromeric complexes with Kir3.2, Kir3.3 or Kir3.4. An exception is where Kir4.1 assembles with Kir5.1 (Hibino et al., 2010, Hille, 2001).

1.2.4 Voltage gated potassium channels

Voltage-gated potassium (Kv) channels sense changes in the cellular membrane potential. Owing to the concentration gradient for K^+ that exists across cellular membranes, the opening of Kv channels results in an efflux of positive charge which results in membrane repolarisation. In excitable cells such as neurons or cardiac myocytes, Kv channels are therefore often expressed together with voltage-gated Na^+ (Nav) and/or Ca^{2+} (Cav) channels which cause membrane depolarisation. Activation of Kv channels thus reduces excitability of the cells after action potential firing (Hille, 2001).

Structures of the bacterial KvAP and the mammalian Kv1.2 channels (both thought to be in the open state) have been solved; however structure of a channel with a drug molecule bound is not available till date. This has made understanding of the pharmacology of the channels difficult. About 40 Kv channels encoded by the human genome are known and they are involved in diverse physiological processes ranging from repolarisation of neuronal and cardiac action potentials, to regulating Ca^{2+} signalling and cell volume, to driving cellular proliferation and migration (Hille, 2001). The first Kv channel to be cloned was the *Drosophila Shaker* channel (Papazian et al., 1987). Like the *Shaker* channel, all mammalian Kv channels are homo-tetramers or hetero-tetramers of 6-TM domain α-subunits (Figure 1.1.C). The six transmembrane α-helical segments, S1–S6 and P-loop are arranged circumferentially to form the channel central pore. The four S1–S4 segments, each containing four positively charged arginine residues in the S4 helix, act as voltage sensor domains and 'gate' the pore by 'pulling' on the S4–S5 linker (Long et al., 2005a). The Kv channel α-subunits are classified into 12 subfamilies (Kv1-12) based on their homology. The channels can be grouped according to their function as follows:

- Delayed rectifiers (belong to the shaker family) - (Kv1.x, Kv2.x, Kv3.x, Kv7.x, Kv10.x)
- A-type potassium channels - Kv1.4
- Outward-rectifying - Kv10.2

- Inward-rectifying - that pass current more easily into the inwards direction (Into the cell) - Kv11.1, Kv11.2, Kv11.3
- Slowly activating - Kv12.1, Kv12.2, Kv12.3
- Modifier/silencer - Unable to form functional channels as homo-tetramers but instead hetero-tetramerise with Kv2 family members to form conductive channels- Kv5.1, Kv6.1, Kv6.2, Kv6.3, Kv6.4, Kv8.1, Kv8.2, Kv9.1, Kv9.2, Kv9.3

K^+ channel β-subunits represent a diverse molecular group, which includes cytoplasmic proteins (Kvβ1-3, KChIP and KChAP) that interact with the intracellular domains of the Kv channels, single transmembrane spanning proteins, such as minK and minK-related proteins (MiRPs) encoded by the KCNE gene family. Co-expression of the β-subunits with α-subunits regulates cell surface expression, gating kinetics and drug-sensitivity of the Kv channels (Hanlon and Wallace, 2002, Martens et al., 1999).

1.3 ATP-Sensitive Potassium Channels

1.3.1 Tissue localisation of K_{ATP} channels

ATP-sensitive potassium (K_{ATP}) channels are weakly inwardly rectifying potassium channels which play the central role of coupling cell metabolism to changes in cell membrane potential. These channels were first identified in cardiac myocytes and were found to be inhibited by intracellular ATP but stimulated by Mg-ADP (Noma, 1983, Ashcroft et al., 1984, Ashcroft et al., 1987). The K_{ATP} channels are found in cardiac myocytes (Noma, 1983), pancreatic β-cells (Ashcroft et al., 1984), skeletal muscle (Spruce et al., 1985), vascular smooth muscle (Beech et al., 1993) and neurons (Ashford et al., 1988). They are located either at the plasma membrane, at the inner mitochondrial membrane (mitoK_{ATP}) (Szewczyk et al., 1996) or in secretory granules (Geng et al., 2003).

1.3.2 Structure and stoichiometry

The K_{ATP} channel expressed on the cell surface is an octamer of two distinct subunits: a pore-forming α-subunit, which belongs to the K^+ inward rectifier family (Kir6.x), and a regulatory β-subunit, the sulfonylurea receptor (SURx), see Figure 1.3.A. The Kir subunits are responsible for ATP inhibition and the SUR proteins for nucleoside diphosphate (NDP) activation.

Three isoforms of Kir6.x cloned till date includes the mammalian Kir6.1 (Inagaki et al., 1995), Kir6.2 (Sakura et al., 1995) and the Kir6.3 found in zebra fish (Zhang et al., 2006). The sulfonylurea receptor SUR belongs to the ATP-binding cassette (ABC) family of proteins. Unlike other ABC proteins such as CFTR, it has neither active nor passive intrinsic transport function. SUR associates with the pore forming potassium channel subunits, Kir6.x to form the K_{ATP} channel, where it serves as a regulatory subunit which fine-tunes the gating of Kir6.x in response to alterations in cellular metabolism (Clement et al., 1997, Lorenz et al., 1998). Transcripts of SUR1 occur most abundantly in neurons, brain, and pancreatic β-cells (Aguilar-Bryan et al., 1995). Other members of SUR family identified include SUR2 which has splice variants SUR2A and SUR2B. Transcripts of SUR2A are primarily detected in heart and secondly in skeletal muscles while the SUR2B transcripts are mainly detected in smooth muscle, and

present nearly ubiquitously in many tissue types (Chutkow et al., 1996). Combinations of different SURx and Kir6.x subunits form distinct types of K_{ATP} channels found in different tissues. Kir6.1 is present ubiquitously in many tissue types and its transcripts are abundantly present in heart, ovary, adrenal tissues (Inagaki et al., 1995). The transcripts of Kir6.2 are present in high levels in skeletal muscle, heart, pancreatic islets, lung, liver, brain, stomach (Sakura et al., 1995). The β-cell K_{ATP} channels are an octameric complex made of four pore forming Kir6.2 and four regulatory SUR1 subunits. Cardiac K_{ATP} channels are made of Kir6.2 and SUR2A subunits while those in smooth muscles are made of Kir6.1 and SUR2B (Inagaki et al., 1995, Aguilar-Bryan et al., 1995, Surah-Narwal et al., 1999). The zebra fish Kir6.3 subunits associate with SUR1 to form functional channels (Zhang et al., 2006).

The pore forming Kir6.x subunits have two transmembrane domains and the membrane re-entering pore-loop like typical Kir channels. The ATP-binding site present on the Kir6.x subunit (Tucker et al., 1997), is essentially a binding pocket made of five residues, R50 in the NH_2 terminus and I182, K185, R201, and G334 in the COOH terminus (Antcliff et al., 2005, Hibino et al., 2010). The SURx subunits contain 17 transmembrane regions grouped into three transmembrane domains TMD0, TMD1 and TMD2. Each SUR unit has two nucleotide-binding domains between TMD1 and TMD2 (NBD1) and in the COOH terminus following TMD2 (NBD2), see Figure 1.3.B. SUR2A and SUR2B differ only in 42 amino acids of the COOH-terminal. The TMD0 of SUR has been implicated in controlling both channel gating (Babenko et al., 1999) and association with Kir6.2 and is thus vital for K_{ATP} channel trafficking (Sharma et al., 1999, Zerangue et al., 1999). Co-expression of the Kir6.2 and SUR1 subunits in both *Xenopus oocytes* and mammalian cells results in K_{ATP} current identical to those of native β-cell currents (Sakura et al., 1995); however, the channel subunits expressed on their own failed to give functional currents in *Xenopus oocytes* (Zerangue et al., 1999, Hough et al., 2000). Therefore, association of the K_{ATP} subunits is considered to be critical for expression of functional K_{ATP} channels on the cell surface.

1.3.3 Regulation of Kir6.x

K_{ATP} channel activity is regulated by intracellular nucleotides and by various pharmacological agents. The physiological and pharmacological control of K_{ATP} channels depends on the conformational changes in the Kir6.x pore by interaction with

ATP or through interaction with the SURx subunit. Physiologically the key feature of the K_{ATP} channel is its regulation by ATP in presence of Mg^{2+}. The K_{ATP} channel stays closed as long as ATP is bound to the channel. In native pancreatic β-cells, ATP in its free acid form is a more potent inhibitor of the channel while Mg-ATP has little inhibitory effect (Ashcroft and Kakei, 1989). In smooth muscle cells, Mg-ATP is also less effective (Kajioka et al., 1991, Nelson and Quayle, 1995).

However, cardiac K_{ATP} channels are inhibited by both ATP and Mg-ATP in a similar manner (Findlay, 1988). ADP is essential for the physiological opening of the K_{ATP} channels and they are thought to bear two distinct sites for channel gating, an inhibitory ATP-binding site and a stimulatory NDP-binding site (Tung and Kurachi, 1991). The stoichiometry of ATP binding in one Kir6.2 subunit provides one high-affinity ATP-binding site, and therefore, one functional K_{ATP} channel bears four ATP-binding sites. However, binding of single ATP to any of the identical ATP-binding sites is sufficient to cause channel closure (Markworth et al., 2000, Craig et al., 2008). PIP2 binds to the cytoplasmic region of the Kir6.2 subunit which is close to the ATP-binding site and stabilizes the open state of the channel. The competition between PIP2 and ATP regulates channel closure by ATP-binding (Baukrowitz et al., 1998).

Activation of the K_{ATP} channels is caused by binding of Mg-ADP to SUR subunit through the cytoplasmic nucleotide binding domains (NBD) which results in conformational change in the subunits. The NBD2 domain has ATPase activity and hydrolyses Mg-ATP to Mg-ADP with a twofold higher rate compared to NBD1 in presence of Mg^{2+} (Matsuo et al., 1999). Binding of Mg-ADP to NBD2 stabilises the binding of ATP to NBD1, which then stimulates channel activity (Bienengraeber et al., 2000). Upon removal of Mg-ADP from NBD2, ATP dissociates from NBD1 and channel activity is reduced. The ATP/ADP ratio therefore dictates channel activity and when the ATP/ADP ratio is high, ATP inhibition predominates. Conversely, when the ratio is low, Mg-ADP stimulation dominates, the channel is activated directly and the channel sensitivity to ATP is reduced. Thus, the K_{ATP} channel complex functions not only as a K^+ conductor, but also as an enzyme regulating nucleotide-dependent channel that is gated through an intrinsic ATPase activity of the SUR subunit. Mutations such as K1348A and D1469N in NBD2 reduce its ATPase activity and produce channels with increased sensitivity to ATP while K_{ATP} channel openers, which bind to SUR, promote ATPase activity (Bienengraeber et al., 2000).
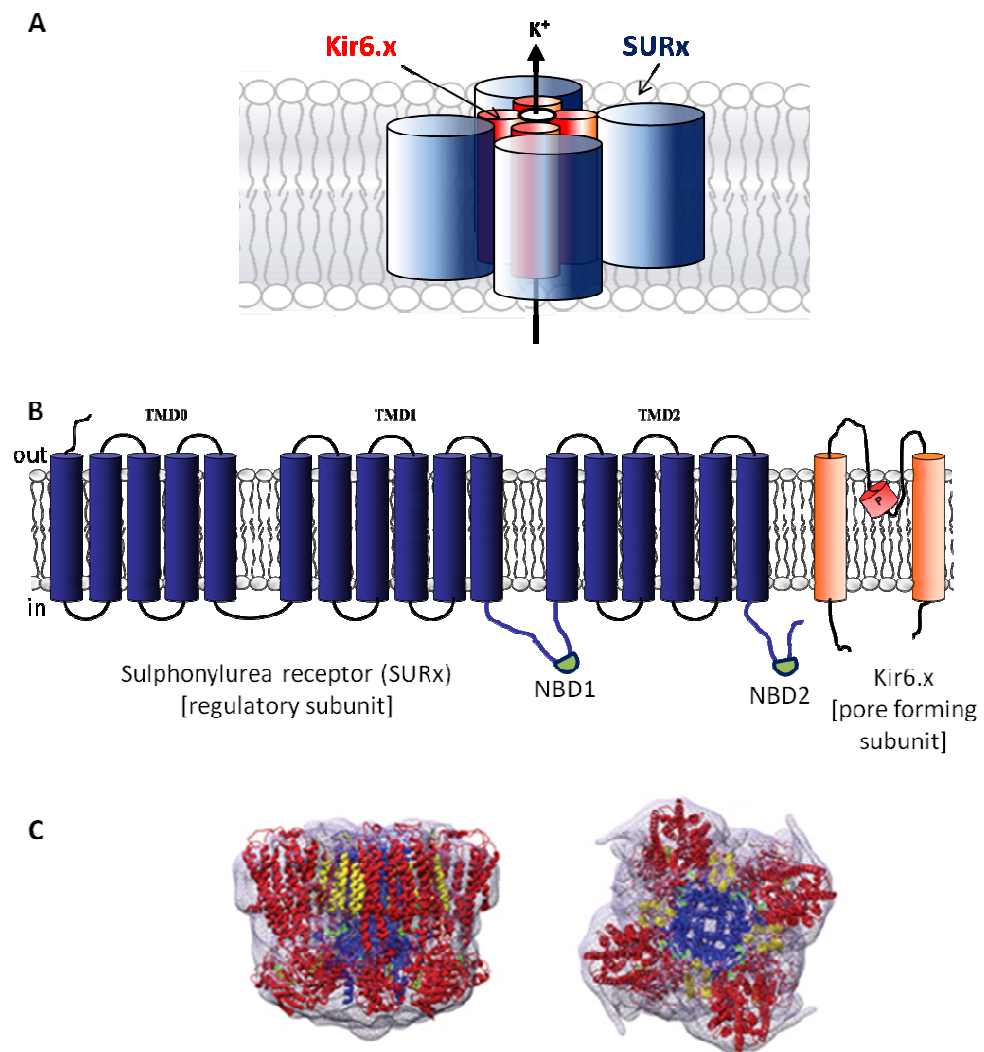
Figure 1.3 Structural organization of K$_{ATP}$ channel and its subunits. (A) Schematic to show the octameric assembly of the K$_{ATP}$ channel. Four subunits of the Kir6.x assemble to form the K$^+$ ion permeable channel pore which is surrounded by the four subunits of SUR1. (B) Schematic representation of Kir6.2 and SUR1 subunits showing the configuration of transmembrane domains (TMD) and the approximate location of the nucleotide binding domains (NBD) on SUR. (C) Top and side views of the EM density along with models of Kir6.2 (blue) and SUR1 with TMD0 (red), TMD0 (yellow) and ATP (green) shown, image from (Mikhailov et al., 2005).

K_{ATP} channels can also be regulated through phosphorylation by PKA signalling pathways particularly in smooth muscles (Lin et al., 2000). PKA phosphorylation sites include S385 in Kir6.1 and T633 and S1465 in SUR2B (Quinn et al., 2004), and S1387 in NBD2 of SUR2B (Shi et al., 2007). Kir6.2 can be phosphorylated at T224 by PKA (Lin et al., 2000) and at T180 by PKC (Light et al., 2000). How phosphorylation of these residues activates the channels is not well understood. Gating of the atrial K_{ATP} channel is mechano-sensitive, and mechanical pressure applied to a cardiac cell leads to an increase in their activity. Disruption of actin filaments with DNase I or cytochalasin B antagonises ATP-mediated inhibition of K_{ATP} channels. Although this mechanism is not well understood, it is considered that mechano-sensitive modulation of the K_{ATP} channels may help to open the cardiac K_{ATP} channels during ischemia or hypoxia when mechanical disturbances of the cytoskeleton can occur (Van Wagoner and Lamorgese, 1994, Terzic and Kurachi, 1996).

1.3.4 Pharmacology of K_{ATP} channels

Sulfonlyureas such as acetohexamide, tolbutamide, glipzide, glebenclamide and glimepriride affect SUR subunits resulting in block of K_{ATP} channels. In pancreatic β-cells, binding of sulphonylurea drugs blocks the K_{ATP} channels which inhibits K^+ efflux, resulting in membrane depolarisation, opening of voltage dependent Ca^{2+} channels, Ca^{2+} influx and insulin secretion. Therefore these drugs are used to stimulated insulin secretion in patients suffering from type 2 diabetes mellitus. The sensitivity of different types of K_{ATP} channels to sulfonlyureas is variable; for example gliclazide and tolbutamide block the K_{ATP} channels in the β-cells, but not the cardiac or smooth muscle cells owing to the different SURx subunits in these tissues. Glibenclamide however blocks all types of the K_{ATP} channels with similar affinity. Effect of tolbutamide and gliclazide on the K_{ATP} channels is reversible however the block of glibenclamide is reversible on cardiac, but not β-cell, K_{ATP} channels (Ashcroft and Gribble, 2000a, Ashcroft and Gribble, 2000b). Potassium channel openers include drugs such as cromakalim, pinacidil, nicorandil, diazoxide, and minoxidil sulfate. These drugs have considered of potential use for a broad range of therapeutic applications including treatment of hypertension and congenital hyperinsulinism (CHI). K_{ATP} channels in vascular smooth muscles are opened by K_{ATP} channel opener drugs which cause relaxation of the muscles resulting in reduced blood pressure. In pancreatic β-cells K_{ATP} channel opener drug diazoxide has been clinically used to treat hyper-secretion of

insulin associated with CHI (Ashcroft and Gribble, 2000a). Since native K_{ATP} channels in different tissue are made of different SUR subunits, i.e. SUR1 in pancreatic, SUR2A in cardiac and SUR2B in smooth muscle tissue, they show different sensitivity to the channel opener drugs that affect the SUR subunits of the K_{ATP} channel. Therefore, the pancreatic K_{ATP} channels are readily activated by diazoxide, weakly activated by pinacidil, and unaffected by cromakalim or nicorandil (Ashcroft and Gribble, 2000a) and the cardiac K_{ATP} channels are activated by pinacidil, cromakalim, and nicorandil but not by diazoxide (Ashcroft and Gribble, 2000a, Reimann et al., 2000), while the smooth muscle channels are activated by all these drugs.

1.3.5 Physiological roles of pancreatic K_{ATP} channels

Insulin-secreting pancreatic β-cells express K_{ATP} channels (Inagaki et al., 1995) which couple blood glucose concentration to insulin secretion (Ashcroft and Kakei, 1989, Ashcroft and Rorsman, 1990). The report (Tokuyama et al., 1996) showed that expression of Kir6.2 mRNA was reduced by >70% in islets from diabetic rats, and this indicated that the channel function was important for β-cell function and depletion of Kir6.2 could cause diabetes mellitus. Mice lacking either Kir6.2 or SUR1 showed transient neonatal hypoglycemia (Seghers et al., 2000, Miki et al., 1998).

Hypoglycemia is defined by low blood glucose concentration below 1-2 mM. It results in the brain being deprived of its main energy source causing rapid loss of consciousness. This condition can lead to brain damage and even death if untreated. Hyperglycemia is an opposite condition where there is elevation of blood glucose levels (>7 mM) and it can lead to complications of diabetes such as neuropathy, retinopathy and cardiovascular disease. Hence it is important for blood glucose levels to be maintained within narrow limits and this is achieved by glucose homeostasis in the fasting and fed states. When food is consumed, liver synthesizes glycogen and triglycerides. Triglycerides are diverted to the adipose tissue as energy stores. When glucose levels decrease during fasting conversion of glycogen by hepatic glycogenolytic enzymes releases glucose. These metabolic processes regulate blood glucose levels through regulation by key endocrine hormones insulin and glucagon. They influence directly or indirectly the enzymes which regulate liver carbohydrate and fatty acid metabolism, and thereby orient metabolic fluxes towards either energy storage or substrate release. Insulin hormone alone is capable of decreasing plasma

glucose concentration, both by inhibiting glucose release from the liver and by increasing glucose uptake in the muscle and adipose tissues (Dunne et al., 2004). Insulin secretion is stimulated by high blood glucose levels by the pancreatic β-cells when the K_{ATP} channels are closed whilst at sub-stimulatory blood glucose levels, the channels are open and no insulin is secreted. As blood glucose levels increase, glucose uptake into the pancreatic β-cell by glucose transporter GLUT2 is followed by it being metabolised to generate ATP. As a result of this metabolic process within the β-cells there is an increase in concentration of ATP while the concentration of ADP is reduced. The property of the K_{ATP} channels to be blocked by ATP underlies the glucose stimulated insulin secretion (GSIS) by the pancreatic β-cells as follows: as the ATP/ADP ratio in the cell increases, ATP concentration increases in the cell and the Mg-ADP concentration decreases. Binding of ATP to Kir6.2 causes channel closure as mentioned before, and the movement of K^+ ions from the cell is reduced and the cell membrane becomes depolarized. Membrane depolarization causes the opening of the depolarization activated Ca^{2+} channels. Ca^{2+} influx into the cell occurs and the resulting high Ca^{2+} levels trigger the insulin granules stored inside the cell to fuse with the plasma membrane and insulin is released into the blood stream (Antcliff et al., 2005, Ashcroft, 2005, Ashcroft, 2006a and Figure 4). Insulin facilitates glucose uptake from blood. When the blood glucose levels fall, the metabolism in the cell decreases and the ATP/ADP ratio decreases and the ATP bound to the K_{ATP} is displaced by PIP_2. The channel opens and K^+ ions move out of the cell causing membrane hyperpolarisation (Hille, 2001, Ashcroft and Kakei, 1989, Ashcroft and Rorsman, 1990, Nichols, 2006). The net activity of K_{ATP} depends on the number of open channels present on the cell surface. The density of K_{ATP} channels increases sharply in presence of low glucose and decreases when blood glucose levels rise in cells that carry out GSIS (Smith et al., 2006). Owing to the key roles of the K_{ATP} channels especially in pancreatic β-cells, any anomalies in the channel function lead to diseases of abnormal insulin secretion.
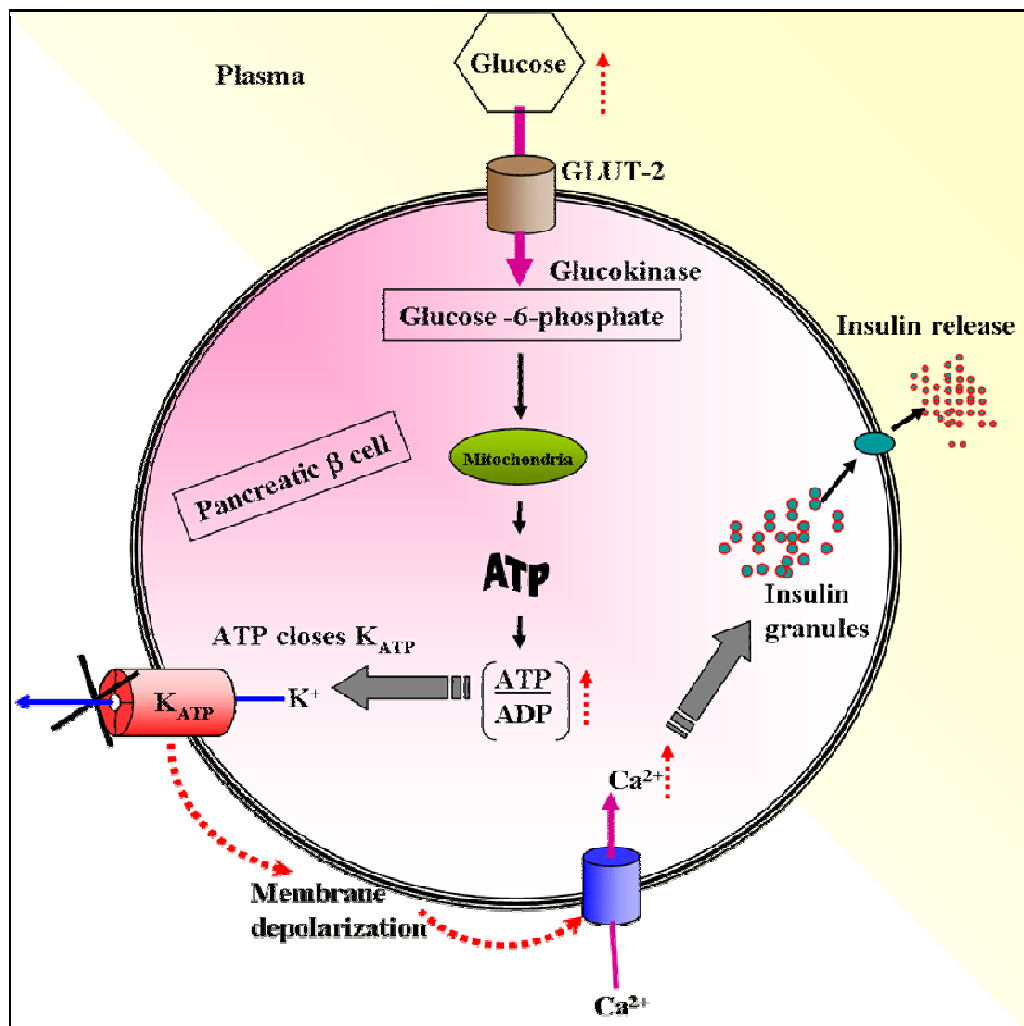
Figure 1.4 Schematic representation of events in glucose stimulated insulin secretion (GSIS). The K_{ATP} channel couples glucose metabolism to insulin secretion. Glucose enters the cell via the GLUT2 transporter. Glucose is metabolised via glycolytic and mitochondrial metabolism which leads to an increase in ATP and a fall in Mg-ADP concentrations. ATP causes the K_{ATP} channels to close, which leads to membrane depolarisation, opening of voltage-gated Ca^{2+} channels, Ca^{2+} influx, and exocytosis of insulin granules.

1.3.6 Pathophysiology of the pancreatic K$_{ATP}$ channels

Polymorphisms in Kir6.2 and SUR1 subunits that alter channel trafficking or function, cause disorders of insulin secretion. The channels have therefore been studied in order to find a cure for affected individuals. Channel function can be altered by mutations in the genes encoding Kir6.2 (*KCNJ11*) and SUR1 (*ABCC8*) that affect channel properties or expression on cell surface (Ashcroft, 2005, Ashcroft, 2006b, Ashcroft and Gribble, 1999, Dunne et al., 2004). Certain mutations lead to the loss-of-channel function by altering channel gating by decreasing the affinity for Mg-nucleotides for SUR1 due to which there is excessive insulin secretion even at sub-stimulatory concentrations of glucose, while others cause defects in trafficking of the functional channels to cell surface (Cartier et al., 2001, Partridge et al., 2001, Smith et al., 2007).

Loss of function mutations

Loss of pancreatic K$_{ATP}$ channel function can cause persistent hyperinsulinaemic hypoglycemia of infancy (PHHI), also known as congenital hyperinsulinism (CHI) which is characterised by excessive secretion of insulin despite hypoglycemia. More than 100 mutations in the SUR1 gene have been reported, some of which cause loss of surface expression of functional K$_{ATP}$ channels (Cartier et al., 2001, Partridge et al., 2001), while others alter channel function. For example, mutations in the NBD of SUR1 lead to formation of K$_{ATP}$ channels that do not open in response to Mg-ADP (Nichols et al., 1996, Ashcroft, 2006a, Gribble et al., 1997). Similarly, several mutations in the Kir6.2 subunits result in channels that remain closed and do not regulate GSIS (Ashcroft, 2005). Although numerous CHI-causing mutations have been identified not many have been characterised to understand how they affect channel trafficking and function.

Apart from the mutations that cause altered channel function, some PHHI causing mutations affect trafficking of the channels to the cell surface thereby reducing surface channel density and thereby channel function leading to increased insulin secretion. For example, mutation delta F1388 in SUR1 prevents normal trafficking of the channels to the cell surface but does not affect channel function. Lack of the channels on cell surface causes disease (Cartier et al., 2001). Another mutation R1394H in SUR1 causes retention of the channels in the trans-Golgi network (TGN), which reduces surface expression of the channels. However, treatment with diazoxide rescues the mutant channels to the cell surface where they form functional channels (Partridge et al., 2001). Some mutations in the transmembrane domains (TMD0, TMD1 and TMD2)

of SUR1 affect trafficking of the channels to the cell surface. Interestingly, mutations of TMD0 domain of SUR1 which cause trafficking defects in the mutant channels respond to treatment with channel blocker sulfonylurea drugs but not to diazoxide. The mutant channels pharmacologically rescued to the cell surface were found to be functional (Yan et al., 2007).

CHI occurrence is rare in general populations with about 1 in 50,000 individuals affected but in certain Finnish and Saudi Arabian people it has a high occurrence of 1 in 2,500 (Smith et al., 2007). The patients require treatment with high glucose to prevent brain damage and are responsive to therapy using exogenous glucagon which stimulates glycogen degradation and gluconeogenesis (Arnoux et al., 2010). Some of the patients are cured by treatment with diazoxide (Dunne et al., 2004) but the majority of the acute cases of hyperinsulinism require subtotal pancreatectomy (Christesen et al., 2007). About 40% of the patients suffering from CHI suffer from the disease of a focal nature where only certain regions of the pancreas are affected and secrete excessive insulin. A near total pancreatectomy is required to cure the CHI in patients with diffuse lesions (Ashcroft, 2005, Verkarre et al., 1998).

Gain-of-function mutations

Gain-of-function mutations in either Kir6.2 or SUR1 cause permanent neonatal diabetes mellitus (PNDM) characterised by reduced insulin secretion and resultant hyperglycemia (Ashcroft, 2005). Mutations in Kir6.2 gene that reduce the sensitivity of the K_{ATP} channels to ATP cause PNDM, while in most extreme cases patients may suffer from severe developmental delay, epilepsy and permanent neonatal diabetes (DEND) syndrome, characterised by marked developmental delay, muscle weakness, epilepsy, dysmorphic feature, and neonatal diabetes (Proks et al., 2004, Gloyn et al., 2004). Mutations such as I182V or R201C/H in Kir6.2, which are located in close vicinity of the putative ATP-binding site, directly impair ATP binding and cause NDM alone (Proks et al., 2004, Gloyn et al., 2004). Mutations including Q52R, V59M/G, and I296L in Kir6.2, indirectly reduce the sensitivity of the channels to ATP as they affect the channel gating properties which increase channel opening. These mutations cause DEND syndrome along with severe NDM (Trapp et al., 1998). NDM can also be caused due to mutations that affect channel trafficking. For example mutations Y330C and F333I in Kir6.2 increase surface density of the K_{ATP} channels by reducing their internalisation the cell surface (Mankouri et al., 2006). Most patients suffering from NDM respond to sulfonylurea therapy (Ashcroft, 2005, Smith et al., 2007).

1.3.7 Physiological roles of cardiac K_{ATP} channels

Cardiac K_{ATP} channels have been implicated in the maintenance of cellular functions and stress adaptation to protect the heart from arrhythmia. Kir6.2-knockout mice show an increased vulnerability to sympathetic stress and acute stress caused arrhythmia and sudden death (Zingman et al., 2002). Native cardiac K_{ATP} channels are considered to be formed of subunits Kir6.2 and SUR2A, although recent reports suggest that in mice Kir6.2 may be expressed with SUR1 in atrial myocytes and with SUR2A in ventricular myocytes (Flagg et al., 2008). Since cardiac tissue has a high concentration of ATP, cardiac K_{ATP} channels are closed under physiological conditions and metabolic insult such as increased cardiac work load, hypoxia, or ischemia causes channel opening (Kane et al., 2005).

1.4 K$_v$11.1 Potassium Channels

1.4.1 Kv11.1 channels in normal activity of the heart

Normal electrical activity of the heart depends on the co-ordinated generation of action potentials in individual cardiomyocytes which result from the opening and closing (gating) of ion channels that are expressed on cardiomyocyte cell membranes. Gating of ion channels allows movement of ions that created different phases of the cardiac action potential which include the resting phase, a depolarisation phase and the repolarisation phase. Different regions of the heart possess ion channels which have distinct pharmacological and gating properties and they function in co-ordination to keep the heart beating in rhythm. Alteration of the ion channel function due to inherited genetic mutations or drugs that modify channel gating properties or expression in the cell surface causes disorders such as cardiac arrhythmias (Sanguinetti and Tristani-Firouzi, 2006, Amin et al., 2010).

In mammalian cardiac ventricular myocytes, the action potential has five phases 0-4 (Figure 1.5.A). In general, the resting potential of atrial and ventricular myocytes during resting phase is stable and negative (approximately -85 mV) due to the high conductance for K$^+$ of the Kir channels. Upon excitation by electrical impulses from adjacent cells, Na$^+$ channels activate (open) and permit an inward Na$^+$ current leading to phase 0 depolarisation (initial upstroke). This is followed by phase 1 (early repolarisation), accomplished by transient outward flow of K$^+$ ions due to opening of voltage-gated K$^+$ channels. Next stage is the phase 2 (plateau) which is a balance between the depolarising L-type inward current from inflow of Ca^{2+} ions through Ca^{2+} channels and the repolarising opening of K$^+$ channels. Currents from the channels that play a role in phase 2 can be categorised as ultra-rapid (Ikur), rapid (Ikr), and slow (Iks) activating. Phase 3 (repolarisation) comprises of the closing of the L-type Ca^{2+} channels and outflow of K$^+$ ions due to opening of K$^+$ channels. Phase 4 represents a return of the action potential to baseline (Amin et al., 2010).

The voltage gated Kv11.1 channels encoded by *KCNH2* in humans are also known as the human *ether a go-go-related* gene (hERG) channels, which have been identified as the potassium channels responsible for the IKr currents (also designated as ERG currents) that are a part of the cardiac action potential (Sanguinetti et al., 1995).
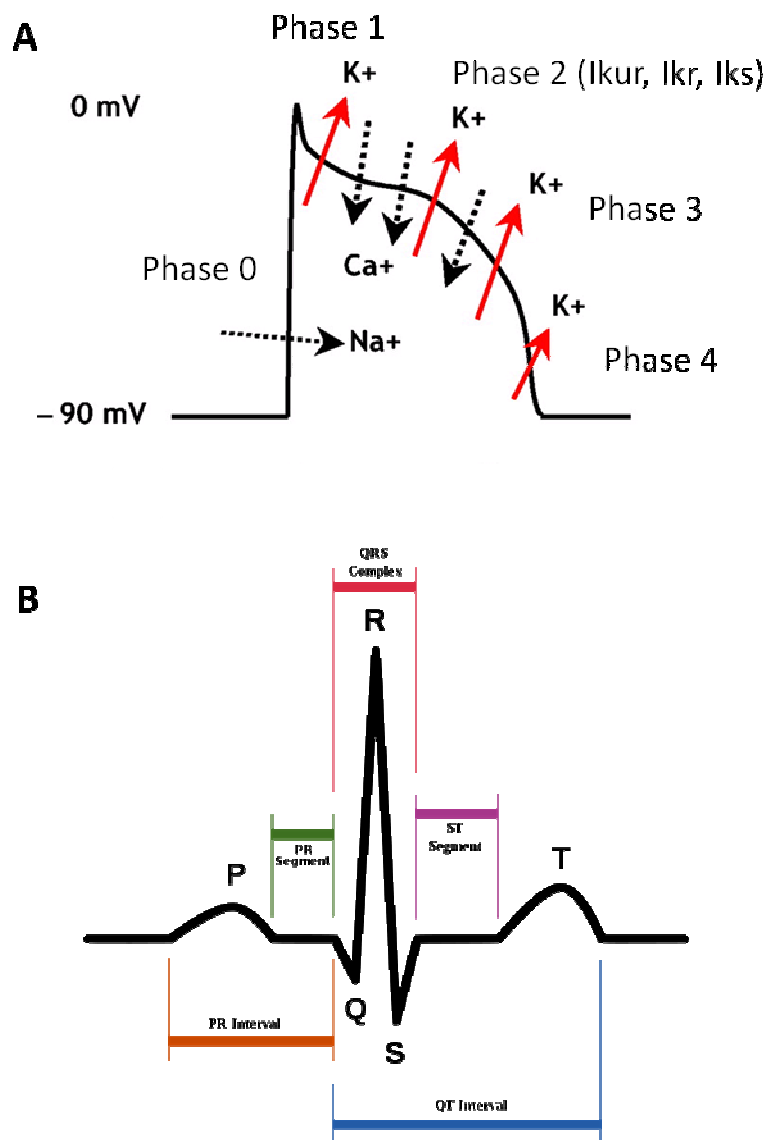
Figure 1.5 Cardiac action potential and ECG. (A) Schematic representation of the normal action potential and the flux of ions, taken from (Brugada et al., 2005). Dashed arrows show currents contributed by influx of Na^+ or Ca^{2+} ions and solid arrows show currents contributed by out flux of K^+ ions. (B) Schematic of the normal electrocardiogram of human heart, created by Anthony Atkielski. The P-wave representing atrial activation, QRS complex representing ventricular activation and the start of ventricular contraction, and T-wave representing ventricular repolarisation are shown along with the QT interval which is the distance from the beginning of the Q-wave to the end of the T-wave (Modell and Lehmann, 2006).

The hERG channels are also important for the pace-making activity of the sinoatrial (SA) and atrioventricular (AV) nodes of the heart and achieving the resting potential in neurons, smooth muscles and tumour cells.

ERG currents have also been recorded in many other excitable cells or neuroendocrine cells, smooth muscle fibres of the gastrointestinal tract, where they contribute to the maintenance of the resting potential related to cell-specific functions like increase in hormone secretion, frequency adaptation or increase in contractility (Gullo et al., 2003, Schwarz and Bauer, 2004).

The channels were first cloned from a hippocampal cDNA library in 1994 and belong to the conserved family of genes related to Drosophila *eag*, which encodes a distinct type of voltage-activated K^+ channels (Warmke and Ganetzky, 1994). The history behind the name of the channel is that *Drosophila* geneticist studying the fly behaviour found that mutant flies, when anaesthetized with ether, exhibited a twitching behaviour that resembled the action of a go-go dancer; hence the mutant phenotype was named as *ether-a-go-go* (EAG) (Warmke and Ganetzky, 1994). The encoded EAG polypeptide is related both to voltage-gated K^+ channels and to cyclic nucleotide-gated cation channels. Homology screens identified a family of *eag*-related channel polypeptides, highly conserved from nematodes to humans, comprising three subfamilies: EAG, ELK, and ERG. The human analogue of EAG gene was named *HERG* derived from the name <u>h</u>uman <u>E</u>AG-<u>r</u>elated <u>g</u>ene. Since *HERG* or *KCNH2* encodes the human Kv11.1 potassium channel it is also known as hERG (Sanguinetti, 2005). The Kv11.1 channels found in mammals other than humans that have been studied include mouse, rat, guinea pig, rabbit and canine channels. In humans, the hERG channels are expressed in tissues throughout the body such as the heart, neurons and smooth muscles but their expression in cardiac tissue is quite high. Role of the channels in many other tissues is unknown.

The mammalian *ERG* family of genes includes three genes *ERG1*, *ERG2* and *ERG3*. The cardiac *ERG* has two N-terminal alternatively spliced variants of ERG1; *ERG1a* and *ERG1b* while the *ERG2* and *ERG3* are found to express in nervous system in rat (Guasti et al., 2005). The ERG1b protein is similar to ERG1a except that it has a shorter N-terminus and is found to express in mouse and human heart (London et al., 1997). Functional ERG channels have been shown to be homo- as well as hetero-

tetramers of both ERG1a and ERG1b proteins in human cancer cells (Crociani et al., 2003) and in rat, human and canine ventricular myocytes (Jones et al., 2004).

The ERG alpha subunits are reported to associate with single transmembrane-domain proteins MinK and MiRP1 (minK-related protein1) and are considered to affect channel function and trafficking (McDonald et al., 1997). For example interaction of hERG α-subunits with β-subunit MiRP1 in heterologous expression systems, causes decreased trafficking of channels to the cell surface and a more rapid rate of deactivation. However looking at the tissue distribution of these subunits as well as the comparisons between hERG currents in presence or absence of MiRP1, it is considered unlikely that the protein has any physiologically critical role in the formation of functional hERG channels (Weerapura et al., 2002).

1.4.2 Stoichiometry and structure of hERG channels

Stoichiometry of hERG

Homomeric channels encoded by *HERG1a* have been used as a model for studying the cardiac Ikr currents. The X-ray crystal structure of the hERG channels is not available till date. Gating properties of the hERG channels have been determined (for detailed review see Tristani-Firouzi and Sanguinetti, 2003), based on the crystal structures of the bacterial KcsA, KvAP and MthK channels and a mammalian channel, Kv1.2, solved by Rod MacKinnon and his colleagues (Long et al., 2005b).

Structure of hERG

hERG channels are tetramers of ERG and each α-subunit is a six transmembrane protein like a typical Kv channel that forms the K^+ selective channel pore where the S4 domain serving as the main voltage sensor. The channels have a Per-Arnt-Sim (PAS) domain in the N-terminus (Morais Cabral et al., 1998) and a cyclic nucleotide binding domain (cNBD) within the C-terminus.

Gating of hERG

The channel pore is asymmetrical and its dimensions change as the channel gates open and close. The extracellular end of the narrow channel pore in hERG has the K^+ selectivity filter that allows the passage of dehydrated K^+ ions as a single file. The

highly conserved sequence Thr-Val-Gly-Tyr-Gly of amino acids line the channel pore in Kv channels but hERG has the Thr and Tyr residues substituted with Ser and Phe. Below the selectivity filter, the pore widens into a water-filled region, called the central cavity, which is lined by the S6 α-helices.

The four S6 domains of the closed channels form a criss-cross near the cytoplasmic interface. This prevents the entry of K^+ ions from the cytoplasm into the channel pore. When the cellular membrane depolarises, the S6 α-helices splay outwards allowing passage of ions into the channel. The S6 domain forms a hinge at the Ile-Phe-Gly motif which allows gating of the channel between the open and inactivated state which cannot close. This is unlike the gating seen in Kv1-Kv4 channels where the channels hinge at the Pro-Val-Pro motif. The bacterial KcsA, MthK, KirBac1.1 and KvAP channels have a conserved Gly residue in S6 is proposed to serve as the hinge which is located two helical turns above the Pro-Val-Pro motif in Kv channels (Sanguinetti and Tristani-Firouzi, 2006). The hERG channels undergo rapid C-type inactivation, deduced by study of Kv channels other than hERG, mediated by a slight constriction of the selectivity filter that may only occur when the outermost K^+ binding site is not occupied by an ion (Kiss and Korn, 1998). The role of the PAS domain in the N-terminus of hERG in channel gating is not well understood although deletion of this domain results in rapid deactivation of the channel. Binding of cAMP to the CNBD domain has a relatively minor effect on channel gating but it is found to be critical for processing of the channels in the ER and disruption of this domain results in lack of functional channels expressed on cell surface (Akhavan et al., 2005). See Figure 1.6.

Drug binding properties of hERG channels

The hERG channels have been shown to be directly blocked in the intracellular pore, leading loss of Ikr currents, by a variety of drugs with diverse structures that include several anti-arrhythmic, psychiatric, anti-microbial and anti-histamine drugs (Fermini and Fossa, 2003). Drug binding is also reported to interfere with trafficking of the hERG channels to the cell surface resulting in reduced channel function leading to acquired or drug induced LQTS (for detailed review see Dennis et al., 2007). This unique property of hERG channels is attributed to their structural features that can more effectively accommodate the binding of drugs as compared to other K^+ channels. Lack of complete understanding of the channel structure limits the predictability for drugs that could bind hERG.
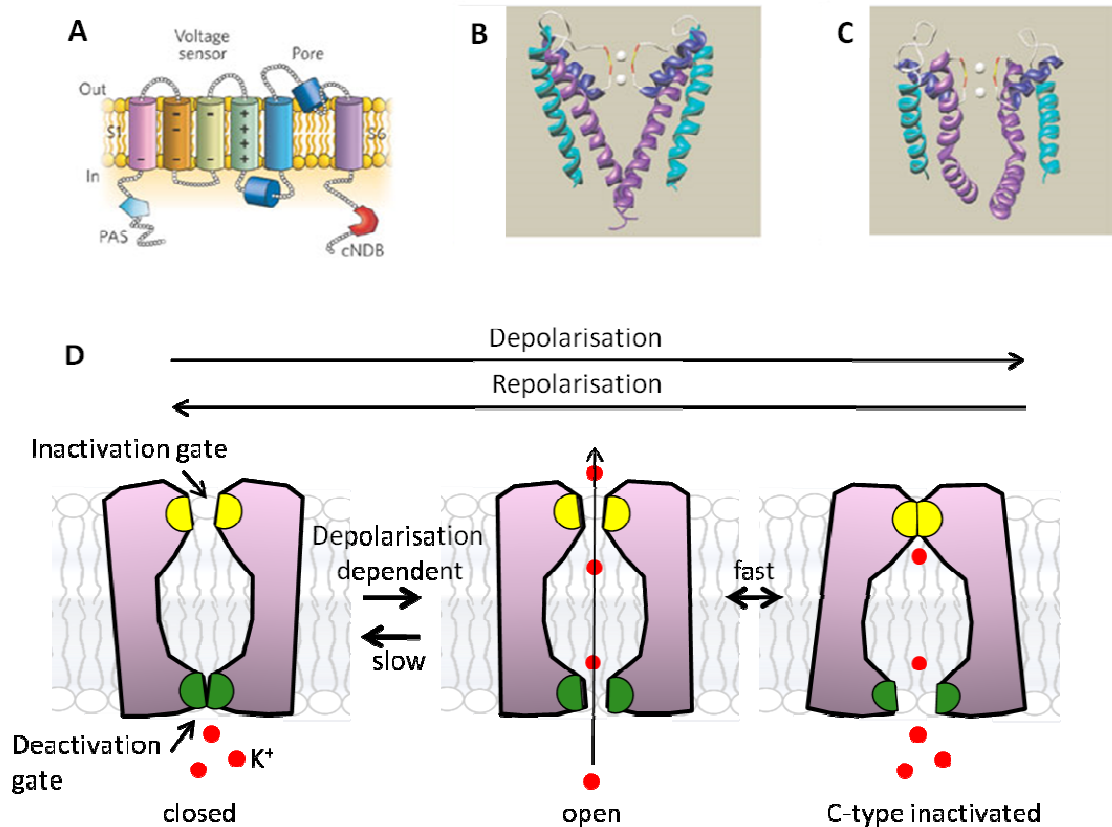
Figure 1.6 Structure and gating of hERG. (A) Diagram of a single hERG subunit containing six α-helical transmembrane domains, S1–S6. (B) Structure of a KcsA K$^+$ channel crystallized in the closed state (Doyle et al., 1998), showing two of the four subunits. White spheres are K$^+$ ions located within the selectivity filter. The Gly (red) and Tyr (yellow) residues of the selectivity filter are also indicated. (C) Structure of the pore domain of a Kv1.2 K$^+$ channel crystallized in the open state (Long et al., 2005a), showing two of the four. (D) Schematic showing gating states of a single hERG channel (pink); channels are closed at negative voltages and slowly open (activation) when the membrane depolarizes and then rapidly inactivate (C-type inactivation) by constriction of the selectivity filter (yellow). Repolarisation of the membrane reverses the transitions between these states, (images are adapted from Sanguinetti and Tristani-Firouzi, 2006).

Two polar residues (Thr623 and Ser624) located at the base of the channel pore helix and two aromatic residues (Tyr652 and Phe656) located in the S6 domain of the hERG subunit were found to be important for interacting with several drugs such as cisapride and terfenadine. The S6 residues (Tyr652 and Phe656) are unique to hERG since most Kv channels have an Ile and a Val in homologous positions. The binding of drugs to the channels is likely to be possible only when the channels are open (Sanguinetti et al., 1995, Sanguinetti and Tristani-Firouzi, 2006, Mitcheson, 2008). The occurrence of drug induced LQTS has resulted in the withdrawal of several blockbuster drugs from the market. Pharmaceutical companies are therefore required to screen compounds for hERG-channel activity early during preclinical safety assessment adding to the developmental costs.

1.4.3 Pathophysiology of hERG channels

The Long QT Syndrome (LQTS)

The rhythmic changes in cardiac action potential are recorded in the electrocardiogram (ECG). A typical ECG tracing of the cardiac cycle (heartbeat) consists of a P wave, a QRS complex, a T wave, and a U wave; the baseline voltage of the electrocardiogram is known as the isoelectric line (Figure 1.5.B). The LQTS is commonly characterised by prolongation of the ventricular action potential duration during cardiac repolarisation, measured as the QT interval on the electrocardiogram (Figure 1.7.A-B). LQTS can lead to life-threatening *torsade de pointes* (TdP), see Figure 1.7.C. The inherited or congenital LQTS is mainly caused by mutations in genes that code for protein subunits of cardiac ion channels. Several genotypes of LQTS are known (LQTS1-10) of which LQTS1-3 have most common occurrence. Mutations in *HERG* (KCNH2) are found to cause the long QT syndrome 2 (LQTS2) which suggests that the channels play a critical role in myocellular repolarisation in the heart (Curran et al., 1995). More than 200 *HERG* mutations have been identified and most of these are located in the hERG channel pore thereby affecting channel gating while others affect the intracellular trafficking of the channels (Anderson et al., 2006, Modell and Lehmann, 2006). Altered channel trafficking causes a reduction in the number of channels expressed on cell surface leading to decreased hERG currents (Ikr). The channels have also been implicated in drug induced LQTS2 where block of hERG channel pore by drugs results in decreased hERG currents (Sanguinetti et al., 1995).
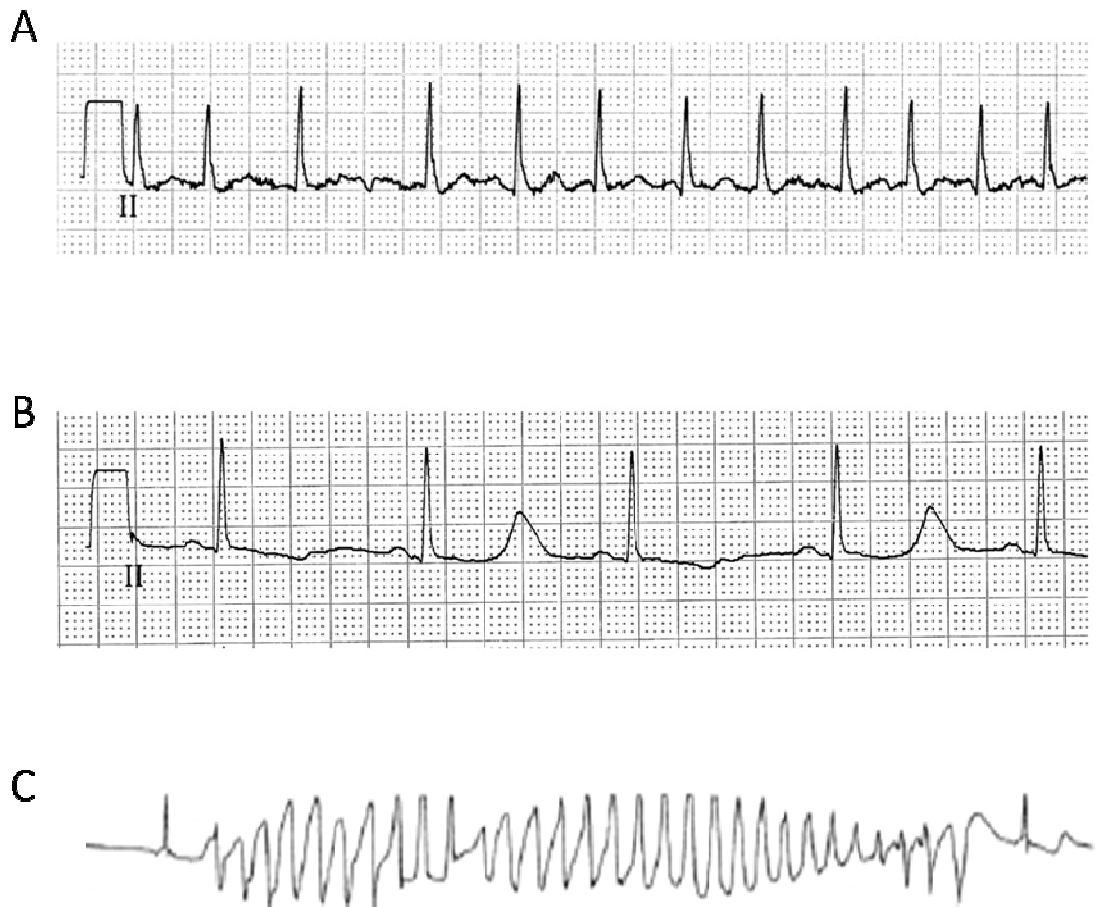
Figure 1.7 ECG traces in health and disease. ECG traces during normal (A), long-QT (B), conditions of the heart (reproduced from Wegener et al., 2008). (C) Resultant electrocardiogram of elongated Q-T interval, resulting in *torsades de pointes* (reproduced from Vandenberg et al., 2001)

Both cardiac drugs as well as non-cardiac medications, antipsychotics (e.g., thioridazine), methadone, antimicrobials (e.g., erythromycin), the gastrointestinal stimulant cisapride, and antihistamines (e.g., terfenadine), may induce LQTS2 and TdP (Modell and Lehmann, 2006). Severity of this form of LQTS varies depending on the drug, dose and individual. In rare instances, drugs may also interfere with trafficking of the hERG channels. Conditions such as hypocalcemia, hypokalemia and hypomagnesemia related to diet, medical conditions and diuretic use can also cause LQTS (Massaeli et al., 2010, Modell and Lehmann, 2006).

The Short QT Syndrome

Short QT syndrome (SQTS) is a disease characterised by a shortened QT interval of the ECG and is associated with cardiac tachyarrhythmia including sudden cardiac death. It usually affects young and healthy people who may have no structural heart disease. SQTS is caused due to mutations in genes that encode for cardiac potassium ion channels. Gain-of-function mutations in *HERG* lead to SQTS (Brugada et al., 2005, Hong et al., 2005). For example, the inherited mutation hERG-N588K causes severely compromised inactivation abilities and faster deactivation kinetics of the mutant channels leading to SQTS (Grunnet et al., 2008).

hERG channels and disorders of insulin secretion

Majority of the patients suffering from diabetes mellitus, characterised by impaired insulin secretion leading to high blood sugar levels, are affected by cardiovascular diseases such as LQTS and show an increased risk of sudden cardiac death. Cardiac disorders are a major cause of death in diabetic patients. Though several ionic currents are found to be depressed in diabetic hearts, any decrease of hERG currents which are required for normal function of the heart (Veglio et al., 2004) would led to cardiac arrhythmia. The channels are also found to be down regulated by hyperglycemia, tumour necrosis factor-alpha (TNF-α), ceramide and the cellular metabolites accumulating in diabetic tissue and this may be due to over production of reactive oxygen species (ROS) which are known to decrease hERG function (Wang et al., 2004a, Nanduri et al., 2008).

A lot remains to be understood about the link between the disorders of insulin secretion and their effect of hERG. It has been reported that expression of the channel protein is reduced in diabetic hearts but not the levels of hERG mRNA which was attributed to

the over-expression of micro-RNA miR-133. This study indicates that apart from trafficking, expression of the channels on cell surface could also be regulated by miRNAs at translational levels (Xiao et al., 2007), However, trafficking of ion channels remains to be a major determinant of the number of channels expressed on the cell surface and is therefore important for understanding channelopathies (Delisle et al., 2004).

1.5 Trafficking of Membrane Proteins

This is an overview of trafficking mechanisms of membrane proteins. The trafficking of the K_{ATP} and hERG channels is discussed in the relevant chapters.

1.5.1 General overview of membrane protein trafficking

Cellular membrane proteins destined for the plasma membrane or for secretory and endocytic organelles are synthesised by ribosomes in the endoplasmic reticulum (ER). Newly formed proteins fold with the help of chaperones into the correct conformation in the ER membrane. Proteins are transported from the ER to an ER-Golgi intermediate compartment (ERGIC) and then are further sorted to the *cis*-Golgi. ER resident proteins are recycled back from ERGIC. For proteins that are multimers of same or different proteins, retention/retrieval to the ER ensures that only properly assembled multimers are transported to the cell surface (Figure 1.8). Misfolded or incorrectly assembled proteins in the ER are generally targeted for degradation through ER-associated degradation (ERAD) pathway. The *trans*-Golgi Network (TGN) serves as a sorting station that either sends proteins to the cell surface or diverts them to endosomes for further distribution within the cell (Ashcroft, 2006a, Bannykh et al., 1998, Bannykh and Balch, 1998).

Thus the ER and Golgi are locations of quality control of the newly synthesised proteins. This includes a general surveillance system that screens for broad conformational characteristics such as appropriate membrane partitioning of hydrophobic domains or unpaired cysteine residues and a more selective mechanism that requires specific motifs interacting with transport proteins that help trafficking of correctly folded/assembled proteins from the ER or Golgi. These motifs are located on the proteins being transported or the 'cargo proteins' and are recognised/bound by the proteins involved in the forward trafficking of these proteins but till date only a limited number of these motifs have been identified (Ellgaard and Helenius, 2003) for particular classes of proteins. Membrane proteins expressed on cell surface by means of forward or biosynthetic trafficking pathways may be removed from the cell surface (internalisation or internalisation), transported back to the cell surface after internalisation (recycling) or transported to endosomes for degradation (Bonifacino and Traub, 2003, Maxfield and McGraw, 2004, Mayor and Pagano, 2007).
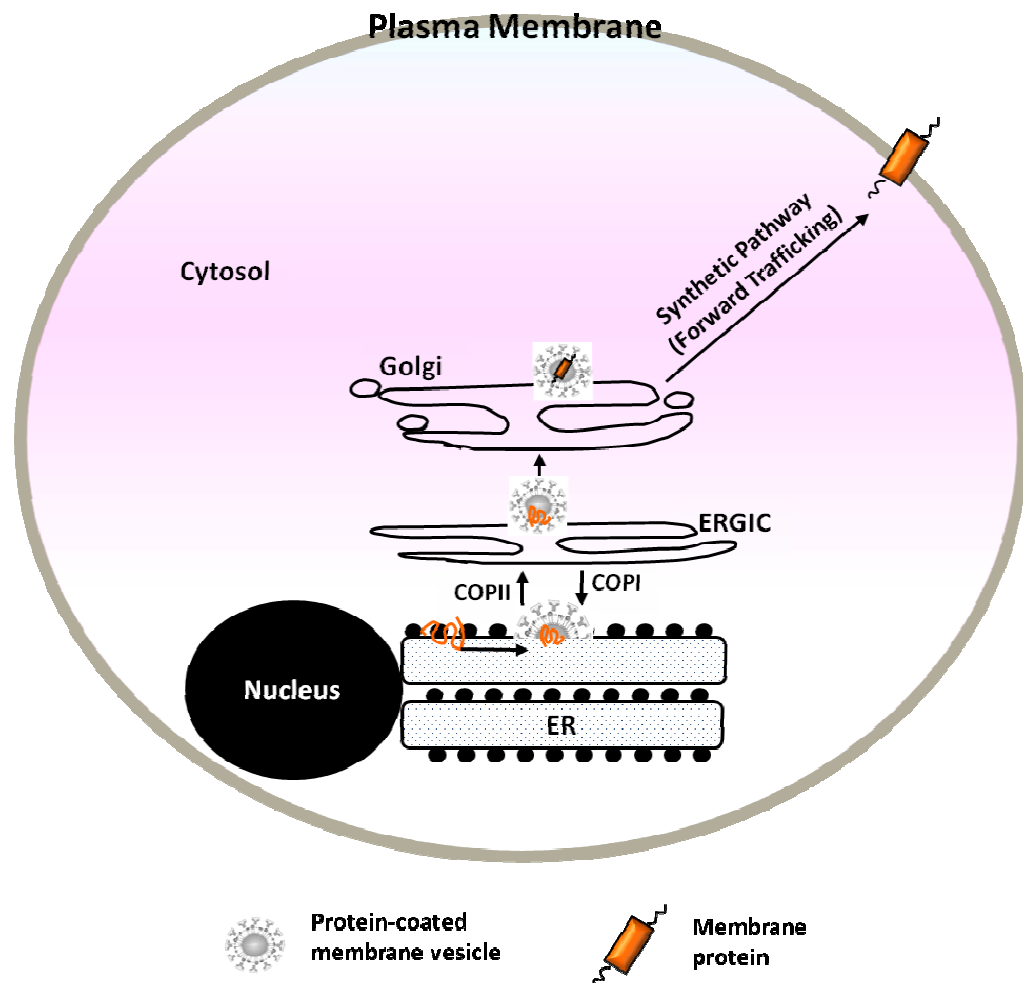
Figure 1.8 Schematic showing forward trafficking of membrane proteins. Membrane proteins are synthesised in the ER membrane and following vesicular transport they enter the ER-Golgi intermediate complex. COPII vesicles mediate regulated transport of proteins out of the ER. Unassembled and ER resident proteins are transported back to the ER in COPI vesicles. Following processing in the Golgi, the membrane proteins are transported to the cell membrane.

Like in the biosynthetic pathway, motifs on the cargo proteins can play an important role in endosomal trafficking of the proteins. Identification and study of these trafficking motifs is critical for understanding the mechanism of trafficking of membrane proteins and is of fundamental importance to cell biology.

1.5.2 Trafficking vesicles

Transport of secretory and membrane proteins between intracellular compartments is generally vesicular, involving proteins of the coat complexes that direct the selection of cargo through recognition of signal motifs (Gorelick and Shugrue, 2001). The vesicles carrying the protein cargo pinch off from donor organelle membrane and then reach recipient organelle to deliver the cargo by fusing with the membrane of the recipient organelle (Aridor and Balch, 1996, Scales et al., 2000, Schekman et al., 1995). These coat complexes include (Bonifacino and Glick, 2004):

- Coat protein complex II (COPII), which exports proteins from the ER. Proteins are sorted by recognition of specific motifs such as DXE on the cargo proteins.
- Coat Protein Complex I (COPI), which binds di-leucine (LL) motifs and functions to direct retrograde transport of proteins from pre-Golgi and Golgi compartments to the ER.
- Clathrin coated vesicles (CCV), which mediate sorting of receptors containing Tyr-based motifs from the TGN and the cell surface.

Vesicular transport generally involves several mediator proteins that act in a cascade. Of several trafficking mediators known, such as the adaptor proteins (AP1, AP2), Sar proteins, Sec proteins and Rab-GTPases, it is evident that these proteins are more or less specific with reference to the site of their action and the kind of cargo they recognize (Doherty and McMahon, 2009, Barlowe, 2003).

1.5.3 Endosomal trafficking of membrane proteins

Changes in the distribution as well as the protein and lipid composition play a key role in regulation of several cell biological processes. Endosomal trafficking mechanisms control the lipid and protein composition of the plasma membrane, thereby regulating how cells interact with their environments (Steinman et al., 1983). Endosomal trafficking processes include:

- internalisation, which allows removal of membrane proteins expressed on cell surface or uptake of proteins into the cell;

- endosomal recycling, which allows the transport of internalised proteins back to the cell surface; and

- degradation, which diverts proteins internalised from the cell surface for degradation.

These interactions can also have patho-physiological implications; for example, alteration of surface density of proteins such as an ion channel can lead to disorders caused by altered channel function (Steele et al., 2007a). Pathogens, such as viral proteins, have been shown to hijack the cellular endocytic mechanisms for entry into the cells and cause infection (Marsh and Helenius, 2006). Therefore, it is important to understand the basic cell biology of endosomal trafficking mechanisms and their regulation.

1.6 Forward Trafficking of Membrane Proteins

1.6.1 ER exit of membrane proteins – COPII vesicles

Some membrane proteins can leave the ER by bulk flow where the ER export is via non-selective vesicle transport while others are transported by a concentrated flow of proteins where proteins leave the ER after being selectively packaged into COPII vesicles that are rich in the protein cargo (Balch and Farquhar, 1995). This selective anterograde pathway involves coat assembly which begins through activation of a small G-protein, Sar1 which recycles between cytosolic and membrane-associated pools, with GTP binding generating the active, membrane-bound state (Barlowe et al., 1994). Several types of ER-exit signals which play a role in transport of specific cargo from the ER exit sites (ERES) have been identified. These include the diacidic motifs [(D/E)X(D/E)], di-hydrophobic motifs (FF, YY, LL or FY), YXXXNPF and LXXLE motifs (Nishimura et al., 1999).

Formation of the COPII transport vesicle begins with selective sorting and recruitment of correctly folded cargo proteins and the components of the COPII vesicle at the ERES and the formation of the COPII vesicles that bud off from the ER. It consists of proteins Sar1, Sec23–Sec24 and Sec13–Sec31 that are sequentially recruited to ER membrane surface. Sar1 is a small 21 KDa GTPase, whereas Sec23–Sec24 and Sec13–Sec31 are large heteromeric protein complexes. Activation of Sar1-GDP to Sar1-GTP is thought to regulate COPII coat assembly. Activation of Sar1-GDP to Sar1-GTP is catalysed by a membrane-bound GDP–GTP exchange factor, Sec12 (a Sar1 specific GDP dissociation stimulator), which is localised to ER (Barlowe and Schekman, 1995). To assemble COPII coat, membrane-bound Sar1-GTP binds to Sec23–Sec24, which in turn attracts Sec13–Sec31 that leads to clustering of the COPII vesicle proteins. Sec24 has several cargo recognition sites through which it binds the transmembrane cargo that is packaged into COPII vesicles. Cargo recognition by Sec24 is due to the specific ER exit motifs present on proteins that get concentrated at the ERES during export (Barlowe, 2003, Nishimura and Balch, 1997, Nishimura et al., 1999, Bi et al., 2002). The cargo containing vesicles pinch off from the membrane following hydrolysis of Sar1-GTP to Sar1-GDP causing their release from the vesicle (Figure 1.9).
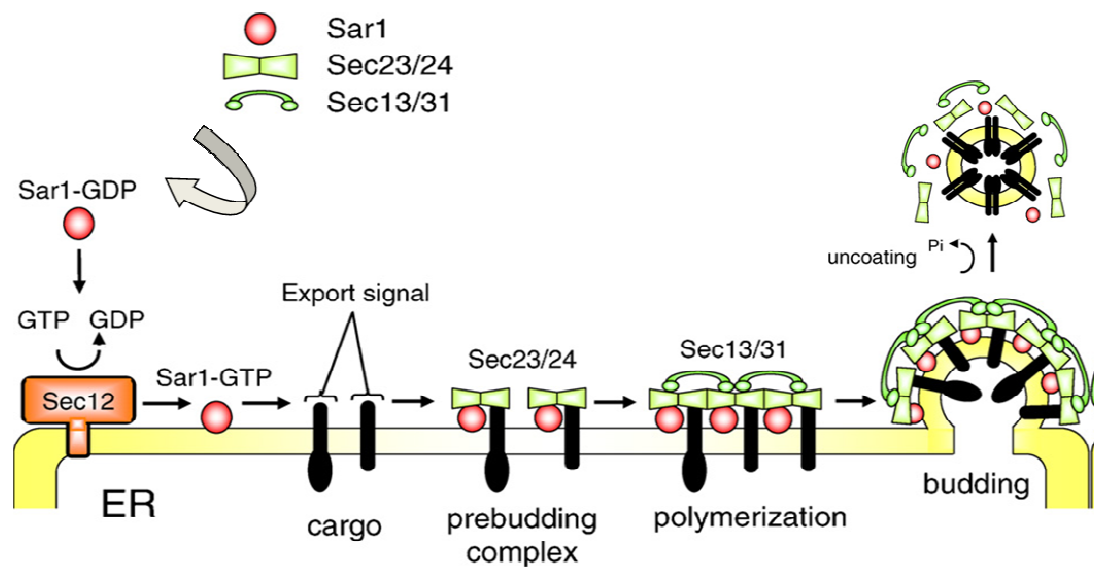
Figure 1.9 Schematic showing the COPII vesicle-mediated ER exit of membrane proteins. The assembly of the vesicle begins with the Sec12-facilitated exchange of GTP for GDP on Sar1 and recruitment of Sar1-GTP to the ER membrane. This is followed by the sequential recruitment of the hetero-dimeric Sec23/24, cargo recognition and binding to Sec24 cargo and finally the recruitment of Sec13/31 coat proteins which lead to the assembly of the cargo loaded COPII vesicle at the ER exit sites. This assembly leads to the formation of a pre-budding complex, which when fully formed is released into the cytoplasm as a COPII-coated vesicle for transport to the Golgi apparatus. Hydrolysis of GTP to convert Sar1-GTP to Sar1-GDP is required for the release of the COPII vesicle from the ERES. (Figure adapted from (Sato and Nakano, 2007b).

The vesicles fuse at the Golgi membrane to deliver the cargo proteins to their destination. GDP/GTP exchange of Sar1 catalysed by Sec12 is critical for initiation of COPII coat assembly (Barlowe and Schekman, 1995).

1.6.2 ER retrieval - COPI vesicles and 14-3-3

Proteins that are returned back to the ER via the COPI vesicles include the ER resident proteins (for example, vSNAREs, ERGIC53/p58, the KDEL receptor), nucleus localised proteins (for example, the epidermal growth factor receptor family protein) and the proteins that do not get transported beyond the *cis*-Golgi (for example, unassembled protein complex components Wang et al., 2010, Lee and Goldberg, 2010).

Additionally, COPI coat proteins have complex functions in intra-Golgi trafficking and in maintaining the normal structure of the mammalian interphase Golgi complex. COPI-coated vesicles form on the Golgi apparatus by the sequential recruitment of an ADP ribosylation factor 1 (ARF1) protein and coatomer, a 550 KDa cytoplasmic complex of seven COPs α-, β-, $\beta 0$-, γ-, δ-, 3-, and ζ-COP (Waters et al., 1991, Yang et al., 2002). Budding of the cargo containing COPI vesicles is initiated by the exchange of GDP for GTP on ARF catalysed by a Golgi-localised guanine nucleotide exchange factor (GEF). See Lee et al., 2010 for a detailed review.

The coatomer COPI proteins are reported to recognise and bind an arginine based RXR motif, where X could be any amino acid, on their cargo (McMahon and Mills, 2004). It was originally suggested that the 14-3-3 proteins bind to the RXR motif; for detailed review see Michelsen et al., 2005 . It was considered that in unassembled K_{ATP} channels the RXR motif on the Kir6.2 and SUR1 subunits is bound by the 14-3-3 protein which causes their ER retention. With further research on the 14-3-3 proteins, it was found that the 14-3-3 proteins bind only dimeric or tetrameric 'RXR' motifs following which the proteins are returned to the ER via COPI vesicles. It was considered that the proteins bind to partially assembled K_{ATP} channel subunits and probe the assembly state of the channel (Heusser et al., 2006, Mrowiec and Schwappach, 2006, Nufer and Hauri, 2003).

The TASK-1 and TASK-3 potassium channels have also been shown to bind to 14-3-3 through tri-basic motif, KRR, which differs in several important aspects from canonical arginine-based (RXR) or lysine-based (KKXX) ER retention signals. Interaction with 14-

3-3 has no significant effect on the dimeric assembly of the channels (Zuzarte et al., 2009). In case of the Major Histocompatibility Complex II (MHCII) protein, 14-3-3 binds to the phosphorylated membrane protein enabling its forward trafficking (Mrowiec and Schwappach, 2006).

1.7 Internalisation of Membrane Proteins

1.7.1 Introduction

Endocytic mechanisms essentially require selection of the cargo protein at the cell surface followed by budding off of the region of the plasma membrane containing the endocytic cargo and tethering of the cargo containing vesicles to their destination endosomal compartment within the cell where the vesicle can fuse to deliver its cargo. Several different endocytic mechanisms have been identified which vary in the cargoes they transport and may use distinct protein machinery, but owing to their complexity a lot still needs to be understood regarding these cellular processes.

Classification of endocytic mechanisms can be based on the requirement for dynamin- pathways that use dynamin-mediated scission mechanism (dynamin-dependent), and those that require other processes (dynamin-independent). Two major classes of dynamin-dependent pathways use either clathrin or caveolin coat proteins. Another basis of classification is pathways that use clathrin (clathrin mediated) or all other pathways (clathrin independent). Clathrin independent mechanisms are classified according to requirement of the small GTPases- CDC42, RhoA and ARF6 (Doherty and McMahon, 2009, Mayor and Pagano, 2007); see Figure 1.10.

Study of endocytic mechanisms of proteins is complicated as the same endocytic cargo may be internalised by different mechanisms in different cell types or may switch pathways in a single cell type under different conditions. For example; albumin is internalised in caveolae in some cell types such as human skin fibroblasts and endothelial cells, whereas in Chinese Hamster Ovary (CHO) cells it is internalised by a RhoA-dependent mechanism (Singh et al., 2003). Another example is cholera toxin (CT), which bind to GM1 at the plasma membrane and is internalised to the Golgi and then transported to the ER. In the ER, catalytic subunits of CT are translocated to the cytosol causing toxicity. CT has been found to be internalised by multiple endocytic pathways which include the clathrin-, caveolin-, ARF6- and CDC42- dependent pathways. Simultaneous block of all these pathways does not prevent toxicity which suggests that additional pathways may exist for internalisation of the CT into the cells (Massol et al., 2004). Choice of endocytic mechanism has also been shown to regulate the fate of its cargo. For example, epidermal growth factor receptors (EGFR) that undergo clathrin mediated endocytosis (CME) have longer life while EGFR receptors

that undergo clathrin independent internalisation (CIE) are diverted for degradation. Thus CME is important for some EGFR-activated signalling pathways and EGF-dependent biological responses, such as DNA synthesis (Torgersen et al., 2001, Sigismund et al., 2008).

1.7.2 Clathrin mediated endocytosis

Clathrin mediated endocytosis (CME) is one of the most common and well studied endocytic mechanisms. It is mediated by the formation of clathrin coated vesicles (CCV) at the cell membrane. CCV can also bud from membranes of intracellular compartments and assist in cargo transfer within the cell. Adaptor and accessory proteins coordinate formation of CCV at the plasma membrane by facilitating membrane curvature and constriction of the vesicle neck. Release of the CCV from the plasma membrane into the cell is mediated by the membrane scission protein, the large GTPase dynamin, which forms a helical polymer around the constricted neck of the CCV (Praefcke and McMahon, 2004). The clathrin coat is removed from the vesicle by auxilin and hsc70 allowing the targeting of the vesicle to its destination within the cell to deliver its cargo by fusion with the cell membrane (Lee and Goldberg, 2010).

Membrane proteins that are endocytosed via the CME have di-leucine (LL) or tyrosine-based (YXXΦ, where Φ is a hydrophobic amino acid) motifs which act as signals that are recognised by adaptor protein-2 (AP2), which form a link between the cargo and the clathrin molecules. For example, the classical CME cargo transferrin receptor has the YTRF motif which is found to be critical for internalisation of the receptor (Collawn et al., 1990); CME of the pancreatic K_{ATP} channels requires an intact YSKF motif in the carboxyl-terminus of Kir6.2 subunits. Mutations Y330C and F333I that disrupt this motif have been shown to abrogate internalisation of reconstituted mutant channels causing permanent neonatal diabetes mellitus (Mankouri et al., 2006). Considering the varied cargoes that are internalised by CME it is being considered that more than one kind of adaptor and accessory proteins are involved in the formation of different subtypes of CCVs that are directed to specific locations within the cell (for detailed review see Doherty and McMohan, 2009).

1.7.3 Clathrin independent endocytosis

Endocytic pathways that do not use clathrin are generally classified as clathrin independent endocytic (CIE) mechanisms. CIE pathways are mostly mediated by lipid-rafts and may or may not require dynamin for membrane fission (Doherty and McMahon, 2009). Rafts are small platforms in membranes and are composed of sphingolipids, phospholipids and cholesterol in the lipid bilayer. Lipid-rafts are present on both the plasma membrane as well as in the membranes of the ER, Golgi and endosomes. Raft components including cholesterol, ceramide and the hydrophobic backbone of sphingolipids are synthesised in the ER and sphingolipid head groups are attached to ceramide in the Golgi complex for the assembly of lipid-rafts which then spread into the endosomal recycling compartments. Cholesterol partitions between the raft and the non-raft phases of the membranes and has higher affinity to raft sphingolipids than to unsaturated phospholipids. Cholesterol molecules act as spacers between the hydrocarbon chains of the sphingolipids and maintains raft structure (Simons and Toomre, 2000). Removal of raft cholesterol using methyl-β-cyclodextrin or saponin, generally leads to dissociation of most proteins from rafts and renders them non-functional. Since the rafts are not solubilised by Triton X-100 or with CHAPS at 4°C they are also referred to as detergent-resistant membranes (DRMs) (Simons and Ehehalt, 2002). The partitioning of proteins into and out of rafts can be tightly regulated. For example; peripheral membrane protein such as non-receptor tyrosine kinase, can be reversibly palmitoylated and can lose its raft association after depalmitoylation (Zacharias et al., 2002). Raft mediated membrane trafficking mechanisms are discussed below:

Caveolin-mediated internalisation

Caveolins are coat proteins that have been implicated in the formation of caveolin coated vesicles known as 'caveolae'. Caveolae are 50–80 nm flask shaped invaginations of the cholesterol rich lipid raft membranes (caveolar rafts) that are involved in caveolar internalisation. There are three isoforms of mammalian caveolin proteins, caveolin1-3. Caveolin1 is considered to be muscle specific while caveolin1 and caveolin2 are expressed in most non-muscle cells (Rothberg et al., 1992). Several cargoes such as the SV40, cholera toxin (CT) have been shown to internalise in a caveolin dependent manner to large intracellular structures called as caveosomes. Caveolins have been shown to associate with cholesterol and glycosphingolipid GM1. Cholesterol depletion and phosphorylation of caveolin1 flattens the caveolae. Studies

using phosphomimetic mutant (S80A) of Caveolin1 suggest that dephosphorylation of the protein at ER/Golgi, where the formation of caveolae initiates, may regulate the formation of caveolar micro-domains (Schlegel et al., 2001).
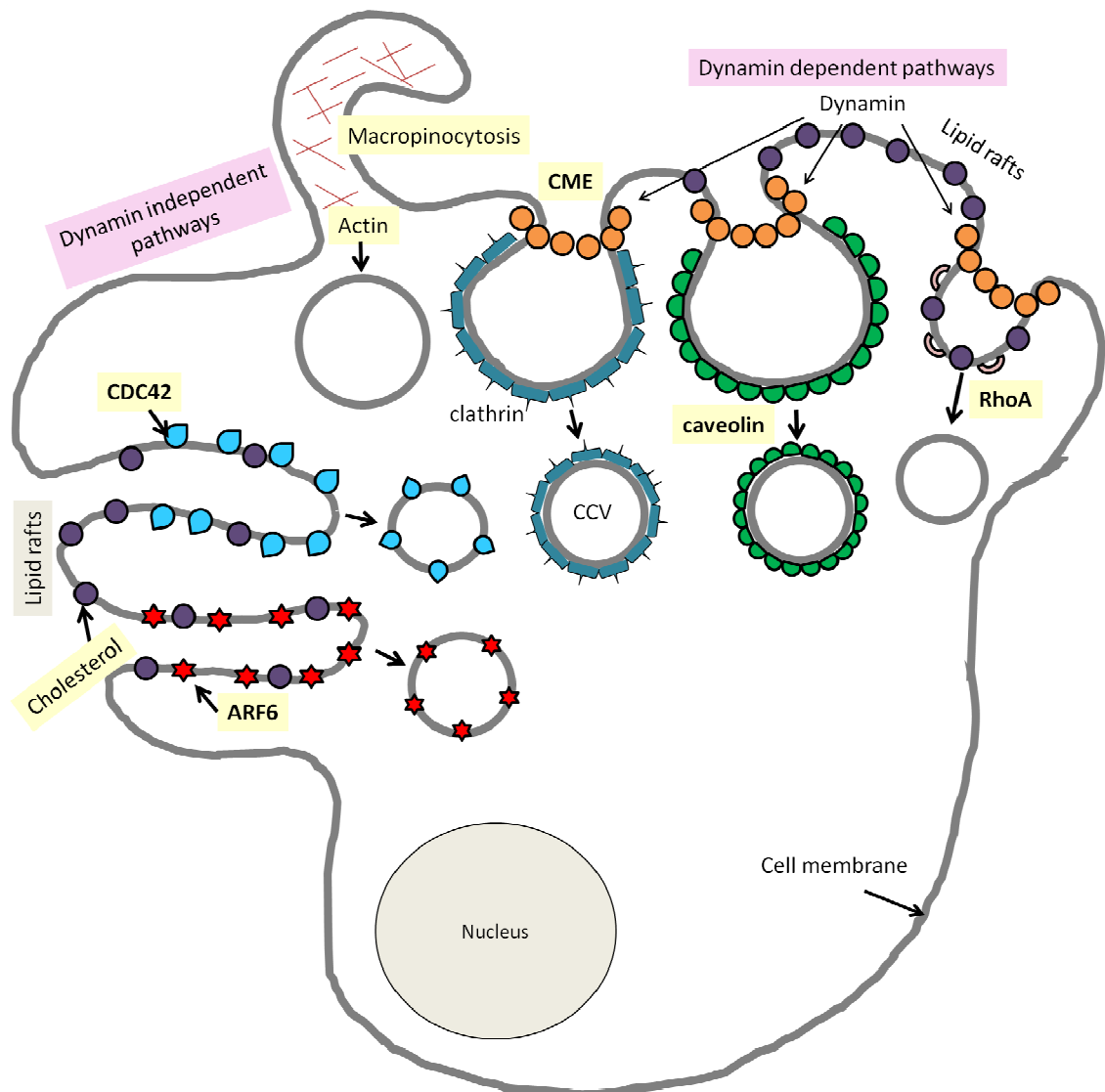
Figure 1.10 Schematic of different endocytic mechanisms. Dynamin-dependent and dynamin-independent endocytic pathways and their mediators are shown, (Mayor and Pagano, 2007). CME, Clathrin mediated endocytosis; CCV, clathrin coated vesicle.

Endocytic nature of caveolae is not well understood and it is considered that caveolae may or may not pinch off from the cell membrane. Apart from internalisation, caveolins have been implicated as being anchors for signalling molecules and caveolae are considered to act as signalling platforms (Krajewska and Maslowska, 2004). For example, localisation of Kv1.5 channels to caveolar rafts has been shown to be critical for regulating the channel function (Martens et al., 2001, Martinez-Marmol et al., 2008).

Flotillin-mediated internalisation

Flotillin proteins (also called reggie proteins) are homologous to caveolin1 and are found to oligomerise and associate into clusters that form scaffolds for membrane micro-domains. The caveolin independent flotillin micro-domains are considered to have a role in facilitating dynamin-dependent internalisation of proteoglycans as well the as epidermal growth factor receptor (EGFR), cellular prion-related protein (PrPc), GFP-GPI and CT (Stuermer et al., 2001, Payne et al., 2007), for review see (Mayor and Pagano, 2007, Sandvig et al., 2008). They form hairpin structures in the plasma membrane and have been shown to undergo cycling to and from the plasma membrane. Scission factors for flotillin based carriers are unknown but their trafficking within the cell is regulated by Rab5. Besides the plasma membrane, flotillin is localised to various intracellular compartments; however, the trafficking pathways used by them is not very clear and they are even considered to act upstream of the clathrin-independent pathways (Langhorst et al., 2008, Langhorst et al., 2005, Stuermer et al., 2004).

CDC42-regulated internalisation

Internalisation of caveolin1-associated cargoes overlap with those of the clathrin-independent carrier (CLIC) and glycoslyphosphatidylinositol anchor protein (GPI-AP) enriched early endosomal compartment (GEEC) pathway. These are examples of clathrin- and caveolin-independent pathways that require lipid-raft domains, also designated as non-caveolar lipid-rafts. Cargoes of non-caveolar raft domains include extracellular fluid, SV40 virions, CT, GM1, GPI-linked proteins, as well as receptors for IL2, growth hormone, AMF and many other molecules (Mayor and Pagano, 2007).

CDC42-regulated endocytic pathway is one of the main routes for non-clathrin, non-caveolar uptake of cargoes such as CT, plant protein ricin, and *Helicobacter pylori*

vacuolating toxin (VacA). GPI-AP are localised to lipid-raft membranes and undergo internalisation via this cholesterol-dependent, clathrin-independent pathway to GEEC instead of the conventional Rab5 positive early endosomal compartments. Membrane constituents are believed to cause membrane budding that is independent of dynamin and requires the small G protein CDC42. Internalisation into GEECs is considered to require CDC42-regulated recruitment of the actin polymerisation machinery. The CDC42-regulated endocytic carriers that bud from the cell surface have long and relatively wide surface invaginations which also allow internalisation of large volume of fluid phase markers in a single budding event compared to clathrin and caveolin mediated mechanisms of internalisation (Chadda et al., 2007, Mayor and Pagano, 2007).

Rac and RhoA-regulated internalisation

A class of CIE pathways are regulated by RhoA GTPase which is considered to cause rearrangement of the actin cytoskeleton. These endocytic processes can be independent of coat proteins and dynamin, and are mediated by cholesterol rich lipid raft membrane regions or use dynamin as a scission factor. The dynamin-dependent, RhoA regulated pathway includes the IL-2 pathway where Rab5 and Rab7 are involved in trafficking within the cell.

Phagocytosis and macropinocytosis

Phagocytosis is the means of internalisation of large particles into the cell which are generally diverted to lysosomes in a Rab7 dependent manner for degradation. It is considered to be mediated by factors such as Rac1 or PKC and involves actin and microtubule rearrangement (Swanson and Baer, 1995).

Macropinocytosis is an actin-mediated endocytic process involving plasma membrane ruffles and internalisation of fluid and particles in large, uncoated, endocytic vacuoles known as macropinosomes (Swanson and Watts, 1995). The ruffles can take the form of lamellipodia or filopodia and are irregular in shape as they are independent of coat proteins and can be up to 10 μm in diameter. It is a clathrin- and caveolin-independent mechanism for uptake of fluids and is considered to be regulated by tyrosine kinases, Ras, Rac1, and Rab34, Na^+/H^+ exchange factors, CDC42 and cholesterol. For detailed review see (Mayor and Pagano, 2007, Mercer et al., 2010, Swanson and Watts, 1995).

ARF6-mediated endocytic pathway

ADP-ribosylation factor 6 (ARF6) localises to the plasma membrane in its GTP state and to a tubulovesicular compartment in its GDP state (Macia et al., 2004). It is expressed widely in different cell types and has been implicated in dynamin- and clathrin-independent, raft-mediated internalisation and recycling of membrane proteins through its GTPase cycle. Apart from membrane trafficking, ARF6 has been shown to function in a variety of biological events, including chromaffin granule exocytosis, Fc-receptor-mediated phagocytosis, epithelial cell migration and adherens junction (AJ) turnover (Sabe, 2003). ARF6 alters the cortical actin cytoskeleton and the lipid composition at the PM through activation of phosphatidylinositol 4-phosphate 5-kinase [PI(4,5)P2] and phospholipase D (PLD) and can facilitate clathrin-dependent as well as clathrin-independent internalisation of ligands (Aikawa and Martin, 2003). ARF6-regulated CME requires AP-2.

ARF6-regulated CI endocytic cargos include MHCI, β1integrin, E-cadherin, GPI-AP, IL-2R-α (Tac) (Eyster et al., 2009). After internalisation, ARF6-GTP and cargo containing endosomal compartments are separate from the classical early endosomal compartments but have been shown to fuse with Rab5 associated early endosomes following hydrolysis of ARF6-GTP. Recycling vesicles derived from clathrin-dependent and independent internalisation might eventually converge in a common endosomal recycling compartment (ERC). For example, after internalisation, MHCI eventually enters the transferrin-positive endosomal compartments from where it can be recycled back to the cell surface (Donaldson and Williams, 2009). Aluminium fluoride (AlF) treatment redistributes ARF6 to the PM and stimulates the formation of actin-rich surface protrusions that prevents internalisation and recycling. ARF6 activation is required for recycling of MHCI from the endosomal membrane back to the PM which can be regulated by Rab11, Rab22, Rab35 and CDC42 (D'Souza-Schorey and Chavrier, 2006, Donaldson, 2003, Donaldson et al., 2009, Eyster et al., 2009), see Figure 1.11.
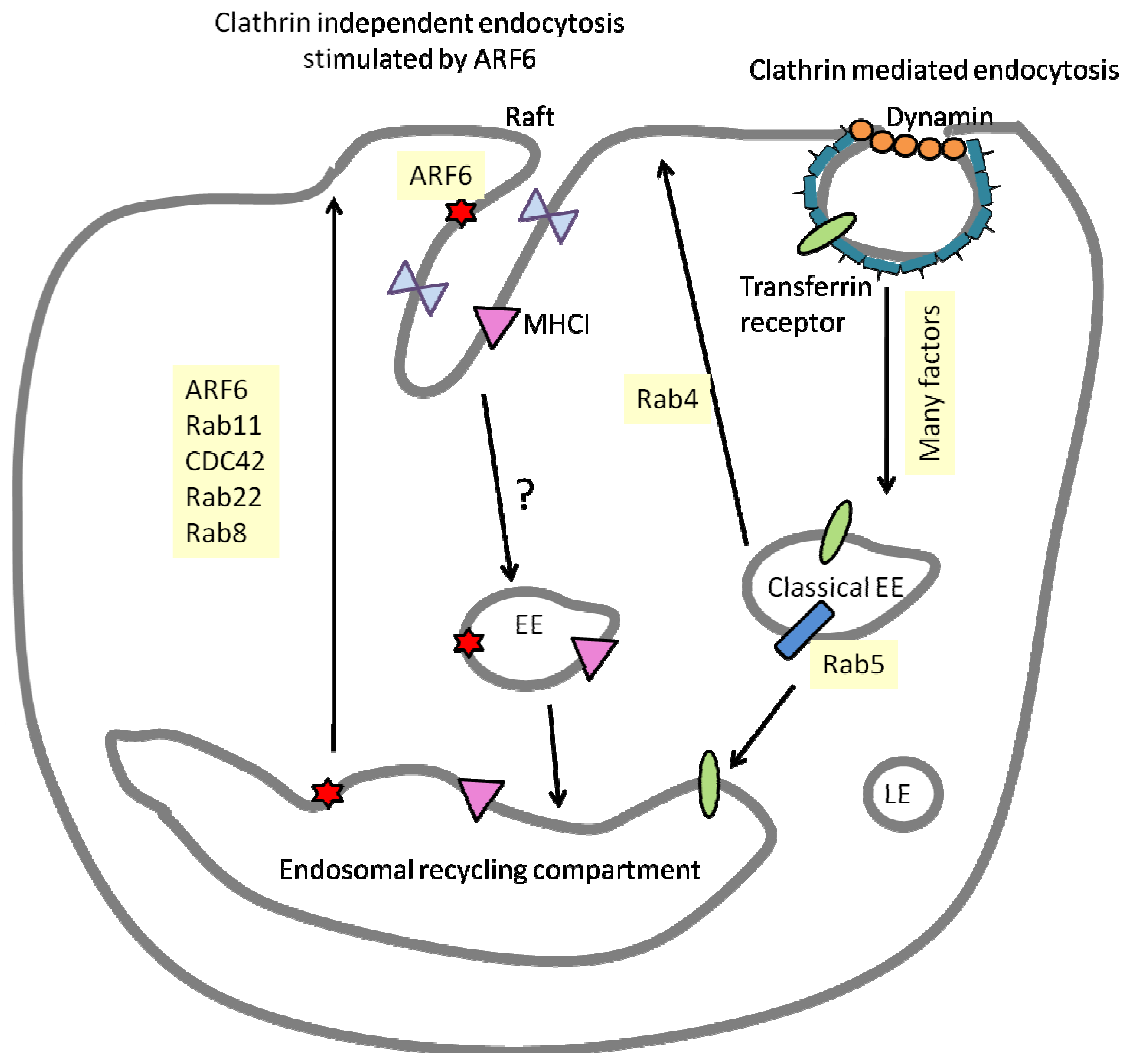
Figure 1.11 Schematic of ARF6-mediated trafficking. A schematic representation of clathrin-independent endocytosis (CIE) that requires membrane cholesterol and is mediated by ARF6 (red star) is shown using MHCl (pink triangle) as an example compared to dynamin (orange circles) and clathrin mediated endocytosis (CME) using the transferrin receptor (green oval) as an example. Cargoes internalised by membrane ruffling due to activation or Src, clathrin coated vesicles fusion with Rab5 (blue bar), EEA1-positive, "classical" early endosomes (EE) containing the CME cargo. From here, CIE cargo may go on to late endosomes (LE). CIE cargo destined for recycling reaches the endosomal recycling compartment (ERC) either directly or after fusion with EE and may be recycled back out to the plasma membrane.

1.8 Endosomal Recycling of Membrane Proteins

Proteins internalised from the cell surface are targeted to specific endosomal compartments from where they may be recycled back to the cell surface or undergo lysosomal degradation by means of vesicular transport. These endosomal recycling processes are regulated by the Rab-GTPases which have been implicated principally in the control of vesicle docking and fusion (Gonzalez and Scheller, 1999).

1.8.1 Rab proteins

Rab proteins are members of the Ras super family of GTPases and are key regulators of intracellular vesicular transport. They undergo a cycle of GTPase activity which allows a cycle of reversible attachment of the Rabs to endosomal membranes. Transport vesicles contain Rab-GTP which is hydrolysed to Rab-GDP when the vesicles fuse with membranes of endosomal compartments. Rab-GDP is then recycled back to their membranes of origin. After delivery to their respective membranes Rab-GDP is activated to Rab-GTP, which allows it to interact with a wide variety of effectors that help in vesicular transport by promoting docking of transport vesicles to their specific target membranes. At steady state most of the Rabs are membrane-associated, however about 10-50% can be detected in the cytosol (for a detailed review see (Schimmoller et al., 1998).

Several Rab proteins have been identified and in most cases they are specifically associated with a particular organelle or pathway. They are tightly regulated by accessory proteins through membrane association, nucleotide binding and hydrolysis. Table 1.2 lists different Rab proteins and their role in endosomal trafficking (for a detailed review see Somsel Rodman and Wandinger-Ness, 2000, Goody et al., 2005, Pfeffer and Aivazian, 2004).

Loss of Rab function due to mutations in the GTPases have been implicated as the cause of several disease conditions such as bleeding and pigmentation disorders (Griscelli syndrome), mental retardation, neuropathy, kidney disease (tuberous sclerosis) and blindness (choroideremia). Altered function of regulatory molecules of Rabs can cause cancers (prostate, liver, breast) as well as vascular, lung, and thyroid diseases (for detailed review see Stein et al., 2003).

Table 1.2 Rab proteins and functions mediated by them in endocytic trafficking.

Rab protein	Function mediated by Rab
Rab4	Regulation of sorting and recycling, localised on EE and RE
Rab5	Formation of CCV for internalisation of cargo proteins from PM and facilitating fusion of the CCV with EE or EE with EE
Rab6	Budding and trafficking of vesicles arising from the TGN to recycle cargo such as Shiga toxin to cell surface.
Rab7	Transport from EE to LE and fusion of compartments from LE for fusion with lysosomes for degradation
Rab9	Transport of cargo from LE to TGN
Rab10	Basolateral trafficking
Rab11	Regulation of recycling from the perinuclear ERC, and transport from TGN to PM
Rab14	Internalisation, lysosomal fusion and phagocytosis
Rab20	Internalisation and recycling in epithelial cells
Rab22	Localised to EE and LE, also implicated in recycling from LE
Rab32	Localised to lysosomes related organelles
Rab34	Formation of macropinosomes and lysosomal distribution
Rab35	Slow endocytic recycling through recycling endosomes
Rab38	Localised to lysosomes related organelles
Rab39	Internalisation

EE, early endosomes; LE, late endosomes; ERC, endosomal recycling compartments; CCV, clathrin coated vesicles; (Barr and Lambright, 2010, Stein et al., 2003, Valente et al., 2010)

1.8.2 Rabs and post endocytic trafficking of membrane proteins

Endosomal trafficking of CME cargo

During internalisation, Rab5 facilitates segregation of cargo (for example, the human transferrin receptor) into clathrin coated vesicles (CCV) and together with a number of effector molecules, promotes fusion with early endosomes (EE). Hence Rab5 positive early endosomal compartments are the first destination of post endocytic cargoes of CME (Zerial and McBride, 2001). Generally, proteins from the EE are subsequently sorted for recycling back to the plasma membrane or transported to lysosomes for degradation. EE micro-domains containing Rab4 molecules promote rapid recycling of the proteins back to the cell surface. Rab15 inhibits recycling from early endosomes (Zuk and Elferink, 2000, Zuk and Elferink, 1999). Membrane proteins that do not recycle back from the EE are transported to late endosomes (LE) and recycling endosomes (RE) from where they undergo recycling back to the plasma membrane in a Rab11 and Rme1 dependent manner (Schlierf et al., 2000). Proteins destined for degradation are diverted to lysosomes in a Rab7 dependent transport. Some proteins such as the mannose 6-phosphate receptor (M6PR) are transported to the TGN from LE with the help of Rab9. Apart from the Rabs described here, other cell specific Rabs are also known; for example, Rab25 is involved in the apical recycling of proteins from the LE to TGN (see Figure 1.12).

Endosomal trafficking of CIE cargo

Proteins internalised through the CIE have been shown to enter compartments separate from the EE. These vesicles may bypass entry into EE and fuse with endosomes containing CME cargo and are diverted to distinct tubular endosomes that recycle the proteins back to the PM or get diverted to LE and subsequently to lysosomes for degradation. Some examples of CIE cargo include the MHCl protein, GPI-AP, the cation channel protein mucolipin-2 and E-cadherin. Recycling can be mediated by Rab11, Rab22, Rab35, extracellular signal regulated kinase Erk, CDC42 and Par3 (for a detailed review see Eyster et al., 2009).

ARF6 is one of the key regulators of dynamin and clathrin-independent endocytosis. After internalisation ARF6-GTP and cargo containing endosomal compartments bind phosphatidylinositol 3-phosphate (PI3P) which allows fusion with Rab5 associated early endosomes containing clathrin cargo. Thus endosomal vesicles derived from

clathrin-dependent and independent endocytic events eventually converge in a common recycling compartment (Naslavsky et al., 2003). For example, after internalisation, ARF6 endocytic cargo MHCI eventually enters transferrin positive endosomal compartments from where it enters the tubular recycling compartments (ERC) from where they can be recycled back to the cell surface (Donaldson and Williams, 2009). Expression of a constitutively active form of ARF6, ARF6-Q67L, stimulates CIE and causes accumulation of internalised cargo in enlarged vacuolar-type structures that are coated with actin and PIP2 which prevents further traffic to Rab5 endosomes and recycling. ARF6 cargoes such as CD55, Glut1 and CD59 are transported to the ERC by bypassing entry into EE and recycled back to the cell surface in a Rab22 dependent manner. The 'GDP on' mutant of ARF6 (T27N), has been shown to localise mainly to the ERC, and can block recycling of proteins back to the cell surface. Proteins such as the GPI-AP and the fluid phase markers are internalised by an ARF6-independent mechanism into GEECs which subsequently acquire Rab5 and EEA1 following which they either fuse with other GEECs or with endosomes carrying the CME cargo in a Rab5 dependent manner (Kalia et al., 2006), see Figure 1.13.

Caveolae containing dynamin-dependent cargoes and CIE cargoes are internalised to endocytic caveolar carriers or caveosomes, both of which can fuse back to the cell membrane allowing recycling of the proteins. SV40 virus is transported to the LE from the caveosomes in a Rab5 dependent manner from where they can traffic to the TGN (Parton and Simons, 2007).
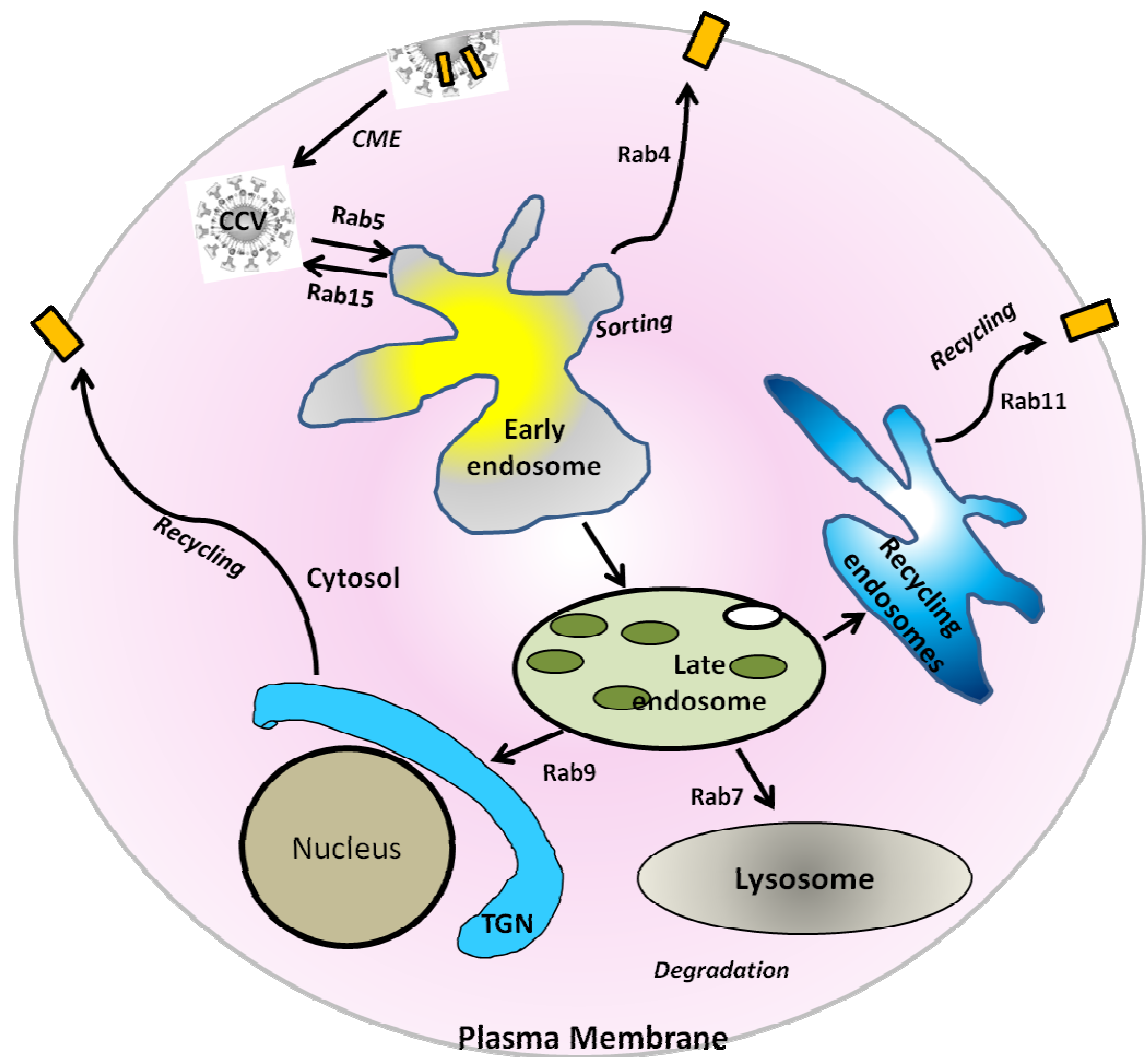
Figure 1.12 Schematic of endosomal trafficking of membrane proteins internalised by CME. Different routes of post endocytic trafficking and recycling of membrane proteins are shown along with the different Rab proteins that help in the process.
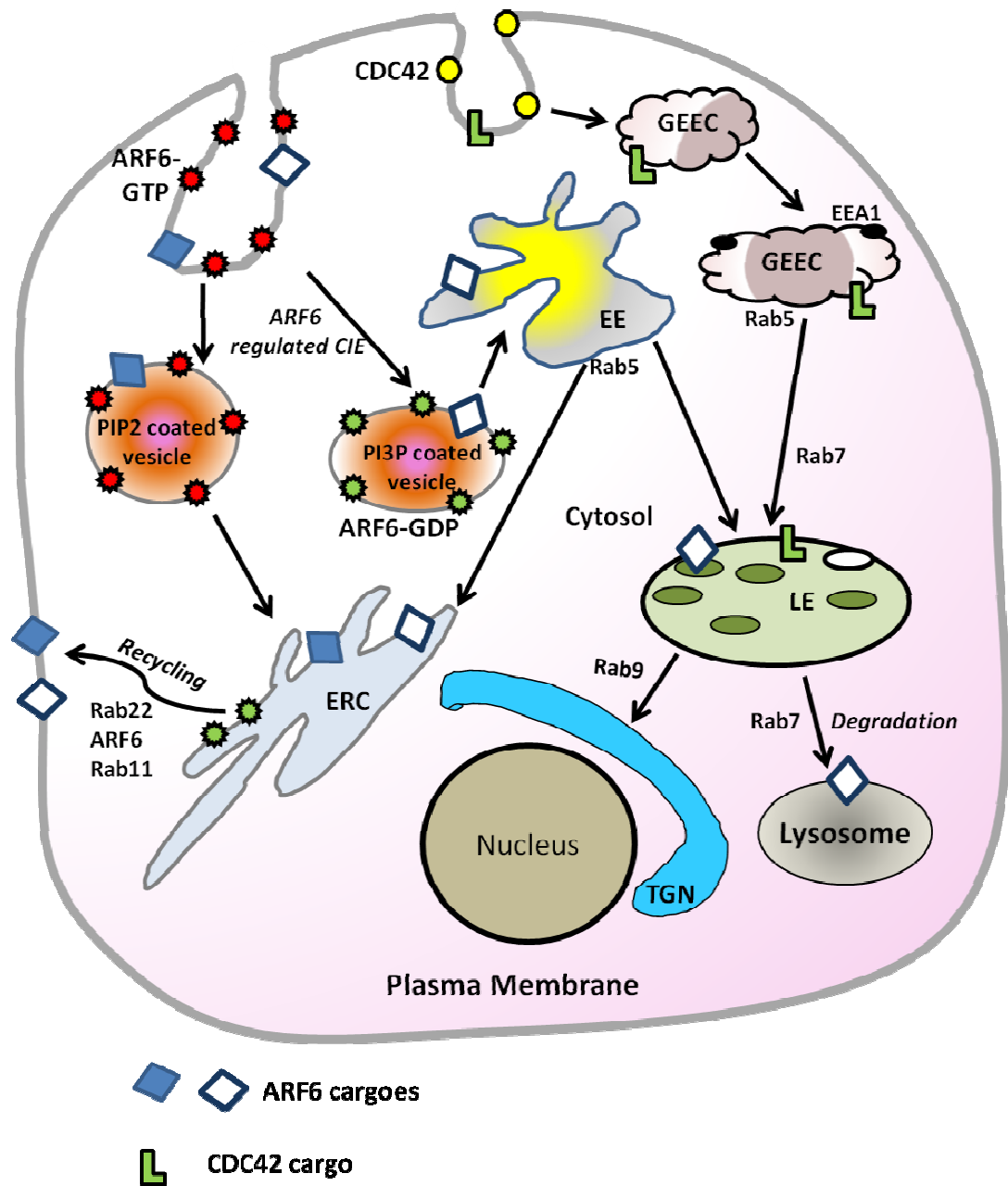
Figure 1.13 Schematic of endosomal trafficking of membrane proteins internalised via dynamin and clathrin independent endocytic mechanisms. Different routes of post endocytic trafficking and recycling of membrane proteins are shown along with the different Rab proteins that help in the process. (EE, early endosomes; LE, late endosomes; ERC, endosomal recycling compartments; TGN, trans-Golgi network; GEEC, GPI-AP-enriched early endosomal compartments; PIP2, phosphatidylinositol 4,5-biphosphate; PI3P, phosphatidylinositol 3-phosphate)

1.9 Aims of the Study

The aim of this study was to investigate the trafficking mechanisms of the pancreatic K_{ATP} and the cardiac hERG ion channels and compare the underlying mechanisms. Although the endosomal trafficking of K_{ATP} channels is better understood, not much is known about the trafficking of hERG channels.

In Chapter 3, the mechanistic details of ER export of the K_{ATP} channels will be investigated using cell biological approaches. A mutation, E282K, in the C- terminus of the Kir6.2 subunit of the K_{ATP} channel has been reported to cause congenital hyperinsulinism (CHI) and previous studies from the group suggested that this mutation causes abrogation of the diacidic ER exit motif on Kir6.2. In this chapter, it will be investigated if E^{282} on the Kir6.2 is a part of the canonical DXE motif required for assembly of the channels into COPII vesicles. Using epitope-tagged constructs for the wild type and the E282K mutant subunits, the molecular basis of the disease phenotype will be examined.

In Chapter 4, it will be investigated if hERG channels are also exported out of the ER in COPII vesicles like K_{ATP} channels. In addition, using C-terminal truncations, the location of the ER exit motifs in hERG will be investigated.

In Chapter 5, the endocytic trafficking mechanism of hERG channels will be investigated using functional, biochemical, pharmacological and cell biological approaches. The mechanism of hERG internalisation will be compared to the clathrin mediated endocytosis of K_{ATP} channels. The mode of hERG internalisation, if understood could help in gaining an insight into how this process may be regulated in health and disease.

In Chapter 6, the endocytic recycling process will be investigated. It will be determined whether internalised hERG channels also recycle back to the cell surface. Factors that may be involved in the regulation of endocytic trafficking of the channels will be investigated using functional, pharmacological and cell biological approaches.

CHAPTER 2

General materials and methods

2.1 Materials

2.1.1 Cell lines

The mammalian human embryonic kidney (HEK293) cells were purchased from the European Collection of Cell Cultures (ECACC, Cambridge, UK). The HEK293-MSRII (HEK-MSRII) cell line, a derivative of the HEK293 cell line with improved adhesion properties was a kind gift from Dr. SP Yusaf, Glaxo-Smith Kline (GSK), Stevenage, UK. HeLa cells were a gift from Dr. Vas Poonambalam, University of Leeds.

2.1.2 Tissues

Neonatal rat hearts were obtained from sacrificed 3-7 day old Wistar rat pups provided by members of Dr. Gamper's lab. Guinea pigs were obtained from the University of Leeds animal house and handled, sacrificed and dissected to obtain hearts by Dr. Matthew Hardy, University of Leeds, following the UK Home Office guidelines. All experimental protocols requiring the use of animals conformed to the Animals Scientific Procedures Act, 1986.

2.1.3 General materials

Sterile plastic-ware for tissue culture was purchased from Sarsted. All solutions for other experimental procedures were prepared using sterile deionised Milli-Q water (18 MΩ, Milli-Pore). Sterile tubes and tips and solutions were used for construction of mutant constructs and general amplification of plasmid DNA. Solution stocks were sterilised by autoclaving. Heat labile solutions were filter-sterilized using 0.2 µm Acrodisc PF filters (Gelman Science).

2.1.4 Tissue culture media

Basal media for tissue culture, DMEM/F-12 with GlutaMax™ was purchased from Invitrogen (Cat: 31331). Medium supplement fetal bovine serum (Cat# F524) and antibiotics penicillin-streptomycin were purchased from Sigma chem. co., G-418 disulphate (Cat# G0175) and Blasticidin (Cat# R210-01) were purchased from Melford.

2.1.5 Growth media

Bacto-tryptone and yeast extract were purchased from Amersham and Difco laboratories. Bacterial agar was purchased from Oxoid, ampicillin sodium salt (Cat# A0104) was purchased from Melford.

2.1.6 DNA cloning – reagents for DNA modification

Restriction endonucleases were purchased from New England Biolabs (NEB). *PfuTurbo*® DNA polymerase was purchased from Stratagene. Electrophoresis grade agarose was purchased from Life Technologies.

2.1.7 Oligonucleotides or DNA cloning

Oligonucleotide primers were designed for site-directed mutagenesis, PCR or DNA sequencing and were from Invitrogen Life Technologies. Primers were reconstituted in sterile deionised water to the concentration of 1 nmol/µl for long-term storage at -20ºC.

2.1.8 Bacterial strains

For general amplification of plasmids competent *E.coli* DH5α cells were prepared. The cells were grown in LB media and incubated in a 37ºC orbital shaking-incubator at 200-250 rpm.

2.1.9 Chemicals and solutions

Laboratory reagents and chemicals were purchased from Sigma, BDH and the Anachem Chemicals Company unless otherwise stated. Isopropanol and ethanol were purchased from BDH.

2.1.10 Plasmid vectors

Most of the constructs used in the study are in mammalian expression vectors pcDNA3 (+), pcDNA6/HIS™A or pEGFP from Invitrogen / Life Technologies. The constructs for expression of the K_{ATP} and hERG channels used in this study are as follows: the HA-tagged Kir6.2 is in pcDNA3 and the myc- and HIS6-tagged SUR1 are in pcDNA6/HIS™A (Figure 2.1 & Figure 2.2), (Mankouri et al., 2006). hERG cDNA (accession number Q12809) was a kind gift from Prof. SA Goldstein (University of

Chicago) and was cloned into pcDNA3 along with the insertion of an HA-tag to generate HA-hERG-pcDNA3 plasmid (Figure 2.3) by Dr. Elliott, a member of the Rao lab. All other plasmid constructs are described in the relevant chapters.

2.1.11 DNA transfection

Transient transfection of cells with plasmids for expression of the required proteins was carried out using Fugene® 6 transfection reagent (Roche) and Optimem® for dilution of reagents (Invitrogen).

2.1.12 Antibodies

Primary antibodies: Anti-HA (YPYDVPDYA) high affinity rat monoclonal antibodies (clone 3F10) were obtained from Roche. Anti-Kv11.1 (hERG) antibodies against extracellular epitope (AFLLKETEEGPPATEC) on hERG channels, raised in rabbit, were purchased from Sigma, mouse monoclonal antibodies against the Myc-tag epitope (EQKLISEEDL) of human c-Myc residues 410-419, clone 9B11 were from Cell Signalling Technology.

Secondary antibodies: Anti-rat, rabbit and mouse fluorescein isothiocyanate (FITC) - conjugated and anti-cyanine-3 (Cy3) - conjugated antibodies were purchased from Jackson Immuno Research Laboratories. Anti-rat and mouse Alexa-488 and Alexa-633 conjugated secondary antibodies were purchased from Invitrogen.

Other antibodies used in the study are described in the relevant chapters.

2.1.13 Materials and reagents for western blotting

All chemicals for polyacrylamide gel electrophoresis (PAGE) were obtained from Sigma. Nitrocellulose membranes (Cat# 162-0115); blotting paper (Cat# 170-3960) and apparatus for gel electrophoresis and western blot transfer (Trans-blot) were purchased from BIORAD. Pre-stained protein ladders were purchased from Fermentas (Cat# SM1811, SM0671).
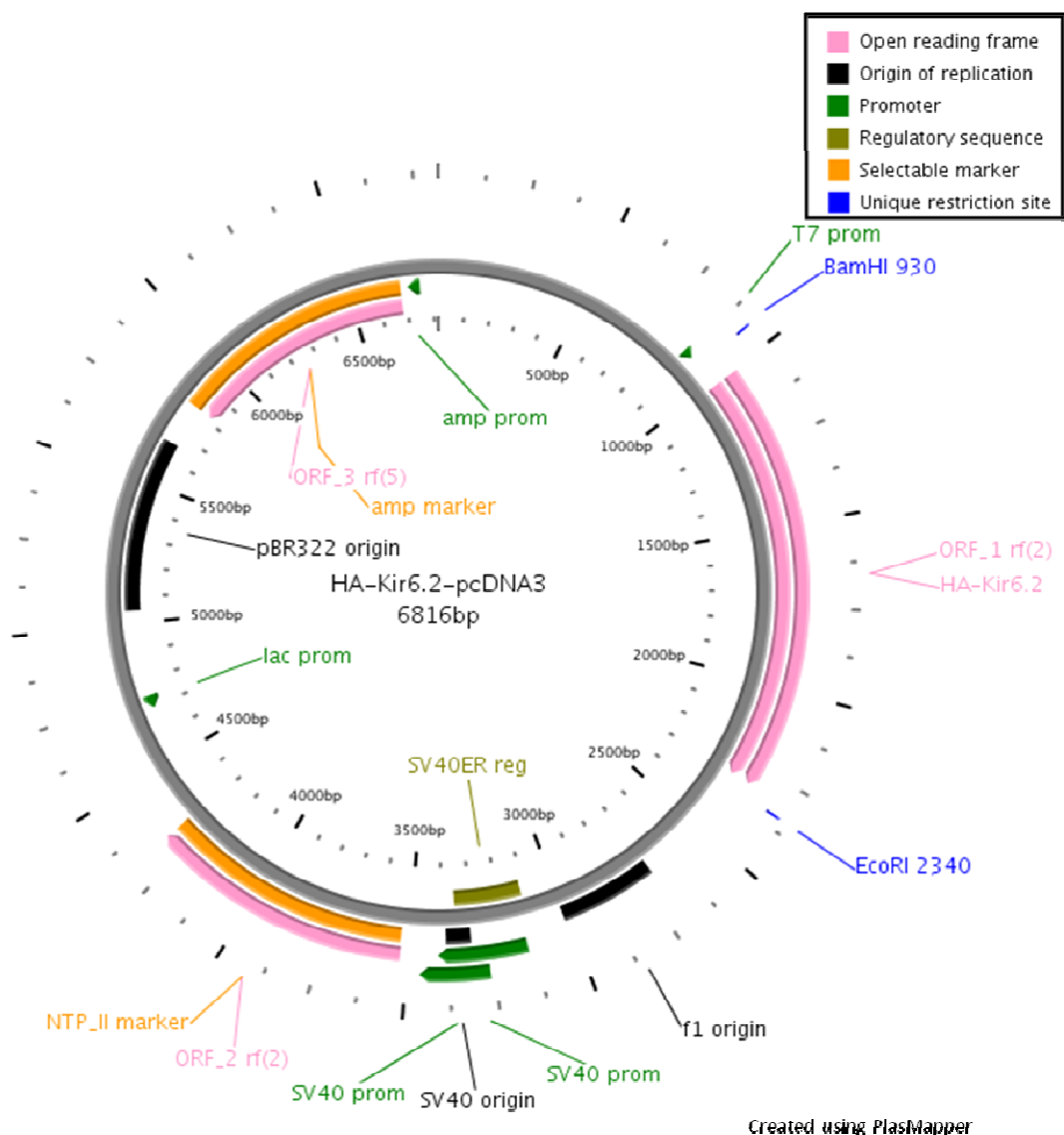
Figure 2.1 Map of the HA-Kir6.2 construct. A haemagglutinin A (HA)- epitope (YPYDVPDYA) and an additional 11 amino-acid linker (IYAYMEKGITD) were introduced into an extracellular loop of mouse Kir6.2 (accession number D50581) by PCR (Zerangue et al,1999) to produce this construct cloned in the mammalian expression vector pcDNA3, with ampicillin as the resistance marker in bacteria and geneticin as selection marker in mammalian cells. Plasmid map prepared using PlasMapper (Dong et al., 2004).
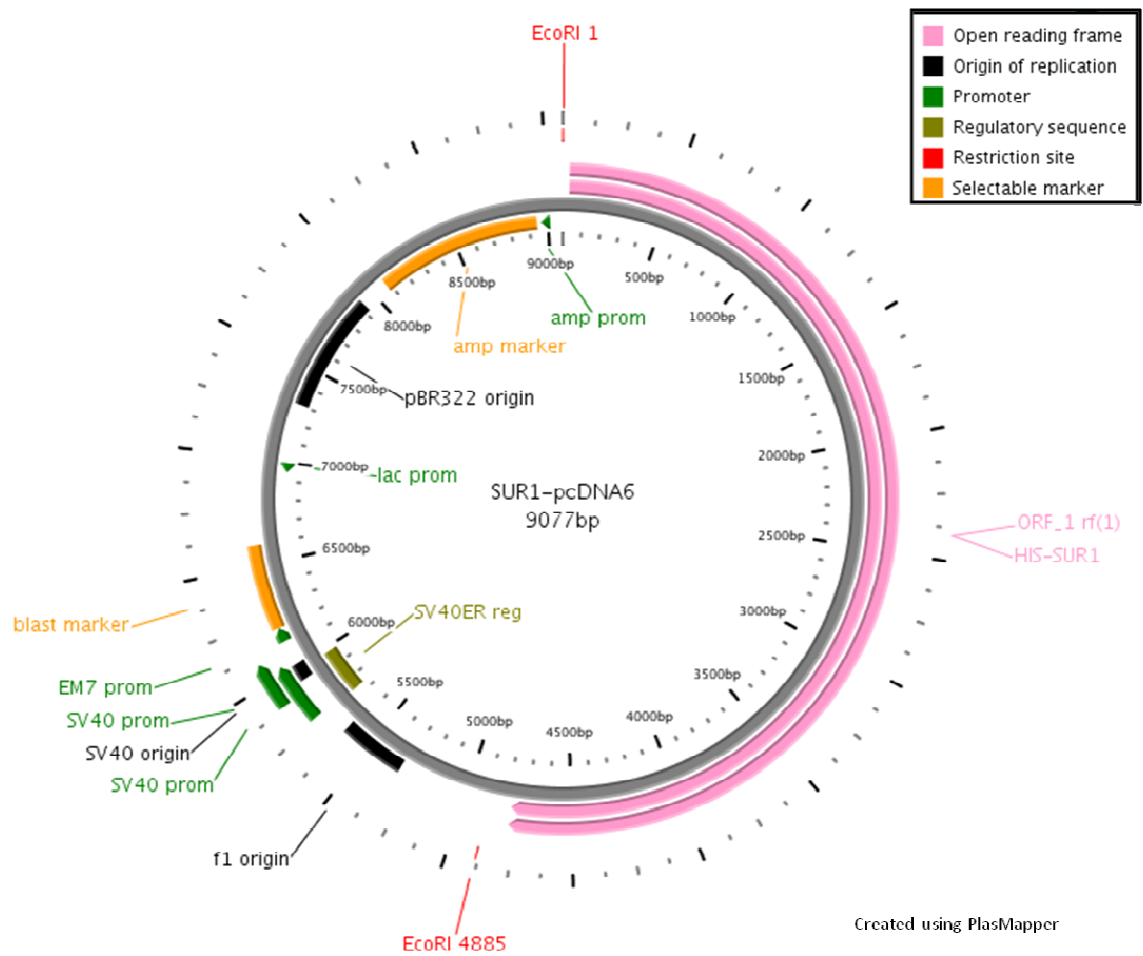
Figure 2.2 Map of the SUR1 construct. The hamster HIS6-SUR1 construct was prepared by cloning hamster SUR1 (accession number L40624) in pcDNA6 (Partridge et al, 2001). HIS6-SUR1-myc construct was prepared by inserting two copies of c-myc epitope into the first extracellular loop of SUR1 after the first nucleotide-binding fold (Sharma et al, 1999); the resultant construct was cloned into the pcDNA6 vector. The constructs have ampicillin as resistance marker in bacteria and geneticin as selection marker in mammalian cells. Plasmid map prepared using PlasMapper (Dong et al., 2004).
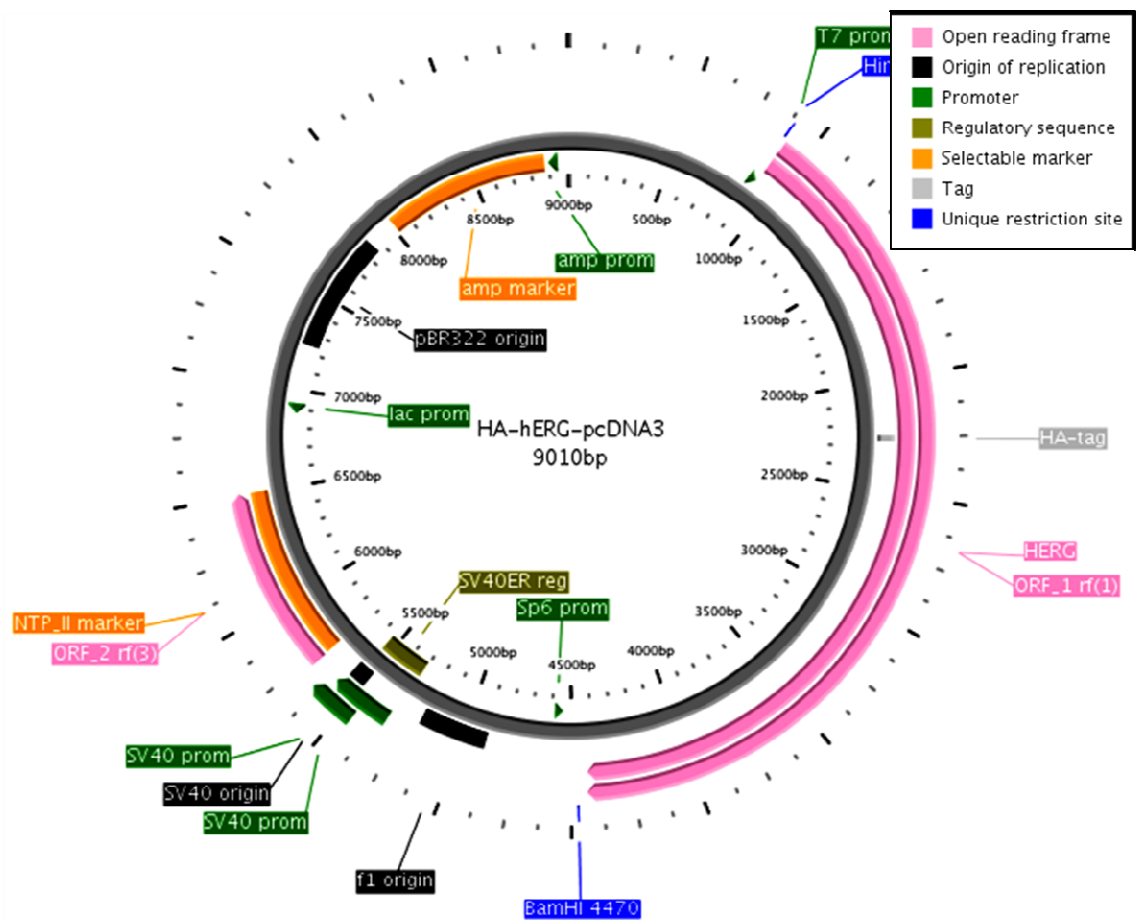
Figure 2.3 Map of the HA-hERG construct. hERG cDNA (accession number Q12809) was a kind gift from Prof. S Goldstein (Department of University of Chicago, Chicago). A HA (hemagglutinin A) epitope and an additional 8-amino acid linker was introduced into an extracellular loop of hERG by polymerase chain reactions (PCR) as described by (Ficker et al., 2003). The resultant construct, hERG-HA was sub-cloned into pcDNA3 for expression in mammalian cell lines. The constructs has ampicillin as resistance marker in bacteria and geneticin as selection marker in mammalian cells. Plasmid map prepared using PlasMapper (Dong et al., 2004).

2.2 General Solutions

2.2.1 Mammalian cell culture medium

HEK-MSRII, HeLa and K_{ATP} stable cells were cultured in DMEM/F12 containing L-glutamine, supplemented with 10% fetal bovine serum (Sigma) and 1X penicillin-streptomycin (Sigma). HEK-MSRII were maintained in 400 µg/ml G-418 and K_{ATP} stable cells were maintained in 500 µg/ml G-418 and 10 µg/ml blasticidin.

2.2.2 Bacterial culture medium

LB Medium (1L)	Autoclaved and cooled before use.
Tryptone	16.0 g
Yeast Extract	10.0 g
NaCl	5.0 g
pH7.2	Adjusted
Water	Made up volume to 1L with water.
Relevant antibiotic as selection marker for plasmid being amplified were added. For preparation of LB Agar plates, LB medium was mixed with 2g of agar and autoclaved. The medium was cooled to ~40°C and mixed with appropriate antibiotic as required before pouring into sterile Petri-dishes and allowed to set. LB Agar plates were stored at 2-8°C.	

SOB Medium (1L)	
Tryptone	20.0 g
Yeast Extract	5.0 g
NaCl	0.5 g
250 mM KCl	10.0 ml
pH 7.0	Adjusted
Water	Made up volume to 1L with water.
Autoclaved and 5 ml sterile 2M $MgCl_2$ was added immediately before use.	

2.2.3 Antibiotic stock solutions

All antibiotic solutions were prepared as concentrated stocks in water and diluted prior to use. Blasticidin was prepared in DMSO. Stock solutions were filter sterilised and stored as aliquots at -20°C.

Antibiotic	Stock concentration	Working concentration
Ampicillin	50 mg/ml	50 µg/ml
Kanamycin	35 mg/ml	50 µg/ml
G-418	50 mg/ml	500 µg/ml
Blasticidin	10 mg/ml	10 µg/ml

2.2.4 Solutions for preparation of competent cells

0.5 M PIPES (100 ml)	Filter sterilised, stored at -20°C
Piperazine-1,2-bis(2-ethane-sulfonic acid)	15.1 g
Water	~ 60 ml
Adjusted pH 6.7 and final volume made up to 100 ml with water.	

Inoue transformation buffer (1 L)	Filter sterilised, stored at -20°C
$MnCl_2. 4H_2O$	10.88 g
$CaCl_2. 2H_2O$	2.20 g
KCl	18.65 g
0.5M PIPES, pH 6.7	20 ml
Final volume made up to 100 ml with water.	

2.2.5 Solutions for DNA preparation

Plasmid DNA amplified in *E.coli* cells was isolated using the alkaline lysis method and purified by phenol-chloroform extraction as described by Sambrook & Russell (2001). Solutions for DNA isolation were prepared as follows:

Solution I (100 ml)	Stored at 2–8°C, stable for 6 months.
Glucose	1.8 g
1M Tris (pH 8.0)	2.5 ml
0.5 M EDTA	2.0 ml
Water	Made up to 99 ml
RNAse A (10 mg/ml)	1.0 ml

Solution II (100 ml)	Prepared fresh before use.
10 M NaOH	2.0 ml
10% SDS	10.0 ml
Water	88.0 ml

Solution III (100 ml)	3M Potassium acetate, pH 5.2. Stored at 2–8°C, stable for 6 months.
Potassium acetate	29.4 g
Acetic acid	11.6 ml, more added if required to adjust to pH 5.2
Water	Made up volume to 100 ml

PEG Solution (25 ml)	Stored at RT, stable for 6 months.
Polyethylene glycol 8000	5.0 g
Water	Dissolved in about 15 ml water, made up volume to 25 ml

TE Buffer, pH 8.0	10 mM Tris-Cl, pH 8.0, 1 mM EDTA. Sterile filtered.

Phenol: Chloroform: Isoamyl alcohol	Stored at 2-8°C
Phenol	25 ml
Chloroform	24 ml
Isoamyl alcohol	1 ml
Phenol phase equilibrated with 10 mM Tris, pH 8.0, 1 mM EDTA.	

Chloroform: Isoamyl alcohol	Stored at RT
Chloroform	24 ml
Isoamyl alcohol	1 ml

2.2.6 Electrophoresis solutions

DNA electrophoresis

Agarose gel running buffer (1L)	Tris-acetate-EDTA (TAE) buffer, 50X. Diluted to 1:50 in sterile water prior to use.
Tris base	242.0 g
Glacial acetic acid	57.1 g
0.5 M EDTA (pH 8.0)	100.0 ml
Distilled water	Made up volume to 1L

Protein electrophoresis

Polyacrylamide Gel running buffer (1L)	Tris-glycine-SDS buffer, 10X. Diluted to 1:10 to get working solution.
Tris base	30.3 g
Glycine	144.0 g
SDS	10.0 g
Water	Made up volume to 1L

2.2.7 Other commonly used buffers

10 X Phosphate buffered saline (PBS) (1L)	Autoclaved and stored at RT. For working solution stock was diluted 1:10 in water (used for western blotting).
KH_2PO_4	2.1 g
$Na_2HPO_4.7H_2O$	7.3 g
NaCl	9.0 g
Dissolved in ~800 ml water, adjusted to pH 7.2. Made up final volume to 1L with water. For washing of cells during immunostaining, tissue culture grade D-PBS was used.	

5X TNE buffer (250 ml)	Autoclaved and stored at RT. For working solution stock was diluted 1:5 in water.
NaCl	10.9 g
Tris base	7.6 g

0.5 M EDTA	5 ml
Dissolved in ~200 ml water, adjusted to pH 7.4. Made up final volume to 250 ml with water.	

2.2.8 Solutions for immunocytochemistry

Antibody dilution buffer (100 ml)	Stored at -20°C as 1 ml aliquots, thawed on ice before use.
Chicken egg albumin (Sigma)	1.0 g
DMEM/F12 Medium	100 ml
Adjusted to pH	7.2

2% Paraformaldehyde (PFA), 1L	Stored at -20°C. Thawed on ice before use.
Water	800 ml (warmed to about 60°C)
PFA (solid)	20.0 g, dissolved in hot water, cooled to RT
10XPBS	100 ml
Adjusted to pH 7.2 using 10 N NaOH.	

RIPA Buffer (100 ml)	For cell lysis. Solution was stored at -20°C as aliquots.
1M Tris-HCl, pH 7.4	1.0 ml
0.5M EDTA	40 µL
NaCl	0.9 g
Sodium deoxycholate	1.0 g
10% SDS	1.0 ml
Nonidet P40	1.0 ml
Water	Made up final volume to 100 ml
Protease inhibitor (Roche)	10 tablets, added before use

2.2.9 Primers for QuikChange® mutagenesis PCR

The following primers were designed to introduce mutation by QuikChange® PCR and synthesised by Invitrogen.

E282KFwd   5' CACCACCAGGACCTGAAGATCATTGTCATC 3'

E282KRev   5' GATGACAATGATCTTCAGGTCCTGGTGGTG 3'

2.2.10 Reagents for transfection

2.5 M CaCl$_2$ (10X), 10 ml	Stored in aliquots at -20°C
CaCl$_2$.2H$_2$O (Sigma, tissue culture grade)	3.7 g
Sterile water	to final volume 10 ml
Solution was filter sterilised.	

BBS (2X), 250 ml	BES- buffered solution, stored in aliquots at -20°C
BES Na$_2$ salt (Calbiochem)	2.94 g
NaCl	4.091 g
150 mM Na$_2$HPO$_4$, pH 6.95	2.5 ml
Sterile water	230 ml
pH adjusted to	6.97
Final volume made up to 250 ml with sterile water. Solution was filter sterilised.	

2.2.11 Reagents for PAGE and Western blotting

Resolving gel (8%)- 10 ml	APS and TEMED added just before casting
5% Glycerol	4.6 ml
30% Acrylamide: bis acrylamide, 30:1 (Sigma)	2.7 ml
1.5 M Tris-HCl, pH 8.8	2.5 ml
10% SDS	0.1 ml
10% Ammonium persulphate (APS)	0.1 ml
TEMED (Sigma)	4.0 µL

3.4 ml of the resolving gel was poured in between the gel plates (BIORAD). The top of the gel was gently layered with water saturated butanol and the gel was allowed to set for 30-60 min at RT. The butanol was poured out before pouring the stacking gel.

Stacking gel (5%) -10 ml	APS and TEMED added just before casting
5% Glycerol	6.8 ml
30% Acrylamide: bis acrylamide, 30:1 (Sigma)	1.7 ml
0.5 M Tris-HCl, pH 6.8	1.25 ml
10% SDS	0.1 ml
10% Ammonium persulphate	0.1 ml
TEMED (Sigma)	10.0 µL
The gel was poured to till the top and a well comb was inserted. The gel was allowed to set for 30-60 min at RT.	

10X SDS PAGE running buffer (1L)	Laemmli buffer diluted 1 in 10 before use.
Tris base	30.3 g
Glycine	144.0 g
SDS	10.0 g
Water	final volume to 1L

10X Transfer Buffer (1L)	Stored at 2-8 °C
Glycine	144.0 g
Tris base	30.3 g
Water	Final volume 1L
Working transfer buffer 1X was prepared by mixing 1 part 10X buffer, 2 parts methanol and 7 parts water.	

SDS Sample Buffer (100 ml)	For loading protein samples on SDS PAGE
1M Tris-HCl, pH6.8	6.0 ml
10% SDS	12.5 ml
50% Glycerol	20 ml
1M DTT	10 ml
1M EDTA	0.8 ml
Water	50.7 ml

2.3 General Molecular Biology Methods

2.3.1 Competent cell preparation

Untransformed *E. coli* DH5α cells were plated out on LB agar plates containing no antibiotics. A starting culture of 25 ml SOB medium was inoculated with one colony. After incubation for 6-8 hrs at 37°C, 3X 250 ml of SOB medium was inoculated with 10 ml, 4 ml or 2 ml of the starting culture. Each culture was incubated at 18°C until the optical density at 600 nm (OD$_{600}$) of the culture reached ~0.55 (requires about 12-16 hours). The culture flasks were transferred to an ice-cold water bath for 10 min and the cultures centrifuged for 10 min at 2500 x g at 4°C [5000 rpm in J-10 rotor]. The medium was carefully removed and the cell pellet gently suspended in 80 ml of ice-cold Inoue transformation buffer. The culture was centrifuged for 10 min at 2500 x g at 4°C. The supernatant was removed carefully and the cells were re-suspended in 20 ml ice-cold Inoue transformation buffer and 1.5 ml of dimethyl sulfoxide (DMSO) was slowly swirled into the cell suspension. The culture was incubated for 10 min in a chilled ice bath. The cell suspensions was dispensed into chilled, sterile micro-centrifuge tubes and snap frozen by immersion in liquid nitrogen or dry ice before storing at -70°C. Competent cells obtained by this method typically showed efficiencies up to 3 x 10^8 transformed colonies per μg of plasmid DNA.

2.3.2 Transformation of *E.coli* with plasmid DNA

For each transformation 100 μl of competent *E. coli* cells were thawed on ice, gently mixed with 25–50 ng of plasmid DNA to be amplified and incubated on ice for 30 minutes. The DNA-cells mixture was then transferred to a 42°C water bath for 40 seconds (heat shocked) and placed on ice for 1 minute following which 900 μl of LB medium was added to the cells and they were placed in a 37°C shaking incubator for 1 hour. The cells were then spun at 7K rpm and 800 μl of the supernatant discarded. The pellet was then re-suspended into the remaining media and plated onto pre-warmed LB-agar plates (containing appropriate selection antibiotics) with a sterile glass spreader. The inoculated plates were then placed in a 37°C incubator and grown overnight.

2.3.3 Preparation of plasmid DNA

The alkaline-lysis method was employed for isolating plasmid DNA from bacterial cells adapted from the protocols described in Sambrook and Russel (2001).

Mini-preparation of DNA

5 ml of 2YT or LB medium supplemented with appropriate selection antibiotic was inoculated with a single bacterial colony transformed with the plasmid DNA or the product of QuikChange® PCR and incubated overnight at 37°C in a shaking incubator at 200 rpm. 1.5 ml of the culture was centrifuged (bench-top microfuge, 4400 g, RT) for 1 minute and the supernatant discarded. This was repeated on more time and the cell pellet from 3 ml culture was then re-suspended in 200 µl of DNA prep Solution I by vortexing and the slurry was incubated at RT for 5 minutes. The cells were then lysed by addition of 400 µl of Solution II from the sides of the tube, gentle mixing by inversion and incubated at room temperature for no further than 5 minutes. 300 µl of Solution III was then added to the lysed cells and the after mixing vigorously the mixture incubated on ice for 10 minutes before spinning at 16000 g at room temperature for 15 minutes. The supernatant was transferred to a fresh tube and mixed with 750 µl isopropanol for 10 minutes at room temperature prior to spinning at 16000 g for ten minutes. The supernatant was then discarded, the pellet washed with 70% ethanol and after drying at 37°C, re-suspended in 30 µl TE Buffer, pH 8.0. 1 µl of the DNA was then analysed by agarose gel electrophoresis to determine quality and approximate yield of the preparation.

Large-scale preparation of DNA (Isolation and purification)

5 ml of 2YT or LB media supplemented with appropriate antibiotic was inoculated with a single bacterial colony from a plate transformed with the plasmid DNA amplified. This seed culture was grown for 16 hrs at 37°C in a shaking incubator. This seed culture was then added to 400 ml 2YT containing appropriate antibiotic and grown at 37˚C in a shaking incubator for a further 16-24 hrs. The cell suspension was centrifuged (Beckman JA10 rotor, 4400 g, 4˚C, 15 min). The supernatant was decanted and the cell pellet re-suspended in 10 ml of Solution I. The cells were then lysed by the addition of 20 ml of Solution II, and gently mixed for one minute prior to incubating on ice for a further 10 min. 10 ml of Solution III (4˚C) was then added and after vigorous shaking the preparation was incubated on ice for 5 minutes prior to spinning as above. The

supernatant was filtered through filter paper and precipitated by the addition of 50 ml of isopropanol. Following centrifugation, the supernatant was then decanted; the pellet dried, and re-suspended in 2 ml TE buffer; pH 8.0. In order to remove all the RNA in the preparation, 50 µl RNase A (10 mg/ ml stock) and incubated at 37°C for 30 min. The plasmid DNA was purified by organic solvent extraction, once with phenol-chloroform and twice with chloroform. The extraction step involved addition of equal volume of solvent to the DNA solution, vortexing and then centrifugation to separate the solvent phase from the DNA containing aqueous phase which was carefully collected and transferred to a new tube. After all steps of extraction, the DNA solution was precipitated by addition of 0.5 ml 20% PEG 8000 and 25 µl 1 M $MgCl_2$. The DNA was then spun at 16000 g for 15 minutes, the pellet washed twice with 70 % ethanol, air-dried, and dissolved in TE buffer; pH 8.0. The DNA concentration was estimated by agarose gel electrophoresis of the DNA preparation.

2.3.4 Agarose gel electrophoresis of DNA

Gel preparation

For 1 % agarose gels 100 ml of 1X TAE buffer was added to 1 g of electrophoresis grade agarose and heated until dissolved. The gel was allowed to cool to ~ 50°C and 7.5µl of 10 mg/ml ethidium bromide was added and mixed. The gel was then poured into a gel cast and allowed to set at room temperature.

Sample preparation and electrophoresis

The agarose gel was placed into the gel electrophoresis tank and immersed in TAE buffer. The DNA samples (1µl of 6X loading buffer and 5µl of the suitably diluted DNA) were loaded into individual wells and electrophoresed at 80 V for ~ 40 minutes. For size estimation of sample DNA, size marker DNA ladder (Fermentas) were run alongside. DNA were visualised on a UV trans-illuminator and the images captured using the Bio-Rad gel documentation system.

2.3.5 QuikChange® mutagenesis

Site-directed mutagenesis was performed using the QuikChange® (Stratagene) and with specifically designed primers which had the desired mutation in the centre of the

primer with ~10-15 bases on each side, (see Section 2.2.9 for primers used in this study). Primers were 25-40 bases in length and possessed a melting temperature of ~10°C above the standard extension temperature of 68°C. Melting temperatures were calculated using the formula: T_m = 81.5 + 0.41(%GC) – 675/N - % mismatch, where *N* is the primer length in base pairs, %GC is the overall guanine and cytosine content. QuikChange® PCR reaction mix was prepared as follows:

Ingredients per reaction	Volume
DNA template (Stock: 100 ng/µl)	1µl
Forward primer (Stock: 10 nmol/µl)	1µl
Reverse primer (Stock: 10 nmol/µl)	1µl
dNTP mix (Stock 2 mM)	5µl
10X *Pfu* reaction buffer	5µl
Pfu Turbo DNA polymerase (2.5 U/µl) (Fermentas)	1µl
DMSO	1µl
Water	35µl

Each reaction was overlaid with mineral oil (Fluka), placed in a DNA thermal cycler and subjected to the following temperature cycles:

95°C for 30 seconds

55°C for 1 minute

68°C for X minutes (X depended on the length of the template, with each 1000 base pairs of template requiring 2 minutes of extension time at 68°C)

Once the 16 cycles were completed, the DNA was extended for 7 minutes at 72°C. Once the PCR reaction was complete 1µl of DpnI restriction enzyme (20U) was added for 2 hours at 37°C to digest the parental super-coiled DNA. The PCR products were then transformed into competent DH5α cells. Plasmid mini-preps were prepared from the colonies obtained from the transformation and sent for sequencing to confirm success of the mutagenesis.

2.3.6 DNA sequencing

All DNA sequencing was performed by Gene service, UK. Sequencing was used to confirm the authenticity of constructs used in the study. The sequences of the primers used for DNA sequencing in this study are as follows:

Primer name	Primer sequence (5' - 3')
T7F	TAATACGACTCACTATAGGG
T7R	TAGTTATTGCTCAGCGGTGG
Kir6.2 C-terminus seq.	GTGCAGAATATCGTCGGGCTG
CMVF	CGCAAATGGGCGGTAGGCGTG

2.4 Mammalian Cell Culture and Manipulation

2.4.1 Growth and maintenance of cell lines

Culture of HEK-MSRII, HeLa and K_{ATP}-stable cells

Cells were grown in 25 cm^2 or 75 cm^2 culture flasks (Sarstedt) at 37˚C in a humidified atmosphere of 5 % CO_2 / 95 % air. When ~70-80 % confluent the cells were passaged as follows: the medium in the flask was removed and the cells were washed with D-PBS (Invitrogen), and detached from the surface of the flask by treatment with 1X Trypsin-EDTA solution [0.05 % (w/v), Invitrogen] for 3-5 min. For the more sticky HEK-MSRII cells, 5 X Trypsin-EDTA solution was used. The detached cells were then re-suspended in pre-warmed media and 1/5th part of the cell suspension was transferred to a new culture flask containing pre-warmed medium and antibiotics where necessary (concentrations as described in section 2.2.1). The cells were then returned to the incubator and allowed to attach and reach confluence for 3-4 days.

Long-term storage of cell lines and their revival

For long-term storage cells were frozen in liquid nitrogen (N_2). Cells were trypsinised, suspended in growth medium and centrifuged at 1000 rpm for 5 minutes to obtain cell pellet. The medium was then decanted and the pellet re-suspended in cell freezing medium (10% DMSO, 80% FBS). The cell suspension was transferred to freezing vials as 1 ml aliquots and stored at -80˚C for 48 hours in cryo-freeze container (Nunc) to allow gradual freezing of the cells. The frozen vials were transferred into a liquid nitrogen storage container for long-term storage. The frozen cells were revived by thawing the frozen vial of cells in a 37°C water bath and inoculating in a 25 cm^2 flask containing 10 ml warm medium. The flask was transferred to the incubator and after about 6-8 hours, the medium from the flask was discarded and new medium was added. The antibiotic selection marker was added as required to the revived cells after 24 hrs of incubation. The cells were used for transfection after one passage.

2.4.2 Transfection methods for HEK MSRII and HeLa cells

Transfection with anionic lipid transfection reagent

Mammalian cells were transfected with plasmid DNA (constructs in pcDNA3, pcDNA6 or pEGFP) using Fugene®6 transfection reagent (Roche diagnostics). Cells were plated at a density of about 30% onto 12 mm or 18 mm glass cover-slips placed in individual wells of a 12 well culture plate and incubated overnight to allow the cells to adhere. The medium was replaced with 2.0 ml of fresh pre-warmed growth media and incubated for 1 hour. The transfection mix was prepared as follows in a sterile micro-fuge tube (per well):

Optimem™	20 μl (warm)
Fugene®6	1 μl (2 μl for HeLa cells)
Mixed by gently flicking the tube and incubated for 5 min at RT	
Plasmid DNA	150-300 ng
Mixed by gently flicking the tube and incubated for 30-45 min at RT.	
The transfection mixture was then transferred to the cells on cover-slips.	

Calcium phosphate method

Calcium phosphate method (adapted from (Jordan and Wurm, 2004) was used for transfection of cells in 25 or 75 cm^2 flasks at a confluence of 50 - 60%. 2 hours prior to transfection the medium from the flask was replaced with new pre-warmed medium (10 ml for 25 cm^2 and 20 ml for 75 cm^2 flasks). The calcium phosphate transfection mixture was prepared as follows in a micro-fuge tube:

For 25 cm^2 flask:

Ingredient	Quantity
Plasmid DNA	20-30 μg
2M $CaCl_2$	50 μl
Sterile water	to a final volume 500 μl, mix well
2X BBS	500 μl, mix

The DNA-calcium phosphate mixture was incubated at RT for 20 min and slowly added drop wise to the flask of cells to be transfected with constant swirling to mix. The cells were incubated at 35°C for 24 hrs before the medium was removed and the cells washed thrice with warm D-PBS. New medium was added to the cells and cells were incubated for further 24 to 48 hrs before use.

2.5 General Immunostaining Methods

All reagents used were purchased as cell culture grade or were prepared and autoclaved as required.

2.5.1 Preparation of adherent cells for immunocytochemistry

For immunostaining experiments involving multiple treatments, the cover-slips were treated with poly-L-lysine for increased adherence of the cells.

Preparation of poly-L-lysine coated cover-slips

Borosilicate glass cover-slips were washed in distilled water and soaked in concentrated hydrochloric acid for 3-6 hours. The cover-slips were rinsed several times in distilled water to remove all traces of HCl. The washed cover-slips were dipped in 1% (w/v) high molecular weight poly-L-lysine solution (44000 to 100000, purchased from Sigma chem. co.), overnight at 4°C or 3 hrs at RT. The poly-L-lysine solution was then removed and stored at 4°C for re-use. The coated cover-slips were rinsed with sterile water 3-5 times and dipped in 70% ethanol.

2.5.2 Immunofluorescence staining

Cells were plated onto glass cover-slips in 12 well tissue culture plates and transfected as required ~40 hours prior to immunostaining. The growth medium was removed using a plastic Pasteur pipette and the cells were washed twice with chilled D-PBS. The D-PBS was removed and ~0.5 ml chilled 2% PFA solution was added to fix the cells for 6 min. The cells were washed thrice with D-PBS. For staining of the channels (or membrane proteins) expressed on cell surface at steady state, the cells were incubated with primary antibodies against extracellular epitope on the membrane proteins for 40 min at RT, followed by D-PBS and incubation with fluorophore conjugated secondary antibodies. For staining of total protein expressed in the cells, following fixing, the cells were permeabilised by treatment with methanol: acetone (1:1) solution (-20°C) for 6 min. Following washing with D-PBS, the cells were immunostained as above. For staining of cells on surface and internal separately, the membrane proteins expressed on the cell surface were first stained following which cells were permeabilised and the internal membrane proteins were stained. For

staining membrane proteins within the cells, the secondary antibody selected was with a different fluorophore to the one used for surface staining. The cells on cover-slips were washed, air dried, mounted on glass slides using Prolong Gold anti-fade reagent with DAPI (Invitrogen), and allowed to set for 24 hrs at RT, before imaging under a Zeiss 510-META laser scanning confocal microscope (LSCM).

2.5.3 Confocal microscopy

Confocal Laser Scanning Microscopy (CLSM) is an optical microscopy in which a focused laser beam is scanned laterally along the x and y axes of a specimen in a raster pattern. The emitted fluorescence (reflected light signal) is collected by the objective lens of the microscope and is focused through a small pinhole, which blocks any light, which originated from above or below the plane of focus. The light, which passes through the pinhole, is then collected by a photomultiplier tube and displayed as pixels on a computer monitor.

Immunofluorescence stained cells were viewed using a Zeiss 510-META laser scanning confocal microscope (LSCM) under an oil-immersed 63× objective lens (NA = 1.40). FITC (494 nm excitation: 519 nm emission) was excited using an argon laser fitted with 488 nm filters and Cy3 (550 nm excitation: 570 nm emission) was excited using a helium / neon laser fitted with 543 nm filters. Cy5 and Alexa 633 were excited using a He/Ne laser fitted with 633 nm filters. The settings of each image were adjusted so that the intensity of each pixel was within the range of sensitivity of the fluorescence detectors i.e. no pixel showed saturation of fluorescence. Images were processed for addition of Scale bars using LSM Image browser. Any adjustments for brightness or contrast on the images was done using LSM Image browser and applied equally on all the image panels without altering the basic information on the image.

2.5.4 Chemiluminescence experiments

Density of HA-K_{ATP} or HA-hERG channels on the cell surface was estimated by the chemiluminescence method as described previously (Mankouri et al., 2006). Transfected cells on cover-slips expressing the channels were fixed and channels on cell surface were labelled with rat anti-HA antibody followed by the HRP conjugated secondary antibody. The cells were washed several times in PBS and solubilised in

RIPA buffer containing Benzonase (5 units) and 1X Protease inhibitors (Roche) by incubation overnight at 4°C on a rocker. Duplicate aliquots (60 μL) of the lysates were transferred to white 96 well plates (Grenier) and 50 μL of Lumigen PS-Atto® substrate was added to each well for 30s and the luminescence was measured using PolarStar Optima (BMG Labteck, GmbH) at a 1 sec interval. Protein content in the lysates was measured on duplicate 60 μL aliquots using the bicinchoninic acid (BCA) assay (Smith et al., 1985). Luminescence values were normalised to the cell protein content. Data were obtained from three separate transfection experiments, each measured in duplicate.

Protein Estimation by BCA Assay

The Bicinchonic acid (BCA) assay was used to determine protein content in mammalian cell lysates. The BCA reagent was purchased from Pierce, Thermo Fisher Scientific. The cupric sulfate reagent was prepared by mixing 0.4 g of $CuSO_4.5H_2O$ in 10 ml distilled water. Working BCA reagent was prepared by mixing 10 ml of the BCA reagent with 100 μl of the cupric sulfate reagent. 60 μL of the lysates were mixed with 200 μL of the working BCA reagent and incubated at 37°C for 30 min. The absorbance of the samples was read at 562nm. For preparation of the protein standard curve, 1 mg/ml BSA standard protein solution (Sigma) was added to the lysis buffer to get 0.1-0.6 μg of protein in 60 μL volume. The absorbance values for the protein standards were plotted against concentration to get standard curve and equation for best fit plot was obtained using the Origin software.

2.5.5 Western Blotting

Lysates of cells or raft fractions were mixed with the SDS sample buffer and loaded on 8% SDS-PAGE gels along with a pre-stained protein molecular weight marker. The proteins were allowed to separate following electrophoresis in the SDS-PAGE running buffer (Figure 2.4.A). The separated proteins on the gel were transferred to a nitrocellulose membrane using Trans-blot apparatus and transfer buffer (Figure 2.4.B). Unbound sites on the membrane were blocked by incubation in 5% SM-PBST (5% skim milk powder, 0.5% Tween-20, PBS) for 2-3 hours and then the membranes were incubated with antibodies against the protein of interest overnight at 4°C followed by wash step using PBST (0.5% Tween-20 in PBS) to remove unbound antibodies. The membranes were then treated with appropriate HRP conjugated secondary antibodies. Working concentration of antibodies is detailed in relevant chapters. Following

incubation with Lumigen (substrate for HRP), blots were exposed to X-ray films (Kodak) and the films were subsequently developed. Positions of the protein bands relative to the molecular weight marker proteins were marked by carefully overlaying the developed X-ray films on the nitrocellulose membranes. For blots of raft fractions where more than one protein of interest were blotted, the membranes were stripped to remove the antibodies following developing for one protein using the western blot strip buffer (2% SDS, 100 mM β-mercaptoethanol, 50 mM Tris-HCl, pH 6.8). The membranes were blocked again 5% SM-PBST for 2-3 hours and blotting was repeated with the next set of antibodies as described above. Scans of relevant portions of the blots are shown.
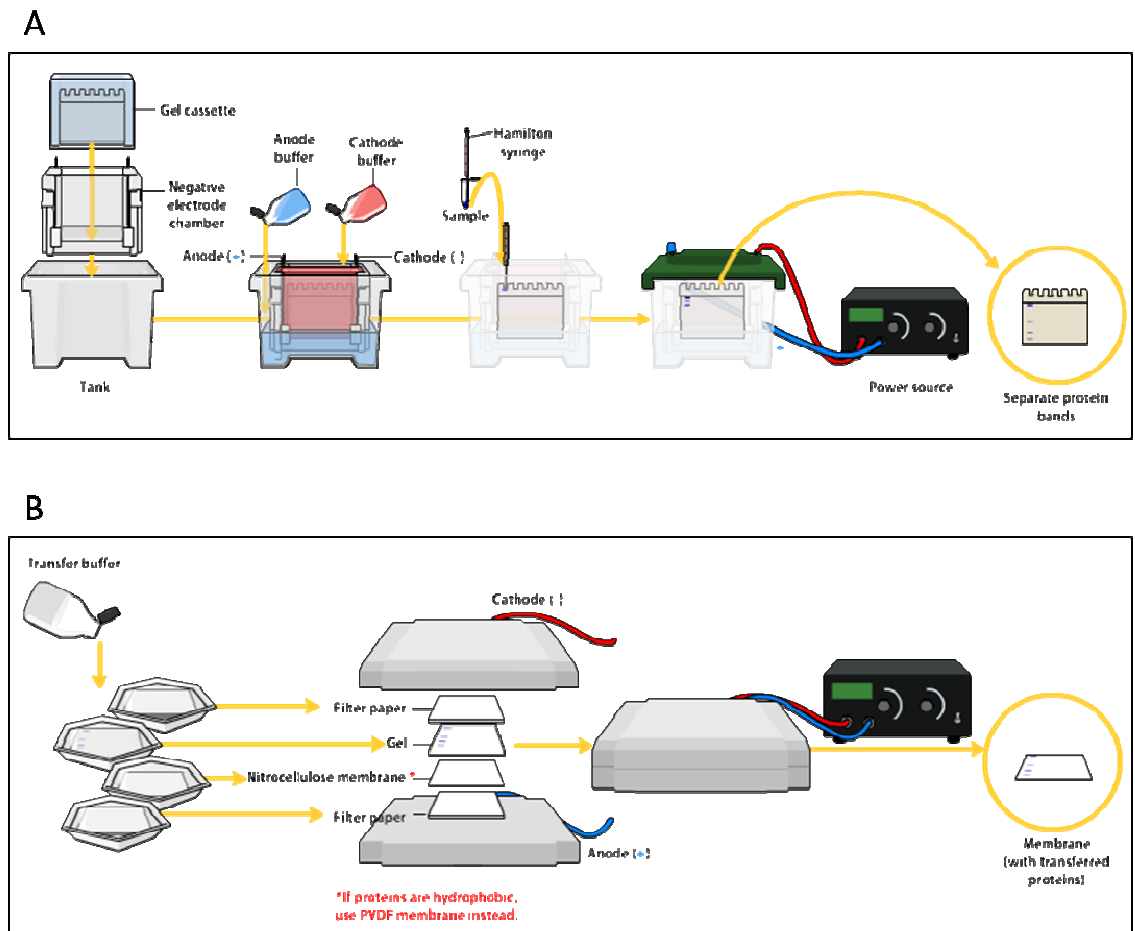
Figure 2.4 Schematic for Western blotting. (A) Steps in SDS-PAGE for separation of proteins. (B) Transfer of separated proteins to nitrocellulose membrane for probing with relevant antibodies. Images prepared by Bensaccount were taken from the public domain at Wikipedia.org.

2.6 Data and Statistical Analysis

For immunocytochemistry experiments, 'n' numbers refer to the number of separate occasions on which the experiment was performed. For chemiluminescence experiments each experiment was performed three or more times where each n number represents the duplicate from individual experiments. The statistical significance of data was determined by performing the Student's t-test or one way ANOVA test. Significance was deemed when the values were less than or equal to the 0.05 P value when compared to the experimental control.

2.7 Electrophysiology

HEK-MSRII cells were co-transfected with pcDNA3-HA-hERG and appropriate constructs (Chapter 4, 5 and 6). Borosilicate patch pipettes (2-3 MΩ resistance) were filled with a recording solution (in mM; 120 KCl, 5 $MgCl_2$, 5 K_2ATP, 5 EGTA, 10 HEPES, pH 7.2 with KOH); the bath solution contained, in mM, 137 NaCl, 4 KCl, 1.8 $CaCl_2$, 1 $MgCl_2$, 10 glucose, 10 HEPES, pH 7.4 with NaOH. Whole currents were recorded at room temperature using an EPC10 patch clamp amplifier under the control of Patch master software (HEKA Electronik). Cells were held at -80 mV and 5 s depolarising pulses from -60 to +60 mV followed by a 5 s step to -60 mV were applied every 20 s. Current-voltage relationships were determined by plotting initial amplitudes of the tail currents at -60 mV against the applied voltage. The data were analysed using the Origin 7.0 software. Recordings in Chapter 4 were done by Paul Manna and all the electrophysiology experiments in Chapter 5 and 6 were carried out by Andrew Smith.

CHAPTER 3

Sar1-GTPase dependent ER exit of pancreatic K_{ATP} channels revealed by a mutation causing congenital hyperinsulinism

3.1 Introduction

K_{ATP} channels regulate insulin secretion from the pancreatic β-cells in response to changes in blood glucose (Ashcroft, 2005, Minami et al., 2004) due to their characteristic property of being inhibited by ATP (Tucker et al., 1998) and activated by Mg-ADP (Shyng and Nichols, 1997). In healthy individuals, K_{ATP} channel function is regulated by the metabolic state of the cell (Miki et al., 1998, Nichols, 2006). Abnormal decrease in pancreatic K_{ATP} channel function has been implicated to be a cause of congenital hyperinsulinism (CHI), a disease characterized by unregulated insulin secretion and severe hypoglycemia (Aguilar-Bryan et al., 1998, Dunne et al., 2004, Ashcroft, 2005, Miki and Seino, 2005). The decrease in K_{ATP} channel activity is attributed to mutations in the genes encoding the K_{ATP} channel subunits. The molecular basis of the effect of these mutations could be classified as follows:

- Mutations causing a decrease in channel function by increasing the sensitivity of the K_{ATP} channel to intracellular [ATP]/[ADP] ratio leading to severe hyperinsulinism (Tucker et al., 1998, Ashcroft, 2005, Burke et al., 2008, Dunne et al., 2004, Shyng et al., 1998).
- Mutations that alter the normal trafficking of the channel leading to reduced or lack of surface channel expression (Cartier et al., 2001, Partridge et al., 2001, Christesen et al., 2007).

The K_{ATP} channel subunits, the pore forming Kir6.2 and the sulphonylurea receptor (SUR1) have been shown to associate directly with each other (Lorenz et al., 1998). Moreover, assembly of the subunits is required for the expression of a functional channel on cell surface (Shyng and Nichols, 1997). Studies on trafficking of the K_{ATP} channel subunits reported that neither subunit were capable of exiting the ER when expressed alone due to the presence of dibasic ER retention/retrieval signal, RKR (arginine–lysine–arginine), present on both the subunits (Zerangue et al., 1999). It was proposed that assembly of the subunits into an octameric complex masks the ER retention signals enabling the channel to escape the ER. A recent study indicated that 14-3-3 proteins play a role in masking these ER retention signals (Heusser et al., 2006). However, the details of the ER exit pathway for the channel were not well understood.

Since the K_{ATP} channel is a key player in regulating glucose-stimulated insulin secretion (GSIS) (Ashcroft, 2005, Nichols, 2006), studies to look at the K_{ATP} channels expressed in individuals suffering from insulin disorders have been undertaken in a quest to

understand the molecular nature of the disease and thereby look for possible cures. One such study reported a heterozygous mutation G844A in *KCNJ11* gene, found in a Swedish baby suffering from a severe focal form of CHI (Christesen et al., 2007) . This mutation replaced glutamate (E) at position 282 with lysine (K) in the C-terminus of the K_{ATP} channel subunit Kir6.2 (hereafter referred to as Kir6.2^{E282K}). The patient was not responsive to therapy that employed the potassium channel activator drug, diazoxide (Arnoux et al., 2010, Christesen et al., 2007). The disease was focal in nature, wherein excessive insulin secretion was occurring only from certain clusters of the patient's pancreatic β-cells (Sempoux et al., 2004). The focal nature of the disease is illustrated in Figure 3.1. Every individual inherits a set of chromosomes each from both parents. The Swedish patient had inherited from his father the heterologous *G844A* mutation in the *KCNJ11* gene on chromosome 11. The patient's pancreatic β-cells had the maternal chromosome 11 which had incurred a mutation that resulted in deletion in the 11p15, an area containing the *KCNJ11*, *ABCC8* and imprinted tumour suppressor genes such as the *p^{57kip2}* gene. Such deletion mutations can occur during cell division in early or later stage of development and result in hemizygosity for the mutant allele and β-cell hyperplasia in case of the patient. The *p^{57kip2}* gene is an imprinted gene for a tumour suppressor protein which is functional only when expressed off the maternal chromosome, therefore the cells in the patient's pancreas with the truncated maternal chromosome 11 were tumorous and out-grew the population of cells without the mutation and expressed excessive insulin (Fournet and Junien, 2004, Fournet et al., 2001, Fournet et al., 2000, Verkarre et al., 1998). Scission of the tumorous hyperinsulinaemic region of the patient's pancreas resulted in the clinical cure of the patient (personal communication by Dr. Christesen).

The study of mutations is often rewarding as it can give unique insights into the understanding of the disease at a molecular level. Previous members of the lab, (J. Mankouri and T. Taneja) initiated experiments to gain an insight into the role of the E282K mutation in the Kir6.2 subunit of the K_{ATP} channel in the cause of CHI in the patient. Constructs to express SUR1, HA-Kir6.2^{wt} and HA-Kir6.2^{E282K} (Kir6.2 with E282K mutation) were created for expression in heterologous eukaryotic expression systems.
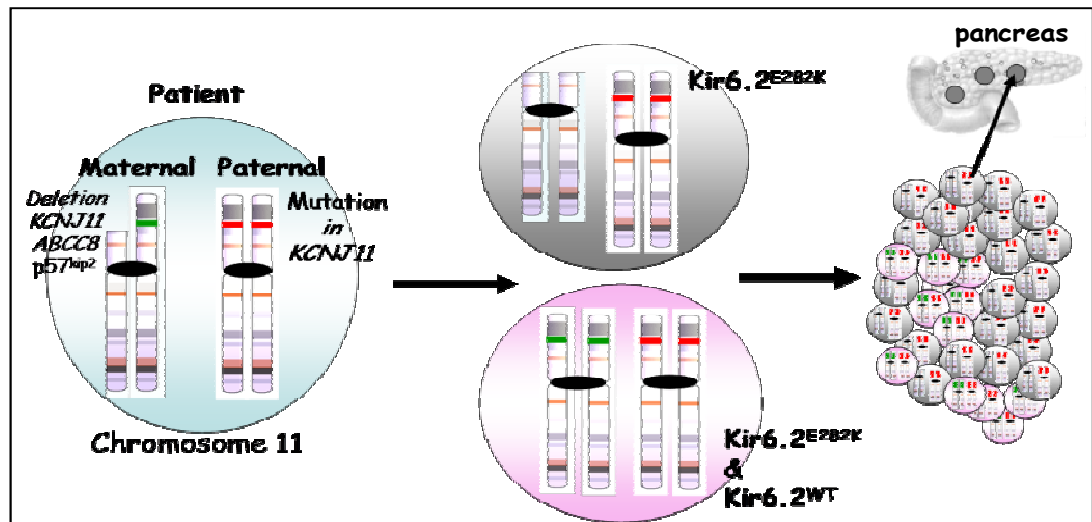
Figure 3.1 Focal nature of disease in patient with E282K mutation in Kir6.2 subunit. The blue cell represents the patient's embryonic cell with the mutated chromosome 11 pair inherited one each from both the parents, destined to form the pancreas. The grey and pink cells represent the tumorous and non tumorous pancreatic β-cells respectively in the patient's pancreas. These tumorous cells express only the E282K mutant channel subunits and out-grow the cells that express channels with heterogeneous wild type and mutant channel subunits. The grey cells clusters depict the focal regions in the patient's pancreas that secrete excessive insulin.

The extracellular hemagglutinin A (HA) epitope on an extracellular domain of Kir6.2 subunit allowed the detection of the channel on cell surface and within the cell (Hu et al., 2003, Mankouri et al., 2006 , see Chapter 2). The K_{ATP} channels were expressed in HEK-MSRII cells by co-transfection of SUR1 and HA-Kir6.2^{wt} constructs. Staining of the channels on HEK-MSRII cell showed that the channels made of wild type Kir6.2 subunits were expressed on cell surface, however the E282K mutant channels were absent from cell surface. The SUR1 subunit of K_{ATP} expressed on the cell surface is known to be glycosylated (Clement et al., 1997). Western blotting experiments described in (Taneja et al., 2009) showed that SUR1 co-expressed with HA-Kir6.2^{WT} but not with HA-Kir6.2^{E282K} matured. Further, anti-HA antibodies were able to co-immunoprecipitate SUR1 from the lysates of cells co-expressing SUR1 and either the HA-tagged wild type or mutant (E282K) Kir6.2, but not SUR1 alone (Taneja et al., 2009). Also when HEK-MSRII cells were co-transfected with HA-Kir6.2^{WT} or HA-Kir6.2^{E282K} constructs along with SUR1 and stained to look at intracellular fluorescence the mutant showed almost complete co-localisation with the ER resident protein, calreticulin (Thesis of J. Mankouri).

ER exit mechanisms of proteins are outlined in detail in the main introduction. Concentrated export of proteins from ER in COPII vesicles requires the small G protein Sar1 (Antonny et al., 2001, Sato and Nakano, 2007b), see Figure 1.9). The COPII cargo is recognised through specific motifs such as the diacidic motifs [(D/E) X (D/E)], di-hydrophobic motifs (FF, YY, LL or FY), YXXXNPF and LXXLE motifs which interact with proteins of the COPII machinery to facilitate their assembly into the COPII vesicle (Barlowe, 2003, Nishimura and Balch, 1997). Preliminary experiments of co-expression of K_{ATP} with dominant negative Sar1 construct (DN-Sar1^{H79G}) showed absence of surface expression of the channel (imaging) and lack of mature SUR1 band (western blotting). Moreover, sequence alignments for the Kir6.2 C-terminus indicated that E282 could be a part of a conserved stretch that constituted a diacidic motif [(D/E) X (D/E)], where X= any amino acid (Nishimura et al., 1999 , See Figure 3.2).

Taken together, these data (Taneja et al., 2009) indicated that the E282K mutation could be responsible for a trafficking defect in the channel causing it to be retained in the ER. What remained and presented itself as an interesting subject of investigation was to confirm if E282 was part of a functional diacidic ER exit motif (DXE) and to determine the mechanistic details of ER exit of the K_{ATP} channel.

```
Kir6.2    DLHHQDLEIIVILE      (274-288)
VSV-G     KRQIYTDIEMNRLGK     (497-511)
Kir2.1    ANSFCYENEVALTSK     (371-385)
sys1p     SPIQLKDLESQI        (192-203)
Gap1p     IPAEKMDIDTGRREV     (558-572)
CFTR      ARAVYKDADLYLLDS     (154-168)
TASK-3    SEDERRDAEERASLA     (251-265)
```

Figure 3.2 Residue E282 in Kir6.2 C-terminus could be a part of a conserved diacidic ER exit motif. Alignment of the partial Kir6.2 C-terminal amino acid sequence with proteins containing the diacidic ER exit motif (highlighted in red); numbers refer to positions in primary sequence.

In this chapter, Sar1-dependent ER exit of the K_{ATP} channels in COPII vesicles was investigated using a temperature sensitive mutant of VSV-G protein which is a reporter for COPII vesicles marking the ERES. The importance of the DXE motif on the Kir6.2 C-terminus (Kir6.2-CT) in the recruitment of the K_{ATP} channels to the cell surface was investigated with the help of CD4-Kir6.2-CT fusion protein as a reporter. The interface of interaction of Kir6.2 with the Sec24 protein in the COPII complex was explored using membrane permeable HIV TAT fusion peptides. The study led to the new finding that K_{ATP} channels contain a diacidic ER exit signal, $D^{280}L^{281}E^{282}$, on Kir6.2, recognised by the COPII coat machinery for mediating ER exit of the channel via COPII vesicles and that the mutation E282K in Kir6.2 blocks ER exit of the channels by disabling the exit signal. Co-expression of the wild type subunit rescued the mutant subunit from ER retention and resulted in functional expression. These results explained the phenotype of the patient as well as response of the patient to resection of the focal area of the pancreas (see Discussion).

3.2 Materials and Methods

3.2.1 Plasmid constructs

HA-tagged Kir6.2 in pcDNA3 and myc-tagged SUR1 in pcDNA6 were transfected in the ratio of 3:1 for transient expression of the K_{ATP} channels in mammalian cell lines as described previously (Mankouri et al., 2006). Constructs of HA-Kir6.2-pcDNA3 with mutations E282K, D280N, L281N, E282N and W91R were generated by the QuikChange® PCR method by members of Rao lab. FLAG-tagged Kir6.2WT construct was without the HA-tag in pcDNA3. Wild type and mutants of hamster Sar1a (acc. AAB30321.1) in pcDNA3.1 were kindly provided by Prof. W.E. Balch, The Scripps Research Institute, La Jolla, CA, USA (Wang et al., 2004b). The constructs were sub-cloned into pEGFP constructs to generate GFP-tagged- constructs GFP-Sar1^{WT}, GFP-Sar1^{H79G} and GFP-Sar1^{T39N} by members of the Rao lab. GFP-VSVG^{ts045} was a gift from Kai Simons, Max Planck Institute of Molecular Cell Biology and Genetics, Dresden, Germany. Human CD4 (M12807) and CD4 containing the substitution of the C-terminal domain (residues 178– 364) of Kir6.2 (CD4-Kir6.2-CT), both in pCDNA3, are as described (Mankouri et al., 2006). CD4-Kir6.2^{E282K}-CT was prepared as described later in the methods section.

3.2.2 Antibodies

All antibodies for immunofluorescence staining were diluted in the Antibody dilution buffer (section 2.2.8). Rat anti-HA antibodies (Roche) were diluted 1:500, mouse anti-FLAG and anti-myc antibodies were diluted 1:250. AlexaFluor^{488}-conjugated anti-rat secondary antibodies (Invitrogen Ltd, Paisley, UK), anti-rat FITC- and Cy3-conjugated secondary antibodies (Jackson Immuno Research, West Grove, PA) were diluted 1:500 in antibody dilution buffer. Mouse anti-CD4 monoclonal antibodies (Q4120) were a gift from Dr P. Beverley (Edward Jenner Vaccine Research, Compton, UK), were diluted 1:100 in antibody dilution buffer for staining. For chemiluminescence assay, the HRP-conjugated anti-rat antibodies were diluted 1:500 in antibody dilution buffer.

3.2.3 TAT- conjugated peptides

TAT (YGRKKRRQRRR), TAT-DXE (YGRKKRRQRRRHHQDLEIIV) and TAT-DXK (YGRKKRRQRRRHHQDLKIIV) peptides were synthesized by Peptide 2.0, Chantilly,

VA. The lyophilised peptides were reconstituted as 1M solutions in sterile distilled water and stored as small aliquots in -20°C. HEK-MSRII cells were grown on cover-slips in 12 well plates and pre-treated for 30 min with 1 ml of 1 μM peptide in Optimem®. 1 ml of cell growth medium was added to the wells and the cells were transfected with the desired constructs and incubated for 48 hours in the presence of 0.5 μM peptide before analysis (immunofluorescence staining or chemiluminescence assay). For cells stably expressing HA-K$_{ATP}$ channels, similar treatment protocol was used as described above without the transfection step.

3.2.4 Preparation of CD4-Kir6.2^{E282K}-CT construct

The wild type CD4-Kir6.2-CT construct in pcDNA3 was used as a template for QuikChange® PCR method (described in Chapter 2, section 2.3.5) using primers (see Chapter 2, section 2.2.9) designed to mutate E to K in the DLE motif of the Kir6.2-CT region. The PCR product was analysed on DNA agarose gel (data not shown) and transformed into competent *E. coli* DH5α cells (prepared as described in Chapter 2, section 2.3.1). The resultant colonies were grown in 5 ml LB medium and plasmid DNA was isolated using the DNA mini-preparation method (as described in Chapter 2, section 2.3.3). The DNA preparations were sequenced using the Kir6.2 C-terminus seq. primer (described in Chapter 2, section 2.3.6). The construct with successful mutation in the sequence was used for large scale preparation of DNA (as described in Chapter 2, section 2.3.3) which was analysed using agarose gel electrophoresis for determination of quality of preparation and concentration of the DNA (data not shown). This plasmid DNA was used for transfection to transiently express the CD4-Kir6.2^{E282K}-CT protein in HEK-MSRII cells.

3.2.5 Immunofluorescence staining

Cells were stained for HA-K$_{ATP}$ channels (wt or mutants) using antibodies against the HA-epitope, myc-SUR1 was stained using anti-myc antibodies and the CD4-Kir6.2-CT constructs (wt or mutant) were stained using anti-CD4 antibodies in concentrations as described in the previous sections. Surface and total proteins were stained for immunofluorescence imaging using the protocols described in Chapter 2. Scale bars were shown for each image using the LSM image browser and zoomed sections of the image were added as insets into the main image.

3.2.6 Determination of surface density of channels (chemiluminescence assay)

For quantification of cell surface density of the K_{ATP} channels, the chemiluminescence assay was used as described in Chapter 2, section 2.5.4. In the assay channels expressed on the cell surface were labelled with rat anti-HA antibodies followed by HRP-conjugated anti-rat antibodies. The concentration of the secondary antibodies is proportional to the number of channels on the cell surface. Addition of Lumigen™ reagent gives a chemiluminescence signal which was measured and this signal is directly proportional to the number of HRP-conjugated secondary antibodies. The luminescence value from each sample was normalized to the protein content in the lysates to equate the number of cells taken into account to obtain a measure of the surface density of the channels. Data were obtained from three separate transfection experiments, each measured in duplicate and expressed as mean ± SEM and represented as bar graphs for each treatment as compared to the control. Statistical significance of differences was determined using One-Way ANOVA and Bonferroni test; $P < 0.05$ was accepted as significant.

3.3 Results

3.3.1 Effect of mutation of $D^{280}L^{281}E^{282}$ residues of the Kir6.2 subunit on surface expression of the channels

The lack of surface expression of the K_{ATP} channel with E282K mutation in its Kir6.2 subunit reported by previous members of the lab was confirmed (Figure 3.3 top panel). Sequence alignment for the C-terminus stretch (Figure 3.2) suggested that residue E^{282} could be a part of a conserved diacidic ER exit motif DXE where X could be any amino acid. The authenticity of $D^{280}L^{281}E^{282}$ as the DXE motif required to be tested. In order to understand if the K_{ATP} channel required an intact DLE sequence for surface expression, HEK-MSRII cells were co-transfected with SUR1 and each of the extracellular HA-tagged Kir6.2 subunits: HA-Kir6.2^{WT} and mutants HA-Kir6.2^{E282K}, HA-Kir6.2^{D280N}, HA-Kir6.2^{L281N} and HA-Kir6.2^{E282Q}. The transfected cells were fixed and stained for channels expressed on cell surface (red) using the extracellular HA-epitope. The channels that were expressed within the cell but did not appear on the cell surface were stained (green) following permeabilisation of the transfected cells (see methods for details). The stained cells were visualised using immunofluorescence confocal microscopy (Figure 3.3).

The wild type (WT) K_{ATP} channels express within the cell as well as on the cell surface while channels with the mutation E282K in the Kir6.2 subunit are expressed within the cell but do not appear on the cell surface. Similarly, mutation of the acidic D^{280} and E^{282} residues to their neutral amide forms (D280N and E282N) in the Kir6.2 subunit prevented surface expression of the channels. Mutant L281N behaved like the wild type in terms of surface expression (Figure 3.3). These experiments confirmed the requirement of an intact $D^{280}L^{281}E^{282}$ stretch in the Kir6.2-CT for surface expression of the K_{ATP} channels. It was however not clear if export of K_{ATP} channels from the ER was mediated by COPII vesicles.
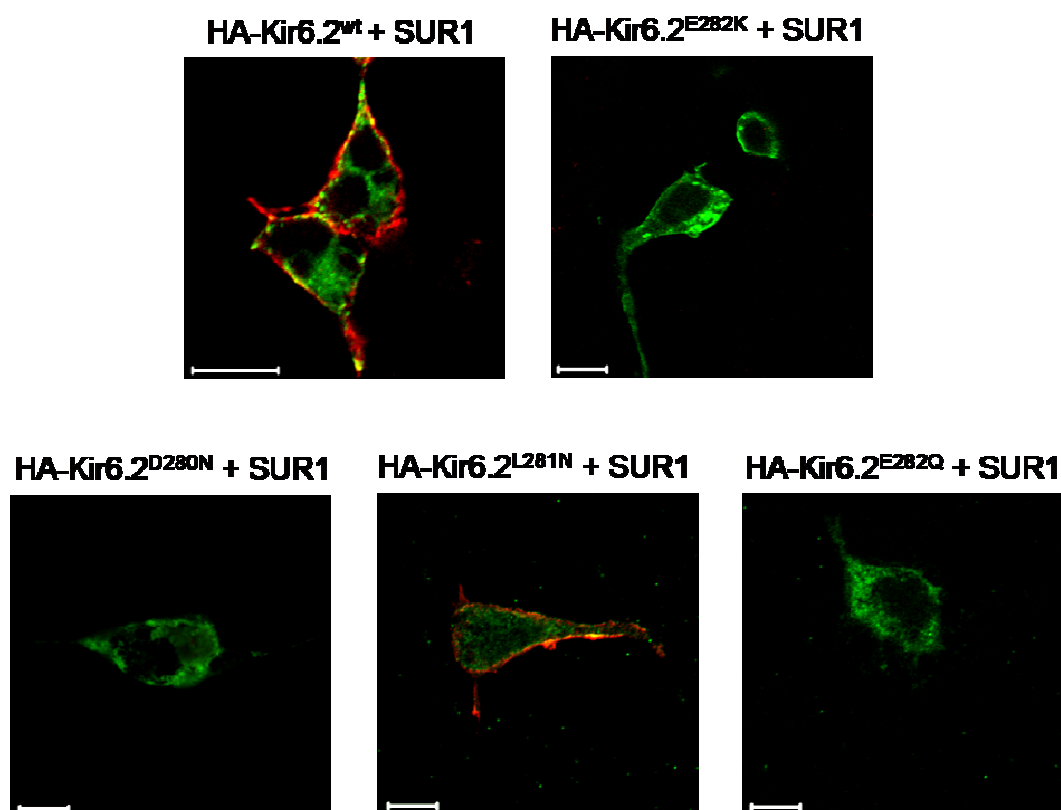
Figure 3.3 Surface expression of the $D^{280}L^{281}E^{282}$ mutants of HA-Kir6.2. HEK-MSRII cells were co-transfected with wild type or mutant Kir6.2 and SUR1 subunits. The cells were fixed and channels expressed on cell surface were stained with primary rat anti-HA antibodies followed by Cy3-conjugated anti-rat IgG secondary antibodies (red). The cells were permeabilised and the channels expressed within the cells were labelled with anti-HA antibody followed by the Alexa^{488}-conjugated secondary antibodies (green). Representative confocal images of four independent experiments are shown; Scale bars: 10 µm.

3.3.2 Sar1-dependent surface expression of K_{ATP} channels

Lack of surface expression of the mutants of the acidic residues D^{280} and E^{282} had opened the possibility that the $D^{280}L^{281}E^{282}$ sequence was an ER export motif on the Kir6.2-CT. The DXE is an ER exit motif recognised and bound by proteins of the COPII machinery that export proteins out of the ER. The formation of the COPII vesicle is dependent on Sar1 (Nishimura et al., 1999, Wang et al., 2004b), see introduction for details). If forward trafficking of the K_{ATP} channel was mediated by the COPII machinery, dominant negative (DN) mutants of Sar1 would prevent its surface expression.

To test this hypothesis, GFP-tagged DN Sar1 mutants, GFP-Sar1^{H79G} and GFP-Sar1^{T39N} were co-expressed with the K_{ATP} channel in HEK-MSRII cells. Both these mutants disrupt normal Sar1 function and prevent COPII vesicle mediated export of cargo proteins from the ER. Surface expression of K_{ATP} channels was absent in presence of both these mutants of Sar1 but not GFP-Sar1^{WT} (see Figure 3.4.A). The GFP tag helped to visualise the expression of the Sar1 proteins in the cells. Further, to eliminate any possible role of the GFP tag in the observed inhibition of K_{ATP} surface expression, experiments were carried out to determine the surface expression of K_{ATP} channels in the presence of the non GFP-tagged versions of the Sar1 proteins (Figure 3.4.B). The K_{ATP} channels were stained (red) on cell surface using the anti-HA antibody on the Kir6.2 subunit. The cells were fixed and permeabilised to stain the K_{ATP} channels expressed within the cells (green). In presence of Sar1^{WT}, the channels are expressed on the cell surface and within the cells. However, in presence of the Sar1 mutants, there was no expression of the channels on cell surface (no red stain) although the channels were expressed within the cells (green stain).

These experiments confirmed that Sar1 activity was necessary for surface expression of the K_{ATP} channels. Although the Sar1 protein has no known role apart from a role in the formation of the COPII coated vesicles that export cargo proteins out of the ER, experimental evidence was required to see if the K_{ATP} channels entered COPII vesicles prior to export out of the ER.
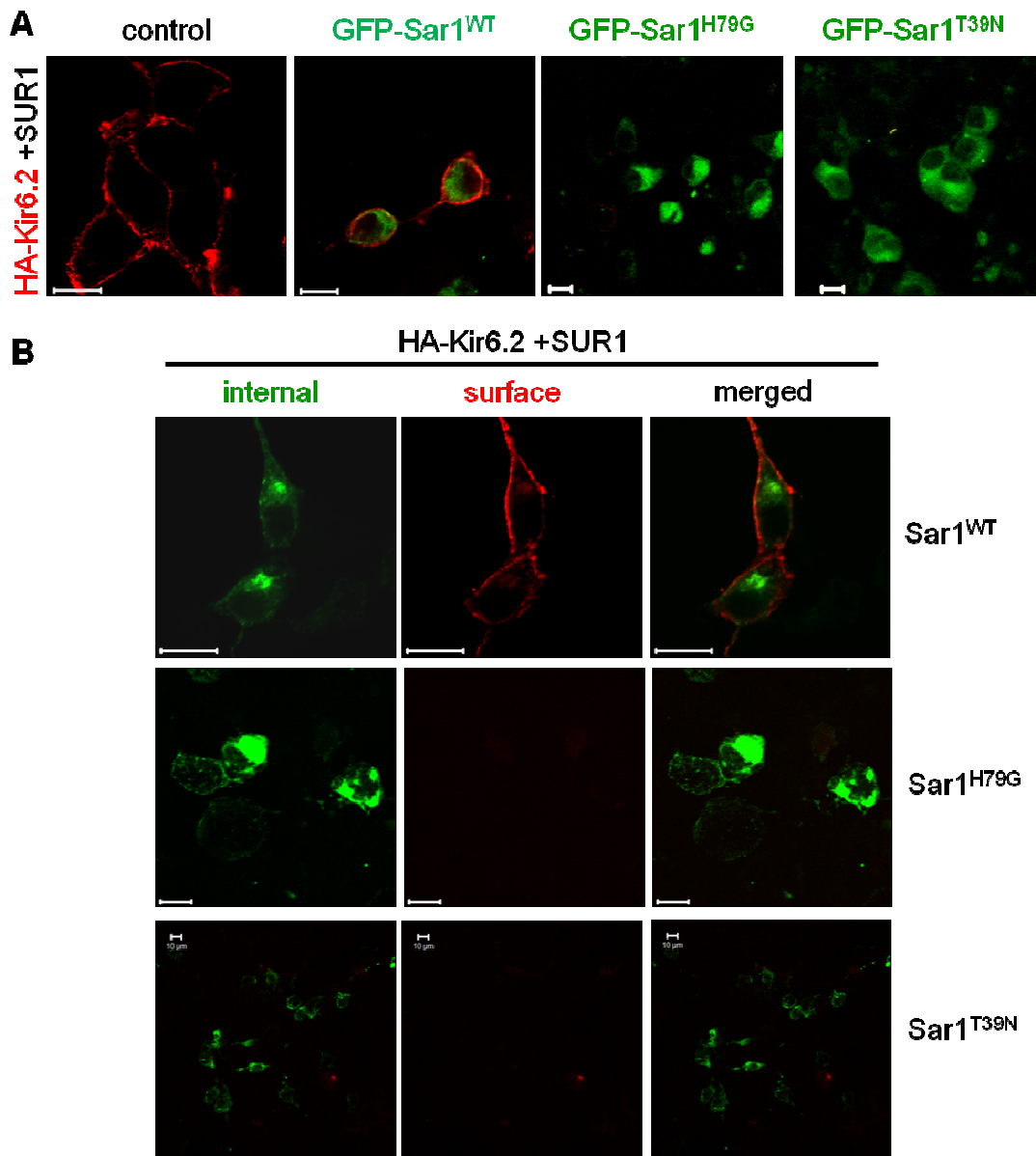
Figure 3.4 Surface expression of K_{ATP} channels is Sar1-dependent. (A) HEK-MSRII cells were transfected to co-express HA-Kir6.2^{WT}+SUR1 (K_{ATP}) and the indicated GFP-tagged Sar1 constructs. Cells expressing K_{ATP} channels alone were experimental control. The cells were stained with anti-HA antibody to detect the channels expressed on cell surface (red). GFP-tagged Sar1 constructs appear green within the cell. (B) Non GFP-tagged Sar1 proteins: Sar1^{WT}, Sar1^{H79G} and Sar1^{T39N} were co-expressed with HA-Kir6.2^{WT}+SUR1. The K_{ATP} channels were stained for the HA-epitope on Kir6.2 subunit on cell surface (red) and internal (green). Representative confocal images of three independent experiments are shown; Scale bars: 10 μm.

3.3.3 Entry of K_{ATP} channels into ERES

GFP-VSVG[ts045] protein as a marker for COPII vesicles at ERES

Packing of the COPII vesicles for selective export of cargo proteins from the ER occurs in specific regions of the ER designated as the ER exit sites (ERES) (Barlowe, 2003, Fromme et al., 2008, Miller et al., 2003, Mossessova et al., 2003). Therefore ERES are sites where COPII vesicles are formed. If the K_{ATP} channels are transported out of the ER in the COPII vesicles, they should enter the ERES. The entry of K_{ATP} channels into ERES could be confirmed by looking at co-localisation of the channels with a known ERES marker protein such as the temperature sensitive mutant of the vesicular stomatitis virus glycoprotein; VSVG[ts045] (Mezzacasa and Helenius, 2002). GFP-tagged VSVG[ts045] (GFP-VSVG[ts045]) is expressed normally on cell surface at 37°C. However, if expressed in cells growing at 39.5°C, the protein misfolds and is not exported out of the ER and accumulates in the ER. If the cells are cooled to permissive growth temperatures (32°C or below), the protein rapidly folds into right confirmation and enters ERES for packing into COPII vesicles. Budding of the COPII vesicles from the ER can be prevented by cooling the cells to 10°C (Mezzacasa and Helenius, 2002). Further, since VSVG has a DXE motif and is known to exit the ER by the Sar1 dependent COPII pathway (Nishimura and Balch, 1997), surface expression of the protein is prevented by the DN Sar1 mutant; GFP-Sar1[H79G]. This mutant of Sar1 is 'GTP on' and allows COPII vesicle assembly but prevents vesicle budding from the ERES (Nishimura et al., 1999, Wang et al., 2004b). Figure 3.5 shows confocal imaging of cells expressing the GFP-VSVG[ts045] at regular growth temperature (37°C). For the temperature shift experiment, HEK-MSRII cells were transfected to transiently express GFP-VSVG[ts045] and grown at successive temperatures of 37°C, 39.5°C, 10°C as outlined in the legend to Figure 3.5. Immunofluorescence images of the cells showed the GFP-VSVG[ts045] protein in green punctate structures that mark the ERES close to the nuclear region and the protein was absent at the cell surface. Similar effect could be reproduced by co-expression of GFP-VSVG[ts045] with mutant Sar1[H79G] that prevents COPII vesicle budding (see Figure 3.5). Based on these data the punctate structures of GFP-VSVG[ts045] were used as markers for COPII vesicles at ERES and also as reporters for the activity of Sar1[H79G].

E282K mutant K_{ATP} channels do not enter ERES

Expression of K_{ATP} channels on cell surface is prevented following co-expression with DN Sar1 mutants (Figure 3.4). If Sar1 prevented COPII mediated ER exit of the channel, it should be able to enter ERES. Both temperature shift treatment and DN Sar1 co-expression approach was used on cells co-expressing WT or the E282K mutant K_{ATP} channels and GFP-VSVG^{ts045}; the latter was used as a marker of ERES. The wild type K_{ATP} channels co-localised with punctate GFP-VSVG^{ts045} marking the ERES (Figure 3.6.A). In contrast, no co-localisation was apparent with the E282K mutant channels (Figure 3.6.B). These data indicated that the K_{ATP} channels enter ERES prior to export out of the ER. Moreover, since the E282K mutation prevented entry of the channels into ERES, $D^{280}L^{281}E^{282}$ appeared to be the diacidic ER exit motif on the Kir6.2 subunit of K_{ATP} required for Sar1 dependent ER exit of the channel. Further, it was important to investigate if the SUR1 subunit has any role in this ER exit mechanism of the K_{ATP} channels.
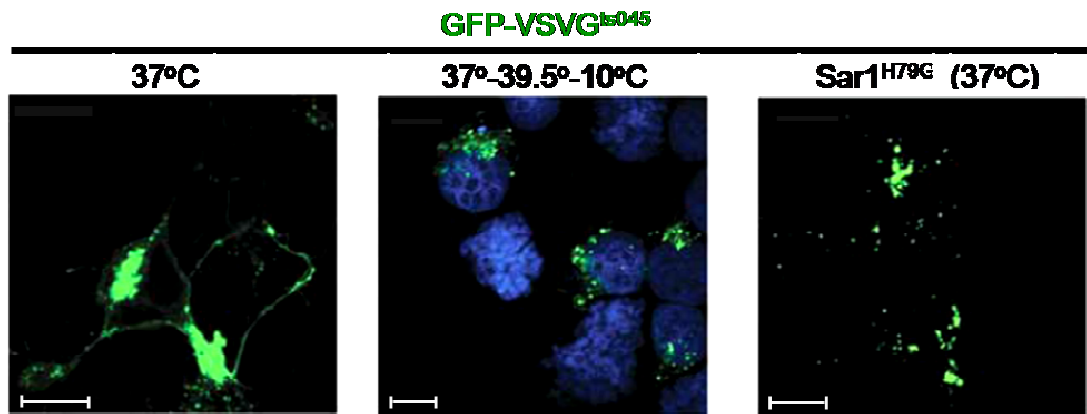
Figure 3.5 GFP-VSVG^{ts045} protein as reporter for ERES. HEK-MSRII cells were transfected with GFP-VSVG^{ts045} at 37°C and then grown at 39.5°C for 18 hrs following which they were shifted to 10°C for 5 hours and then fixed followed by nuclear stain by DAPI. At this temperature, the protein cannot leave the ER and accumulates at ERES. Cells transfected and grown at 37°C expressed the protein on cell surface normally. GFP-VSVG^{ts045} expressed in cells at 37°C along with Sar1^{H79G} arrests the protein at ERES in the COPII vesicle since it cannot dissociate from the ER. Nuclei were stained blue with DAPI. Representative confocal images from four independent experiments are shown; Scale bars: 10 µm.

3.3.4 ER exit of Kir6.2 and SUR1 subunits expressed independently

In the experiments looking at surface expression and ERES entry of the WT and E282K mutant K_{ATP} channels, the importance of the diacidic ER exit motif was apparent. However in these experiments, the SUR1 subunit was co-expressed with the WT or the E282K mutant Kir6.2 subunit as would be the case in native cells (Shyng and Nichols, 1997). Previous studies on trafficking of the K_{ATP} channel reported that the association of the Kir6.2 and SUR1 subunits was critical for masking the ER retention (RXR) motifs on both the subunits and therefore the subunits were thought to assemble in the ER (Zerangue et al., 1999). The subunit assembly was thus considered necessary for surface expression of the channel, yet there was no evidence of it being essential for the entry of the channel subunits into ERES. Moreover, when trafficking experiments with the Kir6.2 WT and E282K mutant subunits were conducted in presence of SUR1 subunit, the influence of the SUR1 subunit in the ER export could not be determined. To address this issue and to get a clearer idea of the ER exit and assembly mechanisms for the channel, the HA-Kir6.2^{WT}, HA-Kir6.2^{E282K} and myc-SUR1 subunits were expressed independently to see if they could enter ERES.

Punctate structures of GFP-VSVG^{ts045} (co-expressed with Sar1^{H79G}) were used as markers of ERES as shown before in Figure 3.5. Both HA-Kir6.2^{WT} and myc-SUR1 co-localised with GFP-VSVG^{ts045} indicating that they are recruited to the ERES while the E282K mutant did not co-localise with GFP-VSVG^{ts045} (Figure 3.7). These results were unexpected, based on the previous reports on the channel assembly where subunit assembly was considered to be a pre-requisite for ER exit (Clement et al., 1997, Shyng and Nichols, 1997, Zerangue et al., 1999, Heusser et al., 2006 ; see discussion.
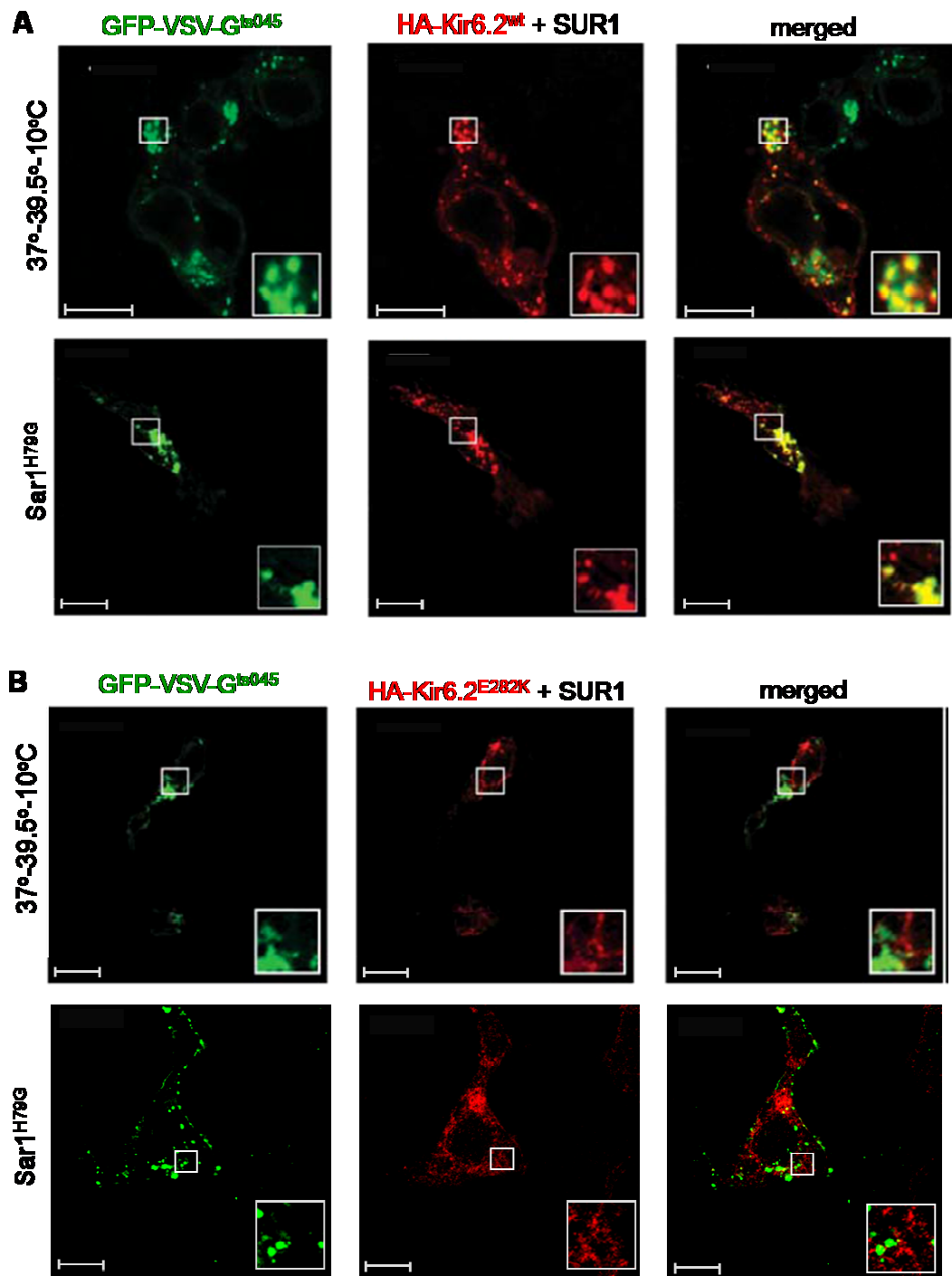
Figure 3.6 WT but not the E282K mutant, K$_{ATP}$ channels enter the ERES. Cells were co-transfected with the indicated channel subunits plus the GFP-VSVG^{ts045} clone. Temperature shift treatments (37°/39.5°/10°C) as well as co-expression of mutant Sar1^{H79G} caused accumulation of GFP-VSVG^{ts045} into punctate structures that mark the ERES. WT-K$_{ATP}$ channels (A) but not the E282K mutant channels (B) co-localise with GFP-VSVG^{ts045} at the ERES. Representative confocal images from three independent experiments are shown; Scale bars: 10µm.

Further, since proteins that enter ERES are expected to exit the ER and enter ERGIC (ER-Golgi intermediate compartment) (Appenzeller-Herzog and Hauri, 2006), an experiment was designed to look at the post-ER itinerary of the individual K_{ATP} subunits. Each of the subunits expressed alone were stained along with the protein ERGIC-53, a marker for the ERGIC (Appenzeller-Herzog and Hauri, 2006 ; see Figure 3.8). Both Kir6.2 and SUR1 co-localised with ERGIC-53, indicating that the individual subunits were able to escape out of the ER and therefore assembly of Kir6.2 and SUR1 is not critical for ER exit of the channel subunits. These data also suggest the possibility of existence of an ER exit motif on SUR1, which seems quite likely considering the fact that SUR1 is a relative of the CFTR, a protein reported to exit ER in COPII mediated vesicles using the diacidic ER exit motif (Wang et al., 2004b).

3.3.5 Kir6.2 interaction with the COPII machinery

These data suggested that Kir6.2 and SUR1 subunits, when expressed independently, can exit the ER. However, in a natural scenario, both Kir6.2 and SUR1 would be co-expressed (Shyng and Nichols, 1997) and therefore it could be argued that in an assembled octamer of Kir6.2 and SUR1 subunits, the diacidic ER exit motif on Kir6.2-CT may not even be stearically accessible for interaction with the COPII machinery (Bi et al., 2002, Mossessova et al., 2003) see discussion. If this was true, the DLE motif on Kir6.2-CT might not even be able to bind to the COPII complex and the effect of the mutation E282K might be indirect.

To test if the DLE motif on the Kir6.2-CT was specifically responsible for interaction with COPII complex, a CD4-Kir6.2-CT fusion protein was used. CD4 is a type I membrane protein expressed on cell surface with no known ER exit/ retention signals and is exported from the ER in a COPII independent manner (Figure 3.9.A). CD4 showed no distinct co-localisation with GFP-VSVG[ts045] puncta in presence of Sar1[H79G] and appeared on the cell surface (Figure 3.9.B).
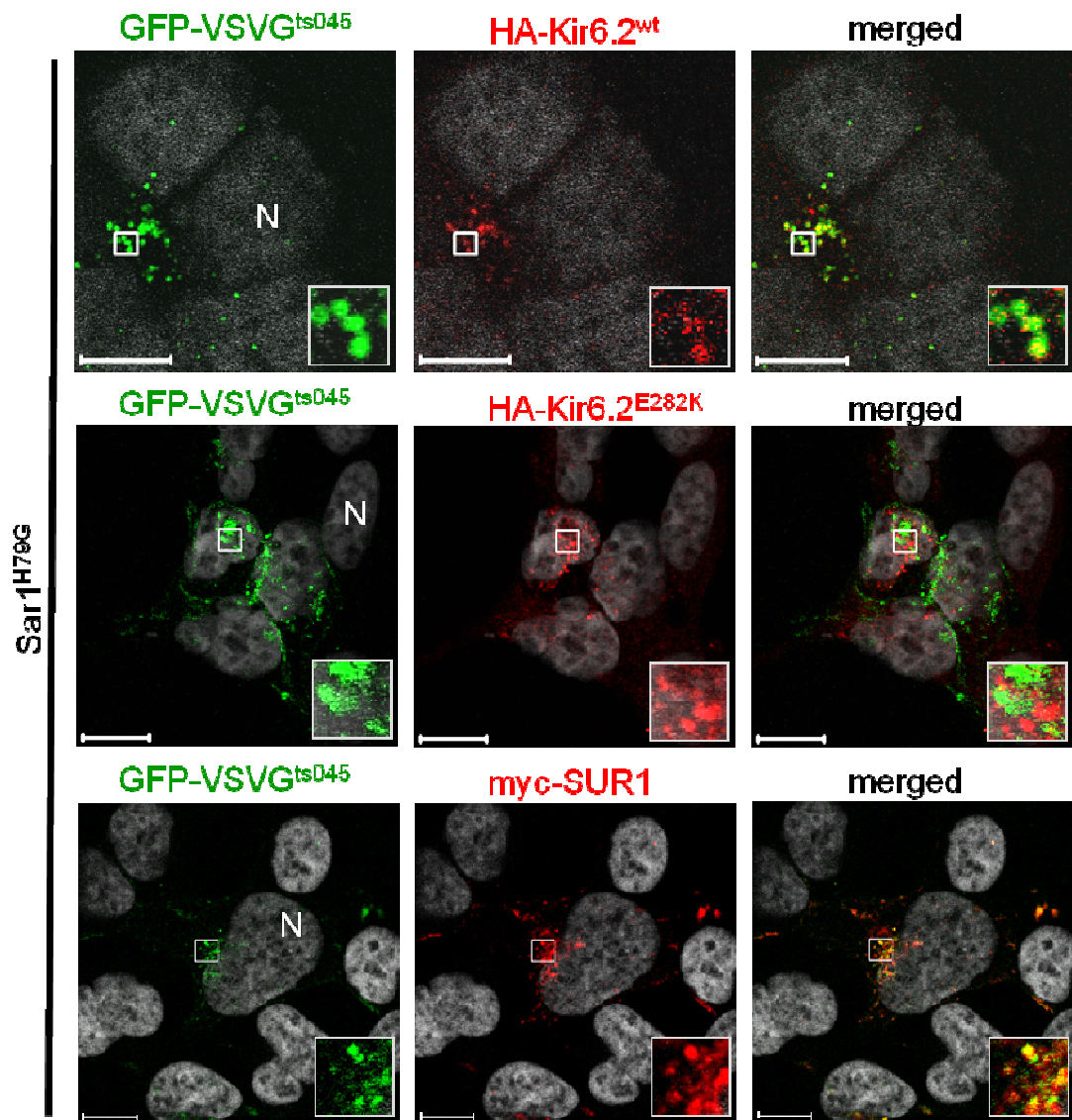
Figure 3.7 Kir6.2 and SUR1 subunits can enter ERES independently, while the mutant E282K cannot. Co-expression of Sar1^{H79G} results in co-localisation of both HA-Kir6.2^{WT} and myc-SUR1 subunits but not HA-Kir6.2^{E282K} with GFP-VSVG^{ts045}. Nuclei (N) in pseudo-grey were stained with DAPI. Representative confocal images from three independent experiments are shown; Scale bars: 10 µm.
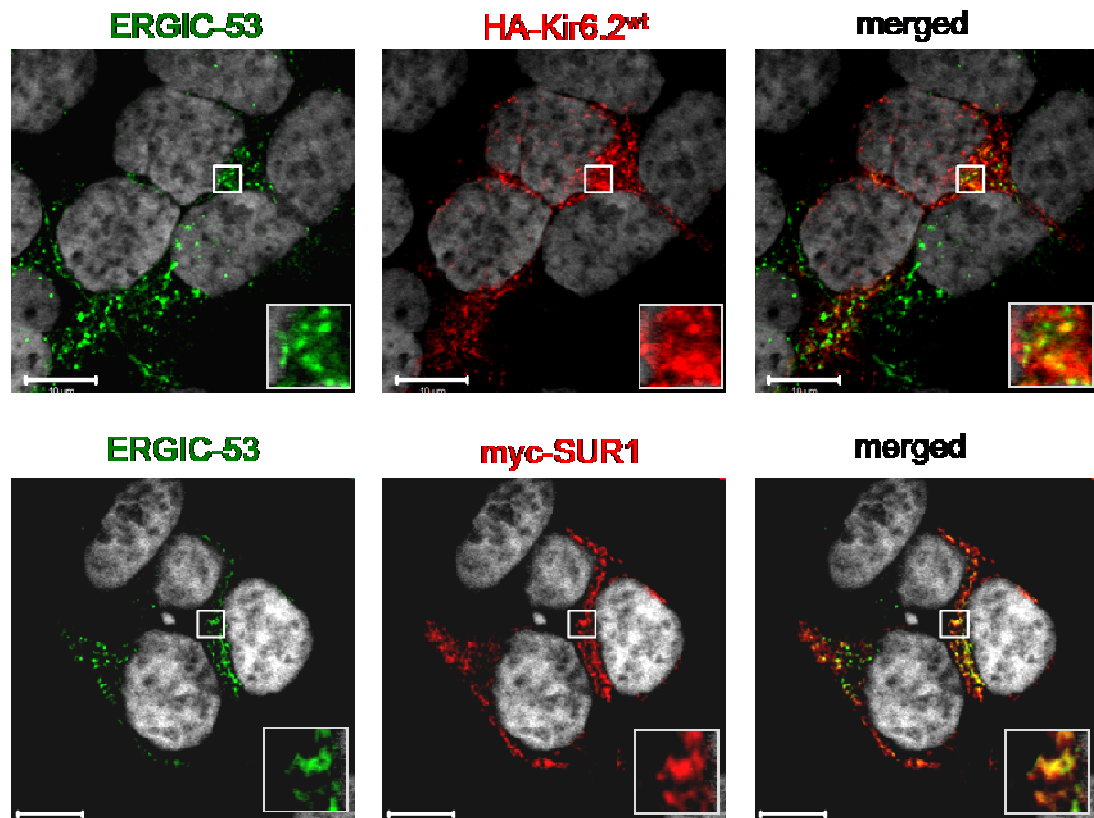
Figure 3.8 Kir6.2 and SUR1 subunits can enter ERGIC independently. Both HA-Kir6.2^{WT} and myc-SUR1 subunits expressed independently were found to enter ERGIC as seen by co-localisation (yellow) with the ERGIC-53 protein (green) stained using ERGIC-53 antibody. Nuclei in pseudo-grey were stained with DAPI. Representative confocal images from three independent experiments are shown; Scale bars: 10µm.
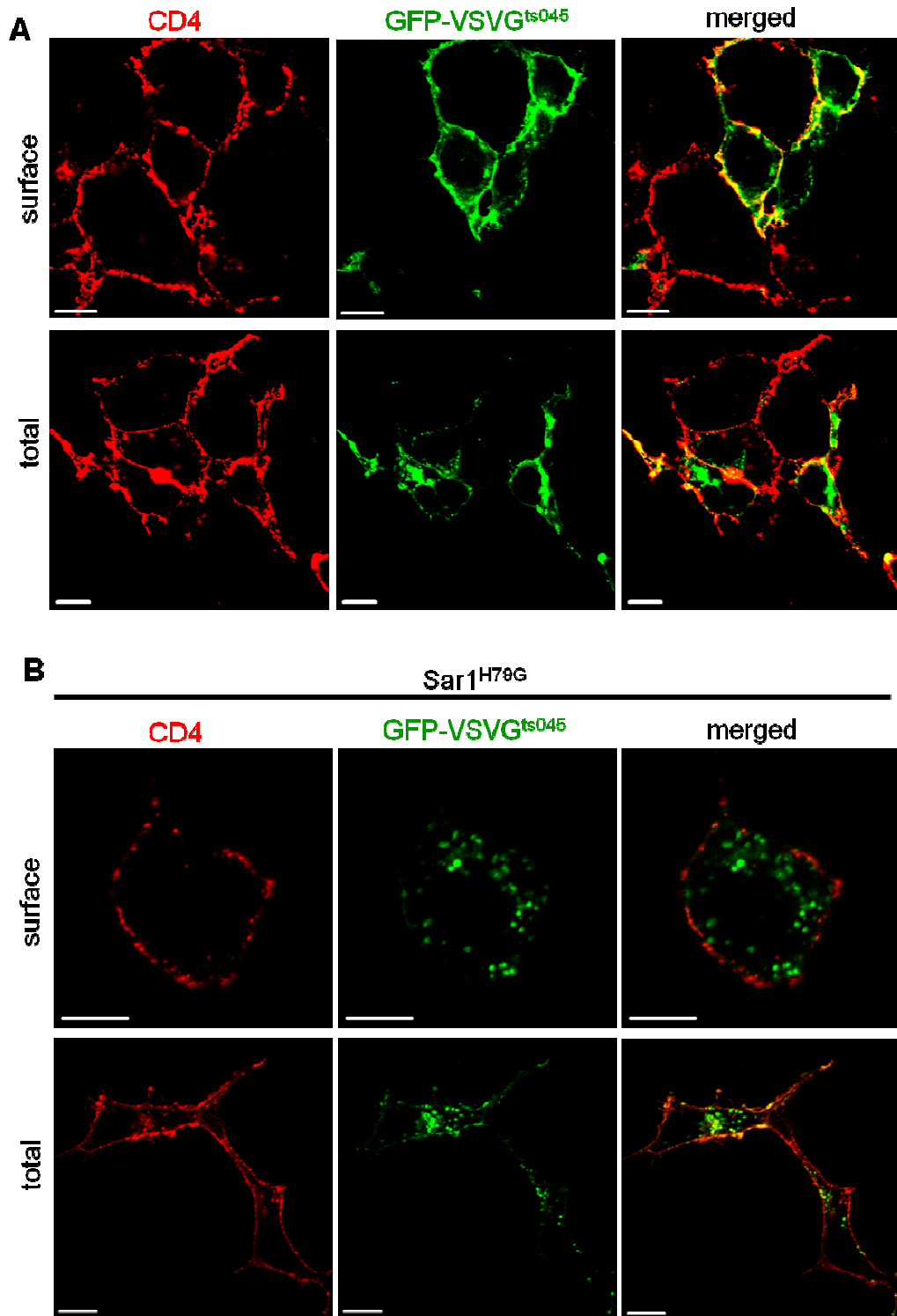
Figure 3.9 CD4 protein expression on cell surface does not depend on Sar1. Cells were transfected with CD4 and GFP-VSVG^{ts045} with or without Sar1^{H79G}. CD4 was immunostained (red) with an antibody against its extracellular domain without (surface CD4) and with permeabilisation (total cellular CD4). CD4 expresses on cell surface (A). Surface expression of CD4 is unaffected by Sar1^{H79G} (B). Representative confocal images from three independent experiments are shown; Scale bars: 10μm.

The C-terminus of CD4 was replaced with the C-terminus of Kir6.2^{WT} devoid of the ER retention signal (Figure 3.10A) because the Kir6.2 subunit with deletion of the last 26 amino acids (Kir6.2Δ26) has been shown to express on cell surface in the absence of the SUR1 subunit in HEK cells (Tucker et al., 1998). This is because the RKR motif on the Kir6.2-CT terminus lies distal to the DLE sequence and is reported to act as the ER retention signal. Interaction with the SUR1 subunit is considered to mask this signal and allow ER exit of the channel subunits (Zerangue et al., 1999). If the ER retention signal is deleted from the Kir6.2-CT, the subunit would not require co-expression with the SUR1 subunit in order to express on the cell surface. This approach allowed the interaction between the COPII complex and the C-terminus of Kir6.2 to be studied independent of the SUR1 subunit.

The rationale behind the use of the fusion protein was that if the diacidic ER exit motif on the Kir6.2-CT was responsible for interaction with the COPII complex then it would cause CD4 to exit the ER in a COPII dependent manner. The fusion protein (CD4-Kir6.2-CT) was expressed on the cell surface and co-localized with GFP-VSVG^{ts045} in the cell and on cell surface (Figure 3.10B). However, when Sar1^{H79G} was also expressed in the cells, the CD4-Kir6.2-CT protein was not expressed on the cell surface and was seen to co-localise with the punctate structures of GFP-VSVG^{ts045} at the ERES (Figure 3.10C). When the DLE motif on the Kir6.2-CT was mutated to DLK, the mutant fusion protein CD4-Kir6.2-CT^{E282K} was found to be expressed within the cell but was absent from the cell membrane (Figure 3.11A).

When the CD4-Kir6.2-CT^{E282K} fusion protein was co-expressed with GFP-VSVG^{ts045} and Sar1^{H79G}, there was no co-localisation seen with punctate VSVG vesicles marking the ERES (Figure 3.11B), indicating the inability of the fusion protein to enter ERES. The CD4-Kir6.2-CT^{E282K} mutant thus behaved like the E282K mutant K$_{ATP}$ channel. Taken together, data from experiments with the fusion proteins indicated that the DLE motif on the Kir6.2 is responsible for interaction with the COPII complex resulting in the concentration of the channel subunits in the ERES and the SUR1 subunit is not required for recognition of the K$_{ATP}$ channels by COPII coat proteins.
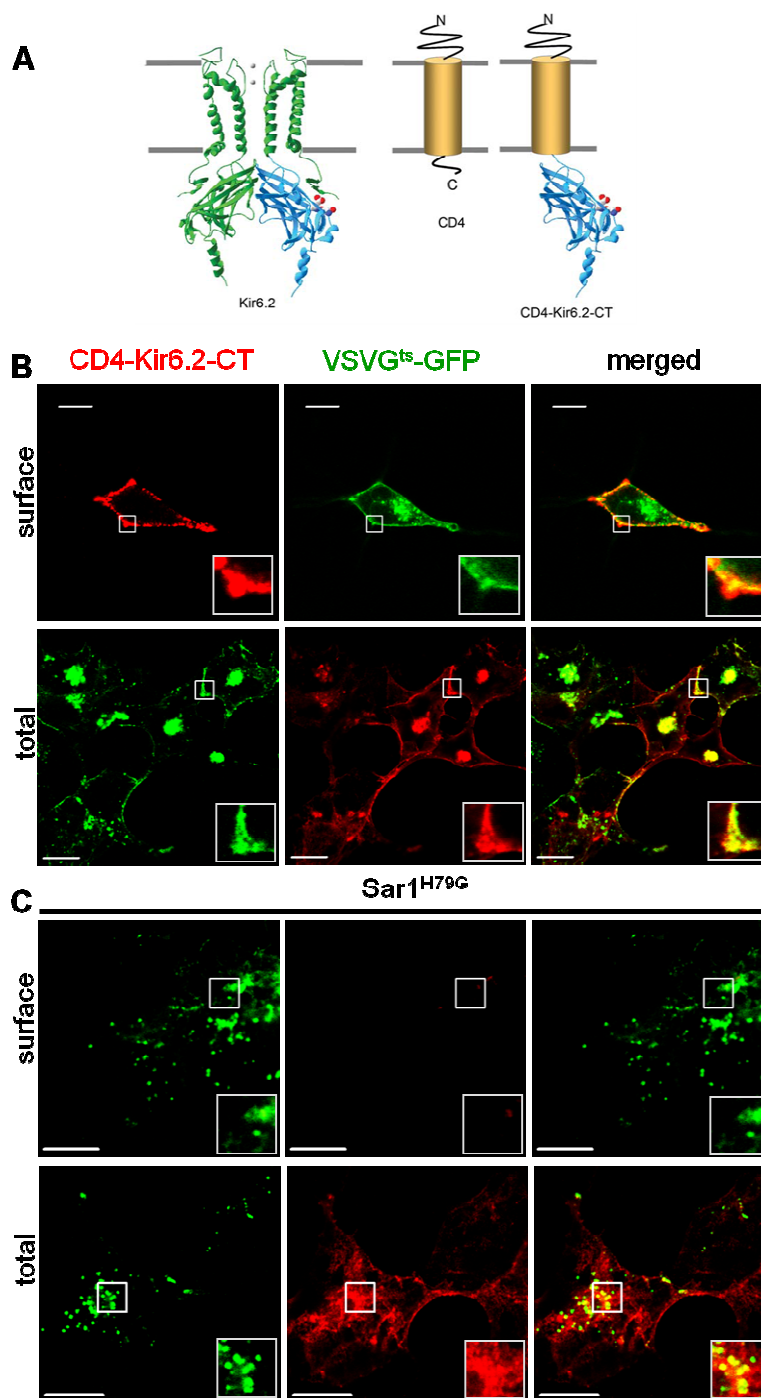
Figure 3.10 DXE motif on Kir6.2 is responsible for entry of K$_{ATP}$ channels into ERES. (A) Structural model of Kir6.2, schematic of CD4 and CD4-Kir6.2-CT fusion protein containing the C-terminus of Kir6.2 (shown in blue); DLE residues are in red; gray lines represent hypothetical membrane borders. (B) Cells were stained for extracellular epitope on CD4 on surface and total. The C-terminus of Kir6.2 confers the ability to enter the ERES on CD4. (C) Sar1^{H79G} prevents surface expression of CD4-Kir6.2-CT and the fusion protein co-localises with GFP-VSVG^{ts045} at the ERES (merged images). Representative confocal images are shown from three independent experiments; Scale bars: 10 µm.
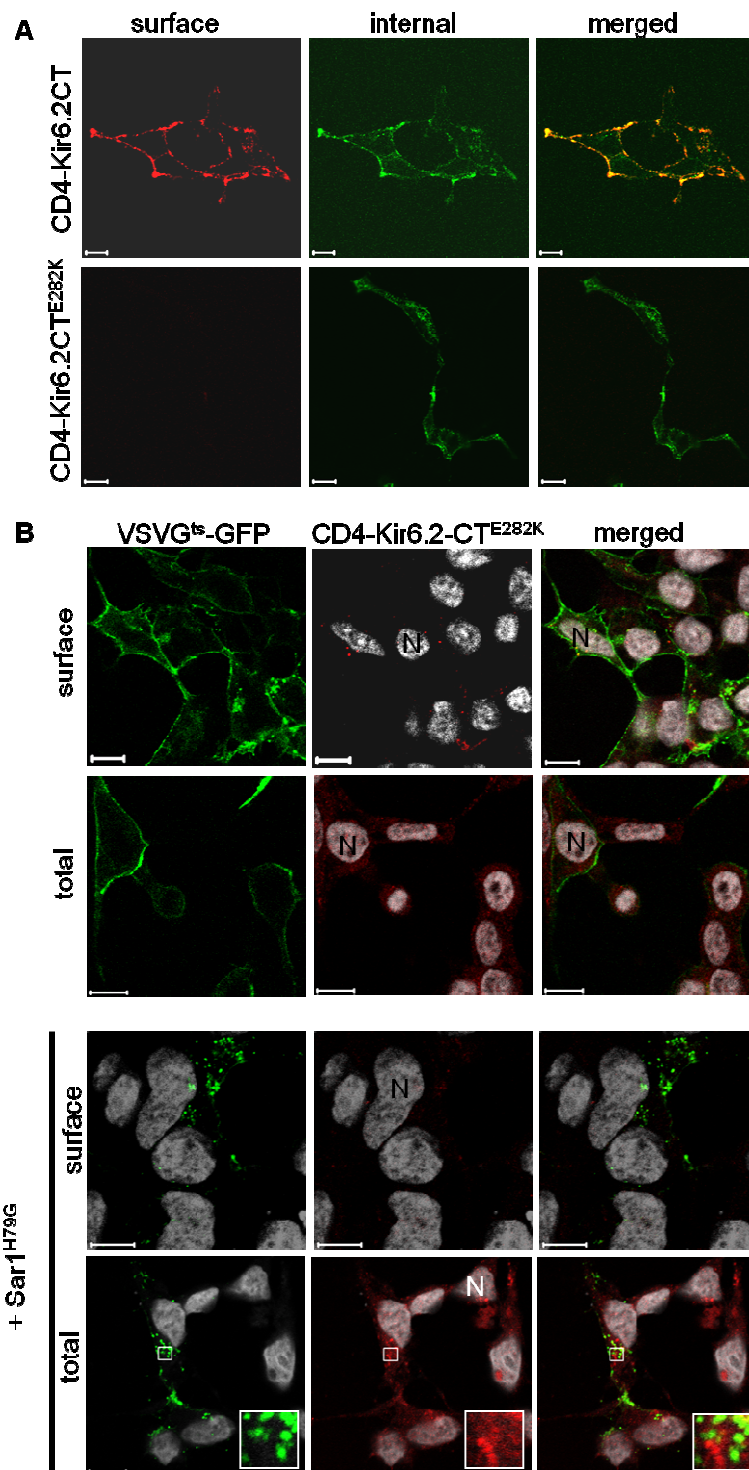
Figure 3.11 Mutation of the DXE motif in the CD4- Kir6.2-CT prevents surface expression and concentration of the protein into ERES. (A) HEK-MSRII cells were transfected to express the CD4-Kir6.2-CT or CD4-Kir6.2-CT[E282K] fusion proteins. Staining for expression on cell surface (red) and internal (green) shows that the mutant fusion protein is not expressed on cell surface. (B) Co-expression with Sar1[H79G] shows that the mutant fusion protein is not expressed on cell surface and does not co-localise with GFP-VSVG[ts045] at the ERES (merged images). Representative confocal images are shown; Scale bars: 10 μm.

3.3.6 Studying interaction between Kir6.2-CT and proteins of COPII coat using membrane permeable TAT-conjugated peptides

The Sec24 subunit of COPII coat complex is known to recognise and bind its cargo through the diacidic motif present on the cargo (Miller et al., 2003). Involvement of the DXE motif on the Kir6.2-CT was evident from the experiments presented in the previous sections. Presence of a competing cargo should disrupt this interaction and affect the ER exit of the K_{ATP} channel. In principle, the TAT-DXE peptide would be expected to compete with the Sec24 binding site and its effect on surface expression of K_{ATP} should resemble that of the mutant Sar1^{H79G}. To test this theory, synthetic peptide (TAT-DXE) containing a stretch of the Kir6.2 channel subunit with the DLE motif (HHQ**DLE**IIV) fused to the HIV TAT peptide sequence was synthesized commercially. The presence of the TAT sequence renders the peptide permeable to the cell membrane (Schwarze et al., 2000). The TAT peptide alone and TAT peptide conjugated to Kir6.2 stretch with mutated DLE motif (HHQ**DLK**IIV) referred to as TAT-DXK were used as controls (See Figure 3.12). HEK-MSRII cells transfected with the K_{ATP} channel subunits were treated with the synthetic TAT peptides (see methods for details). The TAT-DXE peptide treated cells but not the TAT-DXK or TAT peptide treated cells showed lack of surface expression of the K_{ATP} channel as seen by imaging (Figure 3.13.A) and chemiluminescence assay (Figure 3.13.B).

Further, if the TAT-DXE peptide was competitively inhibiting Sec24 binding, then the K_{ATP} channels would not be recruited to the COPII vesicle and would be absent from the ERES. To check if this was true, cells co-expressing the K_{ATP} channel and/or GFP-VSVG^{ts045} were treated with the TAT-conjugated peptides. The cells were fixed, permeabilised and stained for total channel within the cell. Interestingly, GFP-VSVG^{ts045} was completely absent from cell membrane in cells treated with the TAT-DXE peptide (Figure 3.14.A). Moreover, the protein assembled into punctate structures marking ERES as seen in case of co-expression with Sar1^{H79G}. These data suggested that GFP-VSVG^{ts045} bearing COPII vesicles were formed but did not bud off (see discussion). Further, when cells expressing K_{ATP} and GFP-VSVG^{ts045} were treated with TAT-DXE peptide, the channels co-localised with the punctate GFP-VSVG^{ts045} structures marking ERES (Figure 3.14.B). The cells treated with TAT or the TAT-DXK peptide did not cause accumulation of GFP-VSVG^{ts045} in punctate structures. When the cells expressing GFP-VSVG^{ts045} or the K_{ATP} channels were treated with the TAT-DXE peptide and stained (total) for HA-Kir6.2 along with the ERGIC-53, a marker for the ERGIC compartments, no co-localisation could be seen between ERGIC-53 and GFP-

VSVG^{ts045} or K$_{ATP}$ (Figure 3.14.C). Taken together the data indicated that the TAT-DXE peptide prevented the escape of GFP-VSVG^{ts045} and K$_{ATP}$ channels from the ER.

The punctate GFP-VSVG and HA-Kir6.2 both did not show any co-localisation with ERGIC-53 which strengthens the observation that the TAT-DXE peptide locks the DXE motif containing COPII cargo in the ERES. These data further strengthen the importance of the DXE motif in ER exit. Also, the effect of the TAT-conjugated peptides is encouraging for the use of these peptides as tools for COPII mediated ER exit studies.

As in all the above experiments using the peptides, the cells were transiently transfected to express the channel; it was interesting to look at the effect of the peptide on surface expression of the channel in cells stably expressing it. Figure 3.15 shows results from experiments using a K$_{ATP}$ stable cell line that co-expressing HA-Kir6.2 and SUR1. The cells were treated with the TAT-DXE and TAT-DXK peptides for different times and the channels on cell surface were stained. The cells treated with the TAT-DXE peptide showed a decrease in the surface expression of the channel and most of the cells showed nearly complete loss of K$_{ATP}$ from cell surface after 96 hours of treatment with the peptide. The TAT-DXK peptide however had no effect.

Tat **YGRKKRRQRRR**

Tat-DXE **YGRKKRRQRRR**HHQ**DLE**IIV

Tat-DXK **YGRKKRRQRRR**HHQ**DLK**IIV
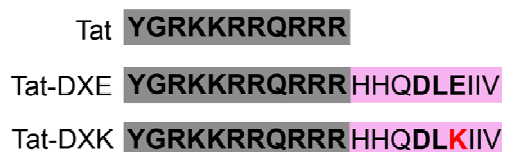
Figure 3.12 Schematic of TAT-conjugated peptides.

HA-Kir6.2^{wt} + SUR1
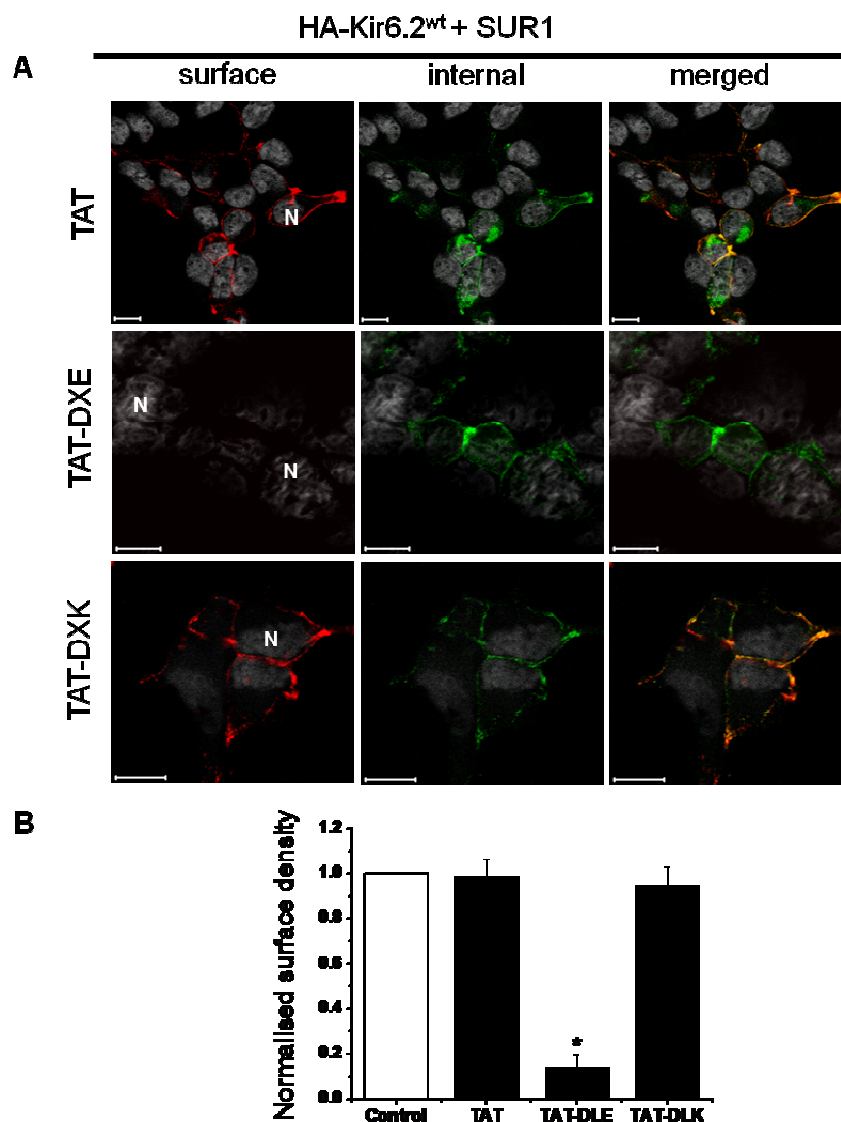
Figure 3.13 TAT-conjugated peptides containing the WT, but not the mutant ER exit signal of Kir6.2 prevents surface expression of K$_{ATP}$ channels. (A) HEK-MSRII cells were transfected with HA-Kir6.2 and SUR1 and treated with the indicated peptides (0.5 mM, made up in Optimem®) and stained for cell surface (red) and intracellular (red) HA-Kir6.2. Representative confocal images of three independent images are shown. Scale bars: 10 µm. (B) Quantitative analysis of the effect of various peptides on the surface expression of K$_{ATP}$ channels using chemiluminescence. All values are normalised to control (untreated); *P > 0.001.
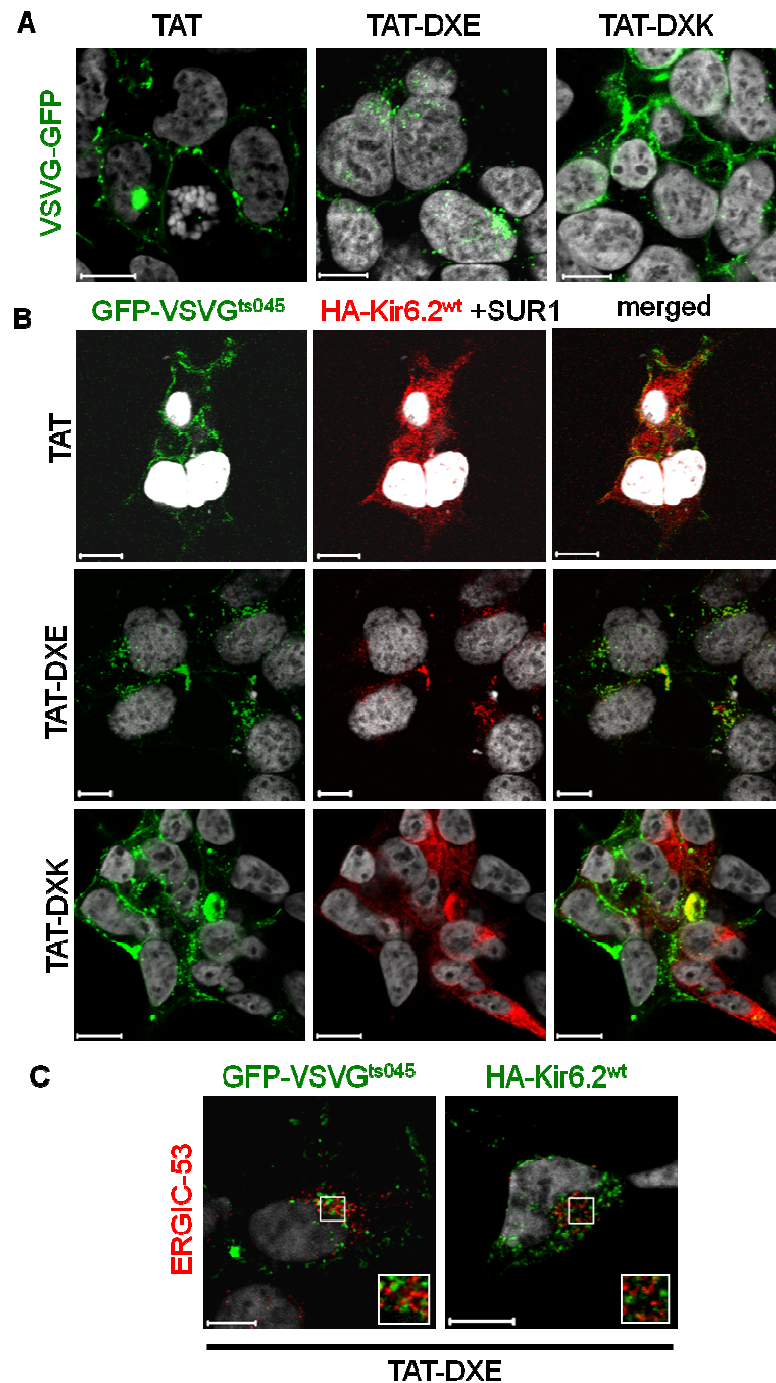
Figure 3.14 TAT-DXE peptide treatment causes accumulation of the cargoes containing the diacidic motif in the ERES. (A) Effect of the TAT peptides on GFP-VSVG^{ts045}. (B) HEK-MSRII cells were transfected to express GFP-VSVG^{ts045} along with HA-Kir6.2^{WT} and SUR1. Following treatment with TAT, TAT-DXE or TAT-DXK peptides as in Figure 3.13, the cells were fixed, permeabilised and stained for total HA-Kir6.2 (red). (C) Cells expressing GFP-VSVG^{ts045} and HA-Kir6.2^{WT} (stained green) following treatment with the TAT-DXE peptide were stained (red) with ERGIC-53 antibody. Nuclei in pseudo-grey were stained with DAPI. Representative confocal images from three independent experiments are shown; Scale bars: 10 µm.
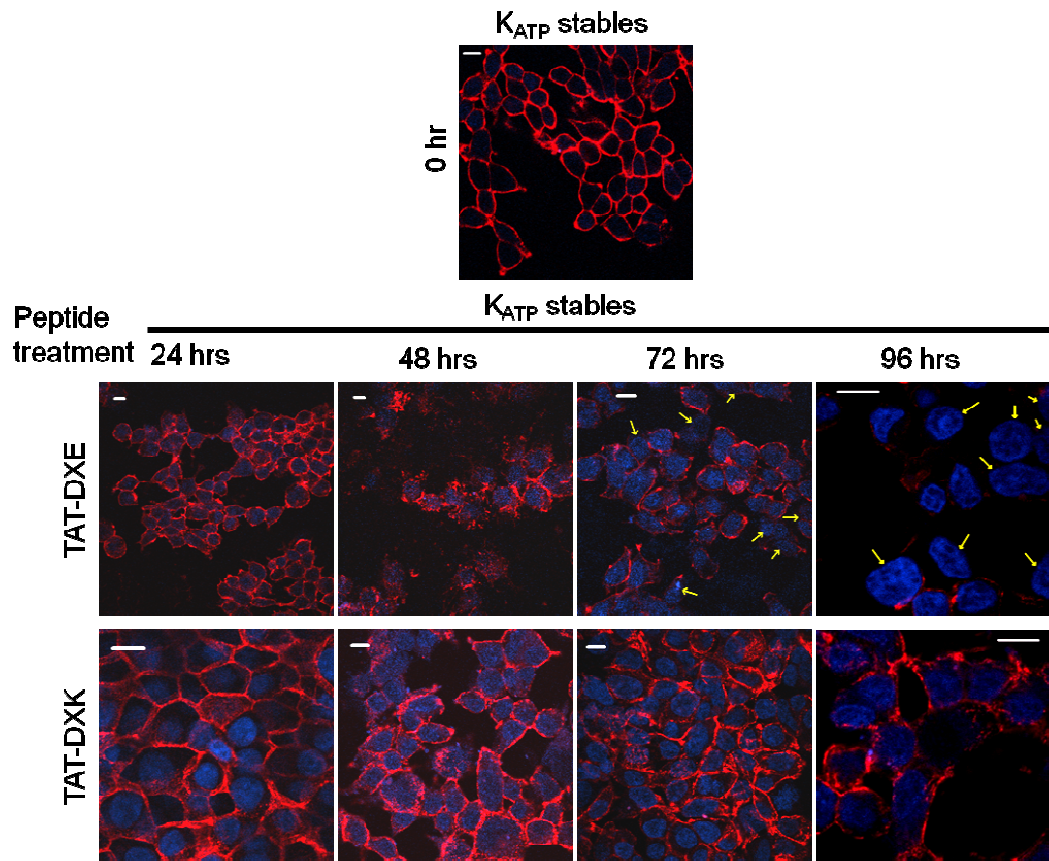
Figure 3.15 TAT-DXE peptide treatments cause loss of K$_{ATP}$ from cell surface in cells stably expressing the channel. HEK293 cells stably expressing the HA-K$_{ATP}$ channels (HA-Kir6.2 + SUR1), were plated out on cover-slips and treated with the TAT-DXE and the TAT-DXK peptides as described in Figure 3.13 for 24, 48, 72 and 96 hrs each. The K$_{ATP}$ channels expressed on the cell surface were stained with the extracellular HA-epitope using the anti-HA antibody. Nuclei were stained with DAPI (blue). Representative confocal images are shown. Scale bars: 10 μm. Yellow arrows point at cells with no HA-K$_{ATP}$ expression.

3.3.7 Rescue of Kir6.2^{E282K} subunit to the cell surface by the Kir6.2^{WT}

The above studies showed that K$_{ATP}$ channels contain a functional diacidic ER exit signal (DLE) which promotes concentration of the channel into COPII enriched ERES prior to secretion and that in the absence of such a concentrative step, delivery of the channel to the cell surface is almost completely prevented. In light of this information it was interesting to understand the effect of the mutation in the DLE motif on Kir6.2 at a functional level. The pancreas of the Swedish patient in whom the E282K mutation in the Kir6.2 subunit was first reported (Christesen et al., 2007 ; see Figure 3.1) had two kinds of cells. The tumorous cells expressed the E282K mutant Kir6.2 subunits and SUR1. Experiments to look at the surface expression of the K$_{ATP}$ channels made up of Kir6.2^{E282K} and SUR1 subunits showed lack of surface expression of the channels (Figure 3.3). The non-tumorous pancreatic cells had a heterozygous mutation in the *KCNJ11* gene and they expressed both wild type and E282K mutant Kir6.2 subunits along with SUR1. Therefore, effect of surface expression of the K$_{ATP}$ channels in cells simultaneously expressing both Kir6.2^{WT} and Kir6.2^{E282K} subunits along with SUR1 was investigated. HEK-MSRII cells were transfected to co-express SUR1, HA-Kir6.2^{E282K} and FLAG-Kir6.2^{WT} (Kir6.2^{WT} subunit with a FLAG tag but no HA-tag). The cells were stained with the anti-HA antibody to label the channels expressed on cell surface (red) and for channels expressed within the cells (green). Interestingly, in cells expressing both FLAG-Kir6.2^{WT} and HA-Kir6.2^{E282K}, the HA-Kir6.2^{E282K} channels were labelled on cell surface which showed that the wild type Kir6.2 subunits were capable of rescuing the E282K mutants to the cell surface. However, when the trafficking deficient mutant of HA-Kir6.2^{W91R} was co-expressed with the FLAG-Kir6.2^{WT}, the HA-tagged mutant subunits were not expressed on the cell surface. The Kir6.2^{W91R} subunits are known to be retained in the ER due to misfolding (Crane and Aguilar-Bryan, 2004) and therefore are not rescued to the cell surface when co-expressed with the Kir6.2^{WT} subunits and SUR1. As an experimental control, when HA-Kir6.2^{WT} subunits were co-expressed with the FLAG-Kir6.2^{WT} subunits, the HA-Kir6.2^{WT} subunits were found to express on the cell surface (Figure 3.16). It was evident from these data that the E282K mutation unlike the W91R mutation only affects the ability of Kir6.2 subunits to be recruited to the COPII vesicles and does not cause subunit misfolding.
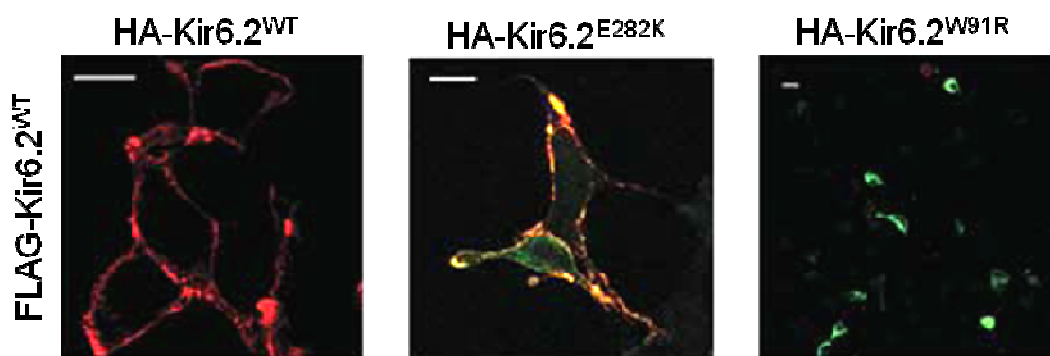
Figure 3.16 Kir6.2^{E282K} can be rescued to the cell surface by the Kir6.2^{WT} subunits. HEK-MSRII cells were co-transfected with SUR1 + FLAG-Kir6.2^{WT} and HA-Kir6.2^{WT} (as control) or HA-Kir6.2^{E282K} or HA-Kir6.2^{W91R}. The channels were stained on cell surface (red) and internal (green) using the anti-HA antibody. This allowed detection of only the HA-tagged constructs. The staining of channels on cells surface (red) in cells transfected with the HA-Kir6.2^{E282K} mutant shows the appearance of the mutant subunits on cell surface due to co-expression with the FLAG-Kir6.2^{WT} subunits. Representative confocal images of three independent experiments are shown. Scale bars: 10 μm

3.4 Discussion

The aim of this study was to investigate the cell biological mechanism by which the genetic mutation E282K in the Kir6.2 subunit of the K_{ATP} channel causes the focal form of CHI (Christesen et al., 2007). The E282K mutant channels were found to be absent from cell surface. Experiments to find out why the mutant channels do not express on cell membrane revealed a previously unrecognised diacidic ER exit motif (DLE) on the C-terminus of the Kir6.2 subunit which is crucial for trafficking of the K_{ATP} channels to the cell surface and that abrogation of this motif leads to the disease (CHI) as reported in the patient.

The lack of surface expression of the E282K mutant K_{ATP} channels observed in confocal imaging (Figure 3.3, top panel) was supported by electrophysiological experiments (Taneja et al., 2009 , J. Mankouri's thesis) which showed that the mutant failed to form functional channels in *Xenopus oocytes*. Taken together, these data classified the E282K into the league mutations that affect forward trafficking instead of those that alter function of the channel (see introduction for details on mutations that alter K_{ATP} channel function but not expression).

Mutations that cause protein misfolding and therefore defective forward trafficking are not uncommon in Kir6.2 or SUR1, as well as in several other membrane proteins such as CFTR (Brown et al., 1996) and hERG (Anderson et al., 2006). Mutations such as delta F1388 in SUR1 lead to lack of surface expression through ER retention of the K_{ATP} channels (Cartier et al., 2001), while others cause retention of the protein in the Golgi (Partridge et al., 2001). CHI caused by lack of functional K_{ATP} channels on β-cell surface due to folding defects in the SUR1 subunit of the channels is a common cause of the disease. Patients suffering this form of CHI can be treated using diazoxide (Partridge et al., 2001). Mutations in the Kir6.2 subunit either introduce a premature stop codon that results in truncated non-functional Kir6.2 protein, or introduce mis-sense mutations that cause rapid degradation of the protein (Aguilar-Bryan and Bryan, 1999, Marthinet et al., 2005). Mutation W91R in Kir6.2 causes misfolding of the subunit that prevents expression of the K_{ATP} channels on cell surface. The misfolded subunit is unable to bind SUR1 subunit stably and is rapidly degraded. The W91R mutation of the Kir6.2 subunit is reported to cause severe hyperinsulinism in patients (Crane and Aguilar-Bryan, 2004). Similarly mutations such as delta F508 in CFTR (Brown et al., 1996) and N470D in hERG (Zhou et al., 1999) cause protein misfolding and forward trafficking defects. The patient with the E282K mutant K_{ATP} channels however had

consistently high insulin levels leading to severe hypoglycemia and did not respond to treatment with diazoxide, a potassium channel activator. Moreover, co-immunoprecipitation studies using myc-SUR1 as bait suggested that HA-Kir6.2^{E282K} was capable of binding SUR-1 (Taneja et al., 2009). Also, co-expression with the wild type channel rescued the E282K mutant subunits to the cell surface (Figure 3.16) and formed functional channels (Taneja et al., 2009, J. Mankouri thesis). These data indicated that the mutation E282K did not affect folding of the Kir6.2 subunit, nor did it affect its association with other Kir6.2^{WT} and SUR1 subunits. Therefore the ER retention of the E282K mutant K$_{ATP}$ channels appears to be mechanistically different from the previously reported mutations where misfolding was the cause of deficient trafficking.

E^{282} was part of the stretch D^{280}L^{281}E^{282} on the Kir6.2 C-terminus. This sequence in which two acidic amino acids separated by a non-acidic amino acid has been identified to act as the diacidic ER exit motif [(D/E) X (D/E)] in several membrane proteins including VSV-G (Nishimura et al., 1999), CFTR (Wang et al., 2004b) and some potassium channels such as TASK-3 (Zuzarte et al., 2007, Barlowe, 2003, Nishimura and Balch, 1997 ; see Figure 3.2). The DXE motif is required for the transport of proteins from the ER in COPII vesicles. Recruitment of cargo into COPII vesicles is initiated by the activation of Sar1 GTPase, which involves exchange of bound GDP for GTP in a reaction catalyzed by the GDP-GTP exchange factor Sec12. This is followed by the attachment of activated Sar1 to the ER membrane, which in turn recruits the Sec23-Sec24 hetero-dimer by binding to the Sec23 protein. Sec24 captures cargo by interacting with the ER export signals. Sec13–Sec31 coat proteins are then added, leading to the formation of the pre-budding complex, which when fully formed is released into the cytoplasm as a COPII-coated vesicle for transport to the Golgi apparatus.

The Sec24 protein can recognize COPII cargo with high specificity through interaction with the ER exit motifs present of COPII cargoes which allows recruitment of the cargo protein into COPII vesicles for exit from ER (Miller et al., 2002). Disruption of the acidic amino acids of this motif causes ER retention (Nishimura et al., 1999). Mutation of the residues D and E of D^{280}L^{281}E^{282} but not L to their neutral amide forms resulted in lack of surface expression like the E282K mutant (Figure 3.3). These data suggested that DLE stretch on Kir6.2 could be acting as the diacidic ER exit motif known to be critical for export of cargo proteins in COPII vesicle.

The assembly of the COPII vesicles at the ERES located on the ER membrane is a part of a concentrative step that ensures efficient delivery of proteins to the cell surface (Barlowe, 2003, Miller et al., 2003, Mossessova et al., 2003, Fromme et al., 2008, Gurkan et al., 2006, Wang et al., 2004b). Formation of the COPII coat is considered to initiate with the recruitment of Sar1-GTP to the ERES and budding of the COPII vesicle containing its cargo requires hydrolysis of Sar1-GTP to Sar1-GDP (Bi et al., 2002, Barlowe, 2002). The Sar1 mutant Sar1^{T39N} is a weak dominant negative and is 'GDP on'; therefore over-expression of this mutant prevents COPII vesicle formation. The mutant Sar1^{H79G} is 'GTP on' and therefore favours COPII vesicle formation but not vesicle budding resulting in the accumulation of cargo in COPII vesicles at ERES (Nishimura et al., 1999, Wang et al., 2004b). Co-expression of K_{ATP} channels with the Sar1 mutants prevented surface expression of the channel (Figure 3.4), indicating that forward trafficking of K_{ATP} channels is Sar1 dependent. Sar1^{H79G} also prevents surface expression of the GFP-VSV-G^{ts045} protein and arrests it in the COPII vesicles in ERES. Effect of Sar1^{H79G} on GFP-VSV-G^{ts045} was similar to that of the temperature shift treatment (37°C-39.5°C-10°C) that arrests the protein in ERES (Mezzacasa and Helenius, 2002). GFP-VSV-G^{ts045} appears as punctate structures in the perinuclear region (Figure 3.5). The wild type K_{ATP} channels (HA-Kir6.2^{WT}+ SUR1) entered the ERES marked by GFP-VSV-G^{ts045} in the temperature shift experiment as well as in presence of Sar1^{H79G} (Figure3.6A). However, the mutant K_{ATP} channels made of the HA-Kir6.2^{E282K} and SUR1 subunits did not enter ERES (Figure 3.6B). Thus an intact DLE motif on Kir6.2 is critical for entry of the channels into ERES for export out of the ER.

Each of the K_{ATP} channel subunits Kir6.2^{WT} and SUR1 expressed independently of each other were capable of entering into ERES (Figure 3.7). These data presented some interesting evidence towards the existence of a signal on SUR1 for sorting into COPII vesicles at ERES. In native cells, both the subunits of the K_{ATP} channels are co-expressed and it has been reported that both Kir6.2 and SUR1 contains an ER retention signal 'RKR' which retains un-assembled subunits in the ER (Zerangue et al., 1999). The study suggested that Kir6.2 subunits assemble into tetramers and the ER retention RKR motifs are exposed. Assembly with SUR1 subunits completes the formation of the octameric channels. This assembly masks the exposed RKR motifs and allows trafficking of fully assembled channels to the cell surface. The evidence towards this theory was that the K_{ATP} channel subunits expressed independently of each other did not express on the cell surface (Zerangue et al., 1999, Crane and Aguilar-Bryan, 2004). Studies on the RKR motif suggested that 14-3-3 proteins have a role in probing the assembly of the K_{ATP} channels in the post ER compartment

(Heusser et al., 2006). If there are any partially assembled channels with exposed RKR signals, they would be bound by 14-3-3 proteins that is recognised by the COPI machinery. The COPI vesicle transports the unassembled channels back to the ER (Heusser et al., 2006, Mrowiec and Schwappach, 2006).

If it was considered that the channel subunits assemble prior to ER exit, then since the E282K mutant Kir6.2 subunit could associate with SUR1 (Taneja et al., 2009), it should be rescued to the cell membrane with the help of the ER exit signal on SUR1 (Sharma et al., 1999). However, the mutant channel co-expressed with SUR1 did not express on cell surface (Figure 3.3 top panel). Therefore, ER exit motif on Kir6.2 was critical for COPII mediated ER exit of the channels. Also, co-expression with the wild type Kir6.2 subunits rescued the E282K mutant to the cell surface. Therefore, the Kir6.2 subunits must assemble prior to ER exit and it was most likely that they formed tetramers. Both Kir6.2 and SUR1 subunits were capable of independently reaching the post-ER destination of ERGIC compartments (Figure 3.7) and the RKR motif did not cause ER retention of the subunits. Taken together these data suggest that the Kir6.2 subunits must dimerise or multimerise in the ER prior to ER exit and the complete assembly of the channel by binding of the SUR1 subunits may be occurring in the ERGIC compartment.

Any unassembled channels or channel subunits must be returned back to the ER in the COPI vesicle due to recognition of the un-masked RXR motifs. Therefore the RKR motif on the K_{ATP} channel subunits is more likely to act as an ER-retrieval signal rather than the ER-retention signal. This model of K_{ATP} channel assembly is further supported by the consideration that in the fully assembled state (Mikhailov et al., 2005), the ER exit signals on Kir6.2 subunits are quite likely to be masked by the SUR1 subunits preventing their recognition by the COPII machinery. Also, the fully assembled complex is 900 KDa and has a diameter of 18 nm (Mikhailov et al., 2005); while the COPII vesicles appear to be about 60-70 nm in diameter (Gurkan et al., 2006, Fromme and Schekman, 2005). Packaging of such a huge channel complex might pose mechanistic problems for the COPII coat machinery while individual subunits and partial complexes of the channel, on the other hand, could be more easily accommodated into COPII vesicles.

The molecular basis of interaction between the COPII complex and the DLE motif on the Kir6.2-CT was intriguing since it was this small stretch of three amino acids which was critical for expression of the channels on the cell surface. An analysis of the available structural information about the Kir6.2 subunits and the COPII proteins

showed that the binding site for the DLE motif on the Sec23.24-Sar1 complex of COPII is at an estimated distance of 20 Å from the membrane interface. The DLE motif on Kir6.2-CT is estimated to be located at a distance of 25 Å from the membrane interface (Figure 3.17). Therefore, the concave shaped Sec23/24-Sar1 complex should be favourably placed to bind the DXE motif and also bend the membrane to form the COPII vesicle (Barlowe, 2002, Fromme and Schekman, 2005, Taneja et al., 2009). However, if it is considered that the channel subunits assemble, it presents the question if the DLE motif is really accessible for binding to the COPII machinery and thereby mediate ER exit. These questions are answered by the data which show ability of the Kir6.2-CT to transfer the ability of Sar1-dependent ER exit in COPII vesicles to CD4 protein (Figure 3.10). The surface expression of CD4 is not Sar1-dependent (Figure 3.9). When the C-terminus of CD4 was replaced by the Kir6.2-CT containing the DLE motif, but no RKR signal, the fusion protein is expressed on cell surface in a Sar1-dependent manner and enters COPII vesicles at ERES (Figure 3.10).

Moreover, mutation E to K in the DXE motif of the fusion protein prevents surface expression of the fusion protein like the E282K mutant channel (Figure 3.11). Thus, the DXE motif on the Kir6.2-CT is required for interaction with the COPII complex for Sar-dependent ER exit. Disruption of the interaction between the DXE motif on Kir6.2 and COPII complex was possible using a membrane permeable TAT fusion peptide that had a stretch of the Kir6.2-CT containing the DLE sequence (Figure 3.12). The HIV TAT peptide stretch has been used to deliver small peptides into the cell (Schwarze et al., 2000). The stretch of DLE motif containing Kir6.2-CT fused to it, acted as a competitive cargo for the Sec24 binding. The TAT-DXE peptide could efficiently saturate the Sec24 binding sites for the diacidic ER exit motif (DXE) as cells treated with the TAT-DXE peptide but not the TAT or TAT-DXK peptide showed lack of surface expression of K_{ATP} (Figure 3.13, 3.15). The K_{ATP} channels in TAT-DXE treated cells were stuck in ER and did not enter ERGIC (Figure 3.16), which confirmed that interaction with Sec23/24-Sar1 complex was necessary for export out of ER. In cells transfected to express the K_{ATP} channel, treatment with the TAT-DXE peptide could significantly reduce the surface expression of the channels within 24 hours of treatment (Figure 3.13) but a similar effect of the TAT-DXE peptide could be seen in the cells stably expressing the K_{ATP} channels after 96 hours of treatment of the cells (Figure 3.15). This is because the peptide treatment affects the channels only during their synthesis and so in cells consistently expressing the channels, treatment of the peptide would not become apparent till all the channels that are already expressed in the cells and are on the cell surface or a part of endosomal recycling pathways reach the end of their lifecycle. The TAT-DXE peptide also prevented surface expression of the GFP-

VSV-G^{ts045} (Figure 3.14), indicating that the saturation of the DXE binding motif on Sec24 (Miller et al., 2002) affects ER export of all proteins that follow Sar1-dependent ER export. The peptide could therefore be used as a tool for studying COPII mediate ER export of proteins. Also, if details of the trafficking mechanisms are known, then with proper delivery systems in place, the TAT-conjugated peptides may be considered for altering surface expression of the channel protein for therapeutic applications.

This study initiated with the report (Christesen et al., 2007) of a Swedish patient who was suffering from a focal from of CHI and had inherited the E282K mutation in the Kir6.2 subunit of the K$_{ATP}$ channel. K$_{ATP}$ channel activity in the pancreatic β-cells regulates insulin secretion in response to the metabolic state of the cell (Ashcroft, 2005, Dunne et al., 2004). Channel closure or absence from the cell surface leads to pancreatic β-cell membrane depolarization which opens the depolarization dependent Ca^{2+} channels. Influx of Ca^{2+} into the cell causes insulin secretion (Ashcroft, 2005, Nichols, 2006 , see Chapter1 and Figure 1.4). Lack of K$_{ATP}$ channel expression on cell surface would result in continued insulin secretion as observed in the patient. The absence of the E282K mutant K$_{ATP}$ channel from the cell surface therefore accounted for the disease phenotype and the molecular basis of this lack of surface expression of the mutant channel presented itself as an interesting point of study.

The patient's pancreas had two populations of cells, one which expressed just the E282K mutant channels which also lacked the tumour suppressor protein. These cells were therefore tumorous and foci of these tumorous cells were secreting insulin in an unregulated manner. Since they expressed mutant E282K channels that are stuck in the ER due to the abrogated DXE motif, absence of the K$_{ATP}$ channels in these cells led to unregulated insulin secretion by the cells. Following resection of the focal hyperinsulinaemic area to remove the tumorous focal region of the pancreas, the patients was clinically cured. This could be explained as follows: the population of cells in the islets of the patient left behind after the pancreactomy expressed both wild type and the E282K mutant channel subunits. The wild type subunits when co-expressed, rescue the mutant channel subunits to the cell surface (Figure 3.16). Moreover, there would be a mixed population of K$_{ATP}$ channels having different combinations of the WT and E282K mutant subunits in the K$_{ATP}$ channels in these cells. Currents recorded from *Xenopus oocytes* (Taneja et al., 2009 and thesis of J. Mankouri) show that the heteromers are functional as well. Thus, having removed the cells secreting excessive insulin, the patient is left with islets that have functional K$_{ATP}$ channels and therefore are capable of normal glucose stimulated insulin secretion (Arnoux et al., 2010). Thus, the

molecular basis of the cure of focal form of CHI is explained in support of the clinical cure of the disease.
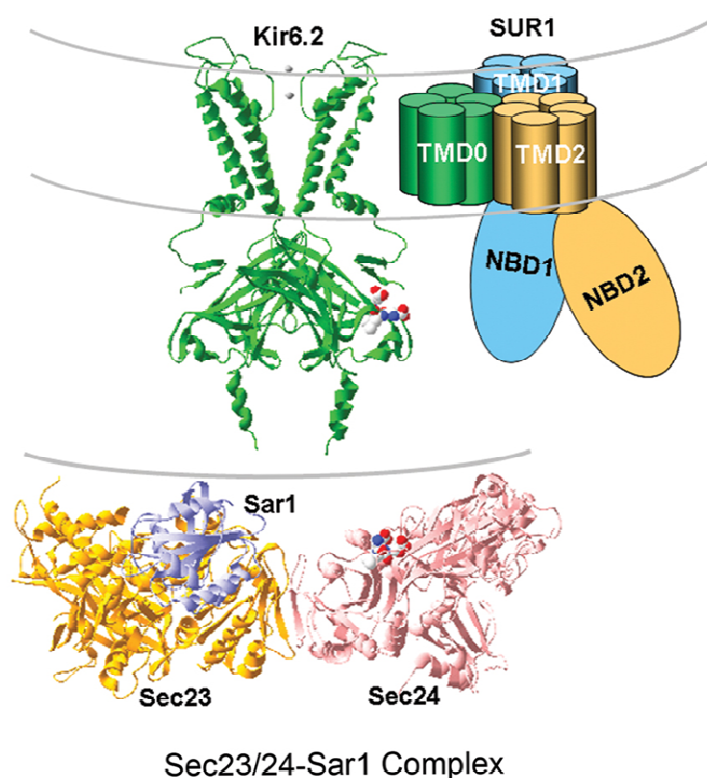
Figure 3.17 K$_{ATP}$ channel and the Sec23-Sec24/Sar1 complex. Structural model of Kir6.2 (Antcliff et al., 2005), schematic of SUR1 and the crystal structure of Sec23/24-Sar1 complex (Bi et al., 2002), shown to the same scale as Kir6.2. In Kir6.2 only two diagonally opposite subunits are shown. The DLE residues of Kir6.2 are highlighted in CPK and are situated approximately 25Å away from the putative membrane border (shown as grey lines). Depicted next to it is the schematic of one SUR1 subunit, containing 17 transmembrane (TM) segments organized into three domains, TMD0 (TM segments 1-5), TMD1 (TM segments 6-11), and TMD2 (TM segment 12-17), and the two cytosolic nucleotide binding domains (NBD1 and NBD2) that follow TMD1 and TMD2. The bottom image shows the structure of the (QLKDLESQI), shown in CPK, bound to the binding pocket; the peptide is located approximately 20Å away from the putative vesicle membrane border (grey line). The Sec23/24-Sar1 complex (Mossessova et al., 2003) has a bow-tie shape and is thus curved to conform to the spherical shape of a vesicle. The complex is an elongated thin particle, measuring ~150Å in the long direction (parallel to the membrane) and about 40Å in the direction away from the membrane. CPK: colouring scheme for atoms where H atoms are in white, carbon in black. Nitrogen in blue and oxygen atoms are depicted in red

3.5 Summary

The study of molecular basis of CHI causing mutation E282K in the Kir6.2 subunits of the K_{ATP} channels has led to the discovery of the presence of a diacidic ER exit motif (DXE) on the Kir6.2 C-terminus formed by the $D^{280}L^{281}E^{282}$ stretch of amino acids. Disruption of this motif due to the mutation E282K in the Kir6.2 prevented the surface expression of the channel. The DXE motif is shown to allow the concentration of the channels in COPII enriched ERES. Entry of the channels into COPII vesicles in a Sar1-GTPase dependent manner is required for entry of the channels into the ERES for transport out of the ER. Co-expression with the wild type Kir6.2 subunits rescues the E282K mutant Kir6.2 subunits to express on cell surface which shows that the mutation has no affect on the channel properties or folding and also explains the clinical cure of the patient following pancreactomy. Further, this study has not only provided explanation to the molecular nature of the disease but has also given insights into the mechanisms of channel assembly. The study suggests that the Kir6.2 subunits assemble in the ER prior to ER exit but rest of the channel assembly with SUR1 subunits is more likely to occur in a post ER compartment. Also, from the experiments that show rescue of surface expression of the E282K mutant subunits by WT-Kir6.2 subunits, it seems that all the four DLE motifs from the four Kir6.2 subunits of the channel are not necessary for entry into the COPII vesicles and ER export. The present data suggest that the RKR motif on the Kir6.2 subunits appears to function as the ER retrieval signal since the channel subunits are on their own able to exit ER and reach ERGIC. The RKR signal is therefore more likely to retrieve partially assembled K_{ATP} channels from the ERGIC to the ER. This model of the K_{ATP} channel assembly and ER export that emerged from the studies presented in this chapter is illustrated in Figure 3.18.

The ER exit signal has physiological importance as its abrogation causes severe CHI. Disease causing mutations have been reported in genes encoding the components of the COPII machinery, including Sar1 (Jones et al., 2003) and Sec23 (Boyadjiev et al., 2006); however, this study provides the first example of a mutation in a cargo protein causing disease in humans. Since the motif works through interaction with the proteins of the COPII machinery it was possible to design and employ a membrane permeable TAT fusion peptide (TAT-DXE) which acts as a competing cargo for binding the COPII complex and prevents surface expression of the K_{ATP} channel. This peptide could be used as a tool in trafficking studies or for altering surface expression of the channel protein for therapeutic applications.
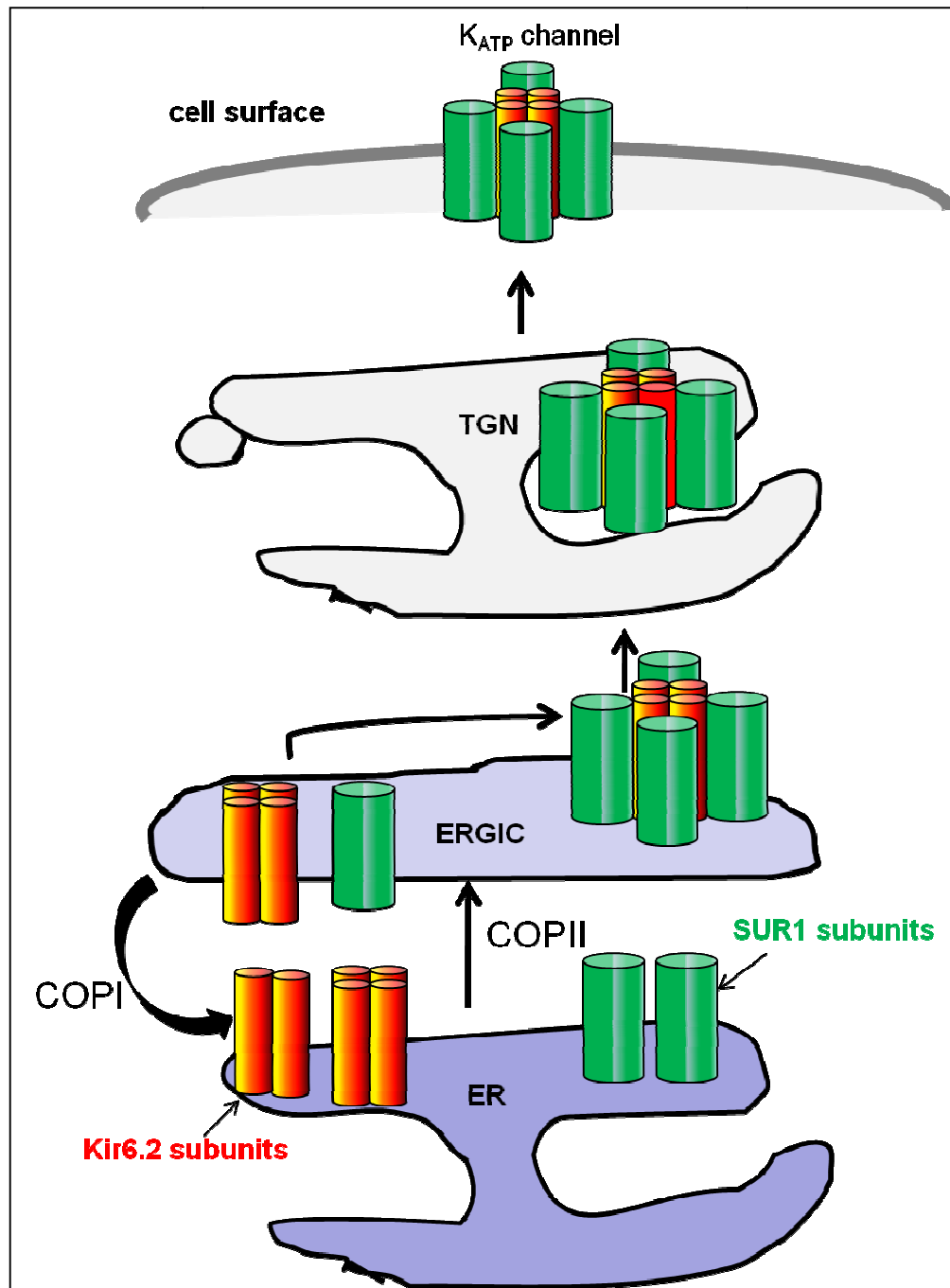
Figure 3.18 Schematic of assembly trafficking of the K_{ATP} channel subunits. The Kir6.2 and SUR1 subunits are expressed in the ER. The Kir6.2 subunits dimerise or multimerise, followed by entry into the COPII vesicles which requires the diacidic ER exit motif (DLE) present on the Kir6.2-CT. All the four subunits do not need to have and intact DLE sequence. The Kir6.2 and SUR1 subunits are exported out of the ER and enter ERGIC compartments where they must be assembled into the octameric K_{ATP} channels with four subunits each of the Kir6.2 and SUR1. Un-assembled channels which have un-masked RKR motifs are transported back to the ER by action of the 14-3-3 proteins. The octameric K_{ATP} channels are processed in the Golgi and expressed on the cell surface.

CHAPTER 4

Sar1-GTPase dependent ER exit of cardiac hERG potassium channels

4.1 Introduction

The hERG (human *ether-a-go-go related gene*) potassium channel (Kv11.1), encoded by the *KCNH2* gene, underlies the rapidly activating delayed rectifier K$^+$ current (IK$_r$), which is the most important component of the repolarisation phase of the cardiac action potential (Sanguinetti et al., 1995, Sanguinetti and Tristani-Firouzi, 2006). Its importance in cardiac function is underscored by the identification of >200 inherited loss-of-function mutations that lead to long QT syndrome 2 (LQTS2) (OMIM: 152427) in which the QT interval of the electrocardiogram is lengthened leading to potentially fatal arrhythmias (Sanguinetti and Tristani-Firouzi, 2006, Anderson et al., 2006, Rajamani et al., 2002, Furutani et al., 1999, Sanguinetti et al., 1995). More alarmingly, a wide range of pharmaceutical agents have been shown to cause LQTS2 through interactions with hERG, leading to the withdrawal of several useful clinical agents (e.g., terfenadine, cisapride and grepafloxacin) (Brown, 2004). Testing of novel therapeutic agents for potential deleterious effects on hERG function has therefore become mandatory and it remains one of the principal causes of failure in pre-clinical testing. A relatively rare but related disorder, short QT syndrome 1 (SQT1) (OMIM: 609620) results from gain-of-function mutation in hERG where the biophysical properties of the channel are altered (Brugada et al., 2005, Hong et al., 2005).

Hereditary LQTS2 mutations and drugs affect the channel in two ways: some inhibit channel function or alter its biophysical properties, whereas others reduce the channel density at the cell surface (Robertson and January, 2006, Sanguinetti and Tristani-Firouzi, 2006, Rajamani et al., 2006, Eckhardt et al., 2005, Ficker et al., 2005). Recent studies suggest that defective trafficking may be the most dominant mechanism for the loss of hERG function (Anderson et al., 2006). Interestingly, defective trafficking caused by many mutations could be rescued pharmacologically in several cases (Robertson and January, 2006, Delisle et al., 2003, Rajamani et al., 2002, Zhou et al., 1999, Ficker et al., 2005, Gong et al., 2006). Several groups have investigated the mechanisms underlying the defective trafficking of the hERG mutant channels and the pharmacological rescue. It seems that most mutations cause misfolding of the channel protein, resulting in retention by the quality control machinery of the ER. Molecular chaperones, including Hsc70 (70 KDa heat shock cognate protein), Hsp90 (90 KDa heat shock protein) (Ficker et al., 2003) and calnexin (Gong et al., 2006) are involved in the ER retention. Studies showed that they bind the misfolded channels more strongly than the wild type channel (Ficker et al., 2003, Gong et al., 2006). Drugs which rescue defective trafficking appear to work by weakening such interactions with chaperones

(Gong et al., 2006, Ficker et al., 2003). Misfolded mutant proteins have been shown to undergo degradation by the cytosolic proteasomes in a process that involves poly-ubiquitinylation and deglycosylation (Gong et al., 2005, Kagan et al., 2000).

Despite the patho-physiological importance, the mechanisms by which hERG channels traffic to the cell surface and how trafficking is regulated are not fully understood. Many membrane proteins contain signals in their primary sequence that control their ER exit (Ellgaard and Helenius, 2003). Some proteins contain ER retention/retrieval signals that play a crucial role in the ER quality control by allowing only properly folded and fully assembled proteins to exit the ER (Ellgaard and Helenius, 2003). Some contain export signals that promote efficient ER export (Barlowe, 2003, Mossessova et al., 2003, Gurkan et al., 2006, Fromme et al., 2008, Ellgaard and Helenius, 2003, Miller et al., 2003). Native IKr channels are made up of two subunits, hERG1a and hERG1b that are products of the alternate transcripts of *KCNH2*; they differ only in the N-terminus. hERG1b has an ER retention signal of the RXR type that prevents its surface expression unless hetero-oligomerisation with hERG1a masks the retention signal (Phartiyal et al., 2007). However, it is not known if hERG has an ER export motif. In a recent study, Delisle et. al. reported that the surface expression of hERG is prevented by a dominant negative construct of Sar1-GTPase (Delisle et al., 2009). Based on this observation, the authors proposed that hERG may exit the ER via COPII vesicles. However, entry of the channel into COPII vesicles was not demonstrated.

Studies showed that membrane proteins destined to exit the ER via COPII vesicles contain discrete ER export signals. These include the diacidic motifs [(D/E)X(D/E)], di-hydrophobic motifs (FF, YY, LL or FY), YXXXNPF and LXXLE motifs (Barlowe, 2003, Mossessova et al., 2003, Fromme et al., 2008, Gurkan et al., 2006, Nishimura et al., 1999, Wang et al., 2004b). The COPII machinery recognizes the ER exit signals on proteins destined to exit the ER and package the proteins into COPII vesicles in a process that requires Sar1-GTPase (Gurkan et al., 2006, Fromme et al., 2008). The cargo-loaded vesicles exit the ER from specialized sites, known as the ER exit sites (ERES) and deliver the cargo protein to the ER-Golgi intermediate compartment, from where the proteins traffic to the plasma membrane via the Golgi (Barlowe, 2003, Fromme et al., 2008, Miller et al., 2003, Mossessova et al., 2003). hERG has several potential ER exit motifs in its C-terminus, including three diacidic motifs (Nishimura et al., 1999), which is consistent with the proposition that hERG might exit the ER via COPII vesicles.

In this chapter, the mechanism of ER exit of hERG was investigated using a temperature sensitive mutant of GFP-tagged VSV-G protein (GFP-VSV-G^{ts045}), as a reporter protein. Dominant negative mutants of Sar1-GTPase required for COPII mediated ER exit and Sec24 blocking peptides (described in Chapter 3) to examine the process of ER exit. Our results demonstrate that hERG exits the ER via COPII vesicles in the same way as GFP-VSV-G^{ts045}. Further, the location of the DXE motif on the distal C-terminus of hERG was investigated. The results show that, unlike VSVG, hERG does not appear to use diacidic ER exit motifs to access the COPII coat machinery.

4.2 Materials and Methods

4.2.1 Plasmid constructs

HA-tagged hERG in pcDNA3 was transfected into HEK-MSRII cells for transient expression of the HA-hERG channels. HA-hERG truncation mutants were prepared by inserting a stop codon using QuikChange® PCR by other members of the Rao lab. For details of the Sar1 constructs and GFP-VSVG[ts045] see Materials and methods section in Chapter 3.

4.2.2 Antibodies

Antibodies against the HA-tag on the hERG channels were diluted and used as in Chapter 3.

4.2.3 TAT-conjugated peptides

Tat (YGRKKRRQRRR), Tat-DXE (YGRKKRRQRRRHHQDLEIIV) and Tat-DXK (YGRKKRRQRRRHHQDLKIIV) peptides were used as in Chapter 3.

4.2.4 Immunofluorescence staining

Cells were stained for HA-hERG channels (wt or mutants) using antibodies against the HA- epitope for immunofluorescence imaging using the protocols described in Chapter2, section 2.5.

4.2.5 Determination of surface density of channels (chemiluminescence assay)

For quantification of cell surface density of the HA-hERG channels, the chemiluminescence assay was used as described in Chapter 3.

4.3 Results

4.3.1 Characterisation of the HA-hERG construct

The aim of this study was to investigate the ER exit mechanisms for the hERG potassium channels. ER exit is a key step in the forward trafficking of the channels and a major determinant of surface density. For this study, a hERG construct (referred to as HA-hERG) with an HA-epitope inserted between the extracellular loop between the S1 and S2 transmembrane domain of the channel (Ficker et al., 2003) was used (Figure 4.2.1A, see Chapter 2, section 2.2.10 for details). HEK-MSRII cells were transfected to express the HA-hERG protein. The channels were immunostained to detect expression on cell surface (red) and within the cell (green), (see Chapter 2, section 2.5 for detailed protocol). A substantial proportion of HA-hERG channels expressed by the transfected HEK-MSRII cells are found at the plasma membrane (Figure 4.1). The channels conducted hERG currents in electrophysiological recordings done by other members of the lab as reported before (Ficker et al., 2003). Taken together, the HA-hERG channels are functional and express on cell surface and therefore suitable for further experiments to study the ER exit mechanisms of the channels.

4.3.2 Sar1-dependency of ER exit of the hERG potassium channels

Proteins can exit the ER via a non-specific, less efficient route, known as 'bulk flow', or via a more efficient, specific route where cargo proteins are concentrated into COPII vesicles in a process that involves Sar1 (Sato and Nakano, 2007c). Formation of the cargo containing COPII vesicles at ER exit sites (ERES) is Sar1-dependent (Barlowe, 2003, Fromme et al., 2008, Matsuoka et al., 1998). In order to examine the mode of hERG ER exit, HA-hERG channels were co-expressed with GFP-tagged, dominant negative constructs of Sar1; GFP-Sar1^{T39N} or GFP-Sar1^{H79G} to intercept the function of endogenous Sar1 protein. Sar1^{T39N} ('GDP-on') binds GTP poorly and prevents recruitment of cargo into COPII vesicles whereas Sar1^{H79G} ('GTP-on') is incapable of hydrolysing bound GTP and prevents release of COPII vesicles (Nishimura et al., 1999, Wang et al., 2004b, Kuge et al., 1994). The channels were immunostained to detect channels on cell surface (red). Both the dominant negative constructs, but not the wild type Sar1, co-expression prevented surface expression of the HA-hERG channels (Figure 4.2).
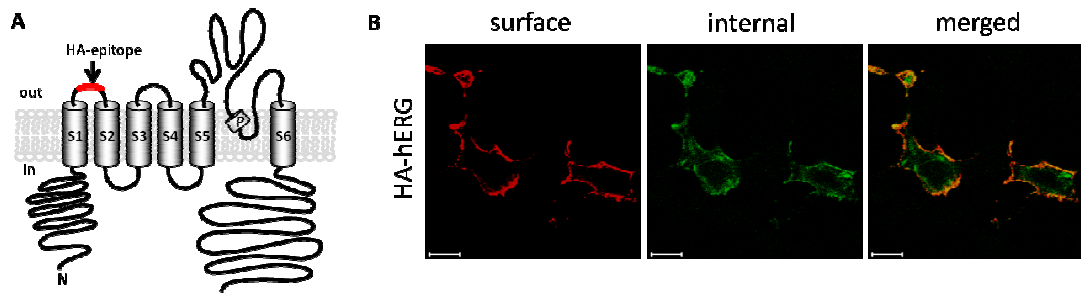
Figure 4.1 HA-hERG construct is expressed on cell surface in HEK-MSRII cells. (A) Schematic of the membrane topology of hERG channel subunit showing the position of the engineered HA epitope. (B) Expression of HA-hERG channels at the plasma membrane (red) and within (green) in transiently transfected HEK-MSRII cells detected by immunostaining with rat anti-HA antibodies, followed by the fluorescent anti-rat secondary antibodies (see methods for details). Representative confocal images from three independent experiments are shown; Scale bars: 10 μm.
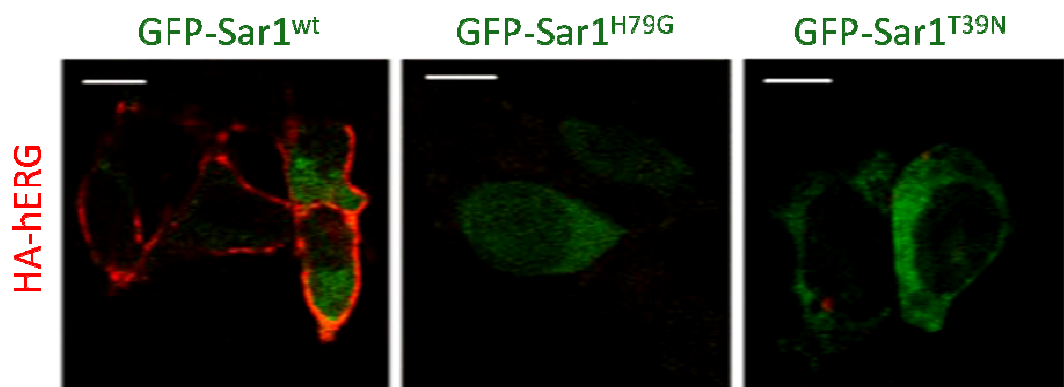
Figure 4.2 Surface expression of the hERG potassium channels is Sar1-dependent. HEK-MSRII cells co-expressing HA-hERG channels and the indicated GFP-Sar1 constructs (green) were stained to label the channel expressed on surface expression (red). Representative confocal images from three independent experiments are shown; Scale bars: 10 μm.

4.3.3 Entry of hERG channels into ERES and ERGIC

The above experimental results showed that surface expression of hERG channels is Sar1 dependent, consistent with the previous report (Mezzacasa and Helenius) that dominant negative mutants of Sar1 block surface expression of proteins that are transported by the COPII complex. However, these results did not indicate if HA-hERG is recruited into COPII vesicles. To address this question, the temperature sensitive mutant version of GFP-tagged vesicular stomatitis virus glycoprotein (GFP-VSVG^{ts045}) was used as a reporter (Mezzacasa and Helenius, 2002).

This protein, has been previously used to label the COPII enriched ERES and to follow forward trafficking of membrane proteins and to study ER exit of the pancreatic K$_{ATP}$ channel described in the previous chapter. At the non-permissive temperature (39.5°C), GFP-VSVG^{ts045} is misfolded and retained in the ER, but does not enter COPII vesicles. Upon shift to the permissive temperature (32°C or lower), it assumes correct folding and exits the ER via COPII vesicles, but this exit step can be arrested by switching from 39.5°C to 10°C, allowing visualization of COPII enriched ERES by confocal microscopy (Mezzacasa and Helenius, 2002). A similar effect could be reproduced by co-expression of the 'GTP-on' Sar1^{H79G} protein that prevents COPII vesicle budding (Kuge et al., 1994). The dominant negative Sar1 construct causes GFP-VSVG^{ts045} to accumulate in ERES, which appear as distinct green puncta that mark COPII vesicles at ERES (Figure 4.3.A). GFP-VSVG^{ts045} co-expressed with Sar1^{H79G} could also therefore be used as a reporter for Sar1^{H79G} activity through the appearance of punctate structures.

Control experiments, suggested that co-expression with GFP-VSVG^{ts045} had no effect on the surface expression of the channels (Figure 4.3.B). These data also suggested that GFP-VSVG^{ts045} and HA-hERG channels co-localise extensively, suggesting that the two proteins may follow a similar traffic route. Co-expression of Sar1^{H79G} prevented surface expression of both proteins and led to their co-localisation in punctate structures, representing ERES (Figure 4.3.C).

Further, when the HA-hERG channels expressed in the cells were seen to co-localise with ERGIC-53 (Figure 4.4), a marker for ERGIC (Appenzeller-Herzog and Hauri, 2006). This proved that the channels enter the ERGIC compartments following exit from the ER.
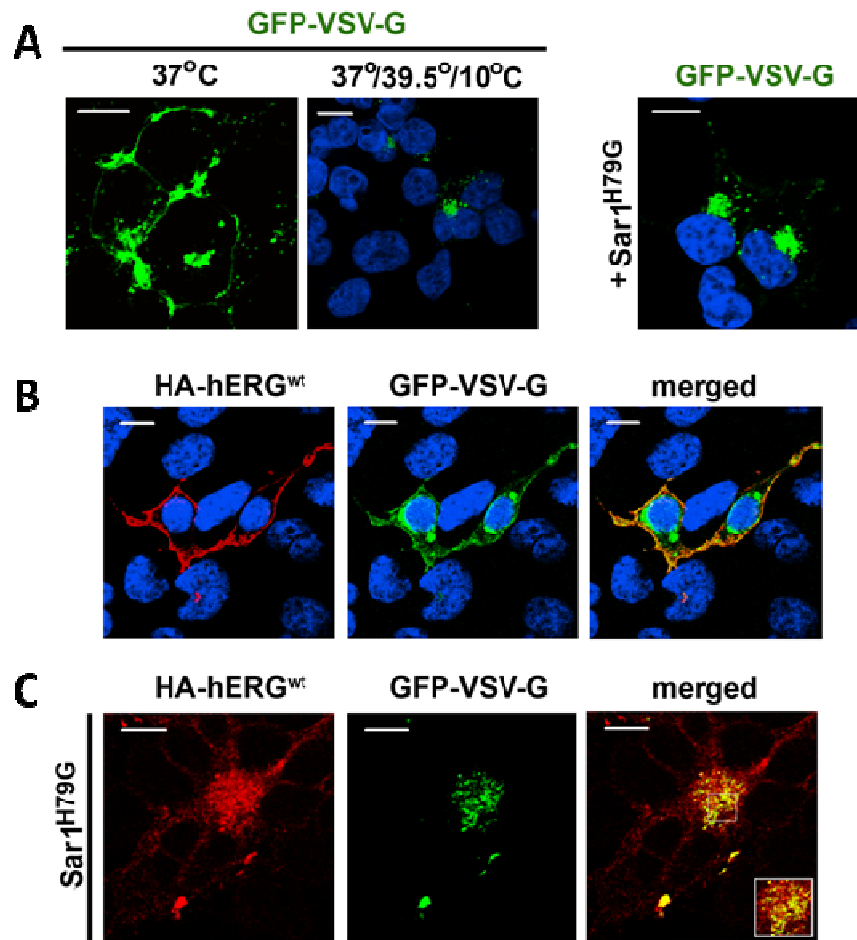
Figure 4.3 hERG enters ERES in the Sar1-dependent trafficking pathway. (A) Labelling ERES with GFP-VSVG^ts045. Shifts in incubation temperatures leads to accumulation of GFP-VSVG^ts045 in ERES; 37°C/39°C/10°C indicates successive incubations at 37°C (24 hrs), 39.5°C (18 hrs) and 10°C (5 hrs) before fixing and imaging. Co-expression of Sar1^H79G leads to the accumulation of GFP-VSVG^ts045 at ERES. (B) Co-expression of GFP-VSVG^ts045 has no effect on the surface expression of HA-hERG; nuclei are stained blue. (C) Co-expression of Sar1^H79G prevents surface expression of HA-hERG and leads to the accumulation of the channel (red) in ERES labelled with GFP-VSVG^ts045 (green); merged images show co-localisation (yellow) of the two proteins. Nuclei stained blue with DAPI. Representative confocal images from three independent experiments are shown; Scale bars: 10 µm.
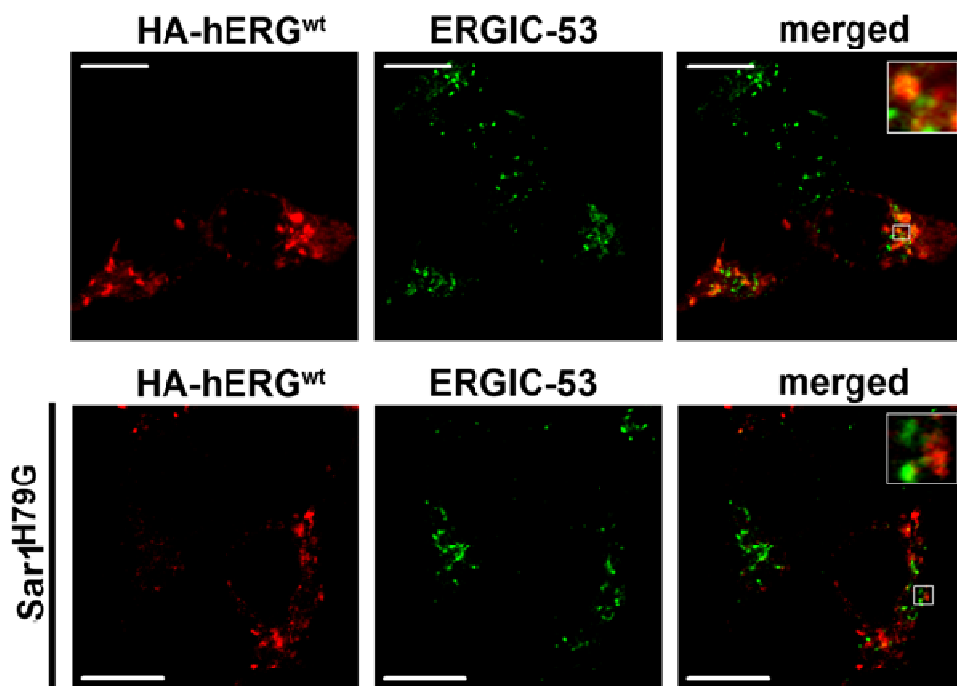
Figure 4.4 hERG entry into ERGIC is blocked by dominant negative Sar1. HA-hERG (red stain) co-stained with ERGIC-53 (green stain), a marker for the post ER compartments ERGIC (top panel). HA-hERG did not co-localise with ERGIC-53, when ER exit is blocked with Sar1^{H79G} (bottom panel). Representative confocal images from three independent experiments are shown; Scale bars: 10 μm.

However, when the Sar1^{H79G} was co- expressed in the HEK-MSRII cells, no co-localisation of HA-hERG with ERGIC-53 was observed which implied that the mutant Sar1 prevented ER exit of the channel. Taken together these data demonstrated that hERG enters COPII enriched ERES before exiting the ER on its way to the ERGIC compartment.

4.3.4 Probing interaction of hERG channels with cargo binding sites on Sec24

The COPII coat machinery binds cargo with its Sec24 subunits (see discussion in Chapter 3). Sec24 has discrete binding sites for ER exit signals located in the cytoplasmic region of cargo proteins (Barlowe, 2003, Mossessova et al., 2003, Wang et al., 2004b, Nishimura et al., 1999). One of the best characterised ER export signal is the diacidic motif, DXE (where D is aspartate, X is any amino acid and E is glutamate) (Wang et al., 2004b, Nishimura et al., 1999, Barlowe, 2003). The diacidic motif was found in a number of cargo proteins including VSV-G (Nishimura et al., 1999) and some potassium channels including the Kir6.2 subunit of the pancreatic K_{ATP} channel in the study presented in the previous chapter (Zuzarte et al., 2007, Taneja et al., 2009). The binding site for the DXE motif on Sec24 has been characterized using structural and biochemical approaches (Mossessova et al., 2003, Bi et al., 2002). Since, the ER export of hERG was Sar1 dependent, the hERG sequence was analysed to screen for a potential ER exit motif on hERG C-terminus which could be responsible for recognition by the COPII machinery. The hERG sequence had three potential DXE motifs (Figure 4.5). In addition, ER export of hERG appeared to be similar to that of VSV-G protein which has a functional DXE motif (Mezzacasa and Helenius, 2002 ; and Figure 4.3). Confirmation of the role of a DXE motif on the hERG C-terminus was therefore required.

The study investigating ER exit of K_{ATP} channels (Chapter 3) had led to the development of the membrane permeable TAT-DXE fusion peptide containing the diacidic ER exit signal (DLE) derived from the K_{ATP} channel (Mezzacasa and Helenius) fused to the HIV-TAT peptide sequence (Schwarze et al., 2000). The rationale underlying this approach was that the TAT peptide derived from a HIV-TAT protein sequence would facilitate penetration of the fusion peptide into the cell and that the peptide would bind the intracellular Sec24 protein of the COPII machinery with its DXE sequence. This interaction would saturate the DXE binding sites on Sec24 (Miller et al., 2002) and prevent the ER exit of any cargo bearing the diacidic ER export motifs.

hERG C-terminus

```
                   870X
860   FNLRDTNMIP| GSPGSTELEG  GFSRQRKRKL  SFRRRTDKDT  EQPGEVSALG


911   PGRAGAGPSS  RGRPGGPWGE  SPSSGPSSPE  SSEDEGPGRS  SSPLRLVPFS
                970X
961   SPRPPGEPPG| GEPLMEDCEK  SSDTCNPLSG  AFSGVSNIFS  FWGDSRGRQY
                                1029X
1011  QELPRCPAPT  PSLLNIPLSS  PGRRPRGDVE  SRLDALQRQL  NRLETRLSAD
         1073X
1071  MATVLQLLQR  QMTLVPPAYS  AVTTPGPGPT  STSPLLPVSP  LPTLTLDSLS


1221  QVSQFMACEE  LPPGAPELPQ  EGPTRRLSLP  GQLGALTSQP  LHRHGSDPGS
```

Figure 4.5 Potential ER exit motifs in hERG C-terminus. Amino acid sequence of the distal C-terminus of hERG showing the location of potential ER exit motifs (underlined) and positions of truncations (indicated with blue vertical lines).

As control, the TAT peptide and a mutant peptide, TAT-DXK was used. The mutant peptide is identical to TAT-DXE except that the conserved glutamate (E) residue is substituted with a lysine (K) which would inactivate the ER exit signal (Taneja et al., 2009 and Figure 4.6.A).

Treatment of cells with the TAT-DXE peptide but not the TAT or TAT-DXK peptides (controls) showed block of surface expression of the K_{ATP} channels (Chapter 3) and the VSV-G protein. GFP-VSV-G^{ts045} was used as a control in the experiment to look at the effect of the TAT peptides on surface expression the HA-hERG channels. (Figure 4.6.B) shows that the Tat-DXE peptide prevented surface expression of the GFP-VSV-G^{ts045} protein while neither of the two control peptides affected its surface expression. When cells expressing the HA-hERG channels were treated with the peptides, the Tat-DXE test peptide, but not the control TAT and TAT-DXK peptides, significantly suppressed the surface expression of HA-hERG (Figure 4.6.C). These data suggested that the hERG channels must contain an ER exit signal to promote its assembly into COPII vesicles and that a binding site for the signal exists on Sec24. Since the DXE peptide prevented the ER exit of the hERG channels, the data suggested that the ER exit signal on hERG channels was likely to be a diacidic motif (DXE). The data also strengthened the finding that ER exit of HA-hERG channels occurs via COPII vesicles in a Sar1-dependent manner.

4.3.5 Locating ER export signals in the distal end of the hERG C-terminus

The above data indicated that hERG channels may have a functional ER exit motif enabling recognition and binding to the Sec24 protein of the COPII complex and that it was more likely to be DXE and it would be interesting to identify this motif. hERG sequence analysis showed that there are three potential diacidic motifs (^{899}DTE, ^{976}DCE and ^{1036}DVE) in the cytoplasmic portion of the channel, all located in the distal C-terminal domain. Other potential signals in the C-terminus include a LXXLE motif (^{1049}LXXLE^{1053}) and a number of di-hydrophobic signals (Figure 4.5). Since there were several potential ER exit signals in the C-terminus, in order to identify the key motif, mutants with a series of truncations, 1073X, 1029X, 970X and 870X, (where X is a stop signal) in the distal C-terminus of the hERG channel were used. These truncations sequentially removed all the three potential DXE motifs, the LXXLE motif and three LL motifs.

A

TAT   YGRKKRRQRRR

TAT-DXE YGRKKRRQRRRHHQ**DLE**IIV

TAT-DXK YGRKKRRQRRRHHQ**DLK**IIV

B

GFP-VSV-G

TAT · TAT-DXE · TAT-DXK

C

HA-hERG
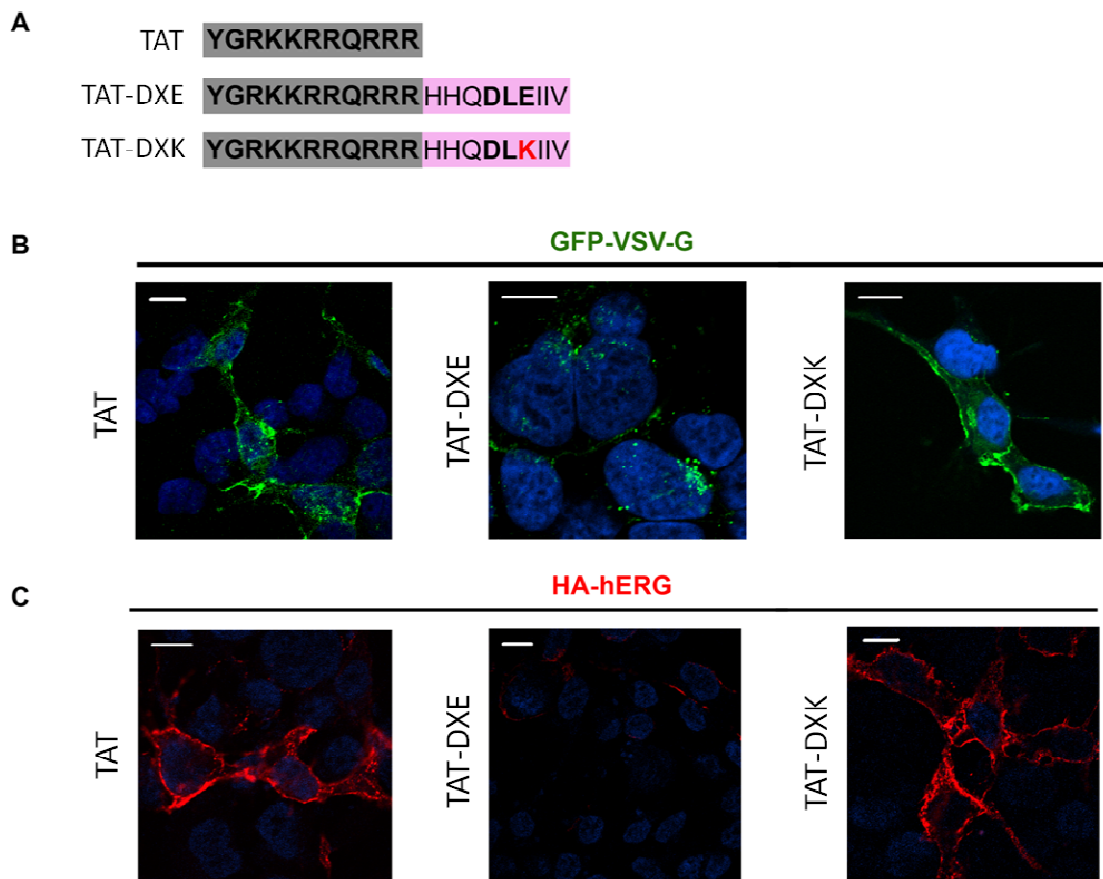
TAT · TAT-DXE · TAT-DXK

Figure 4.6 Peptides that compete for the cargo binding sites on Sec24 prevent surface expression of hERG. (A) Schematic representation of the TAT, TAT-DXE and TAT-DXK peptides. (B-C) HEK-MSRII cells expressing GFP-VSV-G^{ts045} (B) or HA-hERG (C) were treated with the indicated TAT and TAT-conjugated peptides (0.5 μM; see methods). The cells were fixed and the channels expressed on cell surface were stained using anti HA-antibody (red). Nuclei were stained with DAPI. Representative confocal images from three independent experiments are shown; Scale bars: 10 μm.

Truncation mutants extending into the proximal C-terminus of hERG were not used as this region contains the cyclic nucleotide binding domain (CNBD-742-842), which is important for the function of hERG channels (Akhavan et al., 2005). The hypothesis was that if the key motif was absent in the deletion mutant, then the Sar1 dependent expression of the channels on cell surface would be lost. None of the four truncations prevented surface expression of the channel (Figure 4.7.A). These data suggest that none of the three DXE motifs and other motifs found in the distal C-terminus direct the channels to the COPII coat machinery. Furthermore, the truncations failed to prevent dependency of hERG on Sar1 for ER exit: Co-expression of Sar1^{H79G} prevented surface expression of all truncation mutants and led to their accumulation in ERES marked by GFP-VSV-G^{ts045} (Figure 4.7B). This result was somewhat unexpected given the fact ER exit of hERG channels could be blocked with a DXE peptide. The channels were able to enter the COPII vesicles at ERES in a Sar1 dependent manner through interaction by some unidentified signal that allowed recognition and interaction with the COPII machinery.
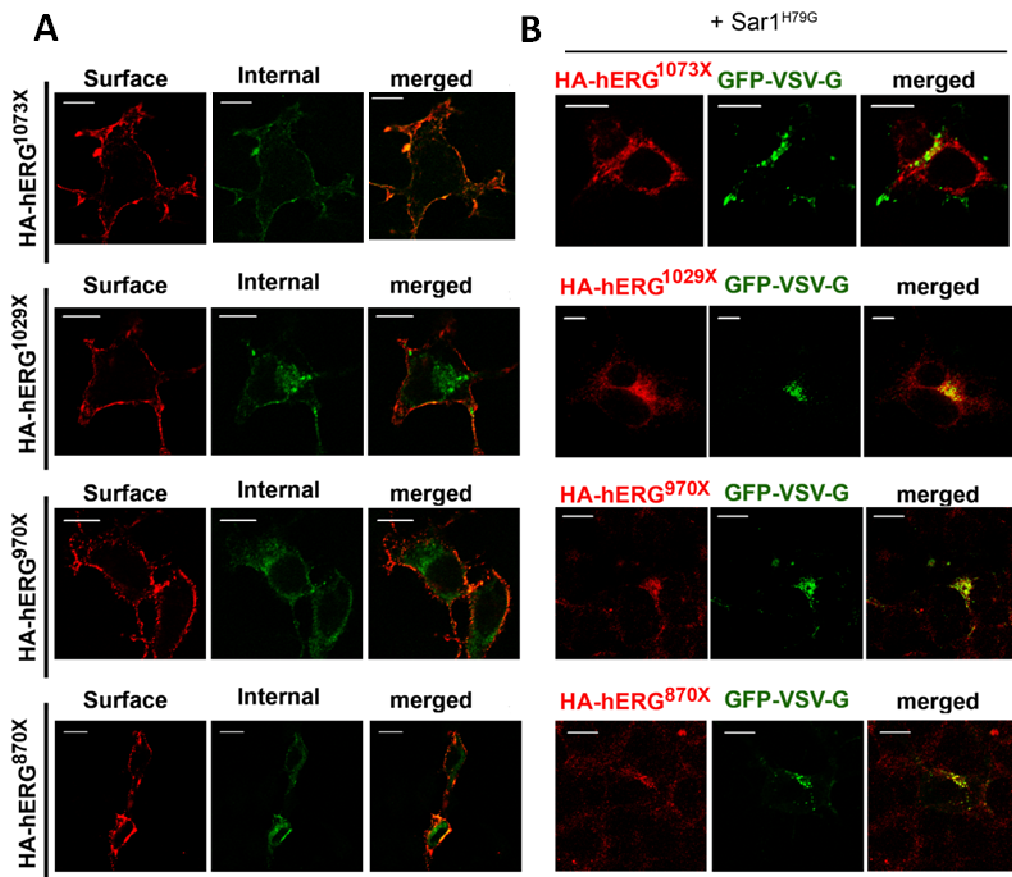
Figure 4.7 ER export signals are absent in the C-terminus of hERG distal to the cyclic nucleotide binding domain. Progressive deletion of the distal C-terminus of hERG fails to prevent surface expression (red) of the channel (A) and Sar1 dependency for ER exit (B). In (B), Sar1^{H79G} expression caused retention of HA-hERG (red) in ERES labelled with the co-expressed GFP-VSV-G^{ts045} (green). Representative confocal images shown from three independent experiments are shown; Scale bars: 10 µm.

4.4 Discussion

The C-terminus of hERG channels has been implicated in its forward trafficking. However, not much is known about the mechanism underlying the ER exit of the channels. The study aimed at investigating the forward trafficking of the channels and found that the ER exit of hERG channels is mediated by COPII vesicles in a Sar1 dependent manner. The channels enter the COPII vesicles and are exported out of the ER from ERES.

The hERG C-terminus is large (462 amino acids) and is reported to be important for proper IKr function (Kupershmidt et al., 1998). Patients suffering from congenital LQTS2 have mutations within the hERG C-terminus. The disease is attributed the lack of channel function. Impaired trafficking of the channel is one of the major causes of the disease. Channel trafficking may be affected due to protein misfolding or due to anomalies in forward trafficking or recycling of the channel (Anderson et al., 2006, January et al., 2000). Therefore, knowledge of how the anterograde trafficking of the hERG channels occurs may be critical for understanding the channel patho-physiology.

Export of the newly synthesised proteins from ER is a key step in the forward trafficking of a protein since it also may regulate entry of only correctly folded proteins into the forward trafficking route. Some proteins can exit the ER either via a nonspecific process known as 'bulk flow' (Barlowe, 2003, Gurkan et al., 2006, Fromme et al., 2008). But an increasing number of proteins appear to exit the ER via a more efficient process, involving selective recruitment of the cargo into COPII vesicles. Concentration of cargo greatly exceeds the bulk flow marker proteins in these vesicles. This selective recruitment is driven by ER export signals located in the cytoplasmic domains of the cargo protein that are recognised and bound by the Sec24 proteins of the COPII complex (Mossessova et al., 2003, Barlowe, 2003, Zuzarte et al., 2007). The mechanism by which cargo is captured into COPII vesicles has been extensively studied using biochemical, cell biological and structural approaches (Mossessova et al., 2003, Bi et al., 2002, Fromme et al., 2008, Gurkan et al., 2006). COPII vesicle formation requires the Sar1-GTPase and involves a cascade of steps (see Figure 1.9 and discussion in Chapter 3).

It has been reported that hERG C-terminus has a putative ER retention motif (R-X-R) (Nufer and Hauri, 2003) at amino acids 1005 to 1007 which is exposed in misfolded hERG proteins with mutations resulting in a reduced number of hERG proteins at the

cell membrane (Kupershmidt et al., 2002, Delisle et al., 2003, Rajamani et al., 2006). Deletion of the RKR motif from the hERG C-terminus has been shown to increase hERG currents. Therefore, this signal is thought to regulate export of correctly folded and assembled hERG protein from the ER. Existence of beta subunits of hERG is not well established. Proteins such as MinK are known to associate with hERG channel; however, their requirement is not considered to be critical for hERG expression and function on cell surface (Sanguinetti and Tristani-Firouzi, 2006). Therefore, these subunits of hERG are unlikely to contribute towards ER export of the channel. Considering the importance of channel subunit assembly as well as correct channel subunit folding, it was less likely that the channel is exported from the ER by bulk flow.

In order to study trafficking of the channel, an HA-epitope tagged construct of hERG was used. The epitope on the extracellular loop of the channel allowed detection of the channel on cell surface and within the cell (Figure 4.1). Experiments showed that trafficking of the HA-hERG channels to the cell surface is significantly reduced by Sar1 mutants (Figure 4.2). Electrophysiological studies (done by other members of the lab) using patch-clamp analysis also showed significant decrease in hERG currents in cells co-expressing $Sar1^{T39N}$ as compared to the $Sar1^{WT}$. Sar1-GTPase is recruited to the COPII vesicle assembly site by conversion from Sar1-GDP to Sar1-GTP, a step that is considered to initiate the COPII vesicle formation. The cargo is packaged into the vesicle which then buds off from the ER following hydrolysis of Sar1-GTP to Sar1-GDP. Disruption of Sar1 function by over-expression of the Sar1 mutants $Sar1^{H79G}$ and $Sar1^{T39N}$ that are 'GTP on' and 'GDP on' respectively would prevent COPII vesicle budding or formation and thereby affect Sar1-dependent COPII mediated ER export of proteins. This effect of Sar1 mutants was observed with the K_{ATP} channel surface expression which was found to be exported out of the ER in COPII vesicles (Chapter 3). Thus, lack of surface expression of the HA-hERG when Sar1 mutants were over-expressed indicated that the ER export of the protein was Sar1 dependent.

The entry the hERG channels into COPII vesicles at ERES was then confirmed through co-localisation with $GFP-VSV-G^{ts045}$. The protein was used as an ERES marker following a temperature shift treatment as described in the results section 4.2.3. Co-expression with $Sar1^{H79G}$ also accumulated the protein in COPII vesicles at ERES and when imaged, the protein appeared as punctate green spots close to the nucleus (Figure 4.3A). Since the co-expression of $GFP-VSV-G^{ts045}$ had no effect on surface expression of the HA-hERG channels (Figure 4.3B), the protein was used as a marker for ERES. The HA-hERG channels were found to co-localise with $GFP-VSV-G^{ts045}$ at the ERES (Figure 4.3C). These data showed that HA-hERG enters the COPII vesicles

at ERES. Moreover, the Sar1 mutant also prevented entry of the channel into the post-ER, ERGIC compartments (Figure 4.4). These data further strengthen the evidence towards requirement of Sar1 for COPII mediated ER export of the hERG channels.

If hERG channels entered the COPII vesicles like the K_{ATP} channels and GFP-VSV-G^{ts045} (Chapter 3), then there should be motifs on the channel C-terminus that allow recognition and binding to the Sec24 protein of the COPII machinery. Studies have shown that VSV-G uses the diacidic DXE motif to exit the ER (Nishimura et al., 1999). Crystallographic studies have shown that Sec24 has three cargo binding sites, A, B and C; the A-site binds YXXXNPF, the 'B' site recognises the DXE motif and LXX (L/M) E site and C-site binds an unidentified motif (Miller et al., 2003, Mossessova et al., 2003, Bi et al., 2002). Although no direct evidence has yet been presented, it is conceivable that recruitment of VSVG into COPII vesicles would involve binding to the 'B' site on Sec24. The K_{ATP} channel was also found to have the DXE motif on its Kir6.2 subunit. Saturation of the DXE binding site on Sec24 using the TAT-DXE peptide which had a small stretch of the Kir6.2 subunit containing the DXE motif affected surface expression of the K_{ATP} channel (Chapter 3). The TAT-DXE peptide was designed to have a stretch of the HIV-TAT protein to allow cell penetration. TAT alone and TAT-DXK (peptide with mutated DXE sequence) were used as controls (Figure 4.6.A). The TAT-DXE peptide was able to prevent surface expression of VSV-G (Figure 4.6.B). This result was consistent with such an expectation, because the peptide would occupy the 'B' binding site on endogenous Sec24, preventing recruitment of GFP-VSV-G^{ts045} into COPII vesicles. Application of the TAT-DXE peptide (but not the TAT and TAT-DXK peptides) onto cells expressing HA-hERG showed it was able to block the ER export of hERG (Figure 4.6.C). These data suggested that hERG was recruited into COPII vesicles by binding to the B site on Sec24. It was therefore interesting to identify if there was a Sec24 binding motif in the hERG C-terminus.

Sequence analysis showed that native sequence of hERG has three DXE sequences in its C- terminus, $^{899}DTE^{891}$, $^{976}DCE^{978}$ and $^{1036}DVE^{1038}$ and three di-leucine motifs on the hERG C-terminus, the first being ^{1022}LL (Figure 4.5). Any of these sequences could be the functional Sec24 binding motifs (Barlowe, 2003) on hERG that mediate ER export of the channel. Experiments showed that hERG proteins with truncations in the C-terminus up to position 870 express on cell surface like the wild type channel (Figure 4.7A) and are retained at the ERES in presence of Sar1^{H79G} (Figure 4.7B). Thus, removal of all the three potential DXE motifs and the only LXX(L/M)E motif from hERG failed to prevent ER export of the channel. It is possible that motifs other than the DXE

signals in hERG bind the COPII machinery, and our understanding of ER exit motifs is incomplete (Sato and Nakano, 2007a).

While the ER exit motif on hERG channels was being investigated, Delisle et al (2009) published their findings on hERG trafficking which were in agreement with the data presented above. Further work on the project was therefore discontinued with the conclusion that further studies to identify how the hERG channels are recognised and packaged into the COPII machinery were required to further the understanding of the forward trafficking of the channels. It would be important to find out, how the channels are recognised by the COPII machinery and if present, what the ER exit signal on the channel is. Use of the TAT-DXE peptides for altering surface density of the channels was an interesting option, considering that defective ER exit of hERG channels is the major cause of the LQTS2 in humans.

4.5 Summary

The hERG potassium channels contribute to the rapidly activating delayed rectifier K^+ current (IKr), responsible for rapid repolarisation of the cardiac action potential. Genetic mutations affecting the function or plasma membrane expression of the channels cause life threatening Long QT syndrome 2 (LQTS2) and therefore understanding of all the biological processes such as forward trafficking of the channels that can play a role in altering surface density of the channels is important. In this chapter, techniques in cell biology, molecular biology were employed to look at the mechanism of Sar1-GTPase dependent ER exit of hERG channels in COPII vesicles. When the function of Sar1 was intercepted, surface expression of hERG is abolished as the channel accumulates in the COPII-enriched ER exit sites and was unable to reach the ERGIC. Blocking the cargo binding sites on the Sec24 component of the COPII coat machinery with membrane-permeable peptides led to inhibition of ER exit of hERG channels. Progressive deletion of the potential diacidic ER exit motifs failed to prevent surface expression of the channels, indicating lack of involvement of canonical diacidic motifs in the ER exit of the hERG channels.

CHAPTER 5

Pathways of hERG internalisation

5.1 Introduction

The cardiac potassium channel hERG (Kv11.1) is responsible for the rapid delayed rectifier current IKr, which plays a central role in terminal repolarisation of human ventricular myocytes (Sanguinetti et al., 1995, Sanguinetti and Tristani-Firouzi, 2006). Loss of hERG/IKr function either by inherited mutations or unintentional drug blockade produces LQTS and is characterised by a prolongation of the QT interval on the ECG which put the patients at an increased risk of suffering from *torsades de pointes* arrhythmias, or sudden cardiac arrest (Sanguinetti and Tristani-Firouzi, 2006). This property of hERG has generated immense interest in hERG biosynthetic trafficking. Therefore, while much is known about hERG biosynthetic delivery (Delisle et al., 2009, Ficker et al., 2005, Ficker et al., 2003), relatively little is known about the fate of channels after they are expressed on the plasma membrane or how the wild type (WT) hERG channel density is regulated under either physiological or patho-physiological conditions. The LQT / SQT disease models demonstrate the necessity of maintaining an appropriate level of hERG channels at the cell surface (Brugada et al., 2005, Thomas et al., 2003a).

Ion channel current is the sum of its biophysical (gating, permeation), biochemical (phosphorylation, etc), and biogenic (biosynthesis, processing, trafficking) processing. The following equation is used for ion channel current:

$$I = n.i.P\mathrm{o}$$

Where I = current, n= number of channels, i= channel conductance and Po is the channel open probability (Delisle et al., 2004, Hille, 2001). Biogenic processes regulate the surface density of a protein through a dynamic balance between the biosynthetic secretion, endosomal trafficking (internalisation, recycling and degradation) of a membrane protein (Kennedy and Ehlers, 2006, Drake et al., 2006). A tilt in the balance could have important patho-physiological consequences as has been demonstrated for ion channels in other physiological conditions by having a direct effect on ion channel currents (Okiyoneda and Lukacs, 2007, Mankouri et al., 2006, Jarvis and Zamponi, 2007).

Research indicates that hERG channels can be removed from the plasma membrane by internalisation. Following stimulation with ceramide the channels were shown to undergo ubiquitinylation and lysosomal degradation (Chapman et al., 2005). It has also

been shown that lowering of extracellular potassium ion concentration accelerates internalisation and degradation of the hERG channels (Guo et al., 2009). This study provides a potential mechanism for hypokalemia-induced LQTS. However, under physiological conditions, the underlying mechanisms of hERG internalisation and the subsequent fate of internalised channels is unclear.

The mechanisms that regulate internalisation of a membrane protein would be largely affected by location of the protein in the cell membrane. The cell membrane is a heterogeneous mixture of proteins, cholesterol, glycero‑, phospho‑ and sphingolipids (Harder and Simons, 1997). The cell membrane has micro-domains that are rich in cholesterol and sphingolipids which are considered to laterally associate with one another and form lipid-rafts that are resistant to detergent solubilisation (Lai, 2003, Lingwood and Simons, 2010). Cholesterol and sphingolipid enriched membranes are believed to coordinate multiple cellular processes, which include second messenger regulation, membrane recycling of proteins, ion channel function and membrane protein internalisation (Mayor and Pagano, 2007, Harder and Simons, 1997).

Membrane proteins are internalised by a variety of mechanisms (Doherty and McMahon, 2009, Mayor and Pagano, 2007) which can be broadly classified as GTPase dynamin-dependent and independent mechanisms (see Introduction for detailed account and Figure 5.1, Mayor and Pagano, 2007). Dynamin is required for the final scission of several types of vesicles that bud off from membranes containing the endocytic cargo. Dynamin-dependent internalisation can be clathrin, caveolin or RhoA mediated (Mayor and Pagano, 2007). The clathrin mediated pathway of internalisation (CME) is the most common and well studied route of internalisation. It relies on the recruitment of the adaptor protein 2 (AP2) complexes by cargo proteins with a subsequent association of clathrin leading to membrane invaginations that form clathrin coated vesicles (CCV) (Doherty and McMahon, 2009, Kirchhausen, 1999). Caveolin coat proteins form flask shaped invaginations termed as caveolae (Mayor and Pagano, 2007) in the cell membrane that contain endocytic cargo. Caveolae require the action of dynamin for pinching off from the cell membrane and are classified under the clathrin independent endocytic mechanisms (CIE) that require dynamin (Mayor and Pagano, 2007). Another class of CIE mechanism is regulated by the small GTPase RhoA and requires dynamin to complete membrane scission (Ellis and Mellor, 2000). CIE internalisation is found to occur in lipid-rafts that are dynamic structures with cholesterol as a linker (Harder and Simons, 1997, Mayor and Pagano, 2007).
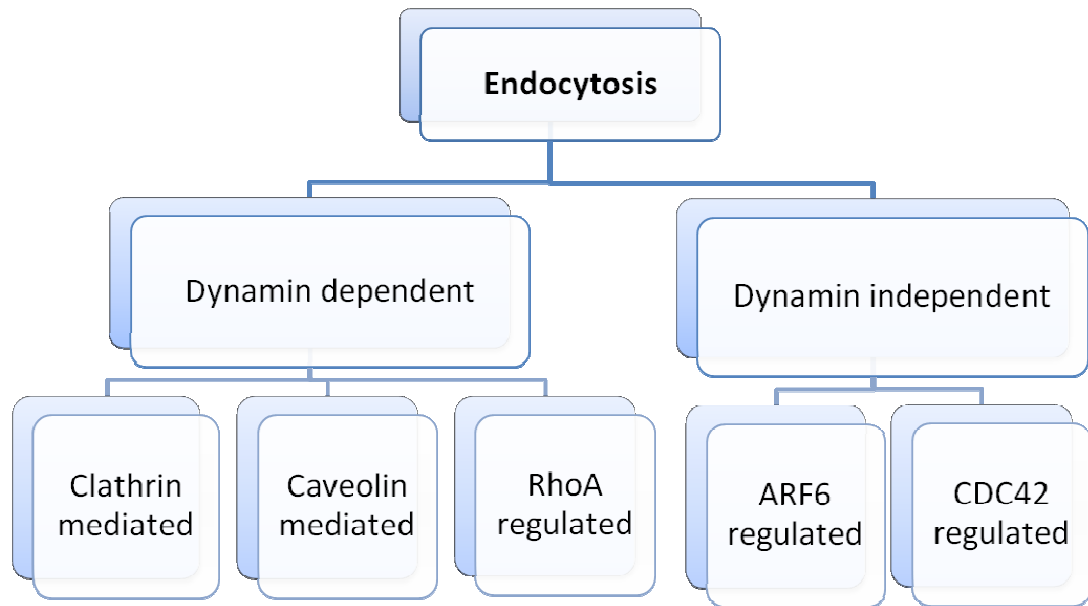
Figure 5.1 Classification of endocytic mechanisms (Mayor and Pagano, 2007)

Although CME is thought to be the most commonly used mechanism (Doherty and McMahon, 2009), recent studies indicate that an increasing number of membrane proteins undergo internalisation via CIE (Eyster et al., 2009, Mayor and Pagano, 2007) that involve lipid-rafts. Unlike CME, however, CIE is not a single mechanism, but comprises several different mechanisms (Mayor and Pagano, 2007, Donaldson et al., 2009). A better understanding of the processes that govern cell surface density of hERG may reveal mechanisms that differentiate hERG from other membrane proteins and potentially reveal targets for future therapeutic interventions. It is therefore important to elucidate the endocytic mechanisms of the hERG potassium channel.

Having understood how the hERG channels undergo internalisation, it would be interesting to understand how the process is regulated. This information would enhance the understanding of mechanisms underlying several cardiac anomalies caused due to altered hERG channel function under physiological and patho-physiological conditions. Protein phosphorylation is one of the most common molecular mechanisms known to modulate the activity of ion channels (Levitan, 1994). Protein kinases have been found to regulate ion channels (Cohen et al., 1996) by altering their biophysical properties. Most common of these are protein kinase C (PKC) and protein kinase A (PKA), (see introduction) which are implicated to regulate a variety of cellular processes including membrane trafficking and internalisation (Alvi et al., 2007, Manna et al., 2010, Herring et al., 2005, Dada et al., 2003). It would be interesting to study how signalling molecules such as protein kinases regulate internalisation of hERG leading to altered surface density of the channels.

In this chapter, the mechanism of hERG internalisation was investigated using a combination of cell biological, pharmacological, functional and biochemical approaches. The study indicated that majority of hERG channels are internalised via a clathrin- and dynamin-independent, lipid-raft and ARF6-mediated pathway. Interestingly, when ARF6 function was suppressed, the channel was found to undergo internalisation via a dynamin-dependent mechanism that was independent of caveolar rafts. Further, the effect of signalling molecules including protein kinase C (PKC) and protein kinase A (PKA) was examined. Activation of PKC was found to inhibit internalisation and increase the surface density of hERG channels.

5.2 Materials and Methods

5.2.1 Cell lines

As described in Chapter 2, section 2.2.1. For experiments involving drug treatments, poly-L-lysine coated cover-slips were used for growing cells (as described in Chapter 2, section 2.5.1). The cells were transiently transfected with the required DNA constructs to express the required proteins using Fugene®6 transfection reagent (as described in Chapter 2, section 2.4.2).

5.2.2 Plasmid constructs

HA-tagged hERG in pcDNA3 was transfected into HEK-MSRII cells for transient expression of the HA-hERG channels as described in Chapter 4. GFP-tagged dynamin constructs dynamin1 (WT), dynamin1 (K44A), dynamin2 (WT) and dynamin2 (K44A) were gifts from H McMahon, Laboratory of Molecular Biology, Cambridge. Other cDNA clones were generous gifts from various researchers (indicated in parenthesis): GFP-tagged Caveolin1 (P132L) (Dr PG Mermelestein, University of Minnesota), HA- or GFP-tagged ARF6 (WT) and ARF6 (T27N) (Prof. Martin, University of Wisconsin), GFP-CDC42 (T17N) (Dr G Bokoch, Scripps Research Institute, La Jolla), GFP-GPI-AP (Dr M. Edidin, Johns Hopkins), and myc-RhoA(T19N), HA-ARF6 (WT) and HA-ARF6 (T27N) (Dr S Poonambalam, University of Leeds), MHCI (Dr E Hewitt, University of Leeds). HA-tagged Kir.2 and SUR1 (subunits of the K_{ATP} channel) are as described in Chapter 3. All the constructs were sequenced to confirm their sequence and large scale DNA preparations were made (as described in Chapter 2) and used for transient transfections in HEK-MSRII and HeLa cells.

5.2.3 Antibodies

Primary antibodies

Antibodies against the HA-tag on the HA-hERG channels and HA-ARF6 (WT) and HA-ARF6 (T27N), rat anti-HA (Roche), were diluted 1:500 in antibody dilution buffer for immunofluorescence imaging and for western blotting the anti-HA antibodies were diluted 1:10000 in SM-PBST (2% skim milk powder, 0.5% Tween-20, PBS). Mouse anti-MHCI (BB7.2, Abcam) were diluted 1:100 and mouse anti-myc (Cell Signalling) antibodies were used at a dilution 1:250 for immunofluorescence staining. For western

blotting, mouse anti-flotilin1 (Abcam) antibodies were diluted 1:1000 in SM-PBST; mouse anti-clathrin (heavy chain; Dr. S. Poonambalam University of Leeds) antibodies were diluted 1:1000 in SM-PBST with 0.2% skim milk. Rabbit anti-Kv11.1 against S1-S2 loop (Sigma) were used at a dilution of 1:50 for immunofluorescence imaging and at 1:5000 in SM-PBST.

Secondary antibodies

Anti-rat, anti-rabbit and anti-mouse Cy3- and Cy5-conjugated secondary antibodies (Jackson ImmunoResearch.), anti rat and anti-mouse Alexa[488]- conjugated secondary antibodies (Invitrogen) were all used at 1:500 dilution. HRP-conjugated goat anti-rat, anti-mouse and anti-rabbit secondary antibodies were obtained from Sigma or Thermo and used at 1:20000 dilution for western blotting. HRP-conjugated anti-rat antibodies for chemiluminescence assays were used at 1:100 dilution.

5.2.4 Cardiac myocytes isolation

Isolation of neonatal rat ventricular myocytes

NRVCM were isolated from ventricles dissected from hearts of 3-7 day old Wistar rats as described previously (Patten et al., 2004). Briefly, cells were dissociated by incubating the minced ventricles with collagenase (0.4 mg/ml, type II, Worthington) and protease (0.6 mg/ml, type XV, Sigma) in a dissociation buffer that contained (in mM): NaCl 116; KCl 5.4; NaH_2PO_4 0.8; Glucose 5.6; HEPES 20; $MgSO_4$ 0.8, pH 7.35; incubation was at 37°C with agitation for a suitable length of time. Cells were filtered through a 70μm nylon filter and cultured on glass cover-slips in DMEM/F12 medium supplemented with 10% horse serum, 5% fetal bovine serum, 50 U/ml penicillin and 50 μg/ml streptomycin for 2-3 days at 37°C and 5% CO_2.

Isolation of Guinea Pig Ventricular Myocytes

All experimental protocols requiring the use of animals conformed to the Animals Scientific Procedures Act, 1986. Single ventricular myocytes were isolated according to methods previously described by (Rodrigo et al., 2002). In brief, adult male Dunken Hartley guinea pigs, weighing between 300 and 500g were humanely sacrificed by cervical dislocation. The heart was then rapidly excised and suspended from a Langendorff apparatus and perfused at 37 °C with Tyrode at a rate of 10 ml/min with a nominally calcium-free solution and then a solution containing 1.66 mg/ml BSA (from

factor V albumin, Sigma Aldrich), 1 mg/ml collagenase (type I, Sigma Aldrich) and 0.66 mg/ml protease (type XIV, Sigma Aldrich). Following enzymatic digestion the heart was perfused with Tyrode solution containing 2 mM calcium (calcium Tyrode). The heart was then cut down and the ventricles were agitated gently in calcium Tyrode. Isolated myocytes were filtered through 300 μm gauze and washed 2-3 times in calcium Tyrode. Cells were stored at room temperature and used within 36 hours of isolation.

5.2.5 Drug treatments

Dynasore, methyl-β-cyclodextrin (MβCD), α-cyclodextrin (α-CD), DAG and forskolin were all purchased from Sigma. PMA, CHE, GÖ6976, H89, were purchased from Calbiochem. Water soluble cholesterol containing a mixture of MβCD and cholesterol was purchased from Sigma (catalogue no. Sigma C4951). Tissue culture grade DMSO was from Sigma. Transferrin-Alexa[488] (Tfn-488), Transferrin-Alexa[633] (Tfn-633) were from Invitrogen and cholera toxin-Alexa[647] (CT-B) was purchased from Molecular Probes. Tfn-488 and Tfn-633 stocks of 5 mg/ml were used at a working concentration of 50 μg/ml (added to cells for 15 min) and CT-B stock at 1 mg/ml was used at a concentration of 1 μg/ml (added to cells for 5 min).

Stock solutions of the pharmacological compounds used in this study were prepared and stored at -20°C as small aliquots. All working concentrations of drugs were prepared in antibody dilution buffer (1% Ovalbumin in DMEM) prior to treatment of cells. Pre-treatment with drugs was for 30 to 60 min at 37°C. Primary antibody treatment for internalisation assay carried out in presence of drugs. Details of drug preparations are as follows:

Compound	Solvent	Stock solution	Working solution
dynasore	DMSO	40 mM	80 μm
genestein	DMSO	200 mM	200 μm
methyl-β-cyclodextrin	water	30 mM	3 mM
α-cyclodextrin	DMSO	10 mM	100 μM
aluminium fluoride (AlF)	ethanol, water water	100 mM $AlCl_3$ 600 μM NaF	100 μM $AlCl_3$ 60 μM NaF
diacylglycerol (DAG)	DMSO	1 mM	10 μm

Compound	Solvent	Stock solution	Working solution
phorbol 12-myristate 13-acetate (PMA)	DMSO	100 µm	100 nM
chelerythrine chloride (CHE)	DMSO	10 mM	10 µm
GÖ6976	DMSO	1 mM	1 µm
forskolin	DMSO	30 mM	30 µM
cholesterol- MβCD	water	5 mmole/L cholesterol plus 5 mmole/L MβCD	0.5 mmole/L cholesterol plus 0.5 mmole/L MβCD
nystatin	DMSO, water	50 mg/ml	50 µg/ml
chlorpromazine	ethanol	25 mg/ml	25 µg/ml

5.2.6 Immunofluorescence staining

Internalisation assay

Cells grown on cover-slips were transfected with HA-hERG or HA-K$_{ATP}$ (HA-Kir6.2 and SUR1) and subjected to internalisation assay as described previously (Lingwood and Simons, 2010). Cells were incubated in presence of primary antibodies and allowed to internalise with the channels, washed, fixed, permeabilised and labelled with a fluorophore (Cy3 or Alexa488) labelled secondary antibodies. Where required, cells were treated with drugs or co-transfected with cDNA clones encoding the wild type or dominant negative isoforms of proteins involved in endocytic trafficking. To assay internalisation in NRVCM, cells were incubated with rabbit anti-Kv11.1 targeted to the S1-S2 loop of hERG, un-internalised antibodies removed by washing with acidic strip buffer (0.5 M NaCl/0.5% acetic acid, pH 2.0) before fixing, permeabilising and staining with fluorescent secondary antibodies, (see Chapter 2 for methods of fixing and permeabilisation of cells). Where MHCI antibodies were used, methanol at -20°C was used for fixing of cells instead of 2% PFA. Stained cells were imaged on a Zeiss 510 META laser scanning confocal microscope (as described in Chapter 2, section 2.5.3).

Co-localisation was scored using Image J macros designed by Dr Gareth Howell, University of Leeds. The macros scored total red pixels and the red pixels in the image that co-localised with the green pixels in the image. Ratio of these values gave percent co-localisation of the red over green. The data from several sets of images obtained

from three independent experiments were analysed and presented in bar graphs as mean ± s.e.m. ANOVA and Student's *t* test were used for statistical analysis.

5.2.7 Quantitation of surface expression

Chemiluminescence assay

Surface density of hERG was assayed as described previously using a chemiluminescence based assay (Mankouri et al., 2006). Transfected cells on cover-slips were given the indicated drug treatment or were co-transfected with HA-hERG and GFP plasmid (control) or with the indicated plasmids. To determine the effect of these factors on channel internalisation, percent internalisation of the channels was determined following 15 minutes of incubation at 37°C. HA-hERG channels were labelled on cell surface for 30 min at 4°C, the cells were washed with chilled PBS and incubated at 37°C to allow internalisation for 15 min. A set of cover-slips with HA-hERG transfected cells were surface labelled for HA-hERG and retained at 4°C where no internalisation of the channel occurs and therefore surface channel density is taken as 100%. The cells were washed, fixed and channels remaining on cell surface after internalisation were labelled with HRP-conjugated secondary antibody. Following several washes in PBS, the cells were solubilised in RIPA buffer supplemented with Benzonase (5 units). Chemiluminescence assay was performed as described in Chapter 2, section 2.5.4, to get the value for density of channels remaining on the cell surface. Percentage of channels internalised from the cell surface was determined using the following equation:

$$\% \text{ Internalisation of the channels} = \frac{\text{channel density after internalisation (37°C)}}{\text{channel density before internalisation (4°C)}} \times 100$$

Data were obtained from three separate transfection experiments, each measured in duplicate and presented in bar graphs as mean ± s.e.m. ANOVA and Student's *t* test were used for statistical analysis. Significant differences as compared to vehicle control are denoted by * (*P*<0.05) and ** (*P*<0.01) in the figures.

5.2.8 Raft isolation and Western blotting

Rafts were isolated using Optiprep^{TM} density gradient centrifugation (Schuck, 2006b). HEK-MSRII cells (~5x10^8) transfected to express HA-hERG and other raft and non-raft

reporter proteins using the calcium phosphate transfection method (as described in Chapter 2, section 2.4.2). The cells were collected and washed twice in PBS. The cell pellet was lysed in chilled TNE buffer (150 mM NaCl, 2 mM EDTA, 50 mM Tris-HCl; pH7.4) containing 1% Triton X-100 at 4°C for 30 min. The lysate was centrifuged at 10,000xg for 5 min to remove the nuclear fraction. 0.5 ml of the lysate was mixed with 1.5 ml of Optiprep^{TM} and overlaid with 3 ml of 30% Optiprep^{TM} and 0.5 ml of TNE before centrifugation at 155,000xg for 16 hrs at 4°C. Fractions were subjected to western blotting for the desired proteins (as described in Chapter 2, section 2.5.5.

For isolation of rafts from neonatal rat heart tissue, hearts from 3-7 seven day old rat pups were excised, washed thrice in chilled TNE buffer and dissected to obtain ventricular tissue. The tissue was chopped finely in chilled tissue homogenisation buffer (TMB, 1XTNE, protease inhibitor, 0.25M sucrose). 1 ml buffer per heart was used. The finely chopped tissue was then dounced in a glass douncer (in chilled conditions) and 10% Triton X-100 was added to a final concentration of 1% w/v. The crude tissue lysate was centrifuged at 10000xg for 5 minutes to obtain a post-nuclear fraction. 0.5 ml of the post-nuclear fraction was mixed with an equal volume of 90% (w/v) sucrose in TNE. On ice, 1 ml of the heavy fraction was overlaid first with 2 ml 30% (w/v) sucrose in TNE then by 2 ml 5% (w/v) sucrose in TNE in an ultracentrifuge tube. Following centrifugation 0.5 ml fractions were collected from the top including the pellet in the bottom fraction that was suspended in 0.5 ml TNE. The proteins in the density gradient fractions were treated with 100 mM DTT and resolved by SDS-PAGE. Proteins of interest were visualised by western blotting.

Rafts from guinea pig myocytes were prepared following lysis of washed cell pellet of myocytes isolated from a guinea pig heart (as described in section 5.2.4) in chilled TNE buffer containing 1% Triton X-100 at 4°C for 30 min. The lysate was centrifuged at 10,000xg for 5 min to remove the nuclear fraction. 0.5 ml of the post-nuclear fraction was mixed with an equal volume of 90% (w/v) sucrose in TNE and rafts were isolated as described above for the rat heart tissue.

5.3 Results

5.3.1 Internalisation of native and recombinant hERG channels

The aim of this study was to investigate the mechanism underlying internalisation of the cardiac hERG potassium channels. To achieve this aim an assay to study internalisation of the channel from the cell surface was standardized (see methods for details). The assay involved the use of anti-hERG antibodies against extracellular epitope on the hERG channel. These monoclonal antibodies were raised against the S1-S2 peptide (AFLLKETEEGPPATEC) which is conserved in human, rabbit, guinea pig and rat ERG channels. The native neonatal rat ventricular cardiac myocytes (NRVCM) (see methods for myocytes isolation procedure) were stained with the anti-Kv11.1 antibodies treated with and without the S1-S2 peptide. Following staining with fluorophore-conjugated secondary antibodies, it could be seen from the confocal images that when the Kv11.1 antibodies were pre-incubated with the S1-S2 peptide against which they were raised, no staining is visible in NRVCM. However, staining can be seen in NRVCM stained using anti-Kv11.1 antibodies without incubation with the peptide (Figure 5.2.A). HEK-MSRII cells that do not express native hERG channels did not show any staining with the anti-Kv11.1 antibodies (Figure 5.2.B). These data established the specificity of the anti-hERG antibody.

In order to look at internalisation of native ERG channels, live NRVCM were incubated in the presence of anti-Kv11.1 primary antibodies at 4°C or 37°C for 60 min. This would allow antibodies that bound the ERG channels on cell surface to be internalised along with the channel. At 4°C, when biochemical processes of a cell are stalled, internalisation of proteins does not occur. The cells were then washed at 4°C, fixed, permeabilised and stained with a fluorescent secondary antibody (red). At 4°C, staining was seen at the cell surface, whereas at 37°C staining was seen on the cell surface as well as within the cell as punctate structures (Figure 5.3.A, top panel). To eliminate the possibility that the punctate structures appeared due to clustering of channels at the cell surface (rather than internalised channels), another set of cells was washed with an acidic buffer (pH 2.5) after the primary antibody incubation step in order to strip any surface bound antibody. Antibodies internalised within the cell along with the channel would be protected from the acid strip and get stained with the secondary antibody.

A NRVCM

B HEK-MSRII (un-transfected)
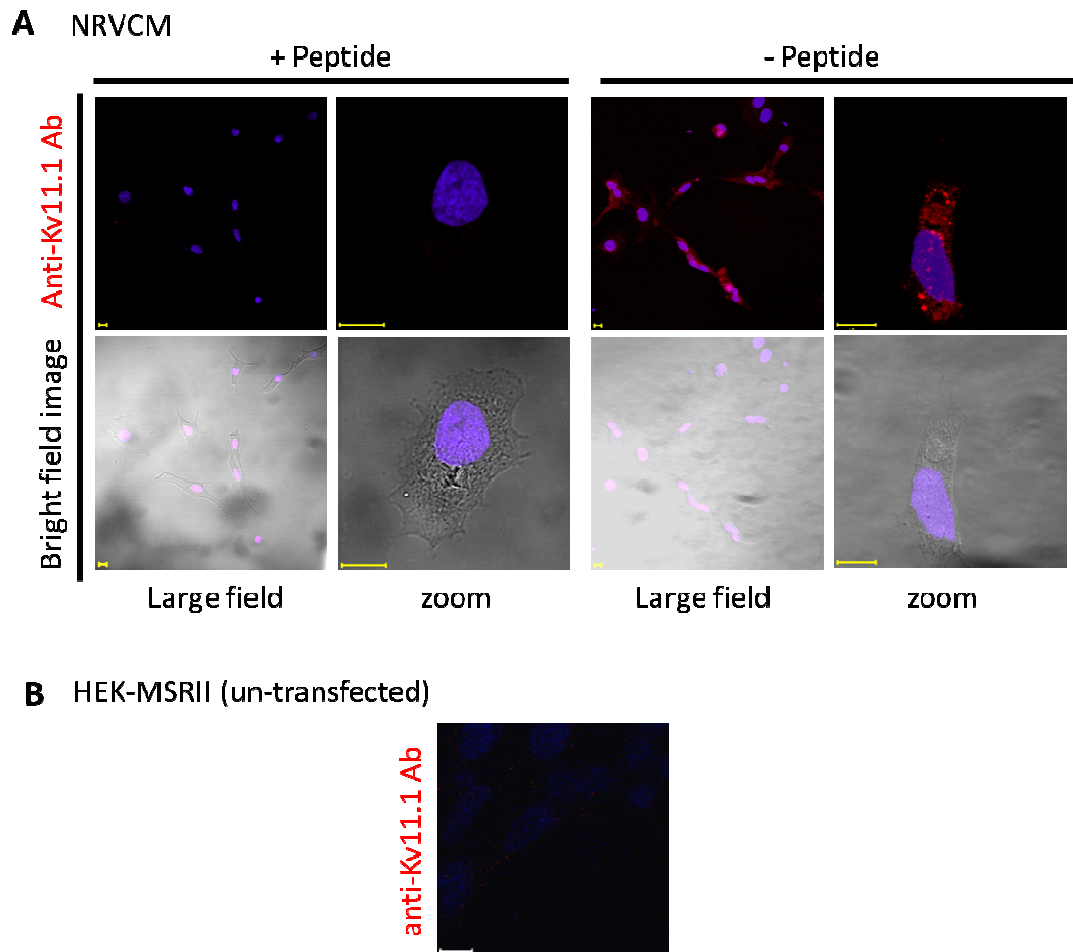
Figure 5.2 Testing the specificity of the anti-Kv11.1 antibody. (A) NRVCM were stained with the anti-Kv11.1 antibody treated with and without S1-S2 peptide. Top panels show staining with fluorophore (red) and bottom panels show bright field images of the cells with nuclear stain. (B) Un-transfected HEK-MSRII cells were stained with the anti-hERG antibody. Nuclei stained blue with DAPI. Representative confocal images from three independent experiments are shown; Scale bars: 10 μm.
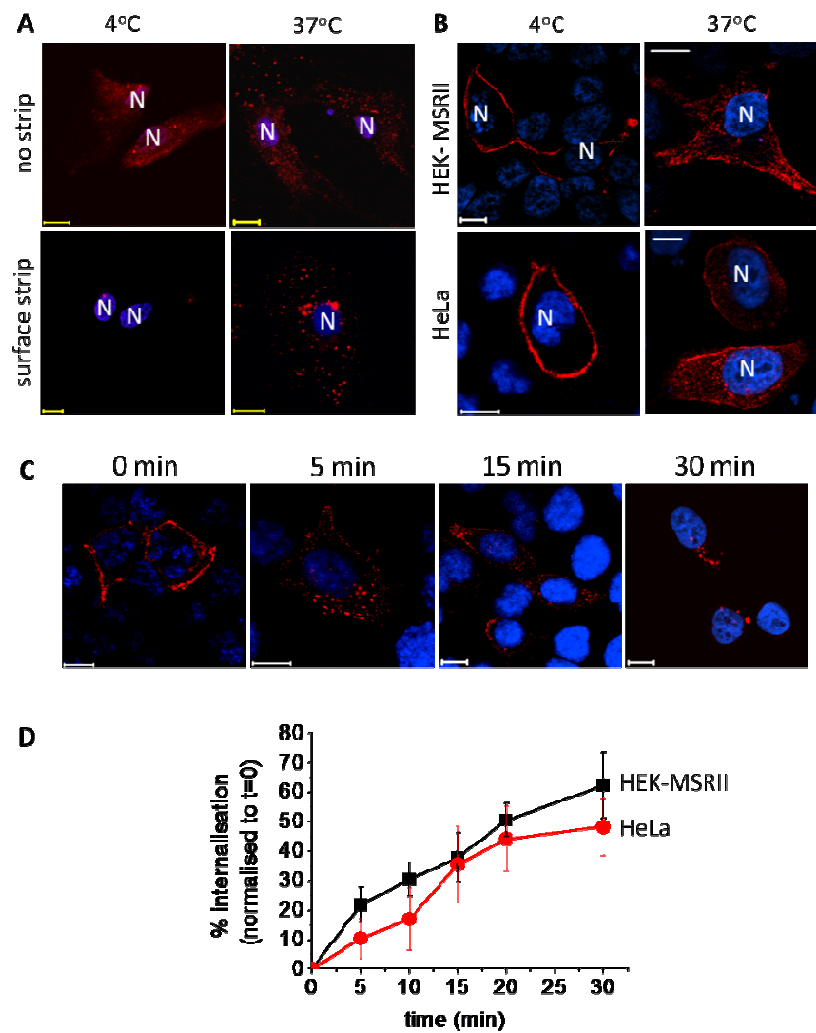
Figure 5.3 hERG undergoes rapid internalisation. (A) Neonatal rat ventricular myocytes (NRVCM) were stained for native ERG channels after incubation at 4°C or 37°C for 60 min. Cells were washed at 4°C with PBS (top panel) or with PBS followed by an acid strip buffer (bottom panel). All the cells were then fixed, permeabilised and stained (red) with Cy3- conjugated secondary antibodies. (B) HEK-MSRII cells (top panels) and HeLa cells (bottom panels) transfected with HA-hERG incubated in presence of anti-HA antibodies at 4°C and 37°C for 60 min. Cells were then washed with PBS at 4°C, fixed, permeabilised and stained. (C) HEK-MSRII cells expressing HA-hERG were labelled with anti-HA antibody on cell surface at 4°C, washed and incubated at 37°C for the indicated time points and then stained as in (A). Nuclei were stained blue with DAPI. Representative confocal images shown from three independent experiments are shown; Scale bars: 10 μm. (D) Quantitative estimation of internalised HA-hERG density in HEK-MSRII and HeLa cells after incubation for the indicated time points at 37°C using the chemiluminescence assay as described in methods; mean ± s.e.m (n = 3) data are shown.

The results (Figure 5.3.A, bottom panel) showed absence of staining in cells incubated at 4°C, but robust staining of ERG in punctate structures was observed in cells incubated at 37°C, indicating that at 4°C all the channels remained on the cell surface but at 37°C channels internalised. Thus in NRVCM, the ERG channels are endocytosed into intracellular structures in a temperature dependent manner. Maintenance and genetic manipulation of native cells is difficult, therefore, HEK-MSRII and HeLa cells were chosen to investigate the mechanisms of hERG internalisation. These cells are easy to transfect and are therefore widely used for trafficking studies. Internalisation of transiently transfected HA-hERG (hERG with extracellular HA-epitope engineered into the S1-S2 loop (Ficker et al., 2003 , Chapter 3) in HEK-MSRII and HeLa cells was looked at. The channels were stained by incubation of the cells in the presence of anti-HA antibodies at 4°C or 37°C. The cells were then fixed, permeabilised and stained with the Cy3-conjugated secondary antibodies. Immunofluorescence imaging showed that in both the cell types, the HA-hERG channels remained on cell surface following incubation at 4°C but they were internalised to punctate structures within the cells at 37°C (Figure 5.3.B).

Next, the time course of internalisation of the HA-hERG channels was investigated. The pool of channels expressed on the cell surface were labelled on the surface with anti-HA antibodies at 4°C and then allowed to internalise at 37°C for different time points. The cells were washed, fixed, permeabilised and stained with Cy3- conjugated secondary antibodies for immunofluorescence imaging. The confocal images indicated that internalisation of HA-hERG channels labelled on the cell surface occurs within 5 min at 37°C, (see Figure 5.3.C). The amount of channels left on the cell surface following internalisation for different time points was quantitatively determined using the chemiluminescence assay described in detail in Methods. The percentage of the channel internalisation was then calculated from the remaining surface density after internalisation for each time point divided by the total channel density prior to internalisation (time 0). The assay showed that in both HEK-MSRII and HeLa cells, the transiently expressed HA-hERG channels are internalised rapidly with ~50 % of the channels expressed on the cell surface being endocytosed within 20 min (see Figure 5.3.D).

Having established that both native and transfected ERG channels undergo rapid constitutive internalisation, the study was then directed towards elucidating the mediators of hERG internalisation.

5.3.2 Dynamin-independent, raft-dependent internalisation of hERG channels

The approach taken to find out the endocytic mechanism of the hERG channels was to use the relevant dominant negative (DN) isoforms or pharmacological compounds known to disrupt function of key proteins of different endocytic pathways and find out which of these affected internalisation of hERG. The internalisation assay followed by immunofluorescence staining (see Methods) was used to look if DN proteins or pharmacological compounds prevented internalisation of the HA-hERG channels. For native ERG channels in NRVCM, the acid strip method was used to confirm internalisation as described in the previous section (Figure 5.2.A). The amount of internalisation of the channel was quantitatively determined using the chemiluminescence assay (see Methods). Both these techniques allowed continuous labelling of channels internalised from the cell surface. Block of internalisation would cause accumulation of the channels at the cell surface and absence of punctate structures within the cells in imaging or a decrease in the internalised channel density in the chemiluminescence assay.

The Figure 5.1 shows the general classification of endocytic pathways with the two major classes of internalisation being dynamin-dependent and dynamin-independent. Dynamin-dependent internalisation can be classified as CME that requires clathrin and CIE that is mediated by caveolar rafts or RhoA-GTPase (Doherty and McMahon, 2009, Mayor and Pagano, 2007). Internalisation of proteins that undergo dynamin-dependent internalisation is prevented by expression of DN-dynamin 1 & 2 (K44E-Dynamin1 & 2) (Bobanovic et al., 2002, Bonifacino and Lippincott-Schwartz, 2003, Mankouri et al., 2006). Co-expression of the GFP-tagged DN-Dynamin1 or 2 did not inhibit internalisation of the HA-hERG channels in HEK-MSRII or HeLa cells (Figure 5.4). These data suggested that internalisation of the hERG channels was independent of dynamin.

As a further confirmation that hERG internalisation was not affected by any of the dynamin-mediated pathways (that are dependent upon proteins: clathrin, caveolin or RhoA); DN-μ2 (D176A/W412A), DN-caveolin1 (P132L) and DN-RhoA (T19N) were each co-expressed with HA-hERG and the channels were stained following the internalisation assay. The images from confocal microscopy showed that internalisation of the HA-hERG channels was largely unaffected by disruption of activity of any of these proteins (Figure 5.5).
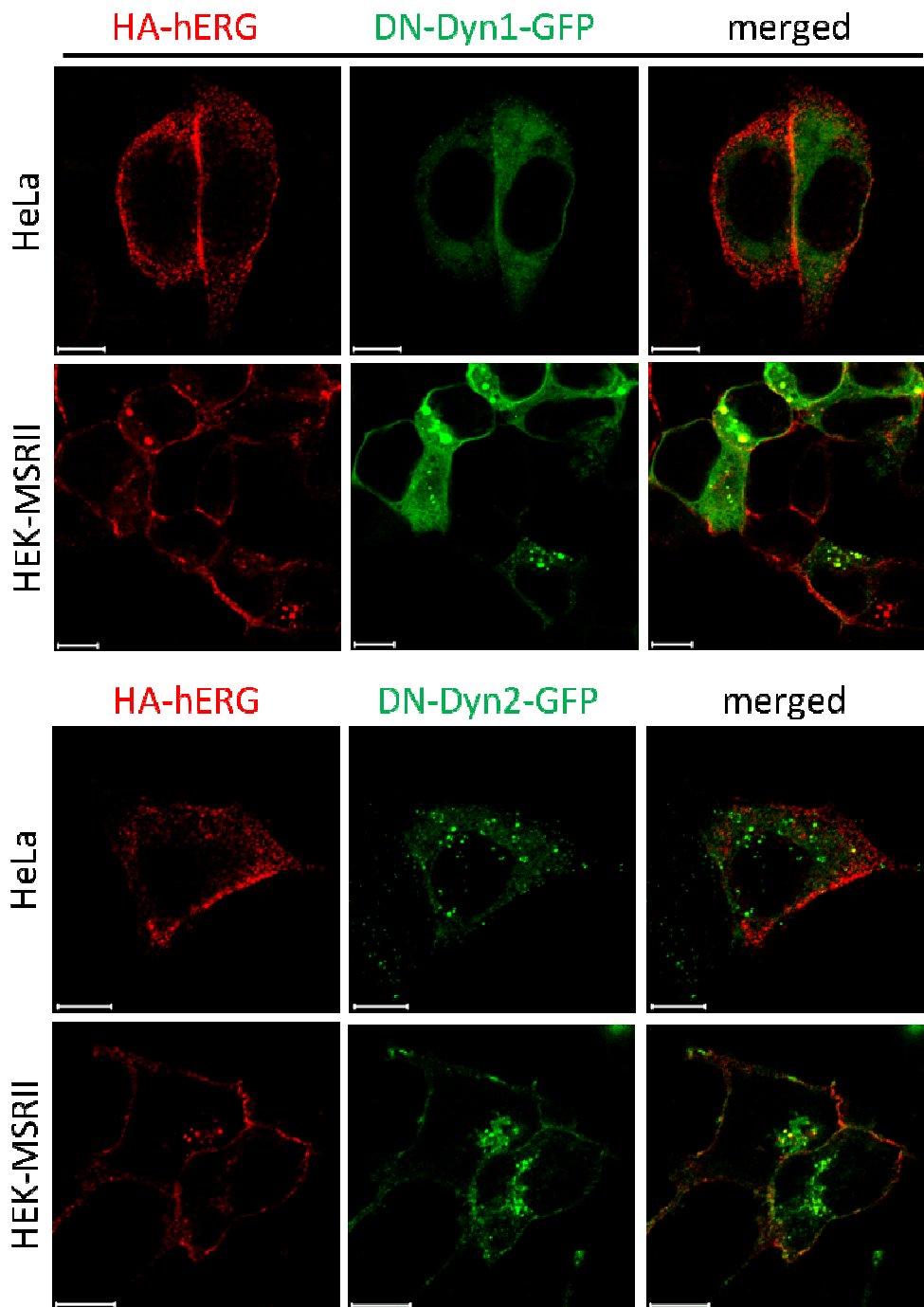
Figure 5.4 Internalisation of HA-hERG channels is unaffected by co-expression of DN-dynamins. HeLa and HEK-MSRII cells were co-transfected to express HA-hERG and the indicated GFP-tagged constructs that would disrupt dynamin-dependent internalisation. The cells were incubated with anti-HA antibodies for 1hr following which they were washed, fixed, permeabilised and stained with Cy3-conjugated secondary antibodies (red) following the internalisation assay. Representative confocal images from three independent experiments are shown; Scale bars: 10 μm.
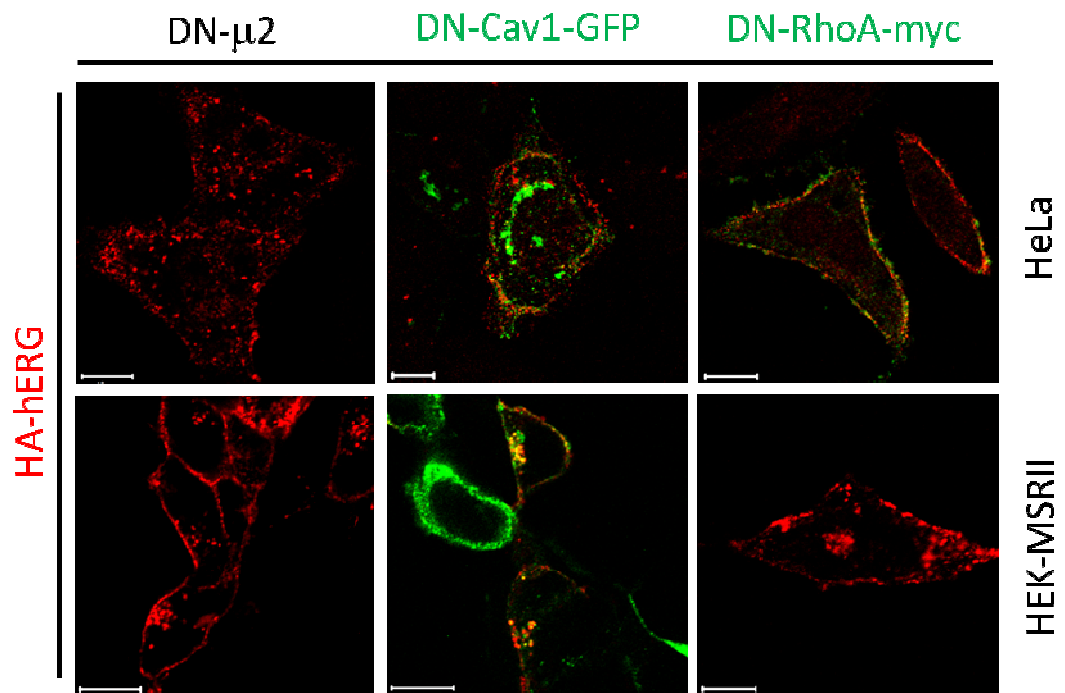
Figure 5.5 hERG internalisation is independent of clathrin, caveolin and RhoA-GTPase. HeLa or HEK-MSRII cells were co-transfected to express HA-hERG and the indicated constructs. HA-hERG was stained (red) following the internalisation assay. DN-RhoA-myc expressed in the HeLa cells was stained (green) using anti-myc antibodies. Representative confocal images from three independent experiments are shown; Scale bars: 10 µm.

Some of the internalised HA-hERG channels however appeared to co-localise with the DN-caveolin1-GFP protein (Figure 5.5), which suggested that a small pool of the hERG channels could be internalised via dynamin mediated pathway. A recent report (Massaeli et al., 2010) suggested that a caveolin-dependent endocytic route is involved in low potassium (0 mM) induced degradation of mature hERG channels. Thus, the major pathway of hERG internalisation in normal physiological conditions appears to be clathrin- and dynamin- independent but some of the channels may also be internalised by alternate dynamin-dependent pathways which might become predominant in altered physiological conditions.

The use of DN constructs (Figure 5.4 and 5.5) indicated that hERG internalisation was not affected by all known dynamin-dependent pathways and left open the possibility that internalisation of the hERG channels could be mediated by lipid-rafts. To check if lipid-rafts but not dynamins were involved in hERG internalisation, pharmacological drugs were used. Treatment of the HA-hERG expressing cells with dynasore, a chemical inhibitor of dynamin function (Macia et al., 2006), failed to inhibit internalisation of hERG while uptake of fluorescently labelled transferrin^{Alexa488} (Tfn-488) was blocked in these cells. Tfn is specifically recognised by the transferrin receptor (TfnR). TfnR is the archetypical cargo for internalisation through dynamin and AP-2 dependent CME (Nesterov et al., 1999, Motley et al., 2003). As a parallel control, cells expressing HA-K_{ATP} (HA-Kir6.2 +SUR1) the pancreatic K_{ATP} channels which are a cargo of CME (Mankouri et al., 2006) showed blocked internalisation of the channels when treated with dynasore (Figure 5.6.A, top panel).

Disruption of lipid-rafts with methyl-β-cyclodextrin (MβCD), a cholesterol sequestering agent (Klein et al., 1995), blocked internalisation of the HA-hERG but not the K_{ATP} channels and Tfn-488 (Figure 5.6A middle panel). As a negative control, α-cyclodextrin (αCD), an inactive analogue of MβCD, was used and it had no effect on internalisation of HA-hERG, Tfn-488 and HA-K_{ATP} (Figure 5.6A, bottom panel). When internalised channel density for HA-hERG channels was quantitatively determined using the chemiluminescence assay (see Methods), cells treated with dynasore showed ~70% internalisation which was similar to the vehicle (no drug) control. However, cells treated with MβCD showed near complete block of internalisation compared to the αCD treated cells (Figure 5.6.B). Preloading of MβCD with cholesterol prior to treatment of cells expressing HA-hERG abolished the ability of the compound to prevent internalisation of the channels in contrast to treatment of cells with cholesterol (Figure 5.6.C). These data confirmed that effect of MβCD was due to cholesterol depletion.
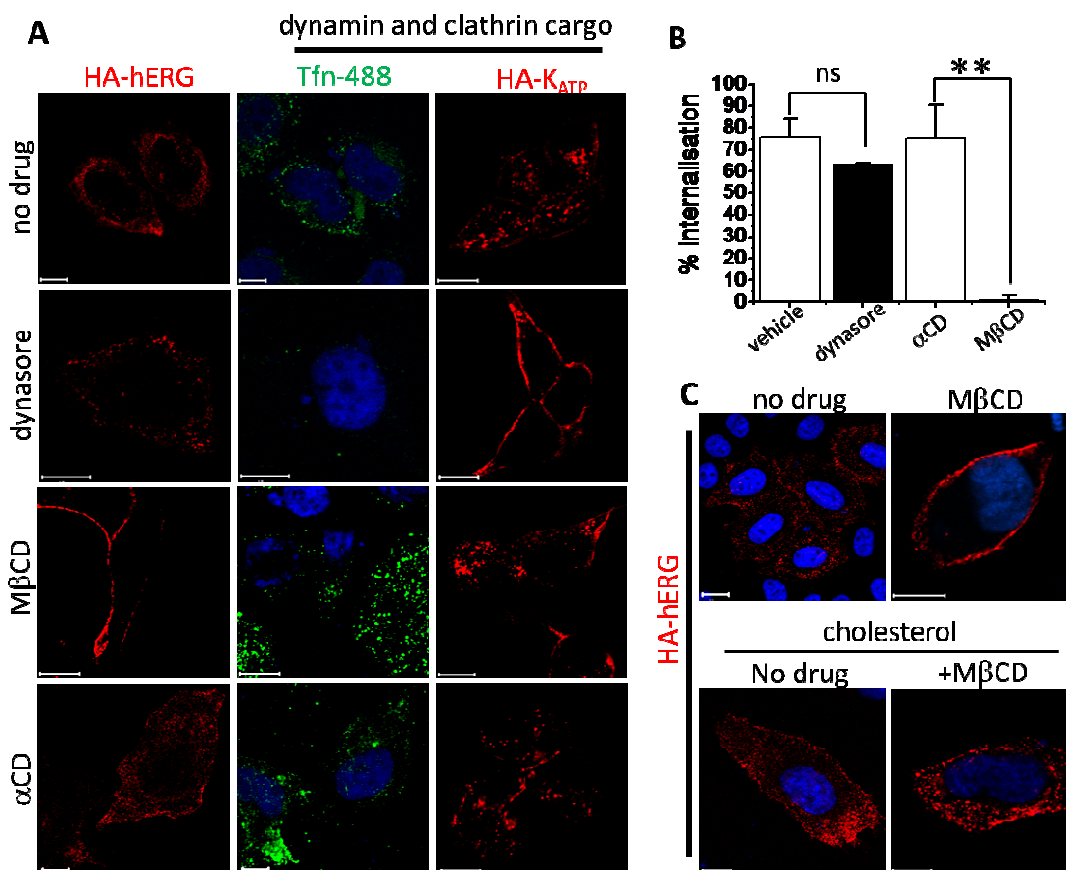
Figure 5.6 Internalisation of hERG channels is dynamin-independent and raft-dependent. (A) HeLa cells transfected with HA-hERG or HA-K$_{ATP}$ were untreated or pre-treated with the indicated drugs (see Methods) for 30 min prior to and during incubation with anti-HA antibodies (60 min, 37°C). Tfn-488 (green), was added to cells during the last 15 min of anti-HA antibody labelling. Cells were washed, fixed, permeabilised and stained with Cy3-conjugated secondary antibodies to label the HA-hERG channels (red). (B) HEK-MSRII cells transfected with HA-hERG were treated with the indicated drugs (vehicle, DMSO) as in (A). Internalisation of pre-bound anti-HA-antibodies was allowed to occur for 15 min prior to assaying the remaining surface density. Following the chemiluminescence assay, percent internalisation of the channels was calculated (ratio of the measure of surface channel density after internalisation and the total surface density of the channels prior to internalisation); mean ± s.e.m (n = 3) data are shown; ** indicates p value <0.01 (p=0.006). (C) HeLa cells were treated with cholesterol saturated MβCD and HA-hERG channels were stained after the internalisation assay as in (A). Cells were treated with no drug, MβCD and cholesterol as experimental controls. Nuclei stained blue with DAPI. Representative confocal images are shown; Scale bars: 10 μm.

The results from the above experiments confirmed that HA-hERG internalisation was dynamin-independent and required the integrity of the cholesterol rich lipid-rafts. Whether this was true for native ERG channels was tested using the pharmacological tools on NRVCM. Treatment of NRVCM with dynasore or αCD did not prevent internalisation of ERG channels, as seen by the presence of stained ERG channels after acid-strip (described in section 5.2.1 and Figure 5.2.A). Treatment with MβCD, on the other hand, inhibited ERG internalisation in NRVCM (Figure 5.7). Taken together these data indicated that hERG internalisation is predominantly dynamin-independent. Moreover, the data also confirmed the validity of the use of recombinant system and the HA-tagged hERG for further investigations into the mechanism of internalisation of the hERG channels.

5.3.3 Localisation of hERG channels to lipid-rafts

Depletion of membrane cholesterol that would disrupt membrane lipid-rafts using MβCD blocked HA-hERG internalisation (Figure 5.6 & 5.7). These data indicated that raft localisation of the channels was important for their internalisation. To strengthen these conclusions it was required to confirm raft localisation of the channel. Towards this, neonatal rat heart lysates were fractionated in the presence of 0.1% Triton X-100 on a sucrose density gradient using high speed centrifugation as described in Methods, (Schuck, 2006a). Western blot analysis of the fractions showed that majority of hERG was localised to the detergent resistant raft membranes (DRM) containing fractions marked by flotillin (Bickel et al., 1997). A small fraction of the channels was also found to be localised to the detergent soluble bottom fraction marked by clathrin (Schuck, 2006a , and Figure 5.8A). Disruption of the detergent resistant raft membranes by treatment of the lysates with MβCD shifted the hERG channels to non-raft, clathrin containing fractions. Similarly the channels were found to be localised to the top raft fractions in Guinea pig cardiac myocytes (Figure 5.8.B). Since the study used HA-hERG transfected in model cells, the localisation of HA-hERG expressed in HEK-MSRII cells was examined.
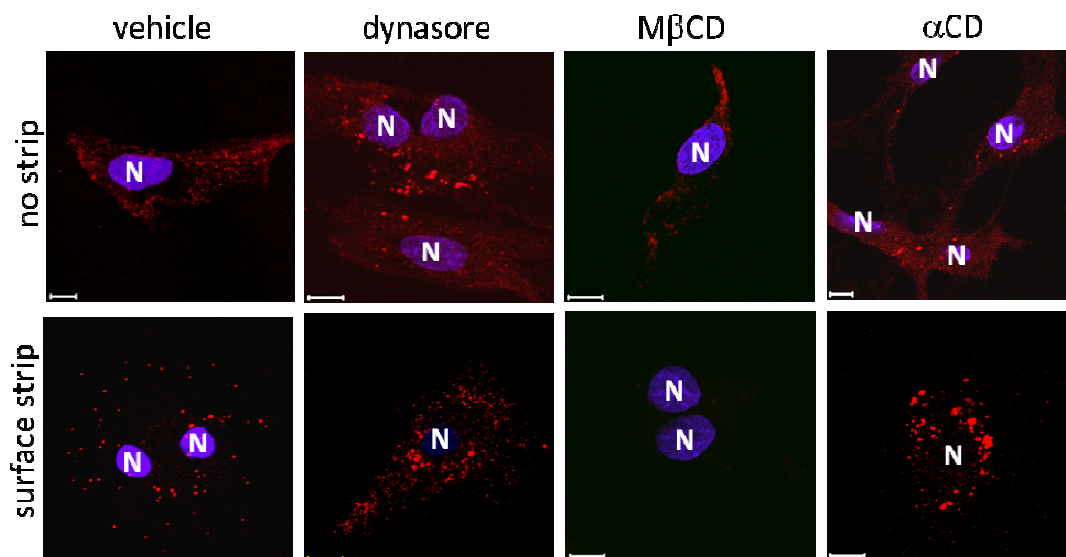
Figure 5.7 Native hERG is internalised by lipid raft dependent pathway independent of dynamin. NRVCM were treated with the indicated drugs for 30 min (see methods) prior to and during 60 min labelling of the native hERG channels on live cells at 37°C (internalisation assay). A set of cells was subjected to acid strip (used in Figure 5.3.A) to confirm internalisation of the channels. The cells were then fixed, permeabilised and stained with Cy3-conjugated secondary antibodies to label the hERG channel (red). Nuclei stained blue with DAPI. Representative confocal images from three independent experiments are shown; Scale bars: 10 μm.
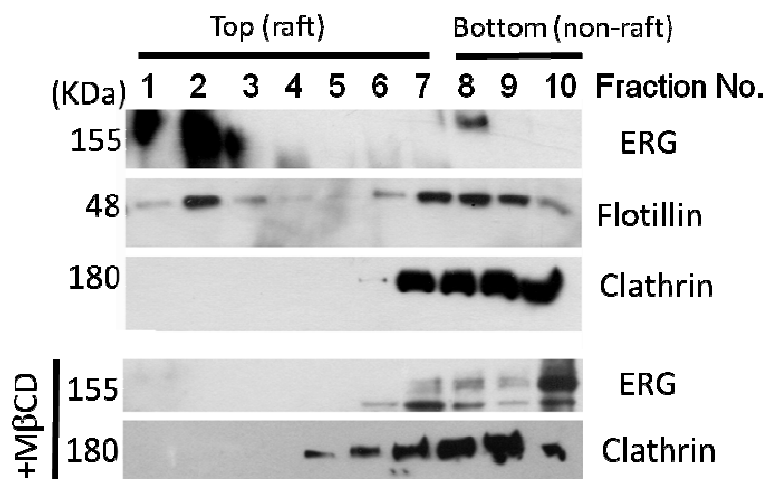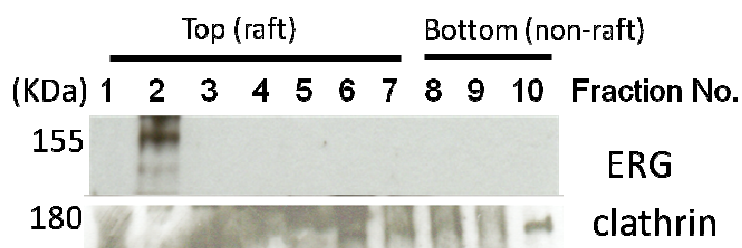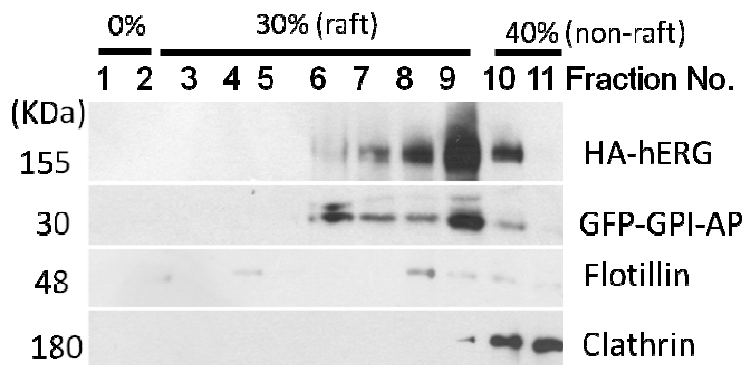
Figure 5.8 ERG channels are localised to lipid-rafts. (A) Neonatal rat heart tissue was homogenised, treated with or without MβCD for 30 min in presence of 1% Triton X-100 and subjected to sucrose density gradient fractionation. Fractions were subjected to western blotting for ERG, flotillin (raft marker), and clathrin (non-raft marker). (B) Guinea pig cardiac myocytes were homogenised and subjected to sucrose density gradient centrifugation as in (A). Fractions were blotted for hERG and clathrin. (C) HEK-MSRII cells co-transfected with HA-hERG and GFP-GPI-AP were homogenised as in (A) and lipid-rafts were purified using Optiprep™ step gradient (see methods). Fractions were blotted for HA-hERG and the indicated raft non-raft marker proteins.

Known raft marker GFP (extracellular)- tagged glycoslyphosphatidylinositol-anchored protein (GFP-GPI-AP) was also co-transfected in these cells which were subjected to detergent extraction followed by raft isolation using the Optiprep™ gradient and high speed centrifugation (see methods for details). As in the heart tissue, majority of HA-hERG in the HEK-MSRII cells was also found to be localised to the raft fractions marked by GFP-GPI-AP and flotillin, but a small proportion was also present in non-raft fractions along with clathrin (Figure 5.8.C). These data established that hERG was localised to lipid-rafts.

Furthermore to investigate if internalisation of hERG occurred in lipid-rafts, internalised HA-hERG in HEK-MSRII cells was labelled along with raft markers (Mayor and Pagano, 2007, Naslavsky et al., 2004, Torgersen et al., 2001), GFP-GPI-AP (Figure 5.9.A) or Alexa^{633} conjugated cholera toxin B (CT-B) (Figure 5.9.B). HA-hERG channels were found to co-localise with both these raft cargos on cell surface and in vesicular compartments within the cells after internalisation. Taken together, the data demonstrated that hERG channels are localised to lipid-rafts in the cell membrane and are internalised by a raft mediated pathway.

5.3.4 CDC42-independent, ARF6-mediated internalisation of hERG channels

The above experimental results left open the possibility that hERG internalisation was mediated by one of the raft dependent pathways which included mediators CDC42 and ARF6 (Chadda et al., 2007, Donaldson et al., 2009, Mayor and Pagano, 2007). Co-expression of GFP-tagged DN isoform of CDC42 (T17N) did not affect the internalisation of HA-hERG (Figure 5.10). Further, immunofluorescence imaging of cells expressing HA-hERG and DN-ARF6 (T27N) did not appear to completely block internalisation of the channel compared to the WT-ARF6 (Figure 5.11.A). However, chemiluminescence assay to determine percent internalisation (as in Figure 5.6.B) showed that there was an increase in the surface density of the channels when DN-ARF6 was co-expressed due to reduced internalisation (Figure 5.11.B). These results were consistent with the electrophysiological assays which showed that co-expression of DN-ARF6 but not CDC42 resulted in a significant increase in the current density of hERG channels in HEK293 cells (Figure 5.10.B&C, experiments done by Andrew Smith, n=4 or more cells for patching).
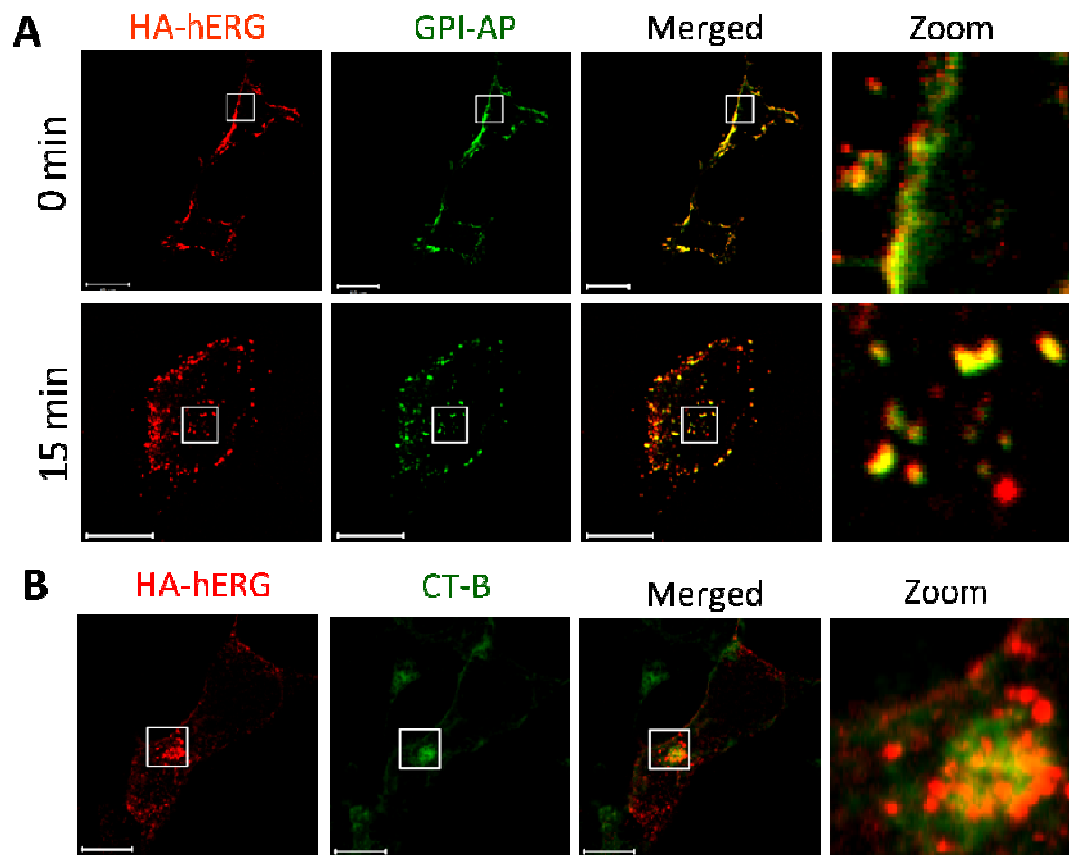
Figure 5.9 Internalised hERG channels co-localise with lipid-raft markers (A) HEK-MSRII cells made to express HA-hERG channels and GFP-GPI-AP were labelled on cell surface with anti-HA and anti-GFP antibodies respectively at 4°C and then incubated at 37°C for 0 and 15 min to allow internalisation. Cells were then fixed, permeabilised and stained for immunofluorescence imaging. (B) HA-hERG channels were labelled following internalisation of anti-HA antibodies for 30 min at 37°C (as described in Fig.5.3.B). Alexa633-conjugated CT-B was added for the last 5 minutes of the assay (pseudo green). Representative confocal images from three independent experiments are shown; panels with zoomed sections highlight co-localisation (yellow) of the lipid-raft markers (pseudo green) with HA-hERG (red); Scale bar:10 μm
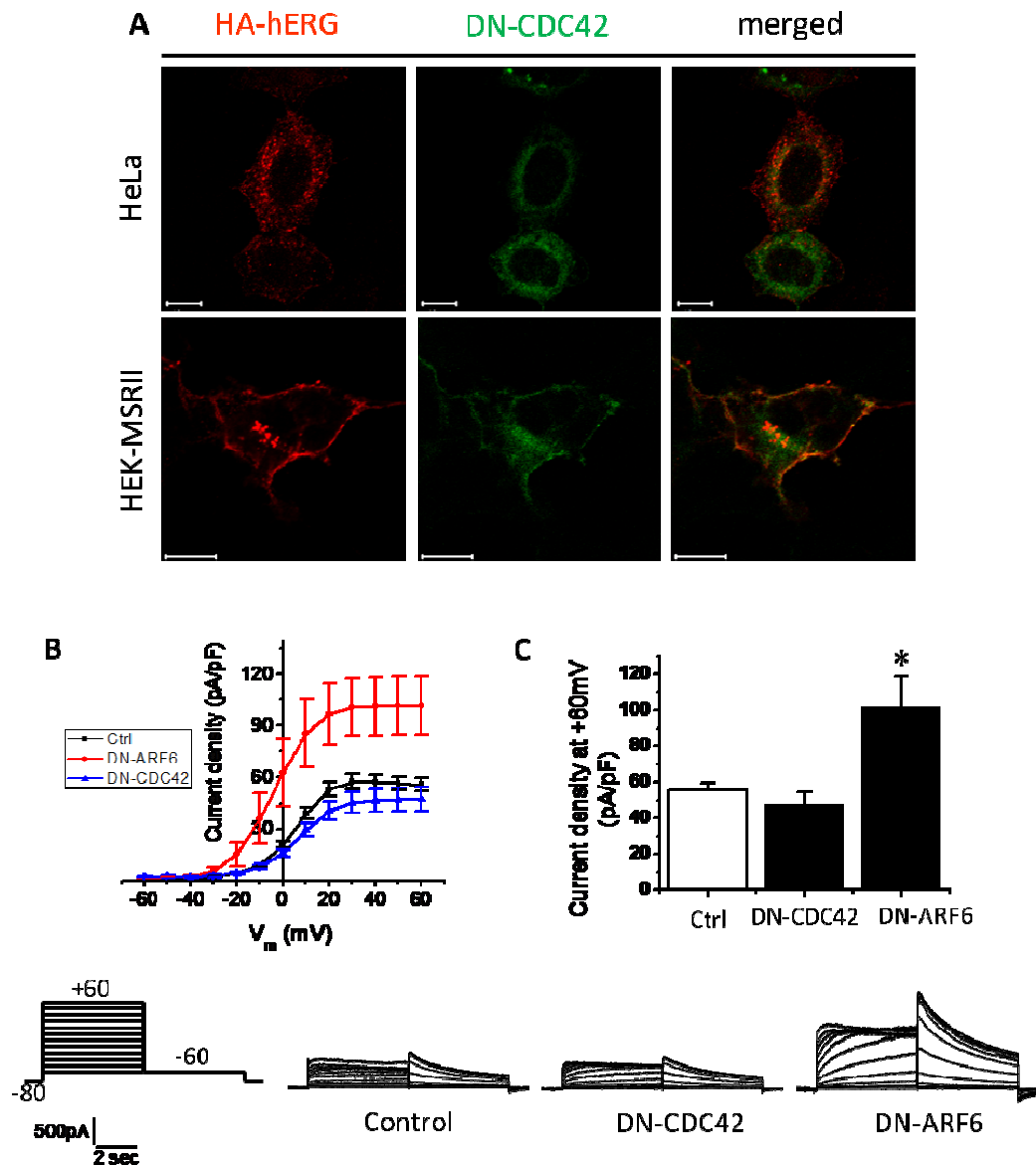
Figure 5.10 CDC42-independent internalisation of hERG channels. (A) HeLa and HEK-MSRII cells were co-transfected with HA-hERG and the indicated GFP-tagged DN constructs were allowed to internalise anti-HA antibodies before staining for endocytosed channels as in Figure 5.3.B. Representative confocal images from three independent experiments are shown; Scale bars: 10 μm. (*B*) Current voltage-relationships of HA-hERG channels co-expressed with the indicated dominant negative constructs; representative current families are also shown. (*C*) Histogram of current densities measured from tail currents (at -60 mV) after +60 mV prepulse. (Data in B and C is from experiments done by Andrew Smith).
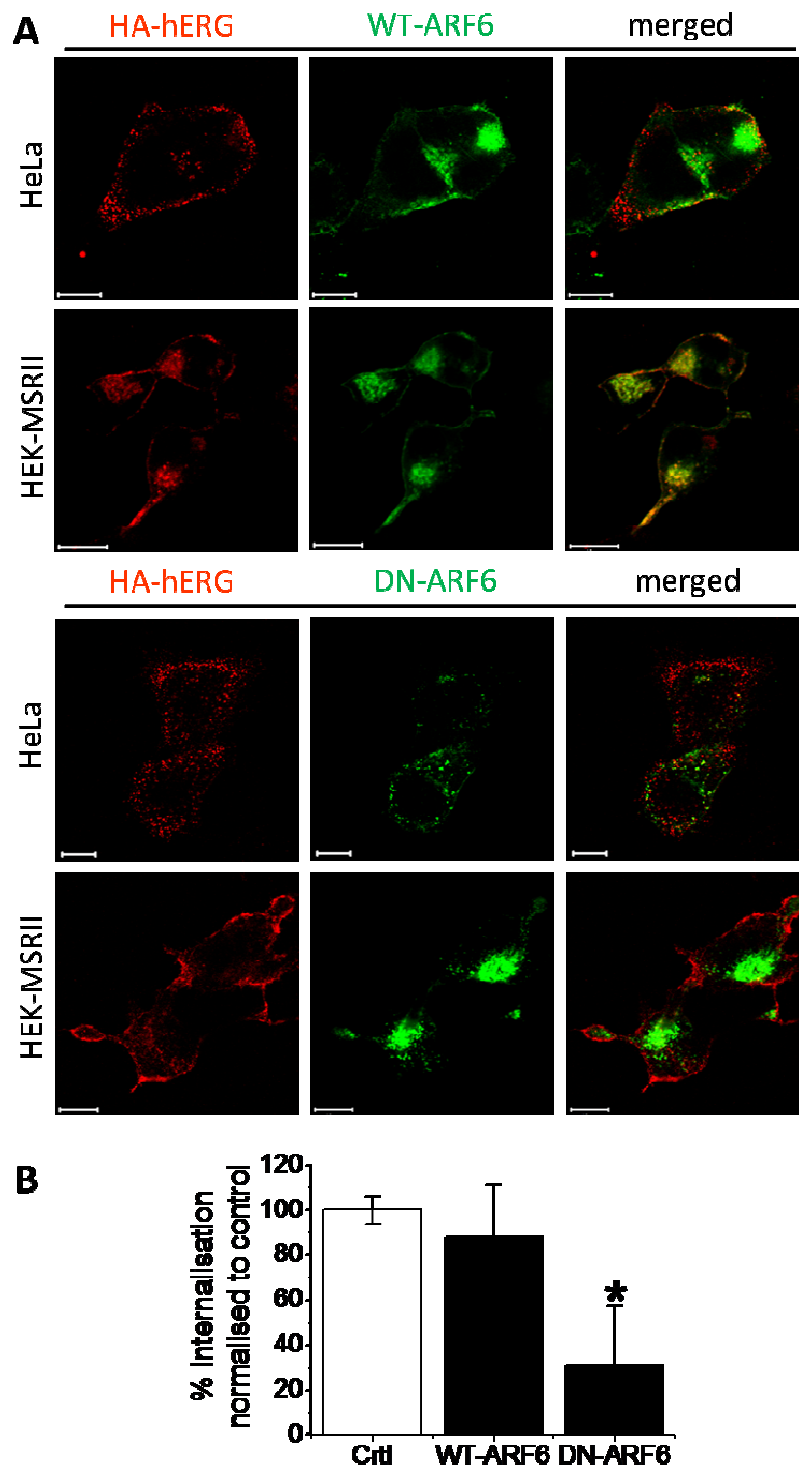
Figure 5.11 hERG internalisation is not completely blocked by DN-ARF6. HeLa and HEK-MSRII cells co-expressing HA-hERG and WT or DN-ARF6, immunostained for HA-hERG (red) following internalisation assay (A) or for remaining surface channels as in Figure 5.6.B and quantified using chemiluminescence assay (B). Representative confocal images from four independent images are shown; Scale bars: 10 μm mean $\pm$ s.e.m (n = 3) data are shown; * indicates p <0.05 (p = 0.01).

Taken together, these data suggested that internalisation of the hERG channels occurs via the ARF6-dependent pathway but could not explain why DN-ARF6 did not cause complete inhibition of internalisation of the channels. One possible explanation was that co-expression of DN-ARF6 and HA-hERG was allowed for about 40 hrs prior to the internalisation assay and staining of the channels for imaging and this long term block of the ARF6 function could be causing diversion of internalisation of the hERG channels by an alternate pathway, independent of ARF6.

To test this hypothesis, cells expressing HA-hERG channels and a known ARF6 cargo, Major Histocompatibility Complex class I protein (MHCI), were treated with aluminium fluoride (AlF: AlF_3 + AlF_4^-), which, unlike DN-ARF6, can disrupt ARF6 function acutely, following 30 min of pre-treatment at 37°C (Radhakrishna et al., 1996, Donaldson et al., 2009). Cells were labelled with anti-HA and anti-MHCI antibodies on cell surface at 4°C and allowed to internalise at 37°C for 0 min and 15 min in presence of AlF. Cells were then fixed, permeabilised and stained for HA-hERG and MHCI. Immunofluorescence staining showed that control (untreated) cells showed robust internalisation of both the cargos (Figure 5.12.A) while treatment with AlF blocked internalisation of both the cargos (Figure 5.12.B). Chemiluminescence assay carried out to determine percent internalisation of the channels showed complete block of HA-hERG internalisation in support of the results from imaging (Figure 5.12.C). Further, treatment of NRVCM with AlF also showed total block of native ERG channel internalisation (Figure 5.13).

The effect of AlF was not non-specific, since treatment of cells expressing the pancreatic K_{ATP} channel known to undergo CME did not block its internalisation (Figure 5.14A). Mediators of CIE, DN-CDC42 and DN-ARF6 did not appear to alter the internalisation of this channel (Figure 5.14B). Moreover, following the prolonged block of ARF6 using the DN isoform, internalisation of MHCI was completely blocked, which is an ARF6 cargo (Donaldson and Williams, 2009 , Figure 5.15). Taken together, it could be concluded from the results that internalisation of hERG channels is ARF6-dependent and that the channels are also capable of internalisation by other alternate pathways.
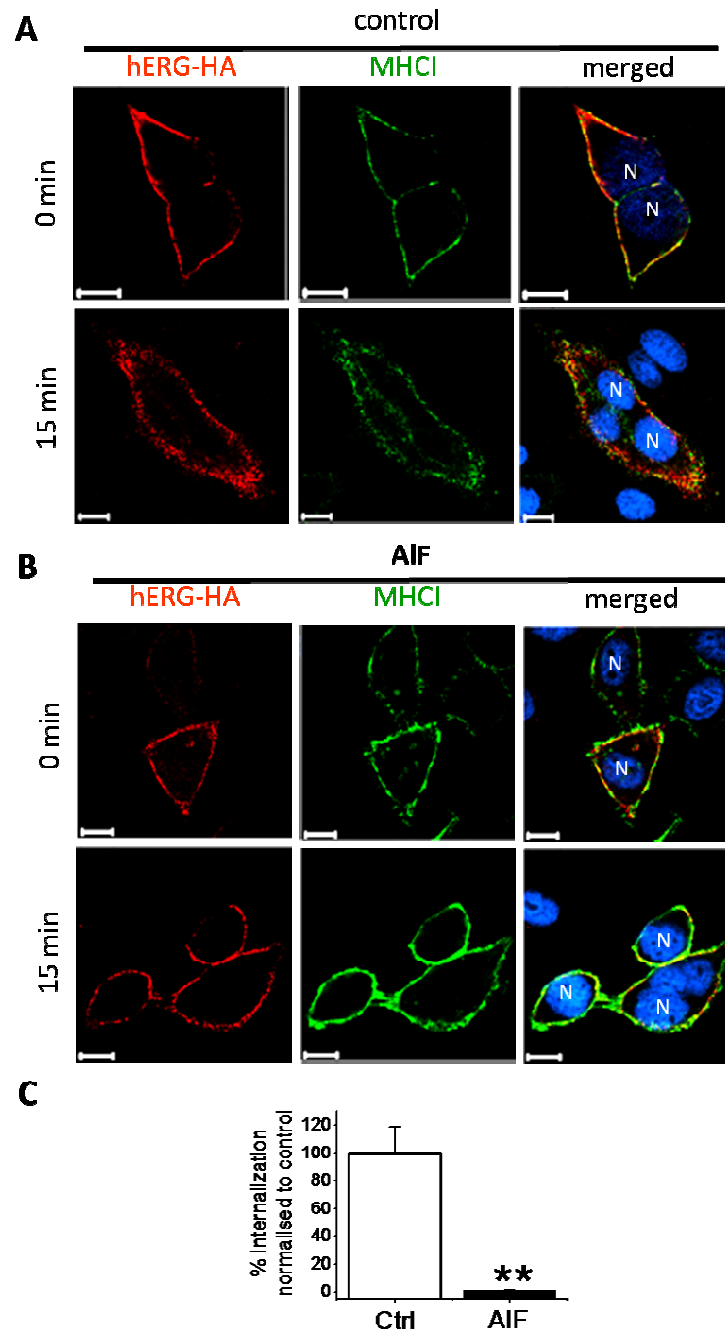
Figure 5.12 Acute block of ARF6 activity prevents hERG internalisation. HeLa cells co-transfected with HA-hERG and MHCI were not treated (control) (A) or pre-treated (B) with AIF and incubated with a mixture of rat anti-HA and anti-MHC antibodies at 37°C for 15 min in the presence of the compound. Cells were permeabilised and stained with appropriate fluorescent secondary antibodies for imaging. (C) Effect of AIF on the surface density of HA-hERG channels was determined as in Figure 5.6.B, using the chemiluminescence assay, mean ± s.e.m (n = 3) data are shown; ** indicates p<0.01 (p=0.01). Representative confocal images of three independent experiments are shown; Scale bars: 10 μm, nuclei (N) were stained blue with DAPI.
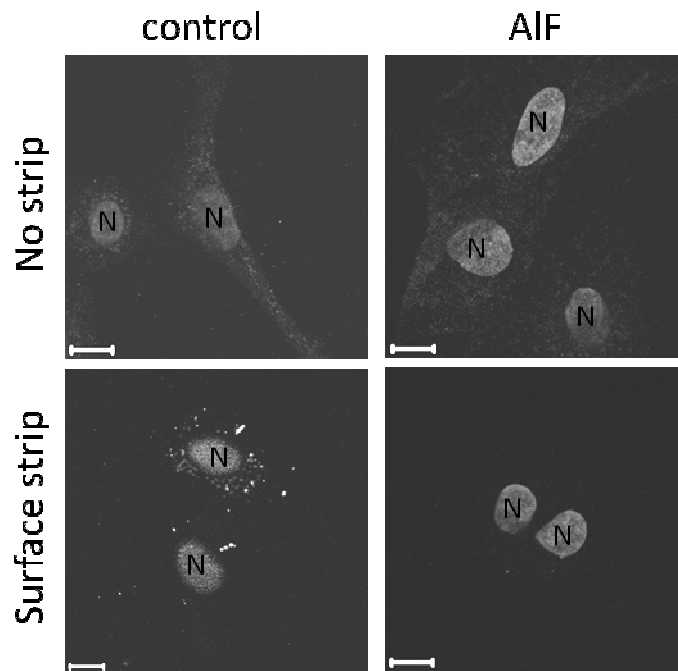
Figure 5.13 Native ERG channel internalisation is ARF6-dependent. Effect of AlF on internalisation of native ERG in NRVCM using acid strip method described in Figure 5.7. Representative confocal images of three independent experiments are shown; Scale bars: 10 μm, nuclei (N) were stained with DAPI.
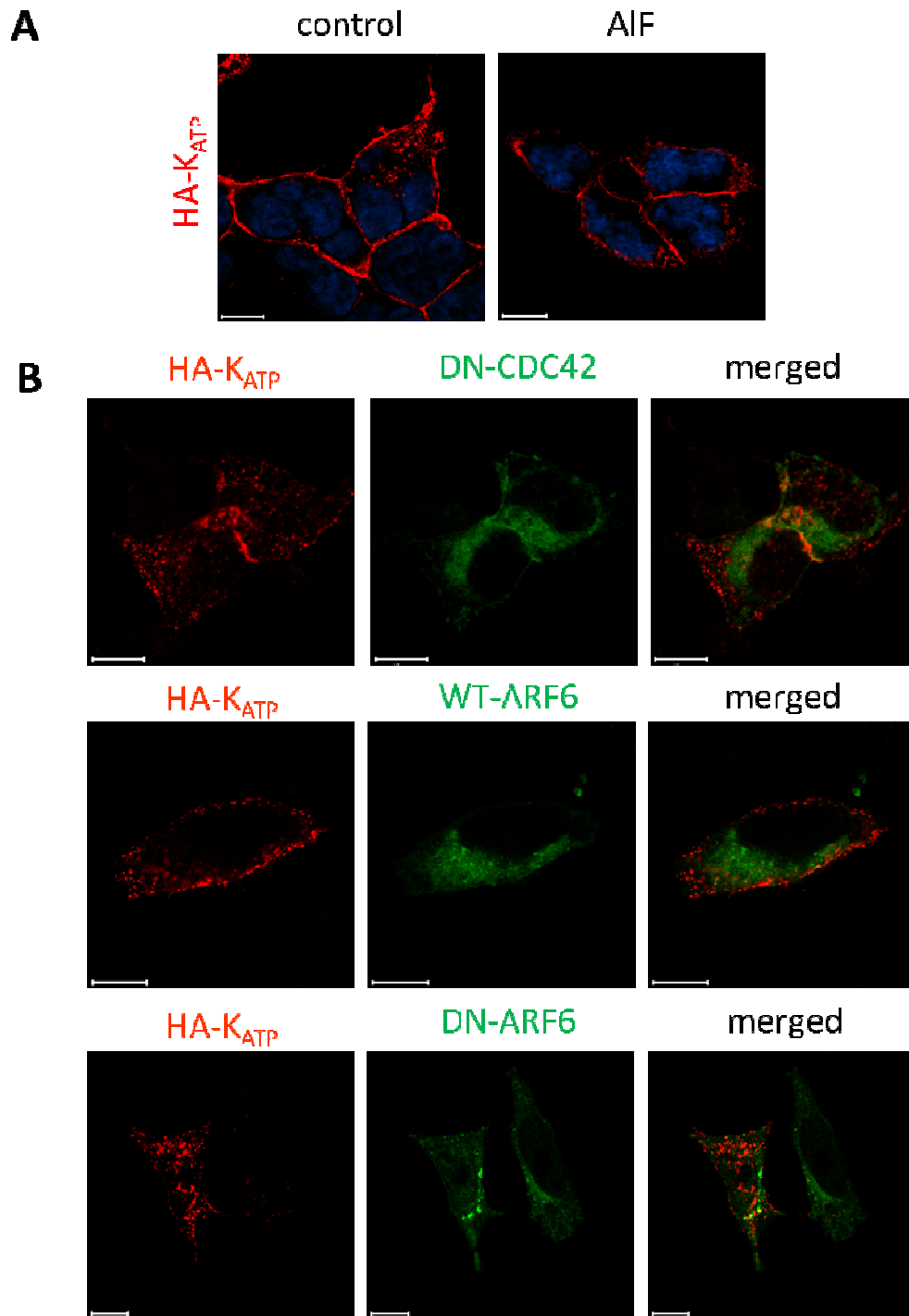
Figure 5.14 Internalisation of clathrin cargo HA-K$_{ATP}$ is unaffected by disruption of ARF6 activity by AlF. (A) Cells expressing pancreatic potassium channels HA-K$_{ATP}$ (HA-Kir6.2 + SUR1) were untreated or treated with AlF (see methods) followed by incubation with anti-HA antibody at 37°C for 1hr. Cells were then fixed, permeabilised and stained with Cy3-conjugated secondary antibodies to label the channel (red); (B) Cells were co-transfected with the indicated DN isoforms and HA-K$_{ATP}$ and the channels were stained (red) following the internalisation assay. Representative confocal images are shown; Scale bars: 10 μm.
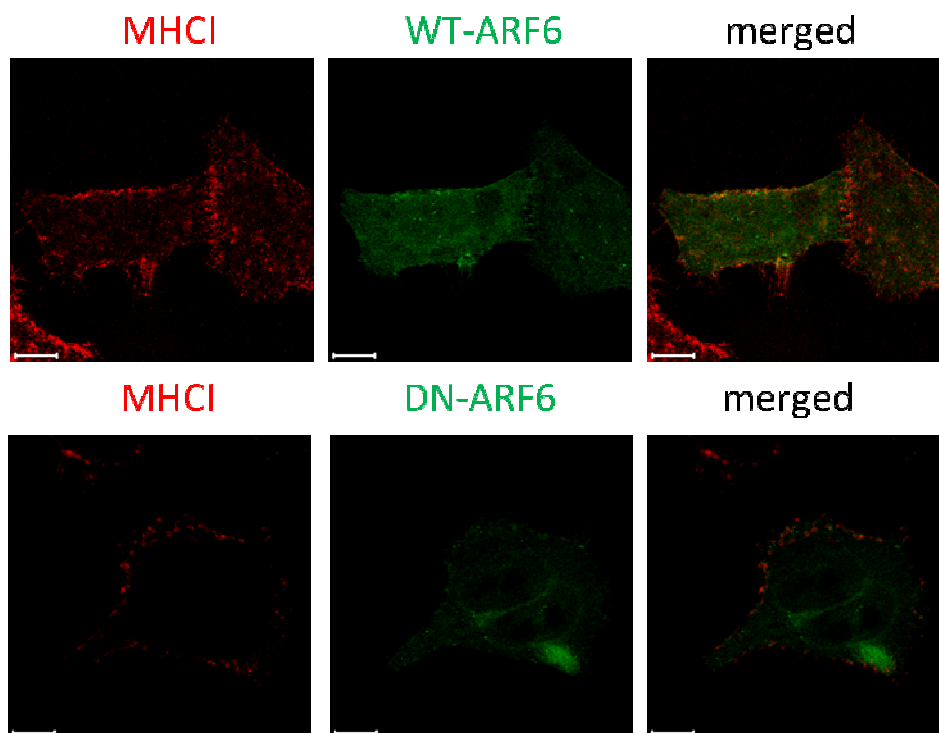
Figure 5.15 Internalisation of MHCI is ARF6-dependent. MHCI and GFP-tagged WT or DN-ARF6 was co-expressed in HeLa cells. Following the internalisation assay using anti-MHCI antibodies, cells were fixed, permeabilised and stained for immunofluorescence imaging (red). Representative confocal images are shown; Scale bars: 10 μm.

5.3.5 Dynamin and clathrin mediated alternate pathway of hERG internalisation

Chronic suppression of ARF6 was found to trigger internalisation of hERG via an alternate pathway (Section 5.2.4). To investigate this alternate pathway of hERG internalisation, HEK-MSRII cells co-transfected to express HA-hERG and DN-ARF6 were treated with drugs to block CME and CIE pathways: dynasore, MβCD and AlF (Figure 5.16). Since functional ARF6 was absent, AlF did not block internalisation. However, dynasore that blocks dynamin-dependent internalisation showed a complete inhibition of internalisation. Also, raft disruption with MβCD failed to inhibit HA-hERG internalisation after chronic suppression of the channel density with ARF6. These effects were exactly opposite to those seen in cells expressing only the hERG channels (Figure 5.6.A & 5.12.A). This dynamin-dependent alternate pathway of internalisation of the hERG channels was also apparent in HeLa cells (Figure 5.16.B). Thus, the alternate pathway of hERG internalisation was dynamin-dependent and raft-independent.

Dynamin-dependent pathways include CME or caveolin and RhoA mediated endocytic pathways (Doherty and McMahon, 2009, Mayor and Pagano, 2007). The latter two are also mediated by lipid-rafts. Treatment of cells expressing HA-hERG and DN-ARF6 with drugs genestein and nystatin, which are known to block caveolin mediated internalisation failed to inhibit internalisation of the channels (Figure 5.17). Moreover, co-transfection with DN-Cav1 (P132L) and DN-RhoA (T19N) also did not block internalisation of HA-hERG in cells expressing HA-hERG (Figure 5.18). These data further confirmed that the alternate pathway was not clathrin independent (raft mediated, dynamin-dependent). The only known pathway of internalisation which requires dynamin and is not mediated by lipid-rafts is CME (Doherty and McMahon, 2009, Mayor and Pagano, 2007). Therefore, effect of ARF6 suppression on co-localisation of endocytosed HA-hERG channels with clathrin cargo transferrin (Tfn) was examined. The results (Figure 5.18) showed that in cells where ARF6 function was chronically suppressed, there was a substantial increase (~ 4-fold; p <0.05) in the co-localisation of the hERG channels with internalised Tfn. Thus, the investigation suggested that though internalisation hERG channel is ARF6-mediated, chronic suppression of ARF6 function causes the channels to internalise via a dynamin-dependent, clathrin-mediated pathway.
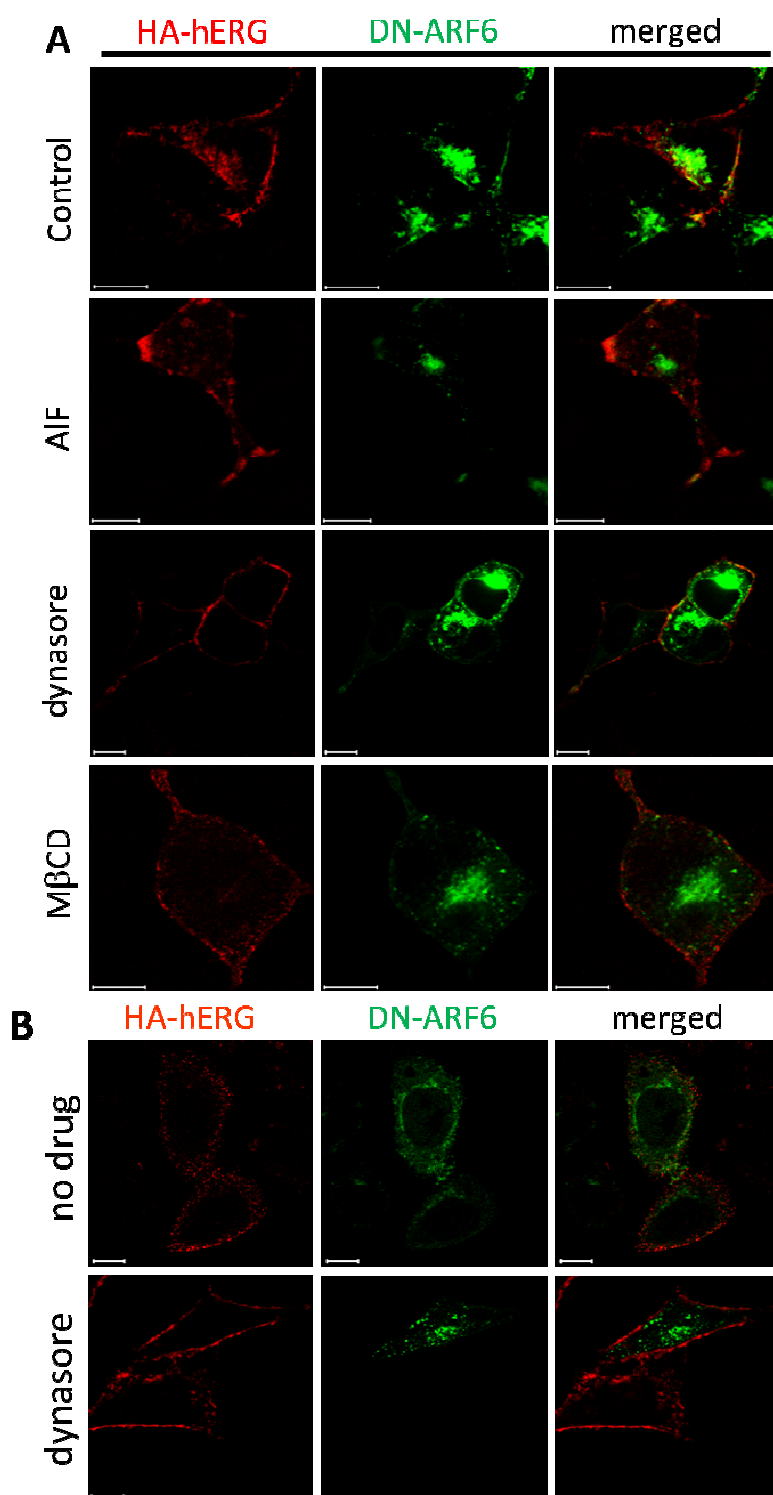
Figure 5.16 Chronic suppression of ARF6 function enables dynamin-dependent internalisation of the hERG channels. HEK-MSRII (A) or HeLa (B) cells co-transfected with HA-hERG and DN-ARF6-GFP were treated with the indicated drugs and internalisation of anti-HA antibodies was determined following the internalisation assay as in Figure 5.6.A except that no transferrin488 was included. Representative confocal images from four independent experiments are shown; scale bars: 10 μm.
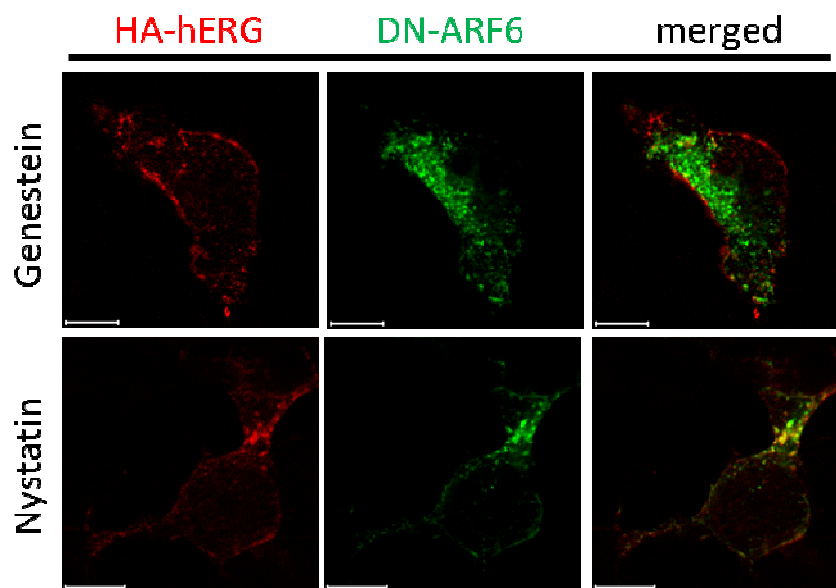
Figure 5.17 Pharmacological blockers of caveolin mediated internalisation do not inhibit internalisation of the HA-hERG channels that are internalised when DN-ARF6 is co-expressed. HEK-MSRII cells co-transfected with HA-hERG and DN-ARF6-GFP were treated with the indicated drugs. Internalisation of anti-HA antibodies was determined following the internalisation assay as in Figure 5.6.A except that no transferrin[633] was included. Representative confocal images from four independent experiments are shown; scale, bar: 10 μm.
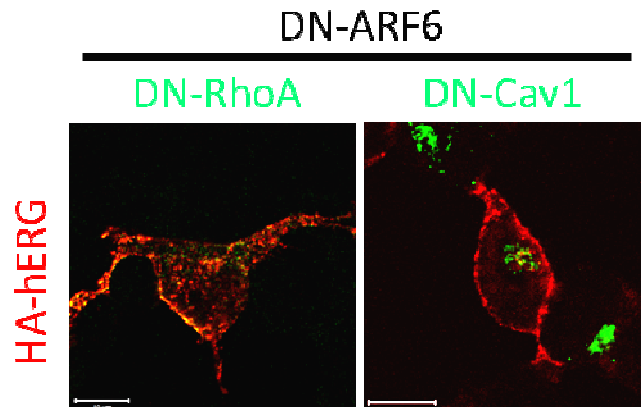
Figure 5.18 DN-RhoA and DN-caveolin do not inhibit internalisation of the HA-hERG channels that are internalised when DN-ARF6 is co-expressed. HEK-MSRII cells were co-transfected to express HA-hERG and DN-ARF6 along with myc- tagged DN-RhoA or GFP-tagged DN-caveolin1 (green). Following internalisation of HA-antibodies for 1hr, cells were fixed, permeabilised and stained with Cy3-conjugated antibodies to label the HA-hERG channels (red). DN-RhoA was stained (green) using anti-myc antibodies and Alexa[488]-conjugated secondary antibodies. Representative confocal images from four independent experiments are shown; scale bars: 10 μm.
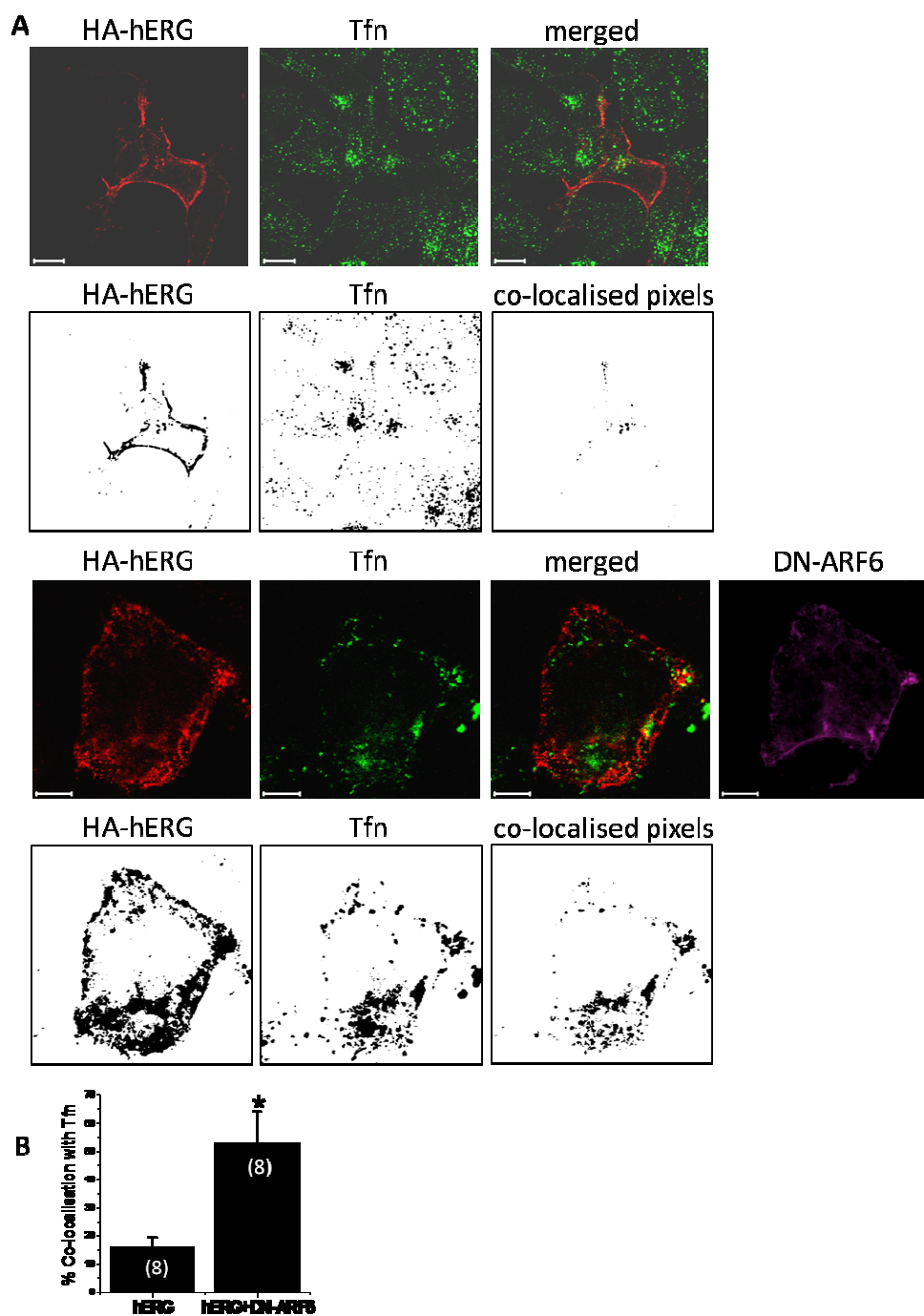
Figure 5.19 Chronic suppression of ARF6 function enables clathrin-dependent internalisation of hERG. (A) HEK-MSRII cells transfected with HA-hERG alone or with DN-ARF6-GFP (pseudo pink) were incubated in presence of anti-HA antibodies as in Figure 5.6.A and Alexa[633]-transferrin (Tfn) was added during the last 15 min of internalisation. Black and white images represent the area scored by ImageJ. Representative confocal images from three independent experiments are shown; Scale bars: 10 μm. (B) Percent co-localisation of Tfn with the HA-hERG channels was calculated using ImageJ (see Methods); mean $\pm$ s.e.m (n = 8) data are shown; * indicates p <0.05 (p = 0.02).

5.3.6 Effect of signalling molecules Protein Kinase A (PKA) and Protein Kinase C (PKC) on internalisation of hERG channels

Autonomic regulation of hERG channels is an area of active investigation with possibility of involvement of kinases, second messengers, and protein–protein interactions. PKA has been shown to affect the rate of hERG channel synthesis (Chen et al., 2009). It has been shown that PKC activators, ceramide, diacylglycerol (DAG) and its precursor phosphatidylinositol 4,5-bisphosphate (PIP_2) modulate hERG function. DAG has been reported to reduce surface hERG density and thereby alter channel function by causing channel internalisation (Ramstrom et al., 2010). Another group has reported that direct activation by PKC increases the hERG channel protein and K^+ current density in a time- and dose-dependent manner (Chen et al., 2010b). The reports however were thus conflicting and a clear effect of the protein kinases on channel internalisation had not been adequately investigated. Having investigated the endocytic pathway of hERG, it was interesting to look further into the regulation of hERG internalisation by PKC and PKA. To fulfil this aim, cells expressing HA-hERG channels were treated with activator and inhibitor drugs for PKC (Figure 5.20) and PKA (Figure 5.21). Following the internalisation assay as in Figure 5.16, cells were fixed, permeabilised and stained to label the channel (red). The imaging data were confirmed using the quantitative chemiluminescence assay as in Figure 5.6.B. Activation of PKC using diacylglycerol (DAG) or PMA was found to inhibit internalisation of the channel and increase surface channel density, while PKA activation or inhibition did not have significant effect on channel internalisation. The physiological significance of these data would be interesting to understand.
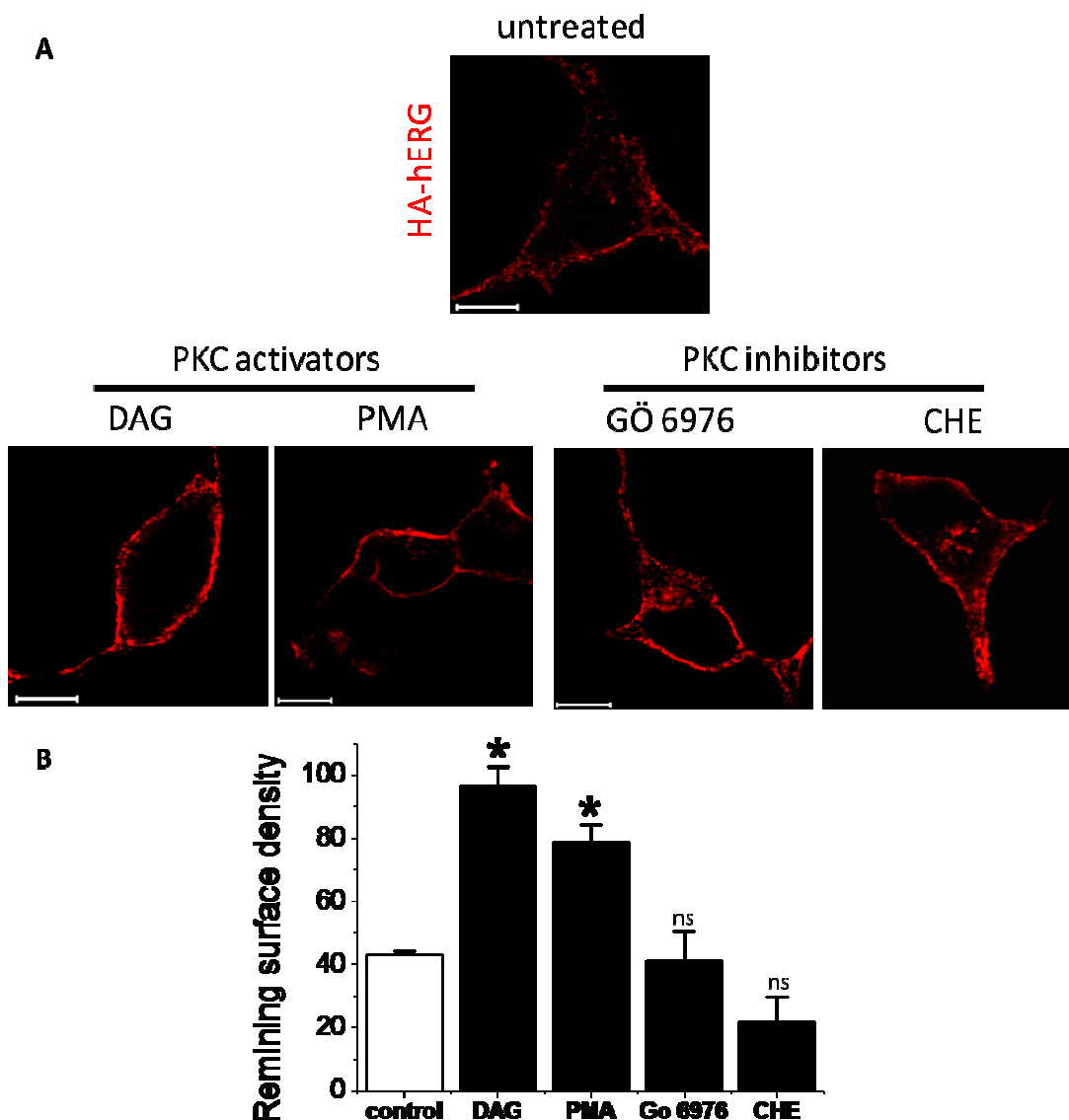
Figure 5.20 Internalisation of HA-hERG channels is blocked by activation of PKC.
(A) HEK-MSRII cells transfected to express HA-hERG channels were treated with PKC activators (DAG and PMA) or PKC inhibitors (GÖ6976 and CHE); see methods for details. HA-hERG channels were stained (red) following the internalisation assay. Representative confocal images of three independent experiments are shown; Scale bars: 10 μm. (B) Cells expressing the HA-hERG channels were treated with the indicated drugs for 30 min prior to and during the internalisation of pre-bound anti-HA-antibodies (15 min, 37°C). The remaining surface density of the channels was determined using the chemiluminescence assay (see Methods). Mean ± s.e.m (n = 2) data are shown, * indicates p value <0.01; ns, not significant.
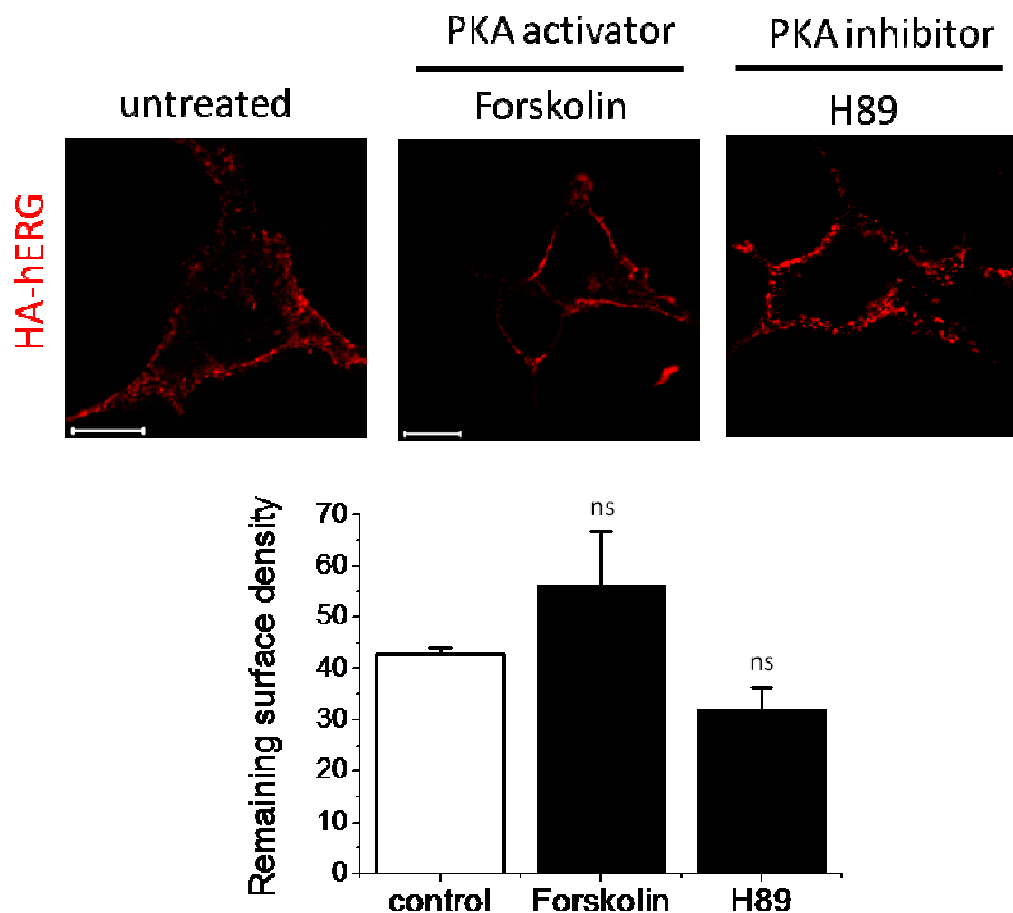
Figure 5.21 hERG internalisation is unaffected by activation of PKA. (A) HEK-MSRII cells transfected to express HA-hERG were treated with PKA activator (forskolin) or PKA inhibitor (H89); see methods for details. HA-hERG was stained (red) after the internalisation assay. Representative confocal images of three independent experiments are shown; Scale bars: 10 μm. (B) Cells expressing HA-hERG were treated with the indicated drugs. Internalisation of pre-bound anti-HA-antibodies was allowed to occur for 15 min prior to assaying the remaining surface density. Mean ± s.e.m (n = 2) data are shown; ns, non significant.

5.4 Discussion

Plasma membrane density of the cardiac hERG channels requires to be critically regulated since altered number of the channels is proven to be associated with life threatening cardiac arrhythmias (Anderson et al., 2006, Sanguinetti and Tristani-Firouzi, 2006). Besides the cardiac tissue, other tissues showing evidence of hERG expression include the pancreatic β-cells (Rosati et al., 2000) and neuronal cells (Selyanko et al., 1999). Also, hERG has been found to express in cancerous tissue that do not normally express the channels in non-cancerous conditions (Cherubini et al., 2000, Wang et al., 2002). Thus the path-physiological importance of hERG is immense and it is important to understand how the channel is regulated in terms of both channel function and expression on the cell surface.

It is known that the plasma membrane density of most proteins is controlled by a balance between biosynthetic delivery and endosomal trafficking processes (Doherty and McMahon, 2009, Drake et al., 2006, Kennedy and Ehlers, 2006). The unique properties of the hERG channels make them susceptible to a huge variety of drugs that directly block the channel (Thomsen et al., 2006) or alter its biosynthetic trafficking (Eckhardt et al., 2005, Rajamani et al., 2006, Anderson et al., 2006), causing drug induced LQTS. Therefore, the channel has become a major target of drug safety screens, which have added to the drug development costs and reduced the number of drugs that get past these screens for use in therapy. However, studies show that approximately 40% of acute hERG blockers also affect trafficking of the channels (Wible et al., 2005). Moreover, another major cause of LQTS is loss of function of mutations in hERG which may lead to any of the following: altered current kinetics, altered ion selectivity, or defective intracellular protein trafficking. Trafficking of the hERG channels attracted more attention, with reports that some of the mutant subunits display wild type current properties when normal trafficking was restored and channels were inserted in the cell membrane in vitro (Thomas et al., 2003b). These studies focused mainly on folding and biosynthetic delivery of the hERG channels and is still an area of interest to researchers (van der Heyden et al., 2008). As a result, while there have been many studies on the biosynthetic delivery of the channels to the membrane (Chen et al., 2010b, Ficker et al., 2003, Kagan et al., 2000), little is known about how the channel density is regulated post biosynthesis under physiological or patho-physiological conditions.

Two studies have reported that hERG channels undergo internalisation (Chapman et al., 2005, Guo et al., 2009); however, the mechanism by which the channels are endocytosed was not clear from either of these studies. Chapman et al., 2005, reported that ceramide treatment causes a time-dependent decrease in hERG current which was attributed to rapid internalisation of the channels from the cell surface. The authors reported that after ceramide stimulation the channel undergo ubiquitinylation and subsequent lysosomal degradation. These results suggested that surface density of the hERG channels expressed on the cell surface must be strictly regulated by endosomal trafficking. Another study by Guo et al., (2009) demonstrated that under hypokalaemic (low serum potassium) conditions, internalised hERG channels undergo increased degradation. The authors used both the heterologously expressed hERG channels in HEK cells and its native counterpart in rabbit hearts for their experiments. HEK cells expressing the channels were grown in medium containing 0 mM extracellular K^+ concentration. The hERG channels expressed in these cells had accelerated internalisation and degradation of hERG channels. The authors suggest that reduction of K^+ ion concentration induces a conformational change in the channel that somehow triggers ubiquitinylation and internalisation (Guo et al., 2009). Moreover, intracellular potassium ions are known to stabilise hERG folding and promote forward trafficking of the channels (Wang et al., 2009). These reports could explain how electrolyte imbalances, such as reduced serum K^+ levels (hypokalemia), trigger potentially fatal arrhythmias (Robertson, 2009), but the mechanism of hERG internalisation in physiological conditions was not understood from these studies. Investigation of endocytic pathways of hERG channels was therefore critical towards better understanding of how the surface channel densities might be regulated.

Membrane proteins are internalised by a variety of mechanisms, of which CDE is best characterised (Figure 5.1 and Doherty and McMahon, 2009, Mayor and Pagano, 2007). Whilst many membrane proteins appear to use CDE to internalise proteins and ligands, there is growing evidence for the existence of a number of other pathways, collectively known as CIE (Doherty and McMahon, 2009, Donaldson et al., 2009, Mayor and Pagano, 2007, Eyster et al., 2009). In order to study internalisation of hERG it was important to be able to track the channels expressed on the cell surface independent of the biosynthetic pathway. Therefore, for this study, the internalisation assay was used to track the internalised channels. In the assay, live cells were incubated with antibodies against extracellular epitope on the hERG channel which allowed only channels expressed on the cell surface and internalised there from to be labelled and immunostained. While anti-HA antibodies were used to label HA-hERG channels, native ERG channels in NRVCM were labelled using the anti-Kv11.1

antibody after confirming their specificity (Figure 5.2). The acid strip ensured that only the internalised channels were being imaged in the NRVCM (Figure 5.2). HEK-MSRII and HeLa cells were used for transient expression of HA-hERG channels. Using this assay it was clearly demonstrated for the first time using immunofluorescence imaging that ERG channels, native (Figure 5.3.A) and recombinant (Figure 5.3.B) undergo internalisation from the cell surface at body temperature but remain on cell surface at 4°C. The time course of hERG internalisation showed that the channel was capable of undergoing internalisation very rapidly with about 50% of the channel internalised within 15 minutes (Figure 5.3.C-D). These data also indicated that the endocytic mechanism was capable of rapidly altering the surface channel density.

Endocytic pathways are broadly classified as dynamin-dependent and independent. Co-expression of dominant negative dynamins did not affect internalisation of HA-hERG (Figure 5.4). These constructs have been shown to inhibit the internalisation of clathrin and dynamin-dependent endocytic cargo K_{ATP} (Mankouri et al., 2006). DN-μ2 (Doherty and McMahon, 2009, Nesterov et al., 1999) also did not affect internalisation of HA-hERG channels as confirmed by the dominant negative approach (Figure 5.5). Thus, hERG internalisation is clathrin-independent (CI). Dynamin-dependent CI endocytic pathways chiefly include caveolae and the less characterised clathrin- and caveolin independent carriers (CLICs), (Mayor and Pagano, 2007). Caveolae are flask shaped invaginations on the cell membrane that are made of caveolin. The caveolae require dynamin for fission from the cell surface to carry the endocytic cargo into the cell (Mayor and Pagano, 2007, Hansen and Nichols, 2010). Several ion channels such as the Kv1.5 and Kv1.3 are known to be targeted to caveolar lipid-rafts for internalisation (Martinez-Marmol et al., 2008). Others, such as Kv2.1, are associated with lipid-rafts that do not contain caveolin (Martens et al., 2001). Co-expression of DN dynamins and DN caveolin1, which are both required for caveolin-mediated internalisation, did not block internalisation of the HA-hERG channels (Figure 5.4 & 5.5). These data suggest that caveolae and CLICs do not have a role in internalisation of channels. A recent report (Massaeli et al., 2010) suggests that under low K^+ conditions, mature hERG channels and caveolin1 (Cav1) co-immunoprecipitate and knockdown of cavolin1 or dynamin2 using siRNA transfection significantly reduces the extensive hERG internalisation under low K^+. Another study reported that there is a significant increase in hERG current amplitude in HEK293 cells expressing the hERG channels when membrane lipid-rafts were disrupted or caveolin1 was knocked down by RNA interference. The authors (Lin et al., 2008) claim that hERG channels interact with caveolin1 and are negatively regulated by this interaction. Association with caveolins does not necessarily indicate that the proteins undergo caveolin dependent

internalisation because caveolins have also been implicated in membrane signalling without having a role in internalisation (Nichols, 2002). Another group has provided evidence that ERG channels in physiological conditions do not associate with caveolin through co-immunoprecipitation experiments (Balijepalli et al., 2007). The authors show that the ERG channels localise to cholesterol and sphingolipid enriched membranes and are modulated by membrane cholesterol.

Another group (Massaeli et al., 2010) show that in 0 mM K$^+$, hERG channels co-immunoprecipitate with caveolin1 and are endocytosed in a caveolin dependent manner to the lysosomes for degradation. The data from the present study, using the internalisation assay, clearly indicates that dynamin-dependent pathways, clathrin, caveolin and RhoA do not block internalisation of hERG (Figure 5.4 & 5.5) which is in contradiction to the report by Massaeli et al., 2010 . This may be because in the presented study internalisation of hERG channels in normal conditions was investigated and severe conditions of K$^+$ depletion were not used. Moreover, the channels were found to be capable of internalisation by dynamin-dependent alternate pathway and therefore it is possible that the channels are diverted to different endocytic pathways depending on the physiological state of the cell.

All of the known CI pathways are generally mediated by cholesterol rich membrane lipid-rafts (Nichols and Lippincott-Schwartz, 2001). The pharmacological approach using dynasore to inhibit dynamin function (Macia et al., 2006) suggested that internalisation of hERG channels is dynamin-independent (Figure 5.6.A & B). Disruption of lipid-rafts with MβCD (Klein et al., 1995) inhibited channel internalisation (Figure 5.6). Internalisation of ERG channels in NRVCM was also dynamin-independent but lipid-raft dependent (Figure 5.7). Consistent with these pharmacological data, and previously published biochemical experiments which showed that in canine cardiac cells, the majority of hERG channels are present in lipid-rafts (Balijepalli et al., 2007), HA-hERG in HEK-MSRII cells and ERG in NRVCM and guinea pig myocytes were localised to lipid-rafts (Figure 5.8). The raft localisation of hERG was also apparent with the extensive co-localisation of HA-hERG with GFP-GPI-AP and cholera toxin (Figure 5.9). Both these proteins are used as lipid raft markers (Nichols et al., 2001). GFP-GPI-AP .is internalised to the Golgi by clathrin and Rab5-independent pathway and fractionates to lipid-rafts (Nichols et al., 2001, Singh et al., 2003). The endocytic pathway of GPI-APs is thought to be CDC42-regulated, and the proteins internalised via this route enter the GPI-AP-enriched early endosomal compartments (GEECs), (Chadda et al., 2007).

Cholera toxin (CT), produced by *Vibrio cholera*, binds to the GM1 protein present in lipid raft domains on cell membranes and undergoes internalisation to be delivered to the Golgi and finally to the ER (Massol et al., 2004). CT is an interesting endocytic cargo since it has been shown to be able to undergo internalisation by several alternate routes including CDC42, caveolae, flotillin and even clathrin. Blocking of one or several endocytic pathways simultaneously does not prevent cholera infection (Massol et al., 2004). Co-localisation of internalised HA-hERG with GFP-GPI-AP and CT could aid in studying the post-endocytic destinations of the channel.

The presence of hERG in lipid-rafts is interesting because there is growing evidence from both functional and structural studies that lipids influence both functional properties and trafficking (surface density) of ion channels (O'Connell et al., 2004, Martens et al., 2004). Thus association of ion channels with lipid-rafts can have significant impact on cell signalling and physiology, (for example, depletion of cholesterol with MβCD causes a dramatic hyperpolarising shift in the steady-state inactivation properties of the Kv1.2 channels, Martens et al., 2000). Balijepalli et al (2007) reported that depletion of cholesterol with MβCD results in a positive shift of voltage dependence of activation and an acceleration of deactivation kinetics of the hERG channel. The consequence of these changes to cardiac rhythm is not known, but it is conceivable that removal of cholesterol could prolong the repolarisation phase of the cardiac action potential, increasing the risk of cardiac arrhythmias.

Having established that the hERG channels are internalised via cholesterol rich lipid-rafts, further investigation into the mediators of the endocytic pathway eliminated the role of CDC42. Although HA-hERG channels co-localise with CDC42 cargo, GFP-GPI-AP, disruption of CDC42 activity using the DN isoform approach did not inhibit internalisation of the channels (Figure 5.10). Moreover, DN-CDC42 did not alter functional hERG current density, while the hERG current density was significantly increased in HEK cells co-expressing DN-ARF6 (Figure 5.10.B&C, experiments by Andrew Smith, a member of Rao lab). Immunofluorescence studies did not appear to completely block internalisation of the channels (Figure 5.11A), though internalisation of ARF6 cargo, MHCI (Donaldson, 2003) was completely blocked by co-expression of the DN-ARF6 construct (Figure 5.15). Quantitative measurements of internalisation by the chemiluminescence assay showed that DN-ARF6 was causing a reduction in the internalisation of the channels (Figure 5.11.B).

ARF6 belongs to the family GTP-binding proteins that are expressed in all eukaryotes (see Introduction). ARF6 activity requires it to cycle between GDP-bound, inactive and GTP-bound, active states (Donaldson, 2003). ARF6 influences membrane trafficking (internalisation and recycling) and the actin cytoskeleton at the plasma membrane (PM) (Donaldson, 2003, Balasubramanian et al., 2007, Radhakrishna and Donaldson, 1997). The dominant negative ARF6 (T27N) is 'GDP on' and is mainly localised to intracellular tubulovesicular structures which can block cell surface molecules from recycling back to the cell surface. Majority of the endogenous ARF6 is present at cell surface and in recycling endosomes. Activation by hydrolysis of ARF6-GTP to ARF6-GDP is considered to signal its internalisation along with membrane rafts to recycling compartments (Sabe, 2003). Therefore, since DN-ARF6 was increasing the surface density of the hERG channels (Figure 5.11.B), ARF6 appeared to have a role in channel internalisation.

Aluminium fluoride prevents the GDP-GTP exchange of ARF6 (Radhakrishna et al., 1996) and thereby distrupts the function of the GTPase in a short duration (30 min pretreatment). Treatment with AlF completely blocked internalisation of hERG channels as well as MHCI (Figure 5.12). Internalisation of clathrin cargo, the pancreatic K_{ATP} channels was not affected by either DN-CDC42, DN-ARF6 or AlF treatment indicating that these methods of disruption of ARF6 function were specific (Figure 5.14). Moreover, disruption of ARF6 function in NRVCM with AlF also blocked ERG internalisation indicating the physiological relevance of the findings. Thus, unlike other cardiac ion channels, which are known to use dynamin-dependent clathrin- or caveolin-mediated mechanisms (Steele et al., 2007b, Steele et al., 2007a), hERG channels appear to undergo internalisation largely via a dynamin-independent route which is regulated by ARF6. Proteins known to depend on ARF6 for endocytic recycling are generally viral proteins such as the herpes simplex virus protein (VP22) (Nishi and Saigo, 2007), coxsackievirus type B3 (CVB3) (Marchant et al., 2009) and cellular prion protein (PrP[c]) (Kang et al., 2009). It is interesting why the hERG channel chooses an endocytic pathway that viral elements hijack. One explanation could be that viruses prefer to use robust pathways for entry into the cell that are difficult to disrupt and since regulation of the surface density of the hERG channels is critical, these channels also use this endocytic mechanism.

The only ion channel known to associate with ARF6 is the neuronal TWIK1 channel which is involved in cell volume regulation and excitability (Decressac et al., 2004). However, the role of ARF6 in the TWIK1 channel internalisation and recycling is not established. ARF6 has been shown to influence recycling of the inwardly rectifying

potassium channels, Kir3.4 (Gong et al., 2007a), but it appears to have no role in their internalisation. Thus hERG could represent the first report of an ion channel to use ARF6 for internalisation. Further research might reveal the role of ARF6 in trafficking of other ion channels in the future.

Chronic suppression of ARF6 activity using dominant negative isoform of ARF6, ARF6 (T27N) did not completely block internalisation of HA-hERG (Figure 5.11) unlike that of MHCI (Figure 5.15), while AlF completely prevented internalisation of the channels. Given that effect of AlF was not observed on non-ARF6 cargo, the HA-K_{ATP} channels (Figure 5.14.A), why DN-ARF6 was not able to completely block internalisation of the HA-hERG channels like AlF presented an interesting point of investigation. These differences in block of internalisation of HA-hERG by DN-ARF6 and AlF treatment could be due to the difference in the way these treatments work: whilst application of AlF produces an acute effect, transfection of DN-ARF6 gradually knocks down the ARF6 function. A simple explanation could be that DN-ARF6 was not fully blocking endogenous ARF6 function, However treatment of cells co-expressing HA-hERG and DN-ARF6 with AlF did not block internalisation of the channels (Figure 5.16.A) although AlF treatment should inactivate any remaining functional ARF6 in the cells. These data suggested that HA-hERG channels seen to internalise in cells expressing DN-ARF6 were taking an alternate pathway of internalisation that is ARF6-independent. Interestingly, dynamin inhibitor dynasore, completely blocked hERG internalisation while MβCD did not do so. This effect of the drugs was completely opposite to that seen on cells expressing HA-hERG alone (Figure 5.6, 5.12). These data raised the possibility that prolonged suppression of ARF6 function could promote deployment of alternative mechanisms of hERG internalisation and that the alternative mechanism was dynamin-dependent. Moreover since MβCD, DN-Caveolin1 and caveolae blocker drugs genestein and nystatin did not block the alternate pathway (Figure 5.17 & 5.18); it was considered to be non-caveolar. Increase in co-localisation with clathrin cargo Tfn (Figure 5.19) indicated that the channels are more likely to undergo dynamin and clathrin mediated endocytosis. Although the dynamin-dependent alternate pathway of internalisation of the HA-hERG channels was revealed only when ARF6 function was suppressed, it is possible that under normal conditions a small proportion of the channels undergo internalisation via the alternate pathway. Under patho-physiological conditions the channels may be diverted to internalisation via alternate endocytic pathway/s which are dependent on dynamin and caveolin (Massaeli et al., 2010).

Ability of proteins to undergo internalisation via more than one mechanism has been reported in a few other cases. Cholera toxin can enter cells via multiple endocytic pathways (Massol et al., 2004, Torgersen et al., 2001). A number of signalling receptors which use multiple mechanisms to promote internalisation and to regulate signal output include the epidermal growth factor receptor, EGFR (Sigismund et al., 2008) and TGFbR (Di Guglielmo et al., 2003). CME is the major pathway of internalisation of these receptors which commits the receptors to recycling and thereby sustains signalling. On the other hand, CIE couples the receptors with degradation leading to attenuation of signalling. In the case of Wnt3a activated pathway of low-density-lipoprotein receptor-related protein 6 (LRP6), major endocytic pathway is caveolar. However inhibition of Wnt3a shunts the LRP6 to a CME pathway. The mode of internalisation of the LRP6 determines if β-catenin signalling is activated or inhibited (Yamamoto et al., 2008), showing that the partitioning of the receptors to different endocytic routes has physiological importance. Although the significance of the two pathways for hERG internalisation is unclear at present, whether partitioning of hERG between the ARF6 and clathrin dependent pathways is similarly regulated, and if so, what signalling molecules determine the traffic route, and what effect such changes might have on cardiac rhythm remains to be investigated.

The fact that a variety of signals, including protein kinases (Chen et al., 2010a), lipids (Bian et al., 2004, Chapman et al., 2005) and ions (Guo et al., 2009) influence cardiac action potential, and that these signals also regulate the surface density of hERG, could suggest that differential trafficking might have a physiological role. The effect of protein kinases on hERG function has been demonstrated and autonomic regulation of hERG channels is an area of active investigation.

Protein kinase C (PKC) is known to control the function of proteins through phosphorylation of hydroxyl groups of serine and threonine amino acid residues. Diacylglycerol (DAG) is one of the key lipid second messengers which bind to the C1 domains of all PKC isozymes resulting in their activation (see introduction). Phorbol esters such as PMA bind to C1 domains of PKC isozymes and thus mimic DAG and activate PKC (Yang and Kazanietz, 2003).

Regulation of hERG potassium channels by activation of PKC was reported to be independent of direct phosphorylation of the channel protein by use of hERG mutants lacking the possible PKC phosphorylation sites in the hERG C-terminus (Thomas et al., 2003b). Experiments with activators and inhibitors of protein kinase C (PKC) showed that PKC activation by treatment with PMA and DAG blocks internalisation leading to

increase in surface channel density (Figure 5.20). A more recent publication (Ramstrom et al., 2010) claimed that DAG potently reduces hERG current due to a PKC-evoked internalisation of the channels from the cell surface and the endocytic mechanism requires the dynein–dynamin complex. However, the data presented to support this hypothesis measured total hERG channels instead of channels internalised from the cell surface. On the other hand, direct activation of PKC with PMA has been shown to increase abundance of the hERG protein and K^+ current density in a time- and dose-dependent manner by protecting the channel from degradation and also enhancing channel synthesis (Chen et al., 2010b). The data presented in this chapter show that treatment with PMA and DAG blocks internalisation of the HA-hERG channels leading to an increase in surface channel density (Figure 5.20). If internalisation was blocked by PMA or DAG then the channels would not be diverted to degradation, which would explain the increase in the hERG channel protein reported by Chen et al (2010).

There are reports of regulation of hERG by the α1A-adrenergic receptor (α1A-AR). Stimulation of α1A-AR increases abundance of hERG protein and K^+ current density through the activation of PKC in a time and dose dependent manner (Chen et al., 2009). The block of hERG internalisation by activation of PKC (Figure 5.20) could explain the mechanism behind the up-regulation of hERG by PKC, a process that may have relevance in cardiac diseases and treatment. Activation or inactivation of PKA did not affect surface density of the channel (Figure 5.21). It has been shown that PKA activity is required for functional expression of the channel (Chen et al., 2009). This would imply that short term modulation of the kinase would not alter the surface density of the channel by processes such as internalisation.

In a patho-physiological context, hERG channels have been found to be over-expressed in cancer cells and blocking of the channels is being tested for use in cancer therapy (Felipe et al., 2006). Infection with hepatitis B virus transactivator (HBx) is a known cause of cancer and HBx infection has been shown to cause an increase in DAG and activation of PKC (Luber et al., 1993). Since PKC activation leads to an increase in surface hERG density, it may be one of reasons why elevated levels of hERG channels are found in cancer cells. The patho-physiological role of the channels in cancerous tissue is however not well understood. Another interesting question is how PKC activation regulates hERG internalisation. One explanation could be that PKC activates ARNO, an upstream regulator of ARF6 (Frank et al., 1998) that catalyses exchange of ARF6-GTP to ARF6-GDP (Santy and Casanova, 2001). This would result in blocking of ARF6 function and thereby block internalisation of the channels.

5.5 Summary

The aim of the present study was to investigate the mechanism underlying the internalisation of the cardiac hERG potassium channel. This knowledge was necessary to gain an insight into how the channel density and thereby function might be regulated. The results demonstrated that internalisation of hERG occurs via a lipid-raft and ARF6-dependent mechanism. Such a mode of internalisation is previously unreported for ion channels. Though this was a major pathway of internalisation of the channel, a prolonged block of ARF6 function revealed a dynamin-dependent alternate endocytic pathway of the channel. The alternate pathway appeared to be mediated by clathrin and independent of lipid-rafts. These findings suggested the possibility that the channel internalisation may be differentially regulated in different physiological and patho-physiological conditions. Experiments to look at the effect of PKC on internalisation of hERG channels showed that activation of the kinase inhibits channel internalisation. These data explain the mechanism behind the increase in hERG currents by PKC activators and the α1A-adrenergic receptor stimulation. The hERG channels are known to be different from other members of the Kv potassium channel family since they exhibit unusual biophysical properties and pharmacology, in particular with regard to their susceptibility to promiscuous blockade by several commonly used drugs. It is therefore seems not surprising that the hERG channels differ from other members of the family in terms of how they are internalised from the plasma membrane.

CHAPTER 6

hERG Channels Recycle and Blocking Rab11a Function Increases Channel Degradation

6.1 Introduction

Cells express several membrane proteins on their surface and in most cases these proteins are removed from the cell surface by internalisation. Cell membranes are known to internalise the equivalent of their cell surface one to five times per hour (Steinman et al., 1983). The endocytic machinery plays an important role in delivering membrane components which include membrane proteins, lipids, solute molecules and receptor associated ligands to various intracellular destinations. Following internalisation from the cell membrane the proteins are generally delivered to early endosomal compartments. Depending upon the nature of the regulatory signals, the cargoes undergo sorting which allows some membrane proteins to recycle back to the plasma membrane, while others traffic to lysosomes for degradation or are returned to the trans-Golgi network (TGN) (Kennedy and Ehlers, 2006, Drake et al., 2006, Bonifacino and Traub, 2003, Grant and Donaldson, 2009). Different membrane proteins can take different routes and differ in the recycling kinetics. Generally, it is the dynamic balance between the recruitment (biosynthetic secretion and endocytic recycling) and removal (internalisation) mechanisms that governs the composition of the plasma membrane and thereby contributes to cellular processes that membrane proteins mediate. A tilt in this balance could have important (patho-) physiological consequences (Maxfield and McGraw, 2004, Grant and Donaldson, 2009).

The mechanism by which membrane proteins undergo internalisation is a major determinant of their post- endocytic destination. Endocytic mechanisms can be broadly classified as those that are clathrin-dependent (CDE) and those that are clathrin independent (CI) (Doherty and McMahon, 2009, Mayor and Pagano, 2007). Cargoes of CDE (see introduction), such as receptors for transferrin (TfR), are packaged into clathrin-coated vesicles that pinch off from the cell membrane with the help of dynamins and transported into the cell (Doherty and McMahon, 2009, Mayor and Pagano, 2007). Endocytic recycling of CDE cargo has been extensively studied. Cargoes of CI internalisation such as the Major Histocompatibility Complex Class I (MHCI) (Donaldson and Williams, 2009) depend on membrane lipid-rafts (see introduction). Since these pathways of internalisation are not well studied, a lot remains to be understood about endocytic recycling of CI endocytic cargo (Grant and Donaldson, 2009).

Endosomal trafficking is mediated by Rab GTPases. The functionality of this family of proteins underlies their ability to act as molecular switches that cycle between GTP-

and GDP-bound states. Several Rab proteins are known to play specific roles in endosomal trafficking (see Chapter1). Rab4, Rab11 proteins have been implicated in the regulation of endosomal recycling. Rab4 is localised to the early endosomes (EE) and sorting endosomes (SE) and is considered to be involved in direct recycling of internalised proteins back to the plasma membrane. Rab11 is localised to the late endosomes (LE) and the recycling endosomes (RE) and plays a role in recycling of internalised proteins back to the plasma membrane. The family of Rab11 GTPases include Rab11a, Rab11b and Rab25 (Grant and Donaldson, 2009). Both Rab11a and Rab11b are ubiquitously expressed and Rab11b is enriched in the brain, heart and testis (Lai et al., 1994); while Rab25 expression is limited to certain tissue types (Lapierre et al., 2003). Recent studies have shown that in polarised epithelial cells where Rab11a and Rab11b are thought to regulate the apical transport of different endocytic cargo, Rab11b may have specific functions as it only partially co-localises with Rab11a in polarised, filter-grown, Madin-Darby canine kidney (MDCK) cells (Lapierre et al., 2003). Rab11a has been shown to regulate the apical recycling of several membrane proteins including the immunoglobulin receptor, human transferrin receptor, and bile salt export pump (ABCB11) and CFTR (Silvis et al., 2009). Trafficking by Rab11b is less understood but it has been implicated in the recycling of human transferrin receptor (Schlierf et al., 2000), and exocytosis of the human growth hormone (Khvotchev et al., 2003).

Cargos of CI internalisation such as MHCI and interleukin-2 receptor α-subunit (Tac) have been shown to enter early endosomal compartments which are distinct from the ones that carry cargoes of CME immediately after internalisation. However, on a later time point in the endocytic itinerary, proteins of CME and CI internalisation have been found to converge and enter late endosomes from where can be diverted to lysosomes for degradation in a Rab7-dependent manner or be recycled back to the cell surface (Grant and Donaldson, 2009, Naslavsky et al., 2003).

In this chapter, the role of post endocytic trafficking in regulating surface density of the cardiac hERG channel was investigated. Any change in the steady-state levels of this channel at the cell surface would have a significant impact on the net K^+ conductance and, therefore, on repolarisation of the cardiac action potential and the cardiac rhythm (Anderson et al., 2006). Hence, it is important to understand if hERG undergoes endocytic recycling and how this process affects the surface channel density. Such a study would have a major impact in understanding the patho-physiology hERG related cardiac arrhythmias. Results presented in Chapter 4 showed that forward trafficking of hERG is mediated by COPII vesicles in a Sar1 dependent pathway. Synthesis of hERG

has been shown to be stringently regulated with the help of chaperones and proteins of the COPII machinery (Ficker et al., 2003). It has been reported that Rab11b is required for the expression of mature hERG (Delisle et al., 2009). This was the first report of the Rab11 protein being implicated in forward trafficking rather than endocytic recycling. Studies presented in Chapter 5 showed that hERG was rapidly internalised from the cell membrane mostly in a lipid raft and ARF6 regulated manner. Also, it has been shown that the hERG channels can bind ubiquitin and get degraded subsequent to the ubiquitinylation (Chapman et al., 2005). However, there were no reports on endosomal recycling of the channel.

In this chapter, the endocytic recycling of the hERG channel was investigated with an attempt to understand the time course of turnover of the endocytosed channels. The study revealed that internalised hERG channels recycle back to the cell surface but are eventually rapidly degraded. Co-expression of a dominant negative isoform of Rab11a showed that there was a significant increase in the channel degradation. Degradation of the channels could be prevented if internalisation of the channel was blocked using aluminium fluoride (AlF), a compound that disrupts ARF6 function (described in chapter 5). Thus, inhibition of hERG recycling results in a substantial reduction in the cell surface density of hERG and block of internalisation can protect the channels from degradation. These data suggested that endosomal recycling of the channel may be a major mechanism for regulation of surface hERG density.

6.2 Materials and Methods

6.2.1 Cell lines

As described in Chapter 2, section 2.2.1. For experiments involving drug treatments, poly-L-lysine coated cover-slips were used for growing cells (as described in Chapter 2, section 2.5.1). The cells were transiently transfected with the required DNA constructs using the Fugene®6 transfection reagent (as described in Chapter 2, section 2.4.2).

6.2.2 Plasmid constructs

HA-tagged hERG in pcDNA3 was transfected into HEK-MSRII cells for transient expression of the HA-hERG channels as described in Chapter 4. Other cDNA clones were generous gifts from various researchers (indicated in parenthesis): GFP-tagged EEA1 (Dr H Stenmark, Norwegian Radium Hospital, Oslo), GFP-Rab5 (S34N), (Dr Vas Poonambalam, University of Leeds, UK), GFP-Rme1(G429R) (Dr B Grant, Rutgers University, NY), GFP-Lamp1 (Dr P Boquet, Institut National de laSante et de la Recherché Medicale, Nice), GFP-Rab11b(WT), GFP-Rab11b (N124I) and GFP-Rab11b(S25N), (Dr. Beate Schlierf, Institut für Biochemie, Universität Erlangen-Nürnberg, Erlangen, Germany).

6.2.3 Antibodies

Rat anti-HA antibodies (Roche) were as described in Chapter 5. Anti-CD63 antibodies were purchased from Abcam and used at 1:250 dilution. Anti-rat, Cy3- and Cy5-conjugated secondary antibodies (Jackson ImmunoResearch) are described in Chapter 5.

6.2.4 Drug treatments

Stock solutions of pharmacological compounds and treatment of cells was done as in Chapter 5. Leupeptin (Sigma) was used at a concentration of 10 μM and monensin (Sigma) at 200 μM and cell-permeable C_6-ceramide at 10 μM. Aluminium fluoride was prepared as described in Chapter 5.

6.2.5 Immunofluorescence staining

Immunostaining of HA-hERG channels was performed as described in Chapter 2.

6.3 Results

6.3.1 Recycling of internalised hERG channels to the cell surface

The internalisation assay used in Chapter 5 showed that the hERG channels undergo internalisation. Therefore in this chapter, the question asked was if these internalised channels undergo recycling back to the cell surface. In order to address this question, a recycling assay, previously described for K_{ATP} channels (Manna et al., 2010), was adopted. In this assay cells expressing HA-hERG channels were incubated at 37°C for 60 min in presence of the anti-HA antibodies directed against the extracellular HA-epitope cloned into the channel. When the channels were internalised, the antibodies bound to the channel were internalised along with it. This step of the assay allowed labelling of the channels expressed on the cell surface as well as the channels undergoing internalisation. The cells were then moved to 4°C to stop all endosomal trafficking of the channels and the channels present on the cell surface labelled with the primary antibody were labelled with a no-tag secondary antibody. The cells were then incubated in the presence of Cy3-conjugated secondary antibodies at 37°C or 4°C for 15 min which allowed labelling of the primary antibody bound internalised channels that recycled back to the cell surface. Immunofluorescence imaging indicated that prior to labelling with no-tag antibody; there are a number of HA-hERG channels present on the cell surface which cannot be detected in the cells labelled with no-tag secondary antibody at 4°C (Figure 6.1, first panel). This indicates that the no-tag antibody is able to bind all the channels present at the cell surface after the internalisation assay and that no channels recycle at 4°C (Figure 6.1, second panel). However, in cells incubated at 37°C, the internalised HA-hERG channels recycle back to the cell surface and bind the Cy3-tagged secondary antibody and are stained red (Figure 6.1, third panel). These data indicated that after internalisation the HA-hERG channels are able to recycle back to the cell surface and re-internalised. This protocol allows specific labelling of the recycling pool of channels and has been designated as the recycling assay.
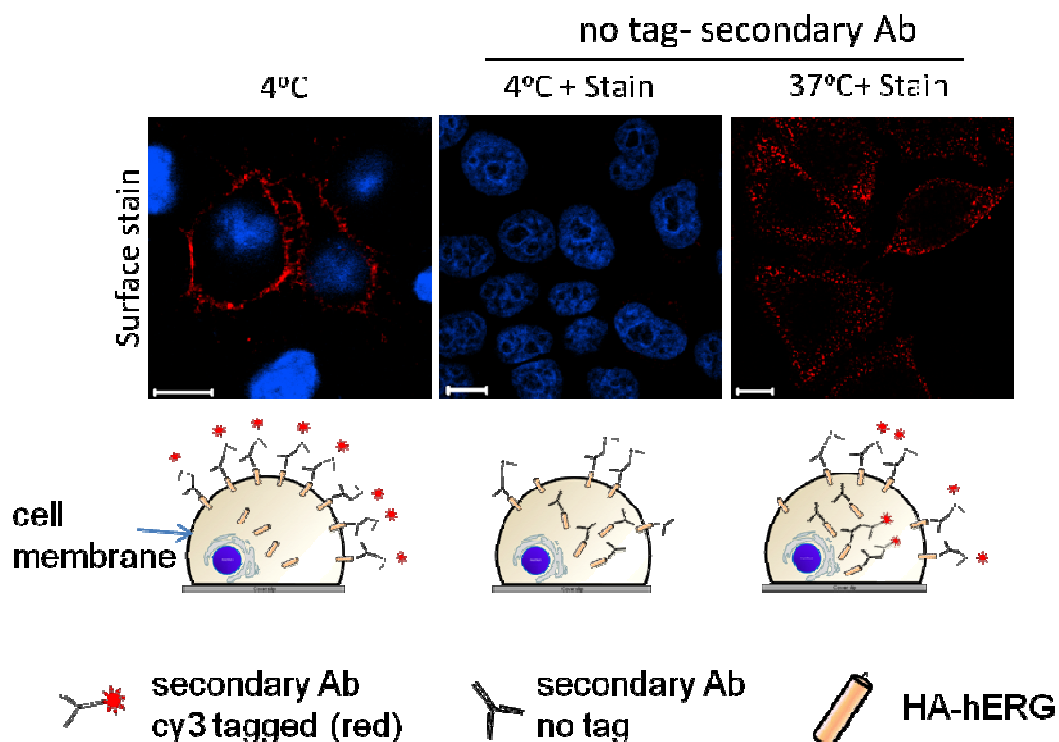
Figure 6.1 HA-hERG channels are recycled to the cell surface. HeLa cells expressing HA-hERG were labelled with anti-HA antibody for 60 min at 37°C and chilled to 4°C. While one set of cells was stained on cell surface, other sets were incubated with no tag-secondary antibodies (Ab) which would not be visible in immunofluorescence imaging. Cells were then incubated at 4°C (control where no recycling would occur) or 37°C in presence of Cy3-conjugated secondary antibodies for 15 min to allow the channels recycled back the cell surface to be labelled (red). The cells were then washed, fixed and mounted for imaging. Nuclei were stained (blue) with DAPI. Representative confocal images of three independent experiments are shown; Scale bars: 10 μm. A schematic representation of the images is included below the image panels to illustrate how the channels are being stained (see methods for more details).

6.3.2 hERG channels recycle rapidly and undergo degradation

Having established that hERG is capable of recycling back to the cell surface after internalisation, it was important to find out how fast the recycling process could occur. Towards this, the recycling assay was modified to examine the rate of recycling. As in the standard recycling assay, channels labelled on the cell surface with primary antibodies (anti-HA) were allowed to undergo internalisation. The channels remaining on the cell surface were allowed to bind no-tag antibodies at 4°C, following which the internalised channels were allowed to recycle back to the cell surface at 37°C in presence of Cy3-conjugated secondary antibodies for different time durations. Recycling of the channels was stopped by moving the cells to 4°C. The cells were washed and fixed with 2% PFA. This protocol allowed the recycled channels for different time points to be stained (red). The non-recycled channels that remained within the cells were stained with Alexa488-conjugated secondary antibody (green) following permeabilisation of the cells (see schematic Figure 6.2.A). Data presented in Figure 6.2.B shows that at time 0, there are no red stained channels since none were recycled. The internalised channels rapidly recycle back to cell surface within 5 minutes of incubation and by 30 minutes, most of the internalised HA-hERG channels have recycled as indicated by the absence of green stained channels in the panel for non-recycled channels. The channels also appear to re-internalise and interestingly by 120 minutes, the recycled channels appeared to have reduced in number which could be because of channel degradation. The following conclusions could be made from these experiments:

    (i)   Internalised HA-hERG channels are rapidly recycled back to the cell surface.

    (ii)   Recycled hERG channels disappear within 2-3 hours, raising the possibility of rapid degradation.

After internalisation, membrane proteins are commonly known to have two fates; they recycle back to the cell surface or are diverted to the lysosomes for degradation (Grant and Donaldson, 2009, Maxfield and McGraw, 2004). Recycling of the hERG channels appeared to be rapid (Figure 6.2B) and could therefore represent a very fast mode of altering surface channel density. Towards this theory, it would be interesting to look at how the process of recycling of hERG might be regulated. The data (Figure 6.2B) also suggested that the channels are rapidly degraded. This raised the question if there was a link between channel recycling and degradation.
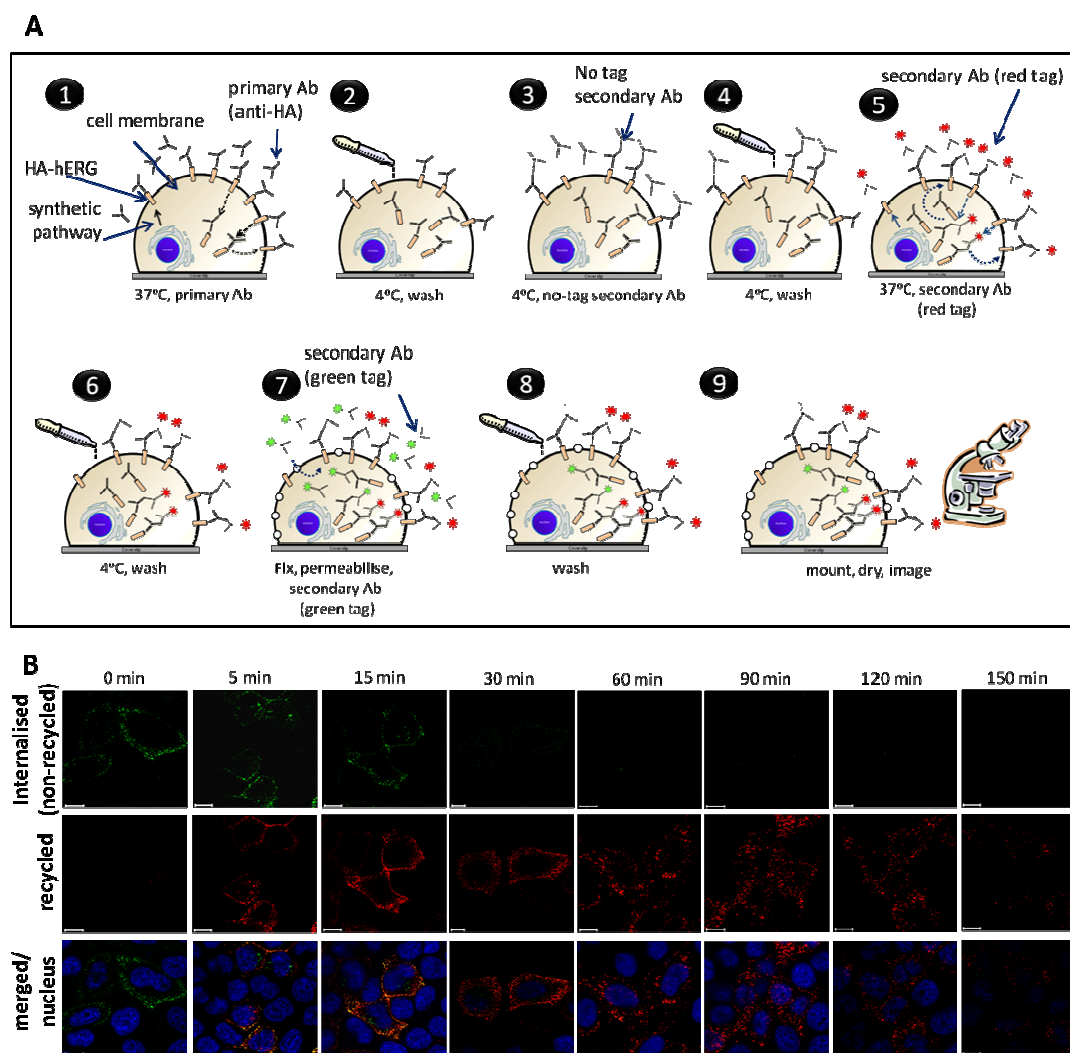
Figure 6.2 Time-course study of recycling of hERG channels. (A) Schematic showing the recycling assay designed to exclusively label the recycled and non-recycled pool of internalised channels (see methods for details). For the time course study, a set of HeLa cells expressing HA-hERG channels was incubated for different time points (0-150 min) in presence of Cy3-conjugated secondary antibody (step 5) to follow the recycling of the channel over a period of 150 min. The cells were fixed, permeabilised and then stained with Alexa[488]-conjugated secondary antibodies to label the non-recycled channels green. Nuclei were stained blue with DAPI and the cells were mounted for imaging. (B) Representative images of the recycling time-course assay are shown. The top panel shows the non-recycled channels, the middle panel shows the recycled channels over the different time points and the bottom panel shows the merged images for the top and bottom panes along with nuclear stain; Scale bars: 10 μm.

6.3.3 Internalised hERG channels undergo degradation

The experiments for time course of recycling of hERG channels showed that the recycled channel pool decreased over a period of time (Figure 6.2.B). These data suggested that the internalised hERG channels might be undergoing both recycling and degradation. To confirm this hypothesis, HA-hERG channels expressed on the cell surface at a given point of time were followed over a period of 90 minutes. Another set of cells were treated with aluminium fluoride (AlF), a drug that disrupts ARF6 function leading to inhibition of internalisation of the hERG channels (shown in Chapter 5). The idea was that if internalised channels were being degraded, then block of internalisation would protect them from degradation. Images of the cells with the internalised channels stained red showed that at time 0 all the channels were on the cell surface. They rapidly internalised within first 5 minutes of incubation and by 60 to 90 minutes, most of them disappeared (Figure 6.3, top panel). In the set of cells treated with AlF, the channels remained on the cell surface and did not disappear even after 90 minutes of incubation (Figure 6.3, bottom panel). These data suggested that following internalisation hERG channels undergo rapid degradation.

It has been reported that following treatment with ceramide, there is a decrease in surface density of the hERG channels. The authors suggested that this decrease was due to an increase in channel degradation. This hypothesis of channel degradation was supported by the authors by comparing the degree of co-localisation of the hERG channels with lysosomal marker protein, Lamp1, in cells treated with and without ceramide (Chapman et al., 2005). The authors used immunostaining of total hERG channels in their study. In order to see if these observations were reproducible with regards to channels internalised from the cell surface, HeLa cells expressing HA-hERG channels were treated without and with C_6-ceramide (10 µM, 60 minutes) prior to and during the internalisation assay. No apparent increase in co-localisation of the stained channels with the GFP-tagged Lamp1 protein co-expressed in these cells could be seen on treatment with ceramide (Figure 6.4.A). Similar results were obtained when the experiment was repeated with staining for another marker for lysosomes, the CD63 protein (Figure 6.4.B).

Internalised hERG undergoes degradation
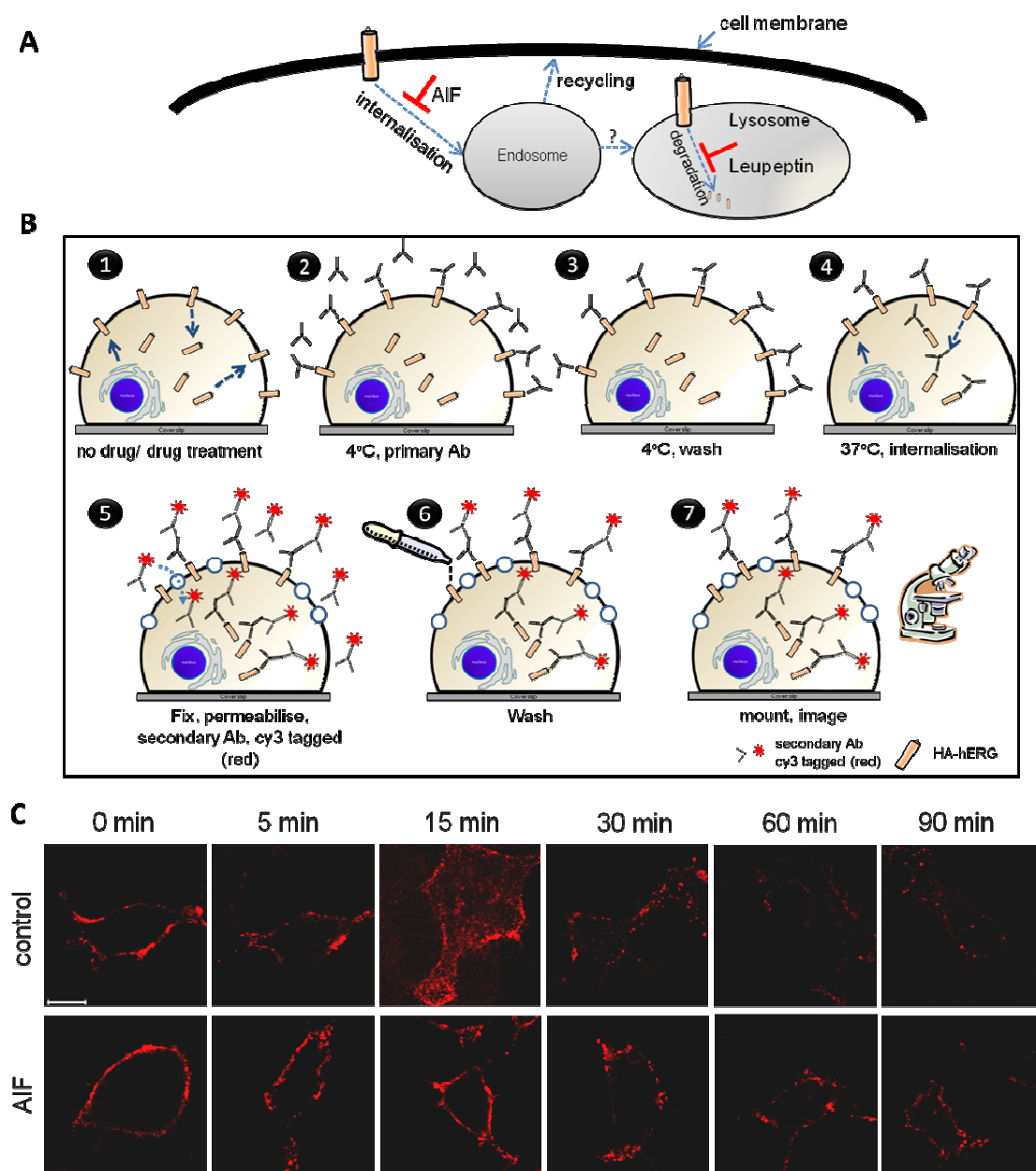
Figure 6.3 Internalised HA-hERG channels degrade. (A) Schematic showing the rationale behind the design of the experiment to examine degradation of internalised channels. (B) Schematic of the internalisation assay. Cells expressing HA-hERG were incubated with anti-HA antibodies at 4°C to label the channels present on the cell surface which were then allowed to internalise for different time points at 37°C. The cells were then fixed, permeabilised and stained with Cy3-tagged secondary antibodies to detect the channels internalised from the cell surface. (C) A set of cells each was treated with no drug (control) or AIF (see methods) for 30 min before and during the internalisation assay described in (B). Representative confocal images from three independent experiments are shown for the indicated drug treatments and times; Scale bars: 10 μm.
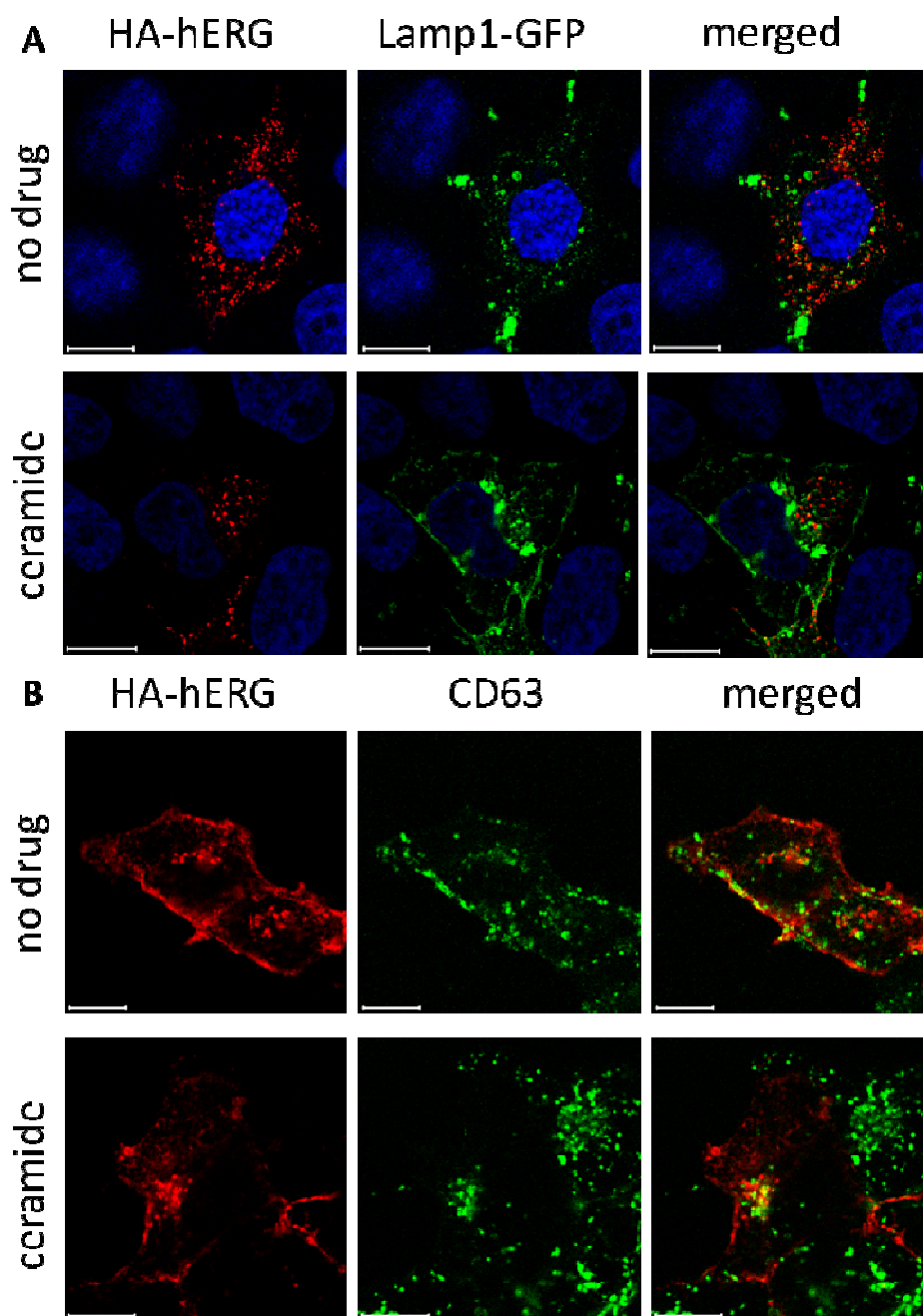
Figure 6.4 Effect of ceramide on hERG degradation. Cells expressing HA-hERG channels were treated with or without ceramide (10 µM) for 60 minutes before and during incubation with anti-HA antibodies for 60 min. The antibodies were internalised along with the channel from the cell surface and stained (red) following fixing and permeabilisation of the cells. As markers for lysosomes, protein Lamp1-GFP (green) was co-expressed in the cells (A) and protein CD63 was stained (green) using anti-CD63 antibodies (B), (see Materials and Methods). Nuclei stained blue using DAPI. Representative confocal images from three independent experiments are shown; Scale bars: 10 µm.

Taken together, these data suggest that internalised hERG channels enter lysosomal compartments resulting in rapid degradation; however, treatment with ceramide did not indicate any significant increase in lysosomal co-localisation of the channels in contrast to the reports by Chapman et al., 2005).

6.3.4 Internalised hERG channels enter recycling endosomes

In order to understand how the surface density of hERG might be regulated by endosomal trafficking, it was important to understand how the internalised channels are recycled back to the cell surface. Towards this aim, localisation of the channels after internalisation was determined by examining the co-localisation of the channel with different endosomal markers. Some hERG channels were seen to co-localise with endosomal marker EEA1 but co-localisation of the channels with GFP-Rab5 (DN) which is also localised to EE was not apparent. These data (Figure 6.5, top two panels) were therefore not conclusive in determining if the internalised hERG channels entered EE. Further, hERG channels co-localised with the GFP-Rme1 (DN) and dominant negative isoform GFP-Rab11a (S25N) which are localised to the perinuclear endocytic recycling endosomal compartments (ERC). These data (Figure 6.5, bottom two panels) suggested that internalised hERG channels enter the recycling endosomes.
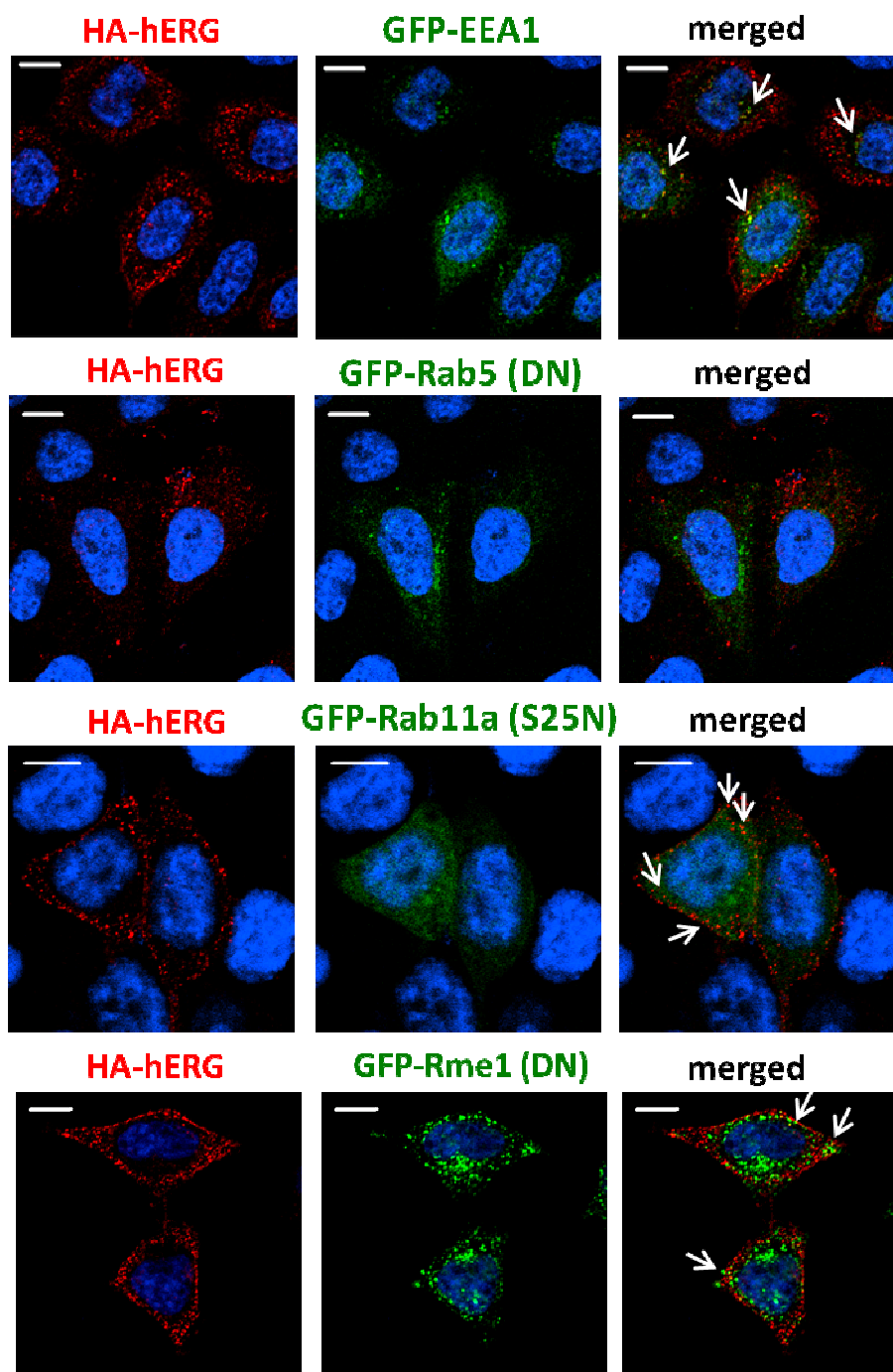
Figure 6.5 Co-localisation of internalised HA-hERG channels with different endosomal markers. HeLa cells expressing HA-hERG channels and the indicated GFP-tagged, DN isoforms (green) of early and recycling endosomal markers were stained (red) for HA-hERG following internalisation, to examine co-localisation (yellow) indicated with arrows (see methods). Nuclei were stained blue with DAPI. Representative confocal images of three independent experiments have been shown; Scale bars: 10 μm.

6.3.5 Role of Rab11a and Rab11b in maintaining surface density of hERG channels

Both Rab11a and Rab11b have been implicated in recycling of membrane proteins from recycling endosomes to the cell surface (Gardner et al., 2010, Grant and Donaldson, 2009, Lapierre et al., 2003). Rab11b has also been implicated in forward trafficking of the hERG channel (Delisle et al., 2009). Internalised HA-hERG channels were found to co-localise with the weak dominant negative isoform, GFP-Rab11a (S25N), (see Figure 6.5). These data suggested that the channels enter recycling endosomes and can undergo recycling in presence of (weak DN) GFP-Rab11a (S25N). However, when the strong DN isoform, GFP-Rab11a (N124I) was co-expressed with HA-hERG channels, there was a substantial decrease in the number of channels expressed on cell surface as compared to the cells expressing no Rab or the GFP-Rab11a (WT), (Figure 6.6, Top and middle panel). Moreover, co-expression with GFP-Rab11b (S25N) also showed a near complete block of surface expression of the channels as opposed to the cells expressing HA-hERG alone or with GFP-Rab11b (WT) (Figure 6.6, Top and bottom panel). Also, it appeared from the confocal image that, more the expression of the GFP-Rab11a (N124I) protein in the cells, lesser was the expression of HA-hERG on cell surface. Taken together these data (Figure 6.6) indicated that both DN-Rab11a (N124I) and DN-Rab11b (S25N) reduce surface density of the hERG channels.

Since the experiments were carried out using transient expression of the channels and the relevant Rab11 constructs, lack of channels on cell surface could also be due to failure of the channels to express in the cells. To eliminate this possibility, a parallel set of cells expressing HA-hERG and GFP-Rab11a (N124I) or GFP-Rab11b (S25N) were fixed, permeabilised and stained for total hERG channels (see methods). HA-hERG channels were stained in both sets of cells (Figure 6.7) which eliminated the possibility of lack of HA-hERG transfection. Further, in cells co-expressing GFP-Rab11a (N124I), the channels appeared to be present in punctate vesicular structures within the cells which showed some co-localisation with GFP-Rab11a (N124I), (Figure 6.7.A, top-panel). Since Rab11a is known to be localised to recycling endosomal compartments (van de Graaf et al., 2006) the data suggested that in cells where Rab11a function was disrupted, some hERG channels were localised to ERC. Immunofluorescence staining for total HA-hERG showed diffuse distribution and extensive co-localisation (Figure 6.7.A, bottom panel) of the channels with GFP-Rab11b (S25N). It has been previously reported that majority of Rab11b is localised to distinct spatial structures that are thought to be reminiscent of the TGN and a small amount of the protein is scattered

throughout the cell (Schlierf et al., 2000). Therefore, co-localisation of the hERG with Rab11b (as seen in Figure 6.7.A bottom panel) suggested that the channels are retained in the TGN in agreement with the report (Delisle et al., 2009). The authors found that mature hERG channels were not formed when co-expressed with DN-Rab11b but not with DN-Rab11a. They also showed that hERG currents were absent in cells co-expressing DN-Rab11b, but not with DN-Rab11a The authors suggest involvement of Rab11b in forward trafficking of the hERG channels and show extensive co-localisation of hERG with Rab11b by imaging. Effect of DN and WT Rab11a constructs on HA-hERG channel function was studied by Andrew Smith, a member of the lab. He used patch clamp recordings to get a measure of current density of the peak tail currents from cells co-expressing HA-hERG channels and DN-Rab proteins (Figure 6.7.B). The results showed that both the strong dominant negative Rab11a (N124I) and the weak dominant negative Rab11a (S25N) significantly decreased hERG currents in patch clamp studies as compared to the WT-Rab11a, (see discussion). These data are consistent with the lack of surface expression of HA-hERG seen in the imaging experiments (Figure 6.6).

Taken together, the data from Figure 6.6 and 6.7, it could be argued that both Rab11a and Rab11b are critical for normal surface expression of HA-hERG channels.
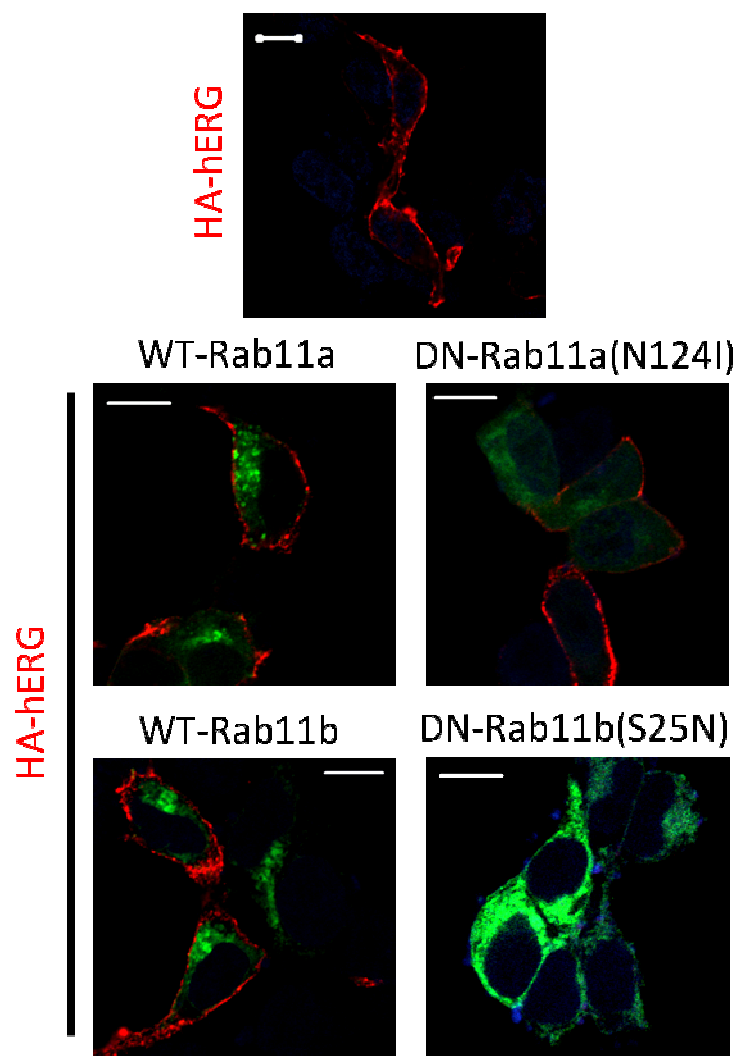
Figure 6.6 Effect of Rab11a and Rab11b on surface expression of HA-hERG. HEK-MSRII cells were transfected to co-express HA-hERG channels and each of the indicated GFP-tagged Rab11 constructs. As control, cells expressing HA-hERG channels alone were used. The cells were fixed and expression of the HA-hERG channels on cell surface was determined by staining with anti-HA antibody followed by Cy3- conjugated secondary antibody. Nuclei were stained blue using DAPI. Representative confocal images from two independent experiments are shown; Scale bars: 10 μm.
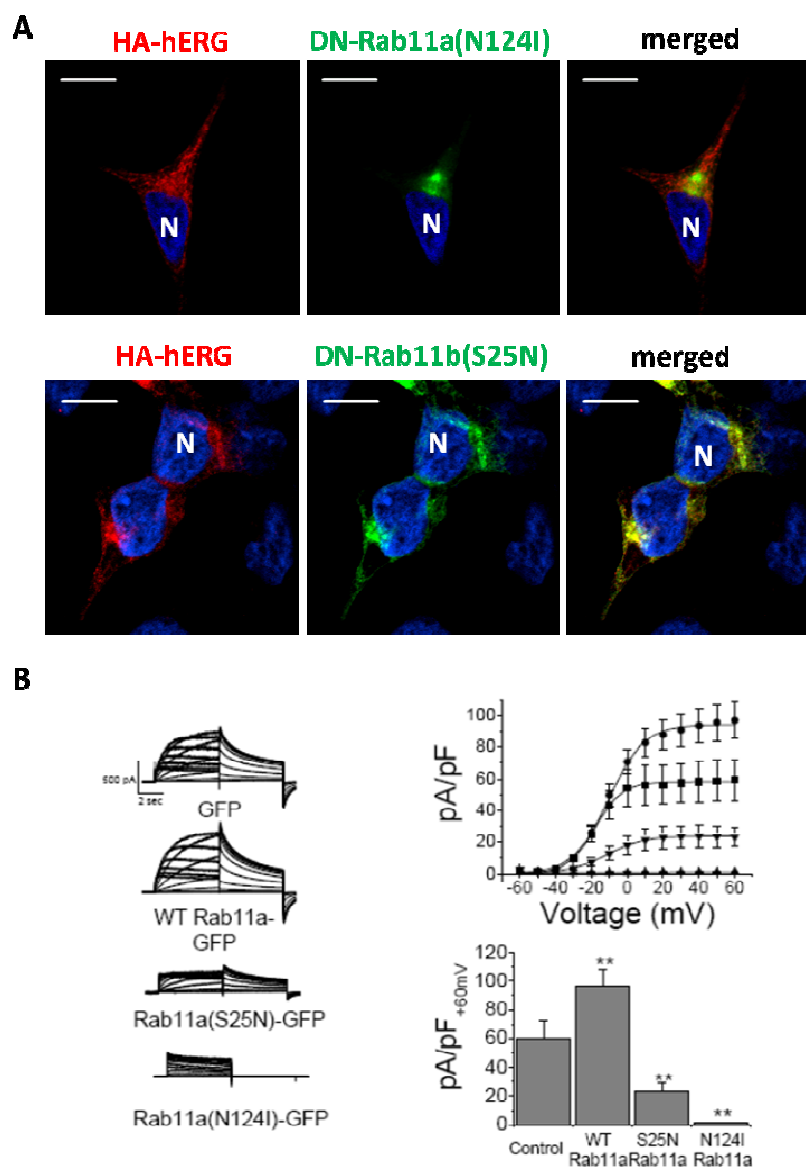
Figure 6.7 Effect of disruption of Rab11a and Rab11b function on HA-hERG function and expression. (A) HEK-MSRII cells expressing HA-hERG channels and the indicated GFP-tagged Rab11 proteins (green) were fixed, permeabilised and the total channel protein was stained (red) to look for distribution of the proteins and their co-localisation (yellow). Representative confocal images are shown. Nuclei (N) stained blue with DAPI; Scale bars: 10 μm. (B) Effect of co-expression of Rab11a mutants on hERG channel currents. Representative current families from patch clamp recordings of cells co-transfected with HA-hERG plus the indicated GFP constructs. E, Current density/ voltage relationships recorded from cells co-transfected with hERG plus empty GFP vector (■), Rab11a WT-GFP (●), Rab11a (S22N)-GFP (▼), or Rab11a (N124I)-GFP (▲). Data points are mean ± s.e.m. (n = 4). (F) Histogram of current density measured from tail currents (at -50 mV) after a +60 mV prepulse, (data by Andrew Smith).

6.3.6 DN-Rab11a diverts HA-hERG channels to lysosomal degradation

Since the Rab11b but not Rab11a appeared to be involved in forward trafficking of HA-hERG channels (Figure 6.7A, top panel) and (Delisle et al., 2009, Gardner et al., 2010), (see discussion), it was interesting to see if the loss of surface expression of the channels in cells expressing DN-Rab11a (N124I) was due increased recycling of the hERG channels to lysosomes for degradation. To achieve this, cells co-expressing HA-hERG and DN-Rab11b (S25N) and DN-Rab11a (N124I) were treated with or without leupeptin to block lysosomal degradation. Following internalisation, the HA-hERG channels expressed on cell surface and internalised there from were stained.

Leupeptin is a protease inhibitor drug used to inhibit lysosomal degradation (Wildenthal et al., 1980, Manna et al., 2010). The rationale behind this experiment was that if disruption of Rab11 function by co-expression of dominant negative isoforms of Rab11a and Rab11b was causing lysosomal degradation of HA-hERG, then leupeptin treatment would prevent the channels from being degraded. In cells expressing the Rab11a (N124I), there was a striking increase in the number of channels stained in cells treated with leupeptin while the drug did not appear to affect the appearance of internalised channels in the cells expressing Rab11b (S25N), see Figure 6.8.A. These data suggested that Rab11a but not Rab11b was required to prevent HA-hERG from being diverted to the lysosomes for degradation following internalisation.

Moreover the loss of channels internalised from the cell surface in the time course experiment (Figure 6.3.C) could be prevented in cells expressing HA-hERG by treatment with leupeptin (Figure 6.8.B). Taken together, these data showed that HA-hERG channels is destined to lysosomal degradation after some cycles of endosomal recycling after internalisation from cell surface. Block of Rab11a function appears to accelerate the degradation of the channels resulting in a substantial decrease in surface channel density (Figure 6.6), presumably by increasing the flux of internalised hERG channels towards the degradative pathway.

Since Rab11a has been implicated in endosomal recycling of proteins (Grant and Donaldson, 2009), it is possible that disruption of Rab11a activity was preventing channel recycling leading to reduced surface density and the non-recycled channels were being diverted to lysosomes for degradation. To check if this hypothesis was correct, firstly, the effect of leupeptin was tested on cells expressing HA-hERG channels alone. Confocal images showed that following recycling (used in Figure 6.2),

there was an increase in the amount of non-recycled channels when lysosomal degradation was blocked (Figure 6.9). Similarly, in cells co-expressing HA-hERG channels and the DN-Rab11a (N124I), there was a significant increase in the non-recycled channel pool when lysosomal degradation was inhibited by leupeptin treatment (Figure 6.10).

Taken together these data indicated that Rab11a activity decides the fate of hERG channels as to whether they recycle back to the cell surface or undergo degradation and this mechanism presents itself to be critical for altering the cell surface density of hERG channels.
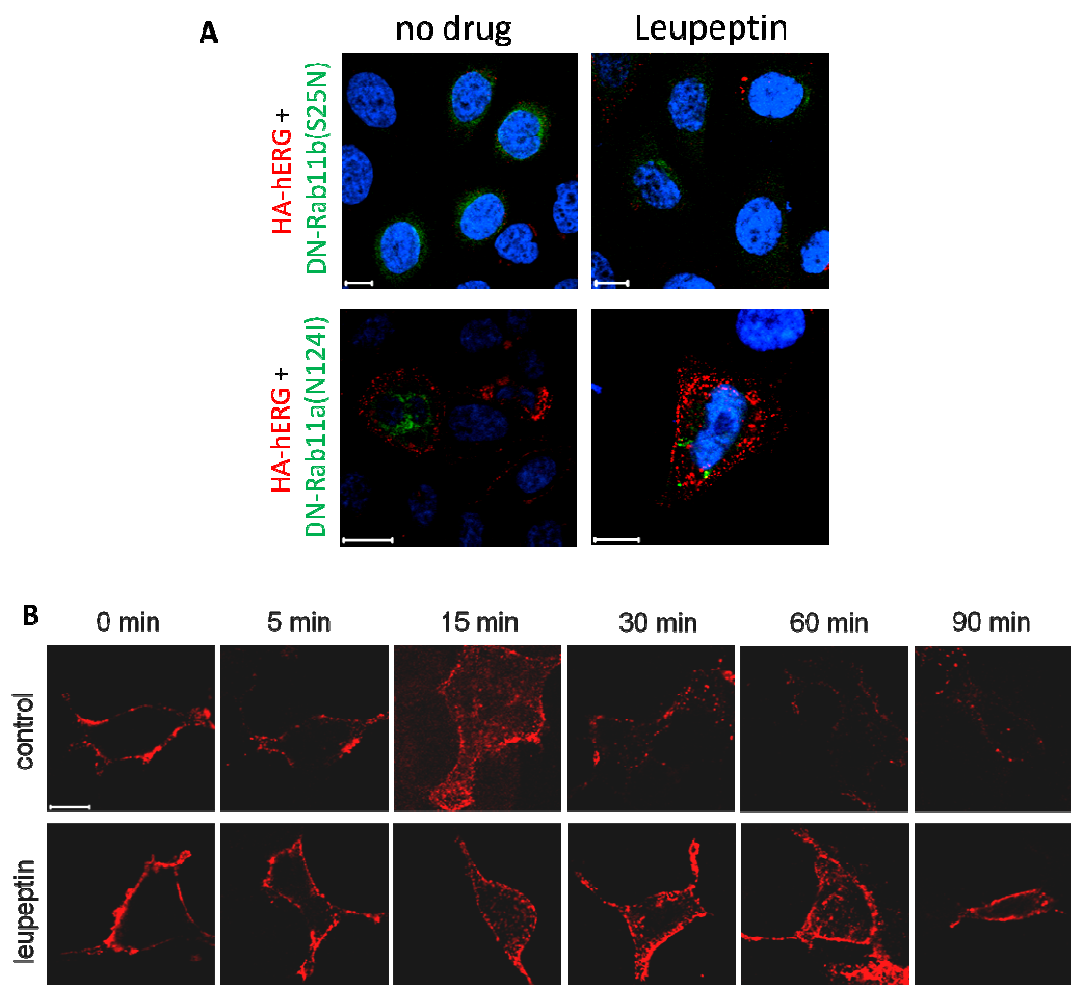
Figure 6.8 DN-Rab11a causes the channels to undergo lysosomal degradation. (A) HeLa cells co-expressing HA-hERG channels and the indicated GFP-tagged Rab11 constructs (green) were treated with or without leupeptin (100 μM), for two hours prior to and during internalisation step (see methods). The channels expressed on cell surface and internalised for 60 min, at 37°C were stained (red). Nuclei stained blue with DAPI. (B) A set of cells were treated with leupeptin as in (A). The channels expressed on cell surface were labelled with anti-HA antibody at 4°C. The cells were washed and a set of cells each was incubated at 37°C for the indicated time points as in Figure 6.3.C. Cells were fixed, permeabilised and stained with Cy3-conjugated secondary antibody to label HA-hERG channels (red). Images for no drug treated cells (control) from Figure 6.3.C. Representative confocal images of three independent experiments are shown; Scale bars: 10 μm.
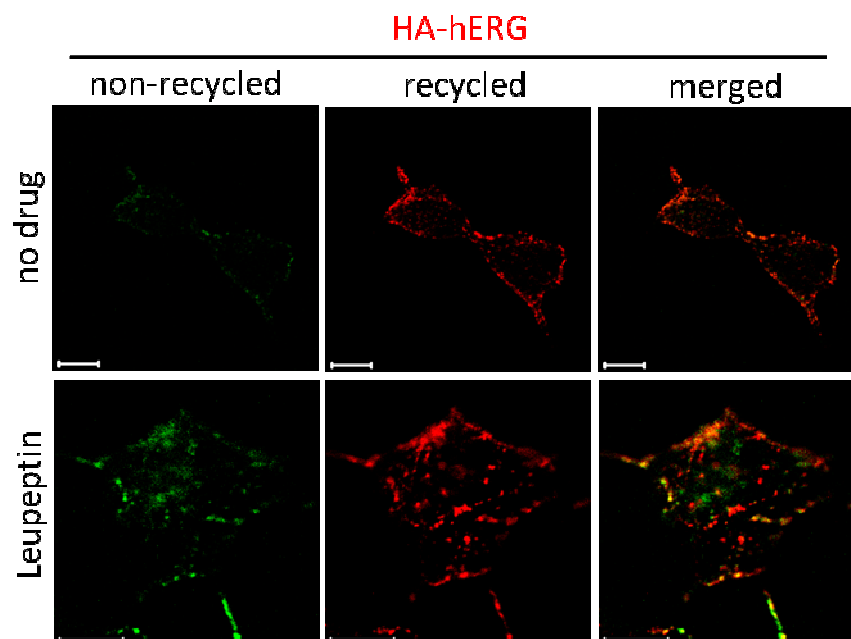
Figure 6.9 Effect of block of Lysosomal degradation on channel recycling. HEK-MSRII cells expressing HA-hERG channels were treated with or without leupeptin (100 μM) for 2 hours before and during incubation in presence of anti-HA antibodies for 60 min to label a pool of channels internalised from the cell surface. Following recycling of the internalised channels for 30 min at 37°C in presence of Cy3-conjugated secondary antibodies, the cells were fixed, permeabilised and stained with Alexa[488] conjugated secondary antibodies. Thus the recycled channels were stained red and the non-recycled pool of channels was labelled green. Representative confocal images are shown; Scale bars: 10 μm.
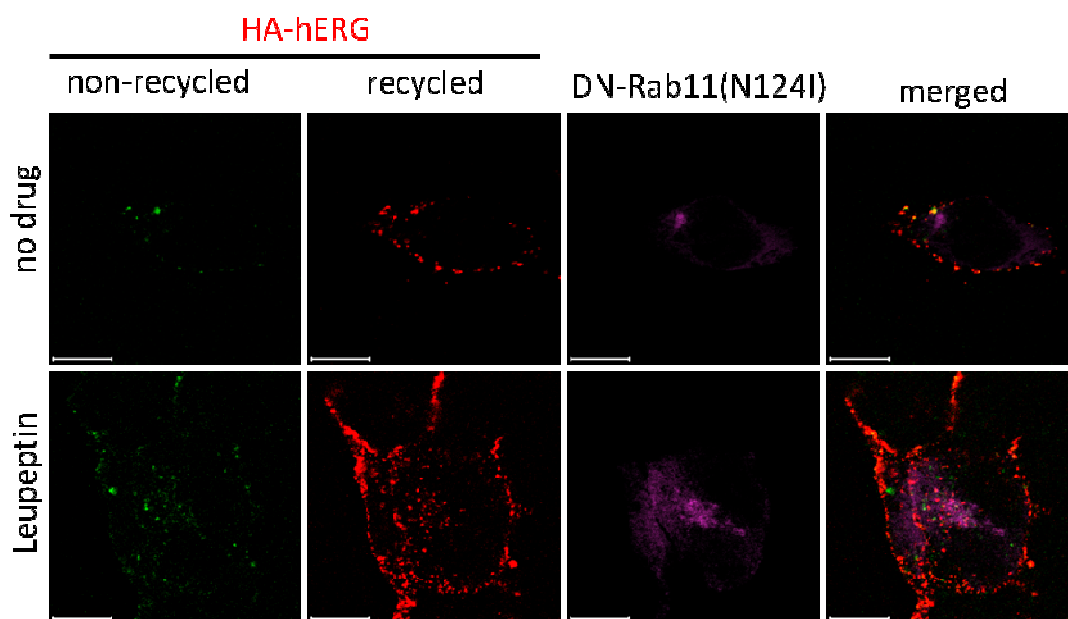
Figure 6.10 Effect of Rab11a (N124I) on HA-hERG recycling. HEK-MSRII cells expressing HA-hERG channels and dominant negative isoform, Rab11a (N124I) were treated with or without leupeptin (100 μM) for 2 hours before and during incubation in presence of anti-HA antibodies for 60 min to label a pool of channels internalised from the cell surface. Following recycling of the internalised channels for 30 min at 37°C in presence of Cy3-conjugated secondary antibodies, the cells were fixed, permeabilised and stained with Alexa[488] conjugated secondary antibodies. Thus the recycled channels were stained red and the non-recycled pool of channels was labelled green. Representative confocal images are shown; Scale bars: 10 μm.

6.4 Discussion

Human ether-a-go-go-related gene (hERG) potassium channels play an important role in cardiac action potential repolarisation, and disruption of hERG channel function can cause cardiac arrhythmias (Anderson et al., 2006). Moreover, recent evidence suggests a role for the hERG channels in the proliferation and progression of multiple types of cancers, Interestingly the hERG channels have been found to express in cancer tissue which did not express the channel in non-cancerous states (Cherubini et al., 2000) making it an attractive target for cancer therapy (Ganapathi et al., 2010). Hence, understanding how hERG channel trafficking regulates or alters their surface density is as important as studying how the channel properties might be regulated. Towards this, the mechanisms of hERG trafficking (forward trafficking and endosomal recycling) need to be studied.

Having investigated the mechanism of hERG internalisation in Chapter 5, this study aimed at investigating the post endocytic itinerary of the HA-hERG channel. Most proteins that undergo internalisation either recycle back to the cell surface or are diverted to lysosomes for degradation (Grant and Donaldson, 2009). Using the recycling assay described in figure 6.1, it was demonstrated that internalised HA-hERG channels are able to rapidly recycle back to the cell surface (Figure 6.2).

Time course experiment to look at the turnover of the internalised pool of channels into the recycled channel pool (Figure 6.2) showed that non-recycled channel pool rapidly disappeared in about 30-60 min indicating that most of the internalised channels might be recycled back to the cell surface.

The recycled channel pool increased over the first few minutes but by 120-150 min the recycled channels became sparse indicating that the channels might be undergoing degradation (Figure 6.2). The fate of the internalised HA-hERG channels to get degraded could be reversed if channel internalisation was blocked using AlF treatment (Chapter 5), (Figure 6.3.B). Since in this experiment, a pool of channels were labelled on cell surface and then allowed to internalise, the channels coming from the synthetic pathway were not stained (Figure 6.3.A). Thus the assay (Figure 6.3) was able to show exclusively the fate of channels expressed on the cell surface at a given point of time and then internalised there from.

Such rapid degradation of an internalised channel pool is uncommon (Maxfield and McGraw, 2004). For example, internalised pancreatic HA-K_{ATP} channels do not degrade for 4 hours or more (Manna et al., 2010) in HEK cells. Since both HA-K_{ATP} and HA-hERG were over-expressed in HEK-MSRII cells, it does not seem likely that the rapid degradation of HA-hERG is merely a result of over expression. These results raised two interesting questions:

- What is the mechanism behind recycling of HA-hERG channels?
- What is the mechanism behind degradation of internalised HA-hERG?

A group (Chapman et al., 2005) investigating regulation of surface density of hERG reported that ceramide evokes a time-dependent decrease in hERG current which they claimed was not due to a change in gating properties of the channel. The rapid decline in hERG protein after ceramide stimulation was attributed by the authors to protein ubiquitinylation and its association with lysosomes leading to lysosomal degradation. The authors stained the entire pool of channels expressed within the cell and showed increase in co-localisation of the channels with lysosomal marker protein LAMP1. However, when co-localisation of internalised HA-hERG with lysosomal markers (LAMP1 or CD63) was examined, (Figure 6.4), there appeared to be no drastic increase in co-localisation of the channels with the lysosomal markers following treatment of cells with ceramide. This could be because the distribution of the total channel pool as seen by Chapman et al. (2005) could be different than and mask the distribution of the internalised surface channels.

Ceramide is a sphingolipid, which due to its pro-apoptotic properties has shown promising results in animal models as an anticancer agent. Ceramide can be formed in the cell membrane from sphingomyelin as a result of various cellular stresses, including reactive oxygen species (ROS), radiation, ischemia reperfusion injury, or treatment with chemotherapeutic or pro-arrhythmic agents (Hannun, 1996). It has also been implicated in the formation/ stabilisation of lipid-rafts affecting the membrane localization of ion channels and their function (Holopainen et al., 1998). A recent finding (Ganapathi et al., 2010) states that ceramide is responsible for recruiting hERG channels to caveolin-enriched lipid-rafts which affects the voltage-dependent gating parameters of the channel inducing inhibition of hERG currents. The authors also use surface biotinylation experiments to label channels on cell surface to show that incubation with C_6-ceramide (10 μM) does not alter the surface channel density over a period of 5 min to 24 hours which is in contradiction to the report that ceramide treatment causes increased degradation of the hERG channels leading to reduced surface expression of the channels (Chapman et al., 2005). The data (Figure 6.4) showed that in untreated

cells the hERG channels enter Lamp1 and CD63 positive lysosomal compartments and the co-localisation of the HA-hERG channels with lysosomes did not increase after treatment with ceramide which indicates that although internalised channels are diverted to lysosomes, treatment with ceramide has little effect on lysosomal targeting of hERG channels.

Moreover, following internalisation, HA-hERG showed complete co-localisation with GFP-GPI-AP (Chapter 5, Figure 5.9A). The GFP-GPI-AP is known to internalise to GPI-AP-enriched early endosomal compartments (GEECs) in a dynamin and clathrin independent, CDC42- or ARF6-mediated pathways (Mayor and Pagano, 2007, Chadda et al., 2007). These data indicated that HA-hERG might be internalised mostly to GEECs. The channels showed some co-localisation with EE marker EEA1 but co-localisation of the channels with GFP-Rab5 (DN) could not be seen (Figure 6.5). Rab5 is known to regulate the fusion between endocytic vesicles that are generally derived from CME and EE as well as the homotypic fusion between early endosomes (Olkkonen and Stenmark, 1997, Grant and Donaldson, 2009). Taking into account the data from Figure 6.5 it could not be determined if the hERG channels can enter the EE after internalisation. Considering that most hERG channels are internalised by CI mechanisms, it is possible that hERG channels do not enter EE.

The channels co-localise with recycling endosomal marker proteins Rab11a and Rme1 (Figure 6.5). The channels also enter lysosomes as seen by co-localisation with lysosomal markers Lamp1 and CD63 (Figure 6.4). These data suggested that after internalisation HA-hERG channels enter the endosomal recycling compartments (ERC) and lysosomes. The Rab11 GTPase is known to be involved in recycling of proteins such as the transferrin receptor and GLUT4 receptor from the recycling endosomal compartments (Grant and Donaldson, 2009, Maxfield and McGraw, 2004). Disruption of activity of both the Rab11 isoforms by the DN isoform over-expression approach led to a drastic decrease in surface channel density and thereby the net channel activity (Figure 6.6). In the patch clamp studies, in cells co-expressing Rab11a (N124I) there was nearly complete absence of hERG currents (Figure 6.7.B). In the imaging, Figure 6.6, in cells showing less fluorescence of GFP-Rab11a (N124I), some HA-hERG staining was seen on cell surface compared to none in cells expressing more of the GFP-Rab11a (N124I). Since, in patch clamp studies, highly fluorescent cells would be selected for the experiment, these cells express very few to no HA-hERG channels on cell surface as is reflected by the complete absence of hERG (Figure 6.7.B).

When Rab11b function was disrupted, very few internalised channels could be seen by immunofluorescence imaging with or without block of lysosomal degradation indicating that the loss of staining was not due to degradation of the internalised channels, but due to lack of internalised channels to begin with. These results were in agreement with the report that Rab11b is required for forward trafficking of the channel (Delisle et al., 2009). However, in cells transfected with DN-Rab11a treatment with leupeptin prevented degradation of internalised channels (Figure 6.8A). The channels appeared to undergo lysosomal degradation within a few minutes after internalisation (Figure 6.8B) and disruption of activity of Rab11a accelerated channel degradation thereby reducing surface channel density.

The differential roles of the two Rab11 isoforms in regulating endosomal recycling have been reported before; for example Rab11b, but not Rab11a, is involved in apical recycling of the cystic fibrosis transmembrane conductance regulator in polarized intestinal epithelial cells (Silvis et al., 2009, Lapierre et al., 2003). However, the regulation of surface density of HA-hERG by two isoforms of the same GTPase by two very different processes is a novel and interesting finding.

Also ARF6 has been shown to be involved in recycling of CI endocytic cargo such as MHCI (Donaldson and Williams, 2009). Although HA-hERG has been found to internalise by the ARF6 dependent pathway like MHCI, the channels did not show extensive co-localisation with MHCI after internalisation (Chapter 5, Figure 5.9.A); therefore ARF6 may not have a role in endosomal recycling of HA-hERG.

Since Rab11a has been implicated in endosomal recycling, it could be said that when HA-hERG reaches recycling endosomes after internalisation, Rab11a mediates recycling of the channels back to the cell surface and disruption of Rab11a function prevents channel recycling and diverts the channels to lysosomes where they get degraded. Thus the activity status of Rab11a in a cell could be a determinant of cell surface density of hERG channels. This hypothesis was supported by the reduced disappearance of non-recycled channels when the cells were treated with leupeptin to block lysosomal degradation prior to and during recycling (see methods). The number of recycled channels has also increased as they were protected from degradation (Figure 6.9). Although this experiment cannot give an idea of the number of recycling events that the HA-hERG channels can undergo before being degraded, it does support that the channels present on the cell surface at a given point of time are all degraded by 60 min after internalisation (Figure 6.8.B). It also shows that most of the channels internalised from the cell surface are recycled back to cell surface within 30-

60 min (Figure 6.8.B). Channels internalised from the cell surface also degrade (Figure 6.9). Thus recycling/degradation of hERG channels appear to occur rapidly.

Half-life of the hERG channels after synthesis and assembly has been reported to be ~12 hrs (McDonald et al., 1997, Ficker et al., 2003, Chen et al., 2009). The post-endocytic fate of the channels from the experiments described in this chapter suggest that the channels expressed on the cell surface undergo several rounds of internalisation and recycling before being diverted to slow degradation.

The experiments investigating the alternate pathway of hERG internalisation (chapter 5, Figure 5.20) show that there is minimal co-localisation of the channels with the clathrin cargo transferrin. However, when the ARF6 function was disrupted with DN-ARF6 to block ARF6-mediated internalisation of the hERG channels, co-localisation with transferrin has significantly increased. Transferrin has been shown to undergo endosomal recycling in a Rab4 (van der Sluijs et al., 1992) and Rab11 (Schlierf et al., 2000, Ren et al., 1998) dependent manner and if hERG also recycles in a Rab11a dependent manner (section 6.2.5 of this chapter), the cargoes should show significant co-localisation. This lack of significant co-localisation could be due to the nature of vesicles transporting the cargoes to the recycling endosomal compartments. Cargoes of CME are located on different regions of the membrane than the CI cargoes which are localised to cholesterol rich raft domains (Lingwood and Simons, 2010). Existence of such micro-domains in the recycling endosomal compartments or even the existence of different kinds of recycling endosomes (Sonnichsen et al., 2000), would explain the lack of co-localisation between transferrin and the HA-hERG channels. The increased co-localisation of HA-hERG with transferrin on co-expression of DN-ARF6 can be attributed to the proteins being packed together in the endocytic CCV. It would be interesting to investigate the mechanism of endosomal recycling of HA-hERG internalised via this CME pathway and to see if the mode of internalisation alters the fate of the channels to undergo lysosomal degradation.

The conclusions from this study could be strengthened if a biochemical approach is used to follow the degradation of HA-hERG channels internalised from cell surface as described for the K_{ATP} channel (Manna et al., 2010). Also, it would be interesting to investigate if Rab7 which plays a role in the transport of proteins from late endosomes to lysosomes (Maxfield and McGraw, 2004) affects trafficking of HA-hERG.

6.5 Summary

While forward trafficking pathways affect expression of the proteins on the cell surface, pathways of endosomal trafficking can rapidly alter the surface density of the proteins (Grant and Donaldson, 2009, Doherty and McMahon, 2009). Co-localisation studies in this chapter and results from co-localisation with marker proteins in chapter 5 indicate that immediately after ARF6 and lipid raft mediated internalisation, HA-hERG channels enter non-clathrin derived structures, likely GEECs, instead of the early endosomal compartments which are generally the destinations of cargoes of CME after which the channels may briefly enter early endosomes like the other CIE cargoes such as MHCI, GPI-AP and Tac (Weigert et al., 2004). From here, the channels can proceed to late endosomes/ lysosomes for degradation or are recycled back to the plasma membrane. Although both Rab11b and Rab11a are required for normal expression of the hERG channels on cell surface, Rab11b plays a role in forward trafficking of the channels (Delisle et al., 2009) while Rab11a is required for channel recycling. Block of Rab11a function diverts channels for degradation, which could be prevented by blocking internalisation. Disruption of Rab11a function results in decreased surface density of the channels. The effect of block of Rab11a function is reflected in the lack of functional hERG currents in HEK cells transiently expressing the channels. This is a novel report of differential regulation of an ion channel trafficking by the Rab11 isoforms.

Both, internalisation and endosomal recycling are the mechanisms by which surface density of hERG can be regulated in health and disease. The mechanism of endosomal trafficking of hERG determined from this study is summarized in the following schematic (Figure 6.11).
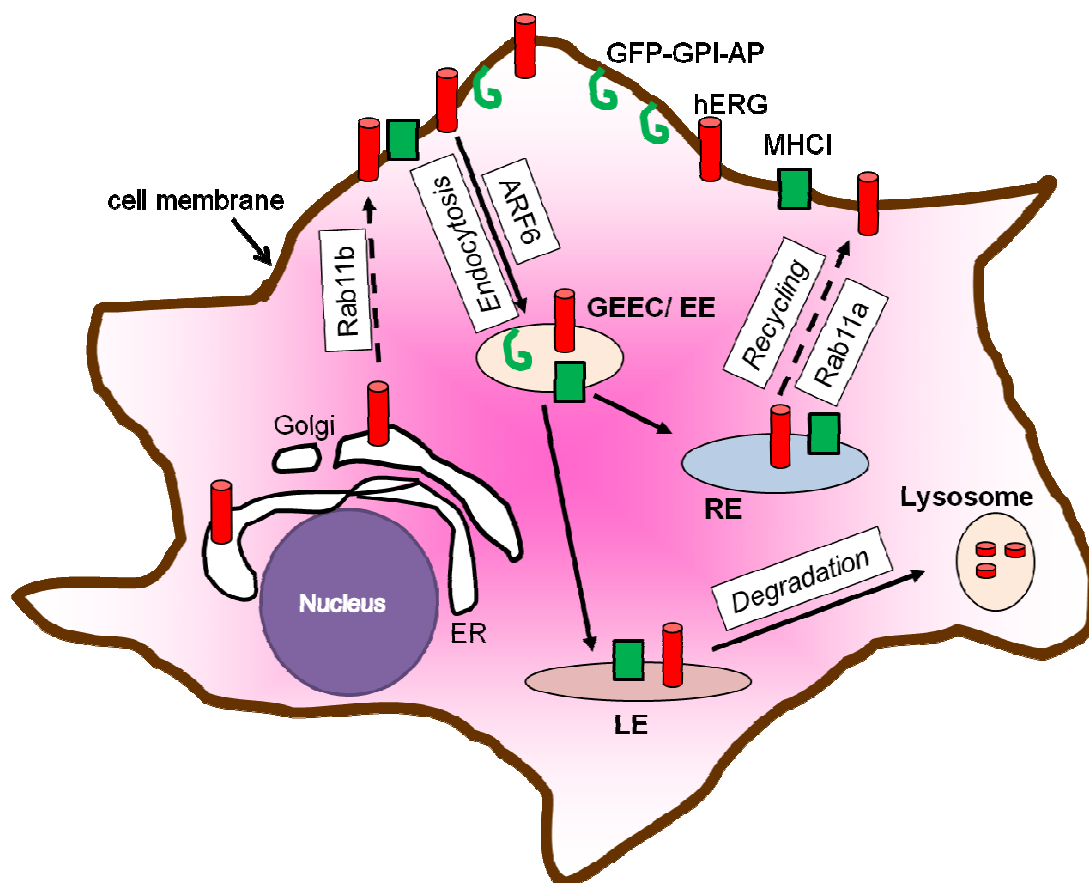
Figure 6.11 Schematic to summarise endosomal trafficking of hERG channels.
hERG channels are expressed on the cell surface in a Rab11b-dependent manner and
internalised via ARF6-mediated pathway to GPI-AP rich GEECs or early endosomal
(EE) compartments. The channels then enter recycling endosomes (RE) from where
they are recycled back to the cell surface. Recycling is mediated by Rab11a. The
channels also traffic to late endosomes (LE) for transport to lysosomes for degradation.
Lysosomal degradation is increased when DN-Rab11a disrupts the normal Rab11a
function.

CHAPTER 7

General discussion

7.1 Overview

The aim of the current study was to understand the trafficking pathways of two physiologically important potassium channels, the pancreatic K_{ATP} and the cardiac hERG. Since channel function is controlled by the channel open probability and the number of channels expressed on the cell surface, it was attempted to a achieve better understanding of the three key trafficking processes (forward trafficking, internalisation and endosomal recycling) that are known to regulate surface density of membrane proteins. Forward trafficking of the proteins was studied with respect to the ER export mechanisms which represent a key step in the biosynthetic delivery of proteins to the plasma membrane.

Firstly, the mechanistic link between the CHI causing mutation E282K in the Kir6.2 subunit of the K_{ATP} channels was investigated (discussed in Chapter 3). The study established the existence of a previously unreported diacidic ER exit motif (^{280}DLE^{282}) on the Kir6.2 subunit which regulates the Sar1-GTPase dependent ER exit of the channels in COPII vesicles and that abrogation of the signal underlies the disease. The study revealed that the complete assembly of K_{ATP} subunits likely occurs after ER exit. Based on the mechanistic information derived from this study, the use of cell penetrating peptides to alter K_{ATP} channel surface expression was explored. A peptide corresponding to the ER exit motif of Kir6.2 was able to prevent the ER exit of the channel, presumably by blocking the recognition of the DLE motif by the Sec24 component of the COPII machinery.

Secondly, the ER exit mechanism of hERG channels was investigated (discussed in Chapter 4). The channels were found to follow Sar1 dependent ER exit of the channel in COPII vesicles like the K_{ATP} channels. However, a functional diacidic ER exit motif was found to be absent on the distal C-terminal of the channel. Interestingly though, peptides that disrupted the ER exit of the K_{ATP} channels were found to inhibit surface expression of the hERG channels, indicating a role for Sec24 in the ER exit of the hERG channels.

Next, the mechanisms of internalisation of the hERG channels were investigated (discussed in Chapter 5). The study revealed that both recombinant hERG and native ERG channels (expressed in neonatal rat cardiac myocytes) are localised to lipid-rafts

and are internalised from the cell surface. Most of the channels were found to undergo internalisation in a cholesterol- and ARF6-dependent manner. This pathway of internalisation appears to be unique to the hERG channels when compared to pathways known to be undertaken by other members of the family of potassium channels. Intriguingly prolonged block of channel internalisation with an ARF6 dominant negative construct revealed that the channels can also undergo internalisation by an alternate pathway which is dynamin-dependent.

Internalised hERG channels were found to rapidly recycle back to the cell surface and undergo lysosomal degradation. Degradation of the channels was enhanced when Rab11a activity was disrupted using dominant negative isoforms (discussed in Chapter 6) indicating that when Rab11a is unavailable for channel recycling, they are diverted for degradation. The endocytic trafficking mechanisms for hERG suggested that endocytic processes could be critical for maintaining the surface density of the channels.

7.2 Sar1-dependent ER Exit of Pancreatic K_{ATP} Channels Revealed by a Mutation Causing CHI

Trafficking of ion channels is often a well regulated process involving specific interactions between the cargo and carrier proteins through trafficking motifs and regulatory molecules. Mutations that disrupt these interactions have been shown to affect channel function and cause disease. Studies of disease causing genetic mutations can be very rewarding as they can provide novel insights into the molecular mechanisms underlying disease. In Chapter 3, the G844A heterozygous paternal mutation in the *KCNJ11* gene of a Swedish patient with the focal form of CHI was studied. This mutation leads to the substitution of lysine (K) for glutamate (E) at position 282 of Kir6.2. The key findings of this study are:

(i)   The E282K mutant channels do not express on the cell surface as they are retained in the ER.

(ii)   The ER exit of K_{ATP} channels requires a functional diacidic ER exit motif (^{280}DLE^{282}) present on C-terminus of the Kir6.2 subunit.

(iii)   The channels enter COPII vesicles at ER exit sites in a Sar1-dependent manner and both the Kir6.2 and the SUR1 subunits are independently capable of exiting the ER to reach the ERGIC compartments.

(iv)   The interaction between the K_{ATP} channels and the Sec24 protein of the COPII machinery, known to recognise and bind the diacidic ER exit motif, can be disrupted by a peptide containing the diacidic ER exit motif.

(v)   The mutant E282K channels can be rescued to the cell surface by co-expression with the wild type subunits.

This study highlights the potential importance of the forward trafficking signal in the surface expression of K_{ATP} channels which are critical for GSIS. It provides a mechanistic explanation to the CHI disease phenotype of the patient. The DXE motif in other membrane proteins has been reported previously to be recognised by the COPII machinery (Nishimura and Balch, 1997, Nishimura et al., 1999, Wang et al., 2004b). Mutation of the motif causes ER retention resulting in complete absence of the mutant K_{ATP} channels on the cell surface which leads to loss of K_{ATP} currents. This results in membrane depolarisation and excessive insulin secretion (Ashcroft and Gribble, 1999, Cartier et al., 2001, Dunne et al., 2004, Ashcroft, 2006b). Misfolding and aggregation of newly synthesised proteins in the ER or alterations in the ER processing of cargo is

responsible for a broad range of diseases including cystic fibrosis, emphysema and neuropathies such as Alzheimer's disease (Cheng et al., 1990, Dimcheff et al., 2003). CHI causing mutations such as the W91R of the Kir6.2 also prevent surface expression of the channels, but this has been attributed to channel misfolding which could explain why these mutant subunits could not be rescued to the cell surface by co-expression with the wild type subunits (Crane and Aguilar-Bryan, 2004). The E282K mutant channels, studied here on the other hand, do not appear to undergo misfolding because co-expression of the wild type subunits with the mutant subunits could rescue the mutant subunits to the cell surface. Functional studies showed that the channels formed of wild type and E282K subunits are functional (Taneja et al., 2009). Therefore, the absence of the E282K mutant channels is mechanistically different from all other mutations reported in the literature. It also explains how the removal of the tumorous pancreatic sections expressing the mutant subunits alone and leaving behind the tissue expressing a mixed population of wild type and E282K mutant subunits (capable of forming functional channels) was able to cure the patient.

The study also revealed that both Kir6.2 and SUR1 can exit the ER and enter ERGIC. These data suggested that complete assembly of the channel likely occurs in the ERGIC or the *cis*-Golgi compartment. Unassembled channel subunits, bearing exposed 'RKR' signals could be recognised by the COPI machinery, and retrieved to the ER via COPI vesicles (Heusser et al., 2006, Mrowiec and Schwappach, 2006). Though the RKR motif on the K_{ATP} channel subunits was well characterised, previous studies could not provide experimental evidence to determine if this motif, which when disrupted caused accumulation of the channels in the ER, was an ER retention or retrieval signal. Assembly of the Kir6.2 and SUR1 subunits was thought to be required to mask these motifs present on both the channel subunits to allow exit of the channels from the ER. The present study showed that the 'RKR' signals on the K_{ATP} channel subunits are more likely to serve as retrieval signals, rather than retention signals because each of the channel subunits were found to be capable of moving out of the ER to reach the ERGIC compartments but only completely assembled channels were expressed on cell surface. Moreover, the rescue experiments suggested that the Kir6.2 subunits must dimerise or multimerise prior to ER exit. These findings provide a valuable mechanistic insight into the channel synthesis and assembly and show that the COPII machinery has an important role in sorting of correctly folded channels for exit out of the ER that can affect surface density of the channels.

Other potassium channels apart from the K_{ATP} channels (shown in this study) have been reported to have a functional diacidic ER exit motif for entry into COPII vesicles in humans which include TASK3, and the Kir1.1, 2.1, 3.2a and 3.4 (Ma et al., 2002, Heusser and Schwappach, 2005). Thus although it has been shown that the diacidic motif is required for ER exit in COPII vesicles, how ion channels are recruited into the COPII vesicles was not fully understood. Selective transport of membrane proteins out of the ER requires the recognition and binding of the Sec24 proteins of the COPII complex with cargo through the ER exit motifs localised to their cytosolic domains. These motifs include the diaromatic, di-hydrophobic motifs and the diacidic ER exit motif (Nishimura and Balch, 1997, Miller et al., 2002). The TAT-DXE peptides used in this study showed that if the diacidic ER exit motif binding site on Sec24 is saturated, the channels are not able to express on cell surface. The TAT-DXE peptides could therefore be used to further understand the interaction between Sec24 and its cargoes and provide a simple tool to screen for other proteins that are recognised by Sec24 and exit the ER in COPII vesicles. Further, the Sec24 has multiple cargo binding sites (Miller et al., 2003) and therefore diverse cargoes can bind to it. Hence it would be interesting to study the mechanism of ER export of proteins that have signals other than the DXE.

7.3 Sar1-dependent ER Exit of hERG Channels

The ER export mechanisms of the hERG potassium channels were investigated in Chapter 4. hERG channels were chosen in this study because the hERG channels are reported to be stringently processed in the ER for preventing expression of misfolded channels (Ficker et al., 2003). Several trafficking deficient mutant hERG channels have been reported that are misfolded and retained in the ER due to strong association with chaperones heat shock proteins (Hsp) 70 and Hsp 90 (Ficker et al., 2003). hERG channels like the K_{ATP} channels, have been reported to posses the putative ER retention signal present in the C-terminus (R-G-R at positions 1005-1007) and the last 104 amino acids of the channel C-terminus are required to mask the signal and prevent ER retention of the channels (Kupershmidt et al., 2002). However, ER exit mechanisms used by the channels are not completely understood. Therefore, the ER exit of the hERG channels was investigated.

Key findings of this study are:

(i)   ER exit of hERG channels is dependent on Sar1-GTPase.

(ii)   The channels enter COPII vesicles at ER exit sites.

(iii)   The TAT-DXE peptide treatment prevents surface expression of the channels which indicated that the channels must interact with the Sec24 proteins of the COPII machinery.

(iv)   The distal C-terminus of hERG channels does not contain a functional ER exit motif.

The present study showed that hERG channels follow a forward trafficking pathway which is dependent on Sar1-GTPase in agreement with the report (Delisle et al., 2009) published when the study was ongoing. Delisle et al however did not present any data to show if hERG channels enter COPII vesicles. Using a temperature-sensitive VSV-G mutant as a marker, this study showed that the channels enter the COPII vesicles at ERES prior to ER exit and entry into ERGIC. This mechanism of ER export of hERG channels appeared to be similar to that of the K_{ATP} channels. Therefore hERG C-terminal sequence was screened for potential ER export motifs and sequential deletions of the distal end of hERG C-terminus were made to remove all the three potential DXE motifs, the LXXLE motif and three LL motifs. Truncations into the proximal C-terminus were not made as this region contains the cyclic nucleotide binding domain (CNBD- 742-842), which is important for the function of hERG

(Akhavan et al., 2005). The truncations did not prevent the Sar1-dependent ER exit of the channels. Thus none of the three diacidic ER exit motifs appeared to be involved in the ER exit of hERG. These results implied that the ER exit motif on the hERG channels may be other that the DXE sequence.

A recent finding showed that glycoslyphosphatidylinositol (GPI)-anchored proteins that are localised to cholesterol rich lipid-raft domains of membranes are incorporated into COPII vesicles after synthesis for export out of the ER (Bonnon et al., 2010). They cannot interact directly with Sec24 since they lack a cytosolic domain and are thought to use membrane-spanning cargo receptors and their ability to interact with the Sec23-Sec24 complex for entry into COPII vesicles. Moreover, the ER export of GPI-anchored proteins was shown to require integrity of the lipid raft domains of the ER membrane (Bonnon et al., 2010). When localisation of the hERG channels (discussed in Chapter 5) was investigated, they were found to be localised to cholesterol rich membrane lipid-rafts unlike the pancreatic K_{ATP} channels (Xia et al., 2004). Thus, it is possible that direct interaction of the hERG channels with Sec24 proteins does not occur.

7.4 Major Pathway of hERG Internalisation Requires Lipid-rafts and is ARF6-mediated

The forward trafficking of the cardiac hERG channels presented distinct features as compared to the pancreatic K_{ATP} channels. Next, the endocytic mechanisms of the hERG channels were investigated and compared to those of the pancreatic K_{ATP} channels (discussed in Chapter 5). The study presented some interesting findings that are listed as follows:

(i)   Recombinant and native cardiac hERG channels are localised to cholesterol rich lipid raft micro-domains.

(ii)   The channels are internalised from the cell surface rapidly.

(iii)   Internalisation of the channels is dynamin-independent, cholesterol dependent and is ARF6-mediated.

(iv)   When ARF6-mediated endocytic pathway of the channels was blocked, an alternate endocytic pathway of the channels was revealed.

(v)   Though most channels are internalised by a lipid raft- and ARF6-mediated pathway, the channels are be able to also internalise via a dynamin-dependent pathway that appears to be clathrin-mediated.

Raft localisation of Kv channels has been reported, for example Kv2.1 and Kv1.5 channels are localised to lipid raft micro-domains and are internalised by dynamin-dependent internalisation in caveolar lipid-rafts (Martens et al., 2001, Martinez-Marmol et al., 2008, Steele et al., 2007a). There is a report that conditions that modify cell membrane cholesterol modulate the electrophysiological properties of Kv11.1 and IKr (Balijepalli et al., 2007). From the results of this study, the raft localisation of the hERG channels may have more physiological effects than regulation of channel function.

Dynamin-independent, ARF6-mediated internalisation of hERG channels in lipid-rafts is novel and previously unreported for ion channels. It is a mechanism generally utilized by proteins such as the MHCI and viruses to gain entry into the cells (Donaldson and Williams, 2009, Mercer et al., 2010). This mechanism of internalisation of hERG channels is a complete contrast to the mechanism used by the pancreatic K_{ATP} channels that have been found to undergo rapid internalisation by CME via a tyrosine-based motif, [330]YSKF[333] located in the C-terminus of Kir6.2 (Mankouri et al., 2006). The hERG channels also showed the ability to undergo internalisation by CME when the ARF6-mediated pathway is blocked. These findings could have important implications on our understanding of signalling events that regulate endocytic trafficking of the

channels which in turn dictate their surface density and function. hERG channel trafficking was found to be affected by PKC. Activation of PKC appeared to inhibit internalisation of the channels and increase their surface density. This is in contrast to the effect of PKC activation seen on the pancreatic K_{ATP} channels which show reduced recycling and are diverted to lysosomal degradation when treated with PKC activator drugs which reduces their net surface density (Manna et al., 2010). The physiological relevance of these findings needs to be studied. Moreover, K_{ATP} channels have been shown to undergo multiple rounds of internalisation and recycling (Manna et al., 2010). If this is also true for hERG channels remains an open question.

7.5 hERG Channels Recycle and Blocking Rab11a Function Increases Channel Degradation

The post-endocytic fate of hERG channels was investigated (discussed in Chapter 6) and the key findings of this study are:

(i)   hERG channels that are internalised from the cell surface undergo recycling back to the cell surface.

(ii)   The recycled channels rapidly are diverted to lysosomes for degradation.

(iii)   Degradation of the channels is enhanced if Rab11a function is disrupted in the cells.

A recent report suggested that Rab11b has a role in the forward trafficking of the hERG channels (Delisle et al., 2009). The present study showed that disruption of Rab11b activity in cells prevent expression of the hERG channels on the cell surface, but another isoform, Rab11a reduces surface expression of the channels as they are diverted to lysosomes for degradation. This can be explained by the following: Rab11a is ubiquitously expressed, whereas Rab11b is expressed primarily in brain and heart and therefore it may have distinct functions in these tissues. Moreover, the role of Rab11a is well established and it is known to associate with recycling endosomes and regulate the recycling of various proteins, such as the transferrin receptor, β-integrin, TRPV5/6 channels, the glucose transporter GLUT4 and the chemokine receptor CXCR. On the other hand Rab11b may be localised to and function distinctly to Rab11a (Lapierre et al., 2003, Silvis et al., 2009).

The hERG channels did not appear to enter or get retained in the transferrin-positive early endocytic compartments. They do however enter the MHCI- and GPI-AP- positive compartments which could be GEECS or some recycling endosomal compartments that sort them for recycling back to the cell surface in a Rab11a dependent manner. If this recycling is blocked, most of the channels are diverted to lysosomal compartments. Thus the sorting of the channels would decide the fate of internalised hERG channels and thereby regulate their surface density.

One of the most well studied membrane trafficking proteins is the glucose transporter GLUT4 (Bryant et al., 2002). GLUT4 is translocated to the cell surface in an insulin stimulated manner and is critical for glucose uptake by muscle and adipose tissues. Rab11a has been found to be present in GLUT4 containing vesicles after insulin stimulation. Rab11a is thought to be activated by the insulin signalling cascade

(Schwenk and Eckel, 2007). Therefore when insulin levels are low, as would be case in conditions such as diabetes, Rab11a activation may be depressed and this might divert the hERG channels for degradation. This could result in reduced hERG surface density and cardiac arrhythmias.

It is also interesting that the hERG channels are able to undergo rapid lysosomal degradation after expression on the cell surface within a couple of hours and it would be interesting to investigate if the mode of internalisation of the channels plays a role in how rapidly the channels are degraded.

7.6 Final Summary

This study has investigated and compared the trafficking mechanisms of two physiologically important potassium ion channels. The mechanism by which the diacidic (^{280}DLE^{282}) motif on the Kir6.2 C-terminus regulates the ER export of the K_{ATP} channels was determined and the molecular basis of CHI caused by the disruption of the motif by the mutation E282K was explained. The unique aspect of this finding is that the mutant channels are not misfolded but are trafficking-deficient because of disruption of the ^{280}DLE^{282} motif. The TAT-conjugated peptides used in the study can be a valuable tool for investigating the interaction between the COPII and its cargo. Its ability to do so was tested on the hERG channel which showed Sar1-dependent surface expression. The study of ER exit mechanisms of the hERG channels showed that the channels can enter COPII vesicles at ERES although they lack the diacidic ER exit motifs on distal C-terminus of the channel. The hERG channels were found to be localised to membrane lipid-rafts and undergo internalisation from the cell membrane via clathrin, caveolin and dynamin-independent mechanism that was mediated by ARF6-GTPase. The channels were also found to be capable of using alternate pathway for internalisation if the major ARF6-mediated pathway was blocked. The mechanism of internalisation of hERG is novel to ion channels. The hERG channels were also found to recycle back to the cell surface and undergo lysosomal degradation which was enhanced when Rab11a function was disrupted. Thus this study adds to the understanding of K_{ATP} and hERG channel trafficking mechanisms which are important processes that regulate that surface levels and thereby the channel functions in health and disease.

BIBLIOGRAPHY

AGUILAR-BRYAN, L. & BRYAN, J. 1999. Molecular biology of adenosine triphosphate-sensitive potassium channels. *Endocr Rev,* 20**,** 101-35.

AGUILAR-BRYAN, L., CLEMENT, J. P. T., GONZALEZ, G., KUNJILWAR, K., BABENKO, A. & BRYAN, J. 1998. Toward understanding the assembly and structure of KATP channels. *Physiol Rev,* 78**,** 227-45.

AGUILAR-BRYAN, L., NICHOLS, C. G., WECHSLER, S. W., CLEMENT, J. P. T., BOYD, A. E., 3RD, GONZALEZ, G., HERRERA-SOSA, H., NGUY, K., BRYAN, J. & NELSON, D. A. 1995. Cloning of the beta cell high-affinity sulfonylurea receptor: a regulator of insulin secretion. *Science,* 268**,** 423-6.

AIDLEY, D. J. 2008. *Ion Channels: Molecules in Action*, Great Britain, Cambridge University Press.

AIKAWA, Y. & MARTIN, T. F. 2003. ARF6 regulates a plasma membrane pool of phosphatidylinositol(4,5)bisphosphate required for regulated exocytosis. *J Cell Biol,* 162**,** 647-59.

AKHAVAN, A., ATANASIU, R., NOGUCHI, T., HAN, W., HOLDER, N. & SHRIER, A. 2005. Identification of the cyclic-nucleotide-binding domain as a conserved determinant of ion-channel cell-surface localization. *J Cell Sci,* 118**,** 2803-12.

ALVI, F., IDKOWIAK-BALDYS, J., BALDYS, A., RAYMOND, J. R. & HANNUN, Y. A. 2007. Regulation of membrane trafficking and internalisation by protein kinase C: emerging role of the pericentrion, a novel protein kinase C-dependent subset of recycling endosomes. *Cell Mol Life Sci,* 64**,** 263-70.

AMIN, A. S., TAN, H. L. & WILDE, A. A. 2010. Cardiac ion channels in health and disease. *Heart Rhythm,* 7**,** 117-26.

ANDERSON, C. L., DELISLE, B. P., ANSON, B. D., KILBY, J. A., WILL, M. L., TESTER, D. J., GONG, Q., ZHOU, Z., ACKERMAN, M. J. & JANUARY, C. T. 2006. Most LQT2 mutations reduce Kv11.1 (hERG) current by a class 2 (trafficking-deficient) mechanism. *Circulation,* 113**,** 365-73.

ANTCLIFF, J. F., HAIDER, S., PROKS, P., SANSOM, M. S. & ASHCROFT, F. M. 2005. Functional analysis of a structural model of the ATP-binding site of the KATP channel Kir6.2 subunit. *EMBO J,* 24**,** 229-39.

ANTONNY, B., MADDEN, D., HAMAMOTO, S., ORCI, L. & SCHEKMAN, R. 2001. Dynamics of the COPII coat with GTP and stable analogues. *Nat Cell Biol,* 3**,** 531-7.

APPENZELLER-HERZOG, C. & HAURI, H. P. 2006. The ER-Golgi intermediate compartment (ERGIC): in search of its identity and function. *J Cell Sci,* 119**,** 2173-83.

ARIDOR, M. & BALCH, W. E. 1996. Principles of selective transport: coat complexes hold the key. *Trends Cell Biol,* 6**,** 315-20.

ARNOUX, J. B., DE LONLAY, P., RIBEIRO, M. J., HUSSAIN, K., BLANKENSTEIN, O., MOHNIKE, K., VALAYANNOPOULOS, V., ROBERT, J. J., RAHIER, J., SEMPOUX, C., BELLANNE, C., VERKARRE, V., AIGRAIN, Y., JAUBERT, F., BRUNELLE, F. & NIHOUL-FEKETE, C. 2010. Congenital hyperinsulinism. *Early Hum Dev,* 86**,** 287-94.

ASHCROFT, F. M. 2005. ATP-sensitive potassium channelopathies: focus on insulin secretion. *J Clin Invest,* 115**,** 2047-58.

ASHCROFT, F. M. 2006a. From molecule to malady. *Nature,* 440**,** 440-7.

ASHCROFT, F. M. 2006b. K(ATP) channels and insulin secretion: a key role in health and disease. *Biochem Soc Trans,* 34**,** 243-6.

ASHCROFT, F. M. & GRIBBLE, F. M. 1999. ATP-sensitive K+ channels and insulin secretion: their role in health and disease. *Diabetologia,* 42**,** 903-19.

ASHCROFT, F. M. & GRIBBLE, F. M. 2000a. New windows on the mechanism of action of K(ATP) channel openers. *Trends Pharmacol Sci,* 21**,** 439-45.

ASHCROFT, F. M. & GRIBBLE, F. M. 2000b. Tissue-specific effects of sulfonylureas: lessons from studies of cloned K(ATP) channels. *J Diabetes Complications,* 14**,** 192-6.

ASHCROFT, F. M., HARRISON, D. E. & ASHCROFT, S. J. 1984. Glucose induces closure of single potassium channels in isolated rat pancreatic beta-cells. *Nature,* 312**,** 446-8.

ASHCROFT, F. M. & KAKEI, M. 1989. ATP-sensitive K+ channels in rat pancreatic beta-cells: modulation by ATP and Mg2+ ions. *J Physiol,* 416**,** 349-67.

ASHCROFT, F. M., KAKEI, M., KELLY, R. P. & SUTTON, R. 1987. ATP-sensitive K+ channels in human isolated pancreatic B-cells. *FEBS Lett,* 215**,** 9-12.

ASHCROFT, F. M. & RORSMAN, P. 1990. ATP-sensitive K+ channels: a link between B-cell metabolism and insulin secretion. *Biochem Soc Trans,* 18**,** 109-11.

ASHFORD, M. L., STURGESS, N. C., TROUT, N. J., GARDNER, N. J. & HALES, C. N. 1988. Adenosine-5'-triphosphate-sensitive ion channels in neonatal rat cultured central neurones. *Pflugers Arch,* 412**,** 297-304.

BABENKO, A. P., GONZALEZ, G., AGUILAR-BRYAN, L. & BRYAN, J. 1999. Sulfonylurea receptors set the maximal open probability, ATP sensitivity and plasma membrane density of KATP channels. *FEBS Lett,* 445**,** 131-6.

BALASUBRAMANIAN, N., SCOTT, D. W., CASTLE, J. D., CASANOVA, J. E. & SCHWARTZ, M. A. 2007. Arf6 and microtubules in adhesion-dependent trafficking of lipid rafts. *Nat Cell Biol,* 9**,** 1381-91.

BALCH, W. E. & FARQUHAR, M. G. 1995. Beyond bulk flow. *Trends Cell Biol,* 5**,** 16-9.

BALIJEPALLI, R. C., DELISLE, B. P., BALIJEPALLI, S. Y., FOELL, J. D., SLIND, J. K., KAMP, T. J. & JANUARY, C. T. 2007. Kv11.1 (ERG1) K+ channels localize in cholesterol and sphingolipid enriched membranes and are modulated by membrane cholesterol. *Channels (Austin),* 1**,** 263-72.

BANNYKH, S. I. & BALCH, W. E. 1998. Selective transport of cargo between the endoplasmic reticulum and Golgi compartments. *Histochem Cell Biol,* 109**,** 463-75.

BANNYKH, S. I., NISHIMURA, N. & BALCH, W. E. 1998. Getting into the Golgi. *Trends Cell Biol,* 8**,** 21-5.

BARLOWE, C. 2002. Three-dimensional structure of a COPII prebudding complex. *Dev Cell,* 3**,** 467-8.

BARLOWE, C. 2003. Signals for COPII-dependent export from the ER: what's the ticket out? *Trends Cell Biol,* 13**,** 295-300.

BARLOWE, C., ORCI, L., YEUNG, T., HOSOBUCHI, M., HAMAMOTO, S., SALAMA, N., REXACH, M. F., RAVAZZOLA, M., AMHERDT, M. & SCHEKMAN, R. 1994. COPII: A membrane coat formed by Sec proteins that drive vesicle budding from the endoplasmic reticulum. *Cell,* 77**,** 895-907.

BARLOWE, C. & SCHEKMAN, R. 1995. [13] Expression, purification, and assay of Sec12p: A Sarlp-specific GDP dissociation stimulator. *In:* W. E. BALCH, C. J. D. A. H. (ed.) *Methods in Enzymology.* Academic Press.

BARR, F. & LAMBRIGHT, D. G. 2010. Rab GEFs and GAPs. *Curr Opin Cell Biol,* 22**,** 461-70.

BAUKROWITZ, T., SCHULTE, U., OLIVER, D., HERLITZE, S., KRAUTER, T., TUCKER, S. J., RUPPERSBERG, J. P. & FAKLER, B. 1998. PIP2 and PIP as determinants for ATP inhibition of KATP channels. *Science,* 282**,** 1141-4.

BEECH, D. J., ZHANG, H., NAKAO, K. & BOLTON, T. B. 1993. K channel activation by nucleotide diphosphates and its inhibition by glibenclamide in vascular smooth muscle cells. *Br J Pharmacol,* 110**,** 573-82.

BI, X., CORPINA, R. A. & GOLDBERG, J. 2002. Structure of the Sec23/24-Sar1 pre-budding complex of the COPII vesicle coat. *Nature,* 419**,** 271-7.

BIAN, J. S., KAGAN, A. & MCDONALD, T. V. 2004. Molecular analysis of PIP2 regulation of HERG and IKr. *Am J Physiol Heart Circ Physiol,* 287**,** H2154-63.

BICHET, D., HAASS, F. A. & JAN, L. Y. 2003. Merging functional studies with structures of inward-rectifier K+ channels. *Nat Rev Neurosci,* 4**,** 957-967.

BICKEL, P. E., SCHERER, P. E., SCHNITZER, J. E., OH, P., LISANTI, M. P. & LODISH, H. F. 1997. Flotillin and Epidermal Surface Antigen Define a New Family of Caveolae-associated Integral Membrane Proteins. *Journal of Biological Chemistry,* 272**,** 13793-13802.

BIENENGRAEBER, M., ALEKSEEV, A. E., ABRAHAM, M. R., CARRASCO, A. J., MOREAU, C., VIVAUDOU, M., DZEJA, P. P. & TERZIC, A. 2000. ATPase activity of the sulfonylurea receptor: a catalytic function for the KATP channel complex. *FASEB J,* 14**,** 1943-52.

BOBANOVIC, L. K., ROYLE, S. J. & MURRELL-LAGNADO, R. D. 2002. P2X receptor trafficking in neurons is subunit specific. *J Neurosci,* 22**,** 4814-24.

BONIFACINO, J. S. & GLICK, B. S. 2004. The mechanisms of vesicle budding and fusion. *Cell,* 116**,** 153-66.

BONIFACINO, J. S. & LIPPINCOTT-SCHWARTZ, J. 2003. Coat proteins: shaping membrane transport. *Nat Rev Mol Cell Biol,* 4**,** 409-14.

BONIFACINO, J. S. & TRAUB, L. M. 2003. Signals for sorting of transmembrane proteins to endosomes and lysosomes. *Annu Rev Biochem,* 72**,** 395-447.

BONNON, C., WENDELER, M. W., PACCAUD, J. P. & HAURI, H. P. 2010. Selective export of human GPI-anchored proteins from the endoplasmic reticulum. *J Cell Sci,* 123**,** 1705-15.

BOYADJIEV, S. A., FROMME, J. C., BEN, J., CHONG, S. S., NAUTA, C., HUR, D. J., ZHANG, G., HAMAMOTO, S., SCHEKMAN, R., RAVAZZOLA, M., ORCI, L. & EYAID, W. 2006. Cranio-lenticulo-sutural dysplasia is caused by a SEC23A mutation leading to abnormal endoplasmic-reticulum-to-Golgi trafficking. *Nat Genet,* 38**,** 1192-7.

BROWN, A. M. 2004. Drugs, hERG and sudden death. *Cell Calcium,* 35**,** 543-7.

BROWN, C. R., HONG-BROWN, L. Q., BIWERSI, J., VERKMAN, A. S. & WELCH, W. J. 1996. Chemical chaperones correct the mutant phenotype of the delta F508 cystic fibrosis transmembrane conductance regulator protein. *Cell Stress Chaperones,* 1**,** 117-25.

BRUGADA, R., HONG, K., CORDEIRO, J. M. & DUMAINE, R. 2005. Short QT syndrome. *Canadian Medical Association Journal,* 173**,** 1349-1354.

BRYANT, N. J., GOVERS, R. & JAMES, D. E. 2002. Regulated transport of the glucose transporter GLUT4. *Nat Rev Mol Cell Biol,* 3**,** 267-77.

BURKE, M. A., MUTHARASAN, R. K. & ARDEHALI, H. 2008. The sulfonylurea receptor, an atypical ATP-binding cassette protein, and its regulation of the KATP channel. *Circ Res,* 102**,** 164-76.

CARTIER, E. A., CONTI, L. R., VANDENBERG, C. A. & SHYNG, S. L. 2001. Defective trafficking and function of KATP channels caused by a sulfonylurea receptor 1 mutation associated with persistent hyperinsulinemic hypoglycemia of infancy. *Proc Natl Acad Sci U S A,* 98**,** 2882-7.

CHADDA, R., HOWES, M. T., PLOWMAN, S. J., HANCOCK, J. F., PARTON, R. G. & MAYOR, S. 2007. Cholesterol-sensitive Cdc42 activation regulates actin polymerization for internalisation via the GEEC pathway. *Traffic,* 8**,** 702-17.

CHAPMAN, H., RAMSTROM, C., KORHONEN, L., LAINE, M., WANN, K. T., LINDHOLM, D., PASTERNACK, M. & TORNQUIST, K. 2005. Downregulation of the HERG (KCNH2) K(+) channel by ceramide: evidence for ubiquitin-mediated lysosomal degradation. *J Cell Sci,* 118**,** 5325-34.

CHEN, J., CHEN, K., SROUBEK, J., WU, Z. Y., THOMAS, D., BIAN, J. S. & MCDONALD, T. V. 2010a. Post-transcriptional control of HERG potassium channel protein by {alpha}-adrenergic receptor stimulation. *Mol Pharmacol*.

CHEN, J., CHEN, K., SROUBEK, J., WU, Z. Y., THOMAS, D., BIAN, J. S. & MCDONALD, T. V. 2010b. Post-transcriptional control of human ether-a-go-go-related gene potassium channel protein by alpha-adrenergic receptor stimulation. *Mol Pharmacol,* 78**,** 186-97.

CHEN, J., SROUBEK, J., KRISHNAN, Y., LI, Y., BIAN, J. & MCDONALD, T. V. 2009. PKA phosphorylation of HERG protein regulates the rate of channel synthesis. *Am J Physiol Heart Circ Physiol,* 296**,** H1244-54.

CHENG, S. H., GREGORY, R. J., MARSHALL, J., PAUL, S., SOUZA, D. W., WHITE, G. A., O'RIORDAN, C. R. & SMITH, A. E. 1990. Defective intracellular transport and processing of CFTR is the molecular basis of most cystic fibrosis. *Cell,* 63**,** 827-34.

CHERUBINI, A., TADDEI, G. L., CROCIANI, O., PAGLIERANI, M., BUCCOLIERO, A. M., FONTANA, L., NOCI, I., BORRI, P., BORRANI, E., GIACHI, M., BECCHETTI, A., ROSATI, B., WANKE, E., OLIVOTTO, M. & ARCANGELI, A. 2000. HERG potassium channels are more frequently expressed in human endometrial cancer as compared to non-cancerous endometrium. *Br J Cancer,* 83**,** 1722-9.

CHILTON, L. & LOUTZENHISER, R. 2001. Functional evidence for an inward rectifier potassium current in rat renal afferent arterioles. *Circ Res,* 88**,** 152-8.

CHRISTESEN, H. B., BRUSGAARD, K., ALM, J., SJOBLAD, S., HUSSAIN, K., FENGER, C., RASMUSSEN, L., HOVENDAL, C., OTONKOSKI, T. & JACOBSEN, B. B. 2007. Rapid genetic analysis in congenital hyperinsulinism. *Horm Res,* 67**,** 184-8.

CHUTKOW, W. A., SIMON, M. C., LE BEAU, M. M. & BURANT, C. F. 1996. Cloning, tissue expression, and chromosomal localization of SUR2, the putative drug-binding subunit of cardiac, skeletal muscle, and vascular KATP channels. *Diabetes,* 45**,** 1439-45.

CLEMENT, J. P. T., KUNJILWAR, K., GONZALEZ, G., SCHWANSTECHER, M., PANTEN, U., AGUILAR-BRYAN, L. & BRYAN, J. 1997. Association and stoichiometry of K(ATP) channel subunits. *Neuron,* 18**,** 827-38.

COHEN, M. V., LIU, Y., LIU, G. S., WANG, P., WEINBRENNER, C., CORDIS, G. A., DAS, D. K. & DOWNEY, J. M. 1996. Phospholipase D plays a role in ischemic preconditioning in rabbit heart. *Circulation,* 94**,** 1713-8.

COLLAWN, J. F., STANGEL, M., KUHN, L. A., ESEKOGWU, V., JING, S. Q., TROWBRIDGE, I. S. & TAINER, J. A. 1990. Transferrin receptor internalization sequence YXRF implicates a tight turn as the structural recognition motif for internalisation. *Cell,* 63**,** 1061-72.

COREY, S., KRAPIVINSKY, G., KRAPIVINSKY, L. & CLAPHAM, D. E. 1998. Number and stoichiometry of subunits in the native atrial G-protein-gated K+ channel, IKACh. *J Biol Chem,* 273**,** 5271-8.

CRAIG, T. J., ASHCROFT, F. M. & PROKS, P. 2008. How ATP inhibits the open K(ATP) channel. *J Gen Physiol,* 132**,** 131-44.

CRANE, A. & AGUILAR-BRYAN, L. 2004. Assembly, maturation, and turnover of K(ATP) channel subunits. *J Biol Chem,* 279**,** 9080-90.

CROCIANI, O., GUASTI, L., BALZI, M., BECCHETTI, A., WANKE, E., OLIVOTTO, M., WYMORE, R. S. & ARCANGELI, A. 2003. Cell cycle-dependent expression of HERG1 and HERG1B isoforms in tumor cells. *J Biol Chem,* 278**,** 2947-55.

CURRAN, M. E., SPLAWSKI, I., TIMOTHY, K. W., VINCENT, G. M., GREEN, E. D. & KEATING, M. T. 1995. A molecular basis for cardiac arrhythmia: HERG mutations cause long QT syndrome. *Cell,* 80**,** 795-803.

D'SOUZA-SCHOREY, C. & CHAVRIER, P. 2006. ARF proteins: roles in membrane traffic and beyond. *Nat Rev Mol Cell Biol,* 7**,** 347-58.

DADA, L. A., CHANDEL, N. S., RIDGE, K. M., PEDEMONTE, C., BERTORELLO, A. M. & SZNAJDER, J. I. 2003. Hypoxia-induced internalisation of Na,K-ATPase in alveolar epithelial cells is mediated by mitochondrial reactive oxygen species and PKC-zeta. *J Clin Invest,* 111**,** 1057-64.

DECRESSAC, S., FRANCO, M., BENDAHHOU, S., WARTH, R., KNAUER, S., BARHANIN, J., LAZDUNSKI, M. & LESAGE, F. 2004. ARF6-dependent interaction of the TWIK1 K+ channel with EFA6, a GDP/GTP exchange factor for ARF6. *EMBO Rep,* 5**,** 1171-5.

DELISLE, B. P., ANDERSON, C. L., BALIJEPALLI, R. C., ANSON, B. D., KAMP, T. J. & JANUARY, C. T. 2003. Thapsigargin selectively rescues the trafficking defective LQT2 channels G601S and F805C. *J Biol Chem,* 278**,** 35749-54.

DELISLE, B. P., ANSON, B. D., RAJAMANI, S. & JANUARY, C. T. 2004. Biology of cardiac arrhythmias: ion channel protein trafficking. *Circ Res,* 94**,** 1418-28.

DELISLE, B. P., UNDERKOFLER, H. A., MOUNGEY, B. M., SLIND, J. K., KILBY, J. A., BEST, J. M., FOELL, J. D., BALIJEPALLI, R. C., KAMP, T. J. & JANUARY, C. T. 2009. Small GTPase determinants for the Golgi processing and plasmalemmal expression of human ether-a-go-go related (hERG) K+ channels. *J Biol Chem,* 284**,** 2844-53.

DENNIS, A., WANG, L., WAN, X. & FICKER, E. 2007. hERG channel trafficking: novel targets in drug-induced long QT syndrome. *Biochem Soc Trans,* 35**,** 1060-3.

DI GUGLIELMO, G. M., LE ROY, C., GOODFELLOW, A. F. & WRANA, J. L. 2003. Distinct endocytic pathways regulate TGF-beta receptor signalling and turnover. *Nat Cell Biol,* 5**,** 410-21.

DIMCHEFF, D. E., PORTIS, J. L. & CAUGHEY, B. 2003. Prion proteins meet protein quality control. *Trends Cell Biol,* 13**,** 337-40.

DOHERTY, G. J. & MCMAHON, H. T. 2009. Mechanisms of internalisation. *Annu Rev Biochem,* 78**,** 857-902.

DONALDSON, J. G. 2003. Multiple roles for Arf6: sorting, structuring, and signaling at the plasma membrane. *J Biol Chem,* 278**,** 41573-6.

DONALDSON, J. G., PORAT-SHLIOM, N. & COHEN, L. A. 2009. Clathrin-independent internalisation: a unique platform for cell signaling and PM remodeling. *Cell Signal,* 21**,** 1-6.

DONALDSON, J. G. & WILLIAMS, D. B. 2009. Intracellular assembly and trafficking of MHC class I molecules. *Traffic,* 10**,** 1745-52.

DONG, X., STOTHARD, P., FORSYTHE, I. J. & WISHART, D. S. 2004. PlasMapper: a web server for drawing and auto-annotating plasmid maps. *Nucleic Acids Res,* 32**,** W660-4.

DORING, F., DERST, C., WISCHMEYER, E., KARSCHIN, C., SCHNEGGENBURGER, R., DAUT, J. & KARSCHIN, A. 1998. The epithelial inward rectifier channel Kir7.1 displays unusual K+ permeation properties. *J Neurosci,* 18**,** 8625-36.

DOYLE, D. A., MORAIS CABRAL, J., PFUETZNER, R. A., KUO, A., GULBIS, J. M., COHEN, S. L., CHAIT, B. T. & MACKINNON, R. 1998. The structure of the potassium channel: molecular basis of K+ conduction and selectivity. *Science,* 280**,** 69-77.

DRAKE, M. T., SHENOY, S. K. & LEFKOWITZ, R. J. 2006. Trafficking of G protein-coupled receptors. *Circ Res,* 99**,** 570-82.

DUNNE, M. J., COSGROVE, K. E., SHEPHERD, R. M., AYNSLEY-GREEN, A. & LINDLEY, K. J. 2004. Hyperinsulinism in infancy: from basic science to clinical disease. *Physiol Rev,* 84**,** 239-75.

ECKHARDT, L. L., RAJAMANI, S. & JANUARY, C. T. 2005. Protein trafficking abnormalities: a new mechanism in drug-induced long QT syndrome. *Br J Pharmacol,* 145**,** 3-4.

ELLGAARD, L. & HELENIUS, A. 2003. Quality control in the endoplasmic reticulum. *Nat Rev Mol Cell Biol,* 4**,** 181-91.

ELLIS, S. & MELLOR, H. 2000. Regulation of endocytic traffic by rho family GTPases. *Trends Cell Biol,* 10**,** 85-8.

EYSTER, C. A., HIGGINSON, J. D., HUEBNER, R., PORAT-SHLIOM, N., WEIGERT, R., WU, W. W., SHEN, R. F. & DONALDSON, J. G. 2009. Discovery of new cargo proteins that enter cells through clathrin-independent internalisation. *Traffic,* 10**,** 590-9.

FELIPE, A., VICENTE, R., VILLALONGA, N., ROURA-FERRER, M., MARTÍNEZ-MÁRMOL, R., SOLÉ, L., FERRERES, J. C. & CONDOM, E. 2006. Potassium channels: New targets in cancer therapy. *Cancer Detection and Prevention,* 30**,** 375-385.

FERMINI, B. & FOSSA, A. A. 2003. The impact of drug-induced QT interval prolongation on drug discovery and development. *Nat Rev Drug Discov,* 2**,** 439-47.

FICKER, E., DENNIS, A., KURYSHEV, Y., WIBLE, B. A. & BROWN, A. M. 2005. HERG channel trafficking. *Novartis Found Symp,* 266**,** 57-69; discussion 70-4, 95-9.

FICKER, E., DENNIS, A. T., WANG, L. & BROWN, A. M. 2003. Role of the cytosolic chaperones Hsp70 and Hsp90 in maturation of the cardiac potassium channel HERG. *Circ Res,* 92**,** e87-100.

FINDLAY, I. 1988. ATP4- and ATP.Mg inhibit the ATP-sensitive K+ channel of rat ventricular myocytes. *Pflugers Arch,* 412**,** 37-41.

FLAGG, T. P., KURATA, H. T., MASIA, R., CAPUTA, G., MAGNUSON, M. A., LEFER, D. J., COETZEE, W. A. & NICHOLS, C. G. 2008. Differential structure of atrial and ventricular KATP: atrial KATP channels require SUR1. *Circ Res,* 103**,** 1458-65.

FOURNET, J. C. & JUNIEN, C. 2004. Genetics of congenital hyperinsulinism. *Endocr Pathol,* 15**,** 233-40.

FOURNET, J. C., MAYAUD, C., DE LONLAY, P., GROSS-MORAND, M. S., VERKARRE, V., CASTANET, M., DEVILLERS, M., RAHIER, J., BRUNELLE, F., ROBERT, J. J., NIHOUL-FEKETE, C., SAUDUBRAY, J. M. & JUNIEN, C. 2001. Unbalanced expression of 11p15 imprinted genes in focal forms of congenital hyperinsulinism: association with a reduction to homozygosity of a mutation in ABCC8 or KCNJ11. *Am J Pathol,* 158**,** 2177-84.

FOURNET, J. C., MAYAUD, C., DE LONLAY, P., VERKARRE, V., RAHIER, J., BRUNELLE, F., ROBERT, J. J., NIHOUL-FEKETE, C., SAUDUBRAY, J. M. & JUNIEN, C. 2000. Loss of imprinted genes and paternal SUR1 mutations lead to focal form of congenital hyperinsulinism. *Horm Res,* 53 Suppl 1**,** 2-6.

FRANK, S. R., HATFIELD, J. C. & CASANOVA, J. E. 1998. Remodeling of the actin cytoskeleton is coordinately regulated by protein kinase C and the ADP-ribosylation factor nucleotide exchange factor ARNO. *Mol Biol Cell,* 9**,** 3133-46.

FROMME, J. C., ORCI, L. & SCHEKMAN, R. 2008. Coordination of COPII vesicle trafficking by Sec23. *Trends Cell Biol,* 18**,** 330-6.

FROMME, J. C. & SCHEKMAN, R. 2005. COPII-coated vesicles: flexible enough for large cargo? *Current Opinion in Cell Biology,* 17**,** 345-352.

FURUTANI, M., TRUDEAU, M. C., HAGIWARA, N., SEKI, A., GONG, Q., ZHOU, Z., IMAMURA, S., NAGASHIMA, H., KASANUKI, H., TAKAO, A., MOMMA, K., JANUARY, C. T., ROBERTSON, G. A. & MATSUOKA, R. 1999. Novel mechanism associated with an inherited cardiac arrhythmia: defective protein trafficking by the mutant HERG (G601S) potassium channel. *Circulation,* 99**,** 2290-4.

GANAPATHI, S. B., FOX, T. E., KESTER, M. & ELMSLIE, K. S. 2010. Ceramide modulates HERG potassium channel gating by translocation into lipid rafts. *Am J Physiol Cell Physiol,* 299**,** C74-86.

GARCIA, M. L. & KACZOROWSKI, G. J. 2005. Potassium channels as targets for therapeutic intervention. *Sci STKE,* 2005**,** pe46.

GARDNER, L. A., HAJJHUSSEIN, H., FREDERICK-DYER, K. C. & BAHOUTH, S. W. 2010. Rab11a and its binding partners regulate the recycling of the ss1-adrenergic receptor. *Cell Signal.*

GENG, X., LI, L., WATKINS, S., ROBBINS, P. D. & DRAIN, P. 2003. The insulin secretory granule is the major site of K(ATP) channels of the endocrine pancreas. *Diabetes,* 52**,** 767-76.

GLOYN, A. L., PEARSON, E. R., ANTCLIFF, J. F., PROKS, P., BRUINING, G. J., SLINGERLAND, A. S., HOWARD, N., SRINIVASAN, S., SILVA, J. M., MOLNES, J., EDGHILL, E. L., FRAYLING, T. M., TEMPLE, I. K., MACKAY, D., SHIELD, J. P., SUMNIK, Z., VAN RHIJN, A., WALES, J. K., CLARK, P., GORMAN, S., AISENBERG, J., ELLARD, S., NJOLSTAD, P. R., ASHCROFT,

F. M. & HATTERSLEY, A. T. 2004. Activating mutations in the gene encoding the ATP-sensitive potassium-channel subunit Kir6.2 and permanent neonatal diabetes. *N Engl J Med,* 350**,** 1838-49.

GONG, Q., JONES, M. A. & ZHOU, Z. 2006. Mechanisms of pharmacological rescue of trafficking-defective hERG mutant channels in human long QT syndrome. *J Biol Chem,* 281**,** 4069-74.

GONG, Q., KEENEY, D. R., MOLINARI, M. & ZHOU, Z. 2005. Degradation of trafficking-defective long QT syndrome type II mutant channels by the ubiquitin-proteasome pathway. *J Biol Chem,* 280**,** 19419-25.

GONG, Q., WEIDE, M., HUNTSMAN, C., XU, Z., JAN, L. Y. & MA, D. 2007a. Identification and characterization of a new class of trafficking motifs for controlling clathrin-independent internalization and recycling. *J Biol Chem,* 282**,** 13087-97.

GONG, Q., ZHANG, L., VINCENT, G. M., HORNE, B. D. & ZHOU, Z. 2007b. Nonsense mutations in hERG cause a decrease in mutant mRNA transcripts by nonsense-mediated mRNA decay in human long-QT syndrome. *Circulation,* 116**,** 17-24.

GONZALEZ, L., JR. & SCHELLER, R. H. 1999. Regulation of membrane trafficking: structural insights from a Rab/effector complex. *Cell,* 96**,** 755-8.

GOODY, R. S., RAK, A. & ALEXANDROV, K. 2005. The structural and mechanistic basis for recycling of Rab proteins between membrane compartments. *Cell Mol Life Sci,* 62**,** 1657-70.

GORELICK, F. S. & SHUGRUE, C. 2001. Exiting the endoplasmic reticulum. *Mol Cell Endocrinol,* 177**,** 13-8.

GRANT, B. D. & DONALDSON, J. G. 2009. Pathways and mechanisms of endocytic recycling. *Nat Rev Mol Cell Biol,* 10**,** 597-608.

GRIBBLE, F. M., TUCKER, S. J. & ASHCROFT, F. M. 1997. The essential role of the Walker A motifs of SUR1 in K-ATP channel activation by Mg-ADP and diazoxide. *EMBO J,* 16**,** 1145-52.

GRIBKOFF, V. K. 2008. The therapeutic potential of neuronal K V 7 (KCNQ) channel modulators: an update. *Expert Opin Ther Targets,* 12**,** 565-81.

GRUNNET, M., DINESS, T. G., HANSEN, R. S. & OLESEN, S. P. 2008. Biophysical characterization of the short QT mutation hERG-N588K reveals a mixed gain- and loss-of-function. *Cell Physiol Biochem,* 22**,** 611-24.

GUASTI, L., CILIA, E., CROCIANI, O., HOFMANN, G., POLVANI, S., BECCHETTI, A., WANKE, E., TEMPIA, F. & ARCANGELI, A. 2005. Expression pattern of the ether-a-go-go-related (ERG) family proteins in the adult mouse central nervous system: evidence for coassembly of different subunits. *J Comp Neurol,* 491**,** 157-74.

GULLO, F., ALES, E., ROSATI, B., LECCHI, M., MASI, A., GUASTI, L., CANO-ABAD, M. F., ARCANGELI, A., LOPEZ, M. G. & WANKE, E. 2003. ERG K+ channel blockade enhances firing and epinephrine secretion in rat chromaffin cells: the missing link to LQT2-related sudden death? *FASEB J,* 17**,** 330-2.

GUO, J., MASSAELI, H., XU, J., JIA, Z., WIGLE, J. T., MESAELI, N. & ZHANG, S. 2009. Extracellular K+ concentration controls cell surface density of IKr in rabbit hearts and of the HERG channel in human cell lines. *J Clin Invest,* 119**,** 2745-57.

GURKAN, C., STAGG, S. M., LAPOINTE, P. & BALCH, W. E. 2006. The COPII cage: unifying principles of vesicle coat assembly. *Nat Rev Mol Cell Biol,* 7**,** 727-38.

HANLON, M. R. & WALLACE, B. A. 2002. Structure and function of voltage-dependent ion channel regulatory beta subunits. *Biochemistry,* 41**,** 2886-94.

HANNUN, Y. A. 1996. Functions of Ceramide in Coordinating Cellular Responses to Stress. *Science,* 274**,** 1855-1859.

HANSEN, C. G. & NICHOLS, B. J. 2010. Exploring the caves: cavins, caveolins and caveolae. *Trends Cell Biol,* 20**,** 177-86.

HARDER, T. & SIMONS, K. 1997. Caveolae, DIGs, and the dynamics of sphingolipid-cholesterol microdomains. *Curr Opin Cell Biol,* 9**,** 534-42.

HEGINBOTHAM, L., LU, Z., ABRAMSON, T. & MACKINNON, R. 1994. Mutations in the K+ channel signature sequence. *Biophys J,* 66**,** 1061-7.

HERRING, D., HUANG, R., SINGH, M., DILLON, G. H. & LEIDENHEIMER, N. J. 2005. PKC modulation of GABAA receptor internalisation and function is inhibited by mutation of a dileucine motif within the receptor beta 2 subunit. *Neuropharmacology,* 48**,** 181-94.

HERRINGTON, J., ZHOU, Y. P., BUGIANESI, R. M., DULSKI, P. M., FENG, Y., WARREN, V. A., SMITH, M. M., KOHLER, M. G., GARSKY, V. M., SANCHEZ, M., WAGNER, M., RAPHAELLI, K., BANERJEE, P., AHAGHOTU, C., WUNDERLER, D., PRIEST, B. T., MEHL, J. T., GARCIA, M. L., MCMANUS, O. B., KACZOROWSKI, G. J. & SLAUGHTER, R. S. 2006. Blockers of the delayed-rectifier potassium current in pancreatic beta-cells enhance glucose-dependent insulin secretion. *Diabetes,* 55**,** 1034-42.

HEUSSER, K. & SCHWAPPACH, B. 2005. Trafficking of potassium channels. *Curr Opin Neurobiol,* 15**,** 364-9.

HEUSSER, K., YUAN, H., NEAGOE, I., TARASOV, A. I., ASHCROFT, F. M. & SCHWAPPACH, B. 2006. Scavenging of 14-3-3 proteins reveals their involvement in the cell-surface transport of ATP-sensitive K+ channels. *J Cell Sci,* 119**,** 4353-63.

HIBINO, H., INANOBE, A., FURUTANI, K., MURAKAMI, S., FINDLAY, I. & KURACHI, Y. 2010. Inwardly rectifying potassium channels: their structure, function, and physiological roles. *Physiol Rev,* 90**,** 291-366.

HILLE, B. 2001. *Ionic Channels of Excitable Membranes*.

HILLE, B. & SCHWARZ, W. 1978. Potassium channels as multi-ion single-file pores. *J Gen Physiol,* 72**,** 409-42.

HO, K., NICHOLS, C. G., LEDERER, W. J., LYTTON, J., VASSILEV, P. M., KANAZIRSKA, M. V. & HEBERT, S. C. 1993. Cloning and expression of an inwardly rectifying ATP-regulated potassium channel. *Nature,* 362**,** 31-8.

HOLOPAINEN, J. M., SUBRAMANIAN, M. & KINNUNEN, P. K. J. 1998. Sphingomyelinase induces lipid microdomain formation in a fluid phosphatidylcholine/sphingomyelin membrane. *Biochemistry,* 37**,** 17562-17570.

HONG, K., BJERREGAARD, P., GUSSAK, I. & BRUGADA, R. 2005. Short QT syndrome and atrial fibrillation caused by mutation in KCNH2. *Journal of Cardiovascular Electrophysiology,* 16**,** 394-396.

HORIE, M. & IRISAWA, H. 1987. Rectification of muscarinic K+ current by magnesium ion in guinea pig atrial cells. *Am J Physiol,* 253**,** H210-4.

HOUGH, E., BEECH, D. J. & SIVAPRASADARAO, A. 2000. Identification of molecular regions responsible for the membrane trafficking of Kir6.2. *Pflugers Arch,* 440**,** 481-7.

HU, K., HUANG, C. S., JAN, Y. N. & JAN, L. Y. 2003. ATP-sensitive potassium channel traffic regulation by adenosine and protein kinase C. *Neuron,* 38**,** 417-32.

INAGAKI, N., TSUURA, Y., NAMBA, N., MASUDA, K., GONOI, T., HORIE, M., SEINO, Y., MIZUTA, M. & SEINO, S. 1995. Cloning and functional characterization of a novel ATP-sensitive potassium channel ubiquitously expressed in rat tissues, including pancreatic islets, pituitary, skeletal muscle, and heart. *J Biol Chem,* 270**,** 5691-4.

ISOMOTO, S., KONDO, C. & KURACHI, Y. 1997. Inwardly rectifying potassium channels: their molecular heterogeneity and function. *Jpn J Physiol,* 47**,** 11-39.

JANUARY, C. T., GONG, Q. & ZHOU, Z. 2000. Long QT syndrome: cellular basis and arrhythmia mechanism in LQT2. *J Cardiovasc Electrophysiol,* 11**,** 1413-8.

JARVIS, S. E. & ZAMPONI, G. W. 2007. Trafficking and regulation of neuronal voltage-gated calcium channels. *Curr Opin Cell Biol,* 19**,** 474-82.

JIANG, Y., LEE, A., CHEN, J., RUTA, V., CADENE, M., CHAIT, B. T. & MACKINNON, R. 2003. X-ray structure of a voltage-dependent K+ channel. *Nature,* 423**,** 33-41.

JONES, B., JONES, E. L., BONNEY, S. A., PATEL, H. N., MENSENKAMP, A. R., EICHENBAUM-VOLINE, S., RUDLING, M., MYRDAL, U., ANNESI, G., NAIK, S., MEADOWS, N., QUATTRONE, A., ISLAM, S. A., NAOUMOVA, R. P., ANGELIN, B., INFANTE, R., LEVY, E., ROY, C. C., FREEMONT, P. S., SCOTT, J. & SHOULDERS, C. C. 2003. Mutations in a Sar1 GTPase of COPII vesicles are associated with lipid absorption disorders. *Nat Genet,* 34**,** 29-31.

JONES, E. M., ROTI ROTI, E. C., WANG, J., DELFOSSE, S. A. & ROBERTSON, G. A. 2004. Cardiac IKr channels minimally comprise hERG 1a and 1b subunits. *J Biol Chem,* 279**,** 44690-4.

JORDAN, M. & WURM, F. 2004. Transfection of adherent and suspended cells by calcium phosphate. *Methods,* 33**,** 136-43.

KACZOROWSKI, G. J., MCMANUS, O. B., PRIEST, B. T. & GARCIA, M. L. 2008. Ion channels as drug targets: the next GPCRs. *J Gen Physiol,* 131**,** 399-405.

KAGAN, A., YU, Z., FISHMAN, G. I. & MCDONALD, T. V. 2000. The dominant negative LQT2 mutation A561V reduces wild-type HERG expression. *J Biol Chem,* 275**,** 11241-8.

KAJIOKA, S., KITAMURA, K. & KURIYAMA, H. 1991. Guanosine diphosphate activates an adenosine 5'-triphosphate-sensitive K+ channel in the rabbit portal vein. *J Physiol,* 444**,** 397-418.

KALIA, M., KUMARI, S., CHADDA, R., HILL, M. M., PARTON, R. G. & MAYOR, S. 2006. Arf6-independent GPI-anchored protein-enriched early endosomal compartments fuse with sorting endosomes via a Rab5/phosphatidylinositol-3'-kinase-dependent machinery. *Mol Biol Cell,* 17**,** 3689-704.

KANE, G. C., LIU, X. K., YAMADA, S., OLSON, T. M. & TERZIC, A. 2005. Cardiac KATP channels in health and disease. *J Mol Cell Cardiol,* 38**,** 937-43.

KANG, Y. S., ZHAO, X., LOVAAS, J., EISENBERG, E. & GREENE, L. E. 2009. Clathrin-independent internalization of normal cellular prion protein in neuroblastoma cells is associated with the Arf6 pathway. *J Cell Sci,* 122**,** 4062-9.

KENNEDY, M. J. & EHLERS, M. D. 2006. Organelles and trafficking machinery for postsynaptic plasticity. *Annu Rev Neurosci,* 29**,** 325-62.

KHVOTCHEV, M. V., REN, M., TAKAMORI, S., JAHN, R. & SUDHOF, T. C. 2003. Divergent functions of neuronal Rab11b in Ca2+-regulated versus constitutive exocytosis. *J Neurosci,* 23**,** 10531-9.

KIRCHHAUSEN, T. 1999. Adaptors for clathrin-mediated traffic. *Annu Rev Cell Dev Biol,* 15**,** 705-32.

KISS, L. & KORN, S. J. 1998. Modulation of C-type inactivation by K+ at the potassium channel selectivity filter. *Biophys J,* 74**,** 1840-9.

KLEIN, U., GIMPL, G. & FAHRENHOLZ, F. 1995. Alteration of the myometrial plasma membrane cholesterol content with beta-cyclodextrin modulates the binding affinity of the oxytocin receptor. *Biochemistry,* 34**,** 13784-93.

KRAJEWSKA, W. M. & MASLOWSKA, I. 2004. Caveolins: structure and function in signal transduction. *Cell Mol Biol Lett,* 9**,** 195-220.

KRAPIVINSKY, G., KENNEDY, M. E., NEMEC, J., MEDINA, I., KRAPIVINSKY, L. & CLAPHAM, D. E. 1998. Gbeta binding to GIRK4 subunit is critical for G protein-gated K+ channel activation. *J Biol Chem,* 273**,** 16946-52.

KUBO, Y., BALDWIN, T. J., JAN, Y. N. & JAN, L. Y. 1993. Primary structure and functional expression of a mouse inward rectifier potassium channel. *Nature,* 362**,** 127-33.

KUGE, O., DASCHER, C., ORCI, L., ROWE, T., AMHERDT, M., PLUTNER, H., RAVAZZOLA, M., TANIGAWA, G., ROTHMAN, J. E. & BALCH, W. E. 1994. Sar1 promotes vesicle budding from the endoplasmic reticulum but not Golgi compartments. *J Cell Biol,* 125**,** 51-65.

KUO, A., GULBIS, J. M., ANTCLIFF, J. F., RAHMAN, T., LOWE, E. D., ZIMMER, J., CUTHBERTSON, J., ASHCROFT, F. M., EZAKI, T. & DOYLE, D. A. 2003.

Crystal structure of the potassium channel KirBac1.1 in the closed state. *Science,* 300**,** 1922-6.

KUPERSHMIDT, S., SNYDERS, D. J., RAES, A. & RODEN, D. M. 1998. A K+ channel splice variant common in human heart lacks a C-terminal domain required for expression of rapidly activating delayed rectifier current. *J Biol Chem,* 273**,** 27231-5.

KUPERSHMIDT, S., YANG, T., CHANTHAPHAYCHITH, S., WANG, Z., TOWBIN, J. A. & RODEN, D. M. 2002. Defective human Ether-a-go-go-related gene trafficking linked to an endoplasmic reticulum retention signal in the C terminus. *J Biol Chem,* 277**,** 27442-8.

LAI, E. C. 2003. Lipid rafts make for slippery platforms. *J Cell Biol,* 162**,** 365-70.

LAI, F., STUBBS, L. & ARTZT, K. 1994. Molecular analysis of mouse Rab11b: a new type of mammalian YPT/Rab protein. *Genomics,* 22**,** 610-6.

LANGHORST, M. F., REUTER, A., JAEGER, F. A., WIPPICH, F. M., LUXENHOFER, G., PLATTNER, H. & STUERMER, C. A. 2008. Trafficking of the microdomain scaffolding protein reggie-1/flotillin-2. *Eur J Cell Biol,* 87**,** 211-26.

LANGHORST, M. F., REUTER, A. & STUERMER, C. A. 2005. Scaffolding microdomains and beyond: the function of reggie/flotillin proteins. *Cell Mol Life Sci,* 62**,** 2228-40.

LAPIERRE, L. A., DORN, M. C., ZIMMERMAN, C. F., NAVARRE, J., BURNETTE, J. O. & GOLDENRING, J. R. 2003. Rab11b resides in a vesicular compartment distinct from Rab11a in parietal cells and other epithelial cells. *Exp Cell Res,* 290**,** 322-31.

LEE, C. & GOLDBERG, J. 2010. Structure of coatomer cage proteins and the relationship among COPI, COPII, and clathrin vesicle coats. *Cell,* 142**,** 123-32.

LEVITAN, I. B. 1994. Modulation of ion channels by protein phosphorylation and dephosphorylation. *Annu Rev Physiol,* 56**,** 193-212.

LIFTON, R. P., GHARAVI, A. G. & GELLER, D. S. 2001. Molecular mechanisms of human hypertension. *Cell,* 104**,** 545-56.

LIGHT, P. E., BLADEN, C., WINKFEIN, R. J., WALSH, M. P. & FRENCH, R. J. 2000. Molecular basis of protein kinase C-induced activation of ATP-sensitive potassium channels. *Proc Natl Acad Sci U S A,* 97**,** 9058-63.

LIN, J., LIN, S., CHOY, P. C., SHEN, X., DENG, C., KUANG, S., WU, J. & XU, W. 2008. The regulation of the cardiac potassium channel (HERG) by caveolin-1. *Biochem Cell Biol,* 86**,** 405-15.

LIN, Y. F., JAN, Y. N. & JAN, L. Y. 2000. Regulation of ATP-sensitive potassium channel function by protein kinase A-mediated phosphorylation in transfected HEK293 cells. *Embo Journal,* 19**,** 942-955.

LINGWOOD, D. & SIMONS, K. 2010. Lipid rafts as a membrane-organizing principle. *Science,* 327**,** 46-50.

LONDON, B., TRUDEAU, M. C., NEWTON, K. P., BEYER, A. K., COPELAND, N. G., GILBERT, D. J., JENKINS, N. A., SATLER, C. A. & ROBERTSON, G. A. 1997. Two isoforms of the mouse ether-a-go-go-related gene coassemble to form channels with properties similar to the rapidly activating component of the cardiac delayed rectifier K+ current. *Circ Res,* 81**,** 870-8.

LONG, S. B., CAMPBELL, E. B. & MACKINNON, R. 2005a. Crystal structure of a mammalian voltage-dependent Shaker family K+ channel. *Science,* 309**,** 897-903.

LONG, S. B., CAMPBELL, E. B. & MACKINNON, R. 2005b. Voltage sensor of Kv1.2: structural basis of electromechanical coupling. *Science,* 309**,** 903-8.

LONG, S. B., TAO, X., CAMPBELL, E. B. & MACKINNON, R. 2007. Atomic structure of a voltage-dependent K+ channel in a lipid membrane-like environment. *Nature,* 450**,** 376-82.

LOPATIN, A. N., MAKHINA, E. N. & NICHOLS, C. G. 1994. Potassium channel block by cytoplasmic polyamines as the mechanism of intrinsic rectification. *Nature,* 372**,** 366-9.

LORENZ, E., ALEKSEEV, A. E., KRAPIVINSKY, G. B., CARRASCO, A. J., CLAPHAM, D. E. & TERZIC, A. 1998. Evidence for direct physical association between a K+ channel (Kir6.2) and an ATP-binding cassette protein (SUR1) which affects cellular distribution and kinetic behavior of an ATP-sensitive K+ channel. *Mol Cell Biol,* 18**,** 1652-9.

LU, Z. 2004. Mechanism of rectification in inward-rectifier K+ channels. *Annu Rev Physiol,* 66**,** 103-29.

LUBER, B., LAUER, U., WEISS, L., HÖHNE, M., HOFSCHNEIDER, P. H. & KEKULÉ, A. S. 1993. The hepatitis B virus transactivator HBx causes elevation of diacylglycerol and activation of protein kinase C. *Research in Virology,* 144**,** 311-321.

MA, D., ZERANGUE, N., RAAB-GRAHAM, K., FRIED, S. R., JAN, Y. N. & JAN, L. Y. 2002. Diverse trafficking patterns due to multiple traffic motifs in G protein-activated inwardly rectifying potassium channels from brain and heart. *Neuron,* 33**,** 715-29.

MACIA, E., EHRLICH, M., MASSOL, R., BOUCROT, E., BRUNNER, C. & KIRCHHAUSEN, T. 2006. Dynasore, a cell-permeable inhibitor of dynamin. *Dev Cell,* 10**,** 839-50.

MACIA, E., LUTON, F., PARTISANI, M., CHERFILS, J., CHARDIN, P. & FRANCO, M. 2004. The GDP-bound form of Arf6 is located at the plasma membrane. *J Cell Sci,* 117**,** 2389-98.

MACKINNON, R. 1991. Determination of the subunit stoichiometry of a voltage-activated potassium channel. *Nature,* 350**,** 232-5.

MACKINNON, R. 2003. Potassium channels. *FEBS Lett,* 555**,** 62-5.

MANKOURI, J., TANEJA, T. K., SMITH, A. J., PONNAMBALAM, S. & SIVAPRASADARAO, A. 2006. Kir6.2 mutations causing neonatal diabetes prevent internalisation of ATP-sensitive potassium channels. *EMBO J,* 25**,** 4142-51.

MANNA, P. T., SMITH, A. J., TANEJA, T. K., HOWELL, G. J., LIPPIAT, J. D. & SIVAPRASADARAO, A. 2010. Constitutive endocytic recycling and protein kinase C-mediated lysosomal degradation control K(ATP) channel surface density. *J Biol Chem,* 285**,** 5963-73.

MARCHANT, D., SALL, A., SI, X., ABRAHAM, T., WU, W., LUO, Z., PETERSEN, T., HEGELE, R. G. & MCMANUS, B. M. 2009. ERK MAP kinase-activated Arf6 trafficking directs coxsackievirus type B3 into an unproductive compartment during virus host-cell entry. *J Gen Virol,* 90**,** 854-62.

MARKWORTH, E., SCHWANSTECHER, C. & SCHWANSTECHER, M. 2000. ATP4-mediates closure of pancreatic beta-cell ATP-sensitive potassium channels by interaction with 1 of 4 identical sites. *Diabetes,* 49**,** 1413-8.

MARSH, M. & HELENIUS, A. 2006. Virus entry: open sesame. *Cell,* 124**,** 729-40.

MARTENS, J. R., KWAK, Y. G. & TAMKUN, M. M. 1999. Modulation of Kv channel alpha/beta subunit interactions. *Trends Cardiovasc Med,* 9**,** 253-8.

MARTENS, J. R., NAVARRO-POLANCO, R., COPPOCK, E. A., NISHIYAMA, A., PARSHLEY, L., GROBASKI, T. D. & TAMKUN, M. M. 2000. Differential targeting of Shaker-like potassium channels to lipid rafts. *J Biol Chem,* 275**,** 7443-6.

MARTENS, J. R., O'CONNELL, K. & TAMKUN, M. 2004. Targeting of ion channels to membrane microdomains: localization of KV channels to lipid rafts. *Trends Pharmacol Sci,* 25**,** 16-21.

MARTENS, J. R., SAKAMOTO, N., SULLIVAN, S. A., GROBASKI, T. D. & TAMKUN, M. M. 2001. Isoform-specific localization of voltage-gated K+ channels to distinct lipid raft populations. Targeting of Kv1.5 to caveolae. *J Biol Chem,* 276**,** 8409-14.

MARTHINET, E., BLOC, A., OKA, Y., TANIZAWA, Y., WEHRLE-HALLER, B., BANCILA, V., DUBUIS, J. M., PHILIPPE, J. & SCHWITZGEBEL, V. M. 2005. Severe congenital hyperinsulinism caused by a mutation in the Kir6.2 subunit of

the adenosine triphosphate-sensitive potassium channel impairing trafficking and function. *J Clin Endocrinol Metab,* 90**,** 5401-6.

MARTINEZ-MARMOL, R., VILLALONGA, N., SOLE, L., VICENTE, R., TAMKUN, M. M., SOLER, C. & FELIPE, A. 2008. Multiple Kv1.5 targeting to membrane surface microdomains. *J Cell Physiol,* 217**,** 667-73.

MASILAMANI, M., NARAYANAN, S., PRIETO, M., BORREGO, F. & COLIGAN, J. E. 2008. Uncommon endocytic and trafficking pathway of the natural killer cell CD94/NKG2A inhibitory receptor. *Traffic,* 9**,** 1019-34.

MASSAELI, H., SUN, T., LI, X., SHALLOW, H., WU, J., XU, J., LI, W., HANSON, C., GUO, J. & ZHANG, S. 2010. Involvement of caveolin in low K+-induced endocytic degradation of the cell surface hERG channels. *J Biol Chem*.

MASSOL, R. H., LARSEN, J. E., FUJINAGA, Y., LENCER, W. I. & KIRCHHAUSEN, T. 2004. Cholera toxin toxicity does not require functional Arf6- and dynamin-dependent endocytic pathways. *Mol Biol Cell,* 15**,** 3631-41.

MATSUO, M., KIOKA, N., AMACHI, T. & UEDA, K. 1999. ATP binding properties of the nucleotide-binding folds of SUR1. *J Biol Chem,* 274**,** 37479-82.

MATSUOKA, K., MORIMITSU, Y., UCHIDA, K. & SCHEKMAN, R. 1998. Coat Assembly Directs v-SNARE Concentration into Synthetic COPII Vesicles. *Molecular Cell,* 2**,** 703-708.

MAXFIELD, F. R. & MCGRAW, T. E. 2004. Endocytic recycling. *Nat Rev Mol Cell Biol,* 5**,** 121-32.

MAYOR, S. & PAGANO, R. E. 2007. Pathways of clathrin-independent internalisation. *Nat Rev Mol Cell Biol,* 8**,** 603-12.

MCDONALD, T. V., YU, Z., MING, Z., PALMA, E., MEYERS, M. B., WANG, K. W., GOLDSTEIN, S. A. & FISHMAN, G. I. 1997. A minK-HERG complex regulates the cardiac potassium current I(Kr). *Nature,* 388**,** 289-92.

MCMAHON, H. T. & MILLS, I. G. 2004. COP and clathrin-coated vesicle budding: different pathways, common approaches. *Curr Opin Cell Biol,* 16**,** 379-91.

MERCER, J., SCHELHAAS, M. & HELENIUS, A. 2010. Virus entry by internalisation. *Annu Rev Biochem,* 79**,** 803-33.

MEZZACASA, A. & HELENIUS, A. 2002. The transitional ER defines a boundary for quality control in the secretion of tsO45 VSV glycoprotein. *Traffic,* 3**,** 833-49.

MICHELSEN, K., YUAN, H. & SCHWAPPACH, B. 2005. Hide and run. Arginine-based endoplasmic-reticulum-sorting motifs in the assembly of heteromultimeric membrane proteins. *EMBO Rep,* 6**,** 717-22.

MIKHAILOV, M. V., CAMPBELL, J. D., DE WET, H., SHIMOMURA, K., ZADEK, B., COLLINS, R. F., SANSOM, M. S., FORD, R. C. & ASHCROFT, F. M. 2005. 3-D structural and functional characterization of the purified KATP channel complex Kir6.2-SUR1. *EMBO J,* 24**,** 4166-75.

MIKI, T., NAGASHIMA, K., TASHIRO, F., KOTAKE, K., YOSHITOMI, H., TAMAMOTO, A., GONOI, T., IWANAGA, T., MIYAZAKI, J. & SEINO, S. 1998. Defective insulin secretion and enhanced insulin action in KATP channel-deficient mice. *Proc Natl Acad Sci U S A,* 95**,** 10402-6.

MIKI, T. & SEINO, S. 2005. Roles of KATP channels as metabolic sensors in acute metabolic changes. *J Mol Cell Cardiol,* 38**,** 917-25.

MILJANICH, G. P. 2004. Ziconotide: neuronal calcium channel blocker for treating severe chronic pain. *Curr Med Chem,* 11**,** 3029-40.

MILLER, E., ANTONNY, B., HAMAMOTO, S. & SCHEKMAN, R. 2002. Cargo selection into COPII vesicles is driven by the Sec24p subunit. *EMBO J,* 21**,** 6105-13.

MILLER, E. A., BEILHARZ, T. H., MALKUS, P. N., LEE, M. C., HAMAMOTO, S., ORCI, L. & SCHEKMAN, R. 2003. Multiple cargo binding sites on the COPII subunit Sec24p ensure capture of diverse membrane proteins into transport vesicles. *Cell,* 114**,** 497-509.

MINAMI, K., MIKI, T., KADOWAKI, T. & SEINO, S. 2004. Roles of ATP-sensitive K+ channels as metabolic sensors: studies of Kir6.x null mice. *Diabetes,* 53 Suppl 3**,** S176-80.

MITCHESON, J. S. 2008. hERG potassium channels and the structural basis of drug-induced arrhythmias. *Chem Res Toxicol,* 21**,** 1005-10.

MODELL, S. M. & LEHMANN, M. H. 2006. The long QT syndrome family of cardiac ion channelopathies: a HuGE review. *Genet Med,* 8**,** 143-55.

MORAIS CABRAL, J. H., LEE, A., COHEN, S. L., CHAIT, B. T., LI, M. & MACKINNON, R. 1998. Crystal structure and functional analysis of the HERG potassium channel N terminus: a eukaryotic PAS domain. *Cell,* 95**,** 649-55.

MOSSESSOVA, E., BICKFORD, L. C. & GOLDBERG, J. 2003. SNARE selectivity of the COPII coat. *Cell,* 114**,** 483-95.

MOTLEY, A., BRIGHT, N. A., SEAMAN, M. N. J. & ROBINSON, M. S. 2003. Clathrin-mediated internalisation in AP-2–depleted cells. *The Journal of Cell Biology,* 162**,** 909-918.

MROWIEC, T. & SCHWAPPACH, B. 2006. 14-3-3 proteins in membrane protein transport. *Biol Chem,* 387**,** 1227-36.

NANDURI, J., WANG, N., BERGSON, P., YUAN, G., FICKER, E. & PRABHAKAR, N. R. 2008. Mitochondrial reactive oxygen species mediate hypoxic down-regulation of hERG channel protein. *Biochem Biophys Res Commun,* 373**,** 309-14.

NASLAVSKY, N., WEIGERT, R. & DONALDSON, J. G. 2003. Convergence of non-clathrin- and clathrin-derived endosomes involves Arf6 inactivation and changes in phosphoinositides. *Mol Biol Cell,* 14**,** 417-31.

NASLAVSKY, N., WEIGERT, R. & DONALDSON, J. G. 2004. Characterization of a nonclathrin endocytic pathway: membrane cargo and lipid requirements. *Mol Biol Cell,* 15**,** 3542-52.

NELSON, M. T. & QUAYLE, J. M. 1995. Physiological roles and properties of potassium channels in arterial smooth muscle. *Am J Physiol,* 268**,** C799-822.

NESTEROV, A., CARTER, R. E., SORKINA, T., GILL, G. N. & SORKIN, A. 1999. Inhibition of the receptor-binding function of clathrin adaptor protein AP-2 by dominant-negative mutant mu2 subunit and its effects on internalisation. *EMBO J,* 18**,** 2489-99.

NICHOLS, B. J. 2002. A distinct class of endosome mediates clathrin-independent internalisation to the Golgi complex. *Nat Cell Biol,* 4**,** 374-378.

NICHOLS, B. J., KENWORTHY, A. K., POLISHCHUK, R. S., LODGE, R., ROBERTS, T. H., HIRSCHBERG, K., PHAIR, R. D. & LIPPINCOTT-SCHWARTZ, J. 2001. Rapid cycling of lipid raft markers between the cell surface and Golgi complex. *J Cell Biol,* 153**,** 529-41.

NICHOLS, B. J. & LIPPINCOTT-SCHWARTZ, J. 2001. Internalisation without clathrin coats. *Trends Cell Biol,* 11**,** 406-12.

NICHOLS, C. G. 2006. KATP channels as molecular sensors of cellular metabolism. *Nature,* 440**,** 470-6.

NICHOLS, C. G., SHYNG, S. L., NESTOROWICZ, A., GLASER, B., CLEMENT, J. P. T., GONZALEZ, G., AGUILAR-BRYAN, L., PERMUTT, M. A. & BRYAN, J. 1996. Adenosine diphosphate as an intracellular regulator of insulin secretion. *Science,* 272**,** 1785-7.

NISHI, K. & SAIGO, K. 2007. Cellular internalization of green fluorescent protein fused with herpes simplex virus protein VP22 via a lipid raft-mediated endocytic pathway independent of caveolae and Rho family GTPases but dependent on dynamin and Arf6. *J Biol Chem,* 282**,** 27503-17.

NISHIMURA, N. & BALCH, W. E. 1997. A di-acidic signal required for selective export from the endoplasmic reticulum. *Science,* 277**,** 556-8.

NISHIMURA, N., BANNYKH, S., SLABOUGH, S., MATTESON, J., ALTSCHULER, Y., HAHN, K. & BALCH, W. E. 1999. A di-acidic (DXE) code directs concentration of cargo during export from the endoplasmic reticulum. *J Biol Chem,* 274**,** 15937-46.

NOMA, A. 1983. ATP-regulated K+ channels in cardiac muscle. *Nature,* 305**,** 147-8.

NUFER, O. & HAURI, H. P. 2003. ER export: call 14-3-3. *Curr Biol,* 13**,** R391-3.

O'CONNELL, K. M., MARTENS, J. R. & TAMKUN, M. M. 2004. Localization of ion channels to lipid Raft domains within the cardiovascular system. *Trends Cardiovasc Med,* 14**,** 37-42.

OKIYONEDA, T. & LUKACS, G. L. 2007. Cell surface dynamics of CFTR: the ins and outs. *Biochim Biophys Acta,* 1773**,** 476-9.

OLKKONEN, V. M. & STENMARK, H. 1997. Role of Rab GTPases in membrane traffic. *Int Rev Cytol,* 176**,** 1-85.

PAPAZIAN, D. M., SCHWARZ, T. L., TEMPEL, B. L., JAN, Y. N. & JAN, L. Y. 1987. Cloning of genomic and complementary DNA from Shaker, a putative potassium channel gene from Drosophila. *Science,* 237**,** 749-53.

PARTON, R. G. & SIMONS, K. 2007. The multiple faces of caveolae. *Nat Rev Mol Cell Biol,* 8**,** 185-194.

PARTRIDGE, C. J., BEECH, D. J. & SIVAPRASADARAO, A. 2001. Identification and pharmacological correction of a membrane trafficking defect associated with a mutation in the sulfonylurea receptor causing familial hyperinsulinism. *J Biol Chem,* 276**,** 35947-52.

PATTEN, R. D., POURATI, I., ARONOVITZ, M. J., BAUR, J., CELESTIN, F., CHEN, X., MICHAEL, A., HAQ, S., NUEDLING, S., GROHE, C., FORCE, T., MENDELSOHN, M. E. & KARAS, R. H. 2004. 17beta-estradiol reduces cardiomyocyte apoptosis in vivo and in vitro via activation of phospho-inositide-3 kinase/Akt signaling. *Circ Res,* 95**,** 692-9.

PAYNE, C. K., JONES, S. A., CHEN, C. & ZHUANG, X. 2007. Internalization and trafficking of cell surface proteoglycans and proteoglycan-binding ligands. *Traffic,* 8**,** 389-401.

PFEFFER, S. & AIVAZIAN, D. 2004. Targeting Rab GTPases to distinct membrane compartments. *Nat Rev Mol Cell Biol,* 5**,** 886-96.

PHARTIYAL, P., JONES, E. M. & ROBERTSON, G. A. 2007. Heteromeric assembly of human ether-a-go-go-related gene (hERG) 1a/1b channels occurs cotranslationally via N-terminal interactions. *J Biol Chem,* 282**,** 9874-82.

PONGS, O. 1999. Voltage-gated potassium channels: from hyperexcitability to excitement. *FEBS Lett,* 452**,** 31-5.

PRAEFCKE, G. J. & MCMAHON, H. T. 2004. The dynamin superfamily: universal membrane tubulation and fission molecules? *Nat Rev Mol Cell Biol,* 5**,** 133-47.

PROKS, P., ANTCLIFF, J. F., LIPPIAT, J., GLOYN, A. L., HATTERSLEY, A. T. & ASHCROFT, F. M. 2004. Molecular basis of Kir6.2 mutations associated with neonatal diabetes or neonatal diabetes plus neurological features. *Proc Natl Acad Sci U S A,* 101**,** 17539-44.

QUINN, K. V., GIBLIN, J. P. & TINKER, A. 2004. Multisite phosphorylation mechanism for protein kinase A activation of the smooth muscle ATP-sensitive K+ channel. *Circulation Research,* 94**,** 1359-1366.

RADHAKRISHNA, H. & DONALDSON, J. G. 1997. ADP-ribosylation factor 6 regulates a novel plasma membrane recycling pathway. *J Cell Biol,* 139**,** 49-61.

RADHAKRISHNA, H., KLAUSNER, R. D. & DONALDSON, J. G. 1996. Aluminum fluoride stimulates surface protrusions in cells overexpressing the ARF6 GTPase. *J Cell Biol,* 134**,** 935-47.

RAJAMANI, S., ANDERSON, C. L., ANSON, B. D. & JANUARY, C. T. 2002. Pharmacological rescue of human K(+) channel long-QT2 mutations: human ether-a-go-go-related gene rescue without block. *Circulation,* 105**,** 2830-5.

RAJAMANI, S., ECKHARDT, L. L., VALDIVIA, C. R., KLEMENS, C. A., GILLMAN, B. M., ANDERSON, C. L., HOLZEM, K. M., DELISLE, B. P., ANSON, B. D., MAKIELSKI, J. C. & JANUARY, C. T. 2006. Drug-induced long QT syndrome: hERG K+ channel block and disruption of protein trafficking by fluoxetine and norfluoxetine. *Br J Pharmacol,* 149**,** 481-9.

RAMSTROM, C., CHAPMAN, H., VIITANEN, T., AFRASIABI, E., FOX, H., KIVELA, J., SOINI, S., KORHONEN, L., LINDHOLM, D., PASTERNACK, M. & TORNQUIST,

K. 2010. Regulation of HERG (KCNH2) potassium channel surface expression by diacylglycerol. *Cell Mol Life Sci,* 67**,** 157-69.

REIMANN, F., GRIBBLE, F. M. & ASHCROFT, F. M. 2000. Differential response of K(ATP) channels containing SUR2A or SUR2B subunits to nucleotides and pinacidil. *Mol Pharmacol,* 58**,** 1318-25.

REN, M., XU, G., ZENG, J., DE LEMOS-CHIARANDINI, C., ADESNIK, M. & SABATINI, D. D. 1998. Hydrolysis of GTP on rab11 is required for the direct delivery of transferrin from the pericentriolar recycling compartment to the cell surface but not from sorting endosomes. *Proc Natl Acad Sci U S A,* 95**,** 6187-92.

ROBERTSON, G. A. 2009. Endocytic control of ion channel density as a target for cardiovascular disease. *The Journal of Clinical Investigation,* 119**,** 2531-2534.

ROBERTSON, G. A. & JANUARY, C. T. 2006. HERG trafficking and pharmacological rescue of LQTS-2 mutant channels. *Handb Exp Pharmacol***,** 349-55.

RODRIGO, G. C., LAWRENCE, C. L. & STANDEN, N. B. 2002. Dinitrophenol Pretreatment of Rat Ventricular Myocytes Protects Against Damage by Metabolic Inhibition and Reperfusion. *Journal of Molecular and Cellular Cardiology,* 34**,** 555-569.

ROSATI, B., MARCHETTI, P., CROCIANI, O., LECCHI, M., LUPI, R., ARCANGELI, A., OLIVOTTO, M. & WANKE, E. 2000. Glucose- and arginine-induced insulin secretion by human pancreatic beta-cells: the role of HERG K(+) channels in firing and release. *FASEB J,* 14**,** 2601-10.

ROTHBERG, K. G., HEUSER, J. E., DONZELL, W. C., YING, Y. S., GLENNEY, J. R. & ANDERSON, R. G. 1992. Caveolin, a protein component of caveolae membrane coats. *Cell,* 68**,** 673-82.

RUSSELL, S. A. 2001. *MOLECULAR CLONING A Laboratory Manual (3-volume set)* Cold Spring Harbor Laboratory; .

SABE, H. 2003. Requirement for Arf6 in cell adhesion, migration, and cancer cell invasion. *J Biochem,* 134**,** 485-9.

SAKURA, H., AMMALA, C., SMITH, P. A., GRIBBLE, F. M. & ASHCROFT, F. M. 1995. Cloning and functional expression of the cDNA encoding a novel ATP-sensitive potassium channel subunit expressed in pancreatic beta-cells, brain, heart and skeletal muscle. *FEBS Lett,* 377**,** 338-44.

SANDVIG, K., TORGERSEN, M. L., RAA, H. A. & VAN DEURS, B. 2008. Clathrin-independent internalisation: from nonexisting to an extreme degree of complexity. *Histochem Cell Biol,* 129**,** 267-76.

SANGUINETTI, M. C. (ed.) 2005. *The hERG cardiac potassium channel: structure, function and Long QT syndrome.*: John Wiley & Sons, Ltd.

SANGUINETTI, M. C., JIANG, C., CURRAN, M. E. & KEATING, M. T. 1995. A mechanistic link between an inherited and an acquired cardiac arrhythmia: HERG encodes the IKr potassium channel. *Cell,* 81**,** 299-307.

SANGUINETTI, M. C. & TRISTANI-FIROUZI, M. 2006. hERG potassium channels and cardiac arrhythmia. *Nature,* 440**,** 463-9.

SANTY, L. C. & CASANOVA, J. E. 2001. Activation of ARF6 by ARNO stimulates epithelial cell migration through downstream activation of both Rac1 and phospholipase D. *J Cell Biol,* 154**,** 599-610.

SATO, K. & NAKANO, A. 2007a. Mechanisms of COPII vesicle formation and protein sorting. *FEBS Lett.,* 581**,** 2076.

SATO, K. & NAKANO, A. 2007b. Mechanisms of COPII vesicle formation and protein sorting. *FEBS Letters,* 581**,** 2076-2082.

SATO, K. & NAKANO, A. 2007c. Mechanisms of COPII vesicle formation and protein sorting. *FEBS Lett,* 581**,** 2076-82.

SCALES, S. J., CHEN, Y. A., YOO, B. Y., PATEL, S. M., DOUNG, Y. C. & SCHELLER, R. H. 2000. SNAREs contribute to the specificity of membrane fusion. *Neuron,* 26**,** 457-64.

SCHEKMAN, R., BARLOWE, C., BEDNAREK, S., CAMPBELL, J., DOERING, T., DUDEN, R., KUEHN, M., REXACH, M., YEUNG, T. & ORCI, L. 1995. Coat

proteins and selective protein packaging into transport vesicles. *Cold Spring Harb Symp Quant Biol,* 60**,** 11-21.

SCHIMMOLLER, F., SIMON, I. & PFEFFER, S. R. 1998. Rab GTPases, directors of vesicle docking. *J Biol Chem,* 273**,** 22161-4.

SCHLEGEL, A., ARVAN, P. & LISANTI, M. P. 2001. Caveolin-1 binding to endoplasmic reticulum membranes and entry into the regulated secretory pathway are regulated by serine phosphorylation. Protein sorting at the level of the endoplasmic reticulum. *J Biol Chem,* 276**,** 4398-408.

SCHLIERF, B., FEY, G. H., HAUBER, J., HOCKE, G. M. & ROSORIUS, O. 2000. Rab11b Is Essential for Recycling of Transferrin to the Plasma Membrane. *Experimental Cell Research,* 259**,** 257-265.

SCHUCK, S., HONSHO, M AND SIMONS, K 2006a. Detergent-resistant membranes and the use of cholesterol depletion.   . *Cell Biology A Laboratory Handbook* Elsevier Academic Press, London.

SCHUCK, S., HONSHO, M AND SIMONS, K,   2006b. Detergent-resistant membranes and the use of cholesterol depletion.

. *In:* CELIS, J. E. (ed.) *Cell Biology A Laboratory Handbook.* London.: Elsevier Academic Press,.

SCHWARZ, J. R. & BAUER, C. K. 2004. Functions of erg K+ channels in excitable cells. *J Cell Mol Med,* 8**,** 22-30.

SCHWARZE, S. R., HRUSKA, K. A. & DOWDY, S. F. 2000. Protein transduction: unrestricted delivery into all cells? *Trends Cell Biol,* 10**,** 290-5.

SCHWENK, R. W. & ECKEL, J. 2007. A novel method to monitor insulin-stimulated GTP-loading of Rab11a in cardiomyocytes. *Cell Signal,* 19**,** 825-30.

SEGHERS, V., NAKAZAKI, M., DEMAYO, F., AGUILAR-BRYAN, L. & BRYAN, J. 2000. Sur1 knockout mice. A model for K(ATP) channel-independent regulation of insulin secretion. *J Biol Chem,* 275**,** 9270-7.

SELYANKO, A. A., HADLEY, J. K., WOOD, I. C., ABOGADIE, F. C., DELMAS, P., BUCKLEY, N. J., LONDON, B. & BROWN, D. A. 1999. Two types of K(+) channel subunit, Erg1 and KCNQ2/3, contribute to the M-like current in a mammalian neuronal cell. *J Neurosci,* 19**,** 7742-56.

SEMPOUX, C., GUIOT, Y., JAUBERT, F. & RAHIER, J. 2004. Focal and diffuse forms of congenital hyperinsulinism: the keys for differential diagnosis. *Endocr Pathol,* 15**,** 241-6.

SHARMA, N., CRANE, A., CLEMENT, J. P. T., GONZALEZ, G., BABENKO, A. P., BRYAN, J. & AGUILAR-BRYAN, L. 1999. The C terminus of SUR1 is required for trafficking of KATP channels. *J Biol Chem,* 274**,** 20628-32.

SHI, Y., WU, Z. Y., CUI, N. R., SHI, W. W., YANG, Y., ZHANG, X. L., ROJAS, A., HA, B. T. & JIANG, C. 2007. PKA phosphorylation of SUR2B subunit underscores vascular K-ATP channel activation by beta-adrenergic receptors. *American Journal of Physiology-Regulatory Integrative and Comparative Physiology,* 293**,** R1205-R1214.

SHYNG, S. & NICHOLS, C. G. 1997. Octameric stoichiometry of the KATP channel complex. *J Gen Physiol,* 110**,** 655-64.

SHYNG, S. L., FERRIGNI, T., SHEPARD, J. B., NESTOROWICZ, A., GLASER, B., PERMUTT, M. A. & NICHOLS, C. G. 1998. Functional analyses of novel mutations in the sulfonylurea receptor 1 associated with persistent hyperinsulinemic hypoglycemia of infancy. *Diabetes,* 47**,** 1145-51.

SIGISMUND, S., ARGENZIO, E., TOSONI, D., CAVALLARO, E., POLO, S. & DI FIORE, P. P. 2008. Clathrin-mediated internalization is essential for sustained EGFR signaling but dispensable for degradation. *Dev Cell,* 15**,** 209-19.

SILVIS, M. R., BERTRAND, C. A., AMEEN, N., GOLIN-BISELLO, F., BUTTERWORTH, M. B., FRIZZELL, R. A. & BRADBURY, N. A. 2009. Rab11b regulates the apical recycling of the cystic fibrosis transmembrane conductance regulator in polarized intestinal epithelial cells. *Mol Biol Cell,* 20**,** 2337-50.

SIMONS, K. & EHEHALT, R. 2002. Cholesterol, lipid rafts, and disease. *J Clin Invest,* 110**,** 597-603.

SIMONS, K. & TOOMRE, D. 2000. Lipid rafts and signal transduction. *Nat Rev Mol Cell Biol,* 1**,** 31-9.

SINGH, R. D., PURI, V., VALIYAVEETTIL, J. T., MARKS, D. L., BITTMAN, R. & PAGANO, R. E. 2003. Selective caveolin-1-dependent internalisation of glycosphingolipids. *Mol Biol Cell,* 14**,** 3254-65.

SMITH, A. J., PARTRIDGE, C. J., ASIPU, A., MAIR, L. A., HUNTER, M. & SIVAPRASADARAO, A. 2006. Increased ATP-sensitive K+ channel expression during acute glucose deprivation. *Biochem Biophys Res Commun,* 348**,** 1123-31.

SMITH, A. J., TANEJA, T. K., MANKOURI, J. & SIVAPRASADARAO, A. 2007. Molecular cell biology of KATP channels: implications for neonatal diabetes. *Expert Rev Mol Med,* 9**,** 1-17.

SMITH, P. K., KROHN, R. I., HERMANSON, G. T., MALLIA, A. K., GARTNER, F. H., PROVENZANO, M. D., FUJIMOTO, E. K., GOEKE, N. M., OLSON, B. J. & KLENK, D. C. 1985. Measurement of protein using bicinchoninic acid. *Anal Biochem,* 150**,** 76-85.

SOMSEL RODMAN, J. & WANDINGER-NESS, A. 2000. Rab GTPases coordinate internalisation. *J Cell Sci,* 113 Pt 2**,** 183-92.

SONNICHSEN, B., DE RENZIS, S., NIELSEN, E., RIETDORF, J. & ZERIAL, M. 2000. Distinct membrane domains on endosomes in the recycling pathway visualized by multicolor imaging of Rab4, Rab5, and Rab11. *J Cell Biol,* 149**,** 901-14.

SPRUCE, A. E., STANDEN, N. B. & STANFIELD, P. R. 1985. Voltage-dependent ATP-sensitive potassium channels of skeletal muscle membrane. *Nature,* 316**,** 736-8.

STEELE, D. F., ELDSTROM, J. & FEDIDA, D. 2007a. Mechanisms of cardiac potassium channel trafficking. *J Physiol,* 582**,** 17-26.

STEELE, D. F., ZADEH, A. D., LOEWEN, M. E. & FEDIDA, D. 2007b. Localization and trafficking of cardiac voltage-gated potassium channels. *Biochem Soc Trans,* 35**,** 1069-73.

STEIN, M. P., DONG, J. & WANDINGER-NESS, A. 2003. Rab proteins and endocytic trafficking: potential targets for therapeutic intervention. *Adv Drug Deliv Rev,* 55**,** 1421-37.

STEINMAN, R. M., MELLMAN, I. S., MULLER, W. A. & COHN, Z. A. 1983. Internalisation and the recycling of plasma membrane. *J Cell Biol,* 96**,** 1-27.

STUERMER, C. A., LANG, D. M., KIRSCH, F., WIECHERS, M., DEININGER, S. O. & PLATTNER, H. 2001. Glycosylphosphatidyl inositol-anchored proteins and fyn kinase assemble in noncaveolar plasma membrane microdomains defined by reggie-1 and -2. *Mol Biol Cell,* 12**,** 3031-45.

STUERMER, C. A., LANGHORST, M. F., WIECHERS, M. F., LEGLER, D. F., VON HANWEHR, S. H., GUSE, A. H. & PLATTNER, H. 2004. PrPc capping in T cells promotes its association with the lipid raft proteins reggie-1 and reggie-2 and leads to signal transduction. *FASEB J,* 18**,** 1731-3.

SURAH-NARWAL, S., XU, S. Z., MCHUGH, D., MCDONALD, R. L., HOUGH, E., CHEONG, A., PARTRIDGE, C., SIVAPRASADARAO, A. & BEECH, D. J. 1999. Block of human aorta Kir6.1 by the vascular KATP channel inhibitor U37883A. *Br J Pharmacol,* 128**,** 667-72.

SWANSON, J. A. & BAER, S. C. 1995. Phagocytosis by zippers and triggers. *Trends Cell Biol,* 5**,** 89-93.

SWANSON, J. A. & WATTS, C. 1995. Macropinocytosis. *Trends Cell Biol,* 5**,** 424-8.

SZEWCZYK, A., CZYZ, A., WOJCIK, G., WOJTCZAK, L. & NALECZ, M. J. 1996. ATP-regulated K+ channel in mitochondria: pharmacology and function. *J Bioenerg Biomembr,* 28**,** 147-52.

TANEJA, T. K., MANKOURI, J., KARNIK, R., KANNAN, S., SMITH, A. J., MUNSEY, T., CHRISTESEN, H. B., BEECH, D. J. & SIVAPRASADARAO, A. 2009. Sar1-

GTPase-dependent ER exit of KATP channels revealed by a mutation causing congenital hyperinsulinism. *Hum Mol Genet,* 18**,** 2400-13.

TAO, X., AVALOS, J. L., CHEN, J. & MACKINNON, R. 2009. Crystal structure of the eukaryotic strong inward-rectifier K+ channel Kir2.2 at 3.1 A resolution. *Science,* 326**,** 1668-74.

TERZIC, A. & KURACHI, Y. 1996. Actin microfilament disrupters enhance K(ATP) channel opening in patches from guinea-pig cardiomyocytes. *J Physiol,* 492 (Pt 2)**,** 395-404.

THOMAS, D., KIEHN, J., KATUS, H. A. & KARLE, C. A. 2003a. Defective protein trafficking in hERG-associated hereditary long QT syndrome (LQT2): molecular mechanisms and restoration of intracellular protein processing. *Cardiovascular Research,* 60**,** 235-41.

THOMAS, D., KIEHN, J., KATUS, H. A. & KARLE, C. A. 2003b. Defective protein trafficking in hERG-associated hereditary long QT syndrome (LQT2): molecular mechanisms and restoration of intracellular protein processing. *Cardiovasc Res,* 60**,** 235-41.

THOMSEN, M. B., MATZ, J., VOLDERS, P. G. A. & VOS, M. A. 2006. Assessing the proarrhythmic potential of drugs: Current status of models and surrogate parameters of torsades de pointes arrhythmias. *Pharmacology & Therapeutics,* 112**,** 150-170.

TOKUYAMA, Y., FAN, Z., FURUTA, H., MAKIELSKI, J. C., POLONSKY, K. S., BELL, G. I. & YANO, H. 1996. Rat inwardly rectifying potassium channel Kir6.2: cloning electrophysiological characterization, and decreased expression in pancreatic islets of male Zucker diabetic fatty rats. *Biochem Biophys Res Commun,* 220**,** 532-8.

TORGERSEN, M. L., SKRETTING, G., VAN DEURS, B. & SANDVIG, K. 2001. Internalization of cholera toxin by different endocytic mechanisms. *J Cell Sci,* 114**,** 3737-47.

TRAPP, S., PROKS, P., TUCKER, S. J. & ASHCROFT, F. M. 1998. Molecular analysis of ATP-sensitive K channel gating and implications for channel inhibition by ATP. *J Gen Physiol,* 112**,** 333-49.

TRISTANI-FIROUZI, M. & SANGUINETTI, MICHAEL C. 2003. Structural determinants and biophysical properties of HERG and KCNQ1 channel gating. *Journal of Molecular and Cellular Cardiology,* 35**,** 27-35.

TUCKER, S. J., GRIBBLE, F. M., PROKS, P., TRAPP, S., RYDER, T. J., HAUG, T., REIMANN, F. & ASHCROFT, F. M. 1998. Molecular determinants of KATP channel inhibition by ATP. *EMBO J,* 17**,** 3290-6.

TUCKER, S. J., GRIBBLE, F. M., ZHAO, C., TRAPP, S. & ASHCROFT, F. M. 1997. Truncation of Kir6.2 produces ATP-sensitive K+ channels in the absence of the sulphonylurea receptor. *Nature,* 387**,** 179-83.

TUNG, R. T. & KURACHI, Y. 1991. On the mechanism of nucleotide diphosphate activation of the ATP-sensitive K+ channel in ventricular cell of guinea-pig. *J Physiol,* 437**,** 239-56.

VALENTE, C., POLISHCHUK, R. & DE MATTEIS, M. A. 2010. Rab6 and myosin II at the cutting edge of membrane fission. *Nat Cell Biol,* 12**,** 635-638.

VAN DE GRAAF, S. F. J., CHANG, Q., MENSENKAMP, A. R., HOENDEROP, J. G. J. & BINDELS, R. J. M. 2006. Direct interaction with Rab11a targets the epithelial Ca2+ channels TRPV5 and TRPV6 to the plasma membrane. *Molecular and Cellular Biology,* 26**,** 303-312.

VAN DER HEYDEN, M. A., SMITS, M. E. & VOS, M. A. 2008. Drugs and trafficking of ion channels: a new pro-arrhythmic threat on the horizon? *Br J Pharmacol,* 153**,** 406-9.

VAN DER SLUIJS, P., HULL, M., WEBSTER, P., MALE, P., GOUD, B. & MELLMAN, I. 1992. The small GTP-binding protein rab4 controls an early sorting event on the endocytic pathway. *Cell,* 70**,** 729-40.

VAN WAGONER, D. R. & LAMORGESE, M. 1994. Ischemia potentiates the mechanosensitive modulation of atrial ATP-sensitive potassium channels. *Ann N Y Acad Sci,* 723**,** 392-5.

VANDENBERG, J. I., WALKER, B. D. & CAMPBELL, T. J. 2001. HERG K+ channels: friend and foe. *Trends in Pharmacological Sciences,* 22**,** 240-246.

VEGLIO, M., CHINAGLIA, A. & CAVALLO-PERIN, P. 2004. QT interval, cardiovascular risk factors and risk of death in diabetes. *J Endocrinol Invest,* 27**,** 175-81.

VERKARRE, V., FOURNET, J. C., DE LONLAY, P., GROSS-MORAND, M. S., DEVILLERS, M., RAHIER, J., BRUNELLE, F., ROBERT, J. J., NIHOUL-FÉKÉTÉ, C., SAUDUBRAY, J. M. & JUNIEN, C. 1998. Paternal mutation of the sulfonylurea receptor (SUR1) gene and maternal loss of 11p15 imprinted genes lead to persistent hyperinsulinism in focal adenomatous hyperplasia. *The Journal of Clinical Investigation,* 102**,** 1286-1291.

WANG, H., ZHANG, Y., CAO, L., HAN, H., WANG, J., YANG, B., NATTEL, S. & WANG, Z. 2002. HERG K+ channel, a regulator of tumor cell apoptosis and proliferation. *Cancer Res,* 62**,** 4843-8.

WANG, J., WANG, H., ZHANG, Y., GAO, H., NATTEL, S. & WANG, Z. 2004a. Impairment of HERG K(+) channel function by tumor necrosis factor-alpha: role of reactive oxygen species as a mediator. *J Biol Chem,* 279**,** 13289-92.

WANG, L., DENNIS, A. T., TRIEU, P., CHARRON, F., ETHIER, N., HEBERT, T. E., WAN, X. & FICKER, E. 2009. Intracellular potassium stabilizes human ether-a-go-go-related gene channels for export from endoplasmic reticulum. *Mol Pharmacol,* 75**,** 927-37.

WANG, X., MATTESON, J., AN, Y., MOYER, B., YOO, J. S., BANNYKH, S., WILSON, I. A., RIORDAN, J. R. & BALCH, W. E. 2004b. COPII-dependent export of cystic fibrosis transmembrane conductance regulator from the ER uses a di-acidic exit code. *J Cell Biol,* 167**,** 65-74.

WANG, Y. N., WANG, H., YAMAGUCHI, H., LEE, H. J., LEE, H. H. & HUNG, M. C. 2010. COPI-mediated retrograde trafficking from the Golgi to the ER regulates EGFR nuclear transport. *Biochem Biophys Res Commun*.

WARMKE, J. W. & GANETZKY, B. 1994. A family of potassium channel genes related to eag in Drosophila and mammals. *Proc Natl Acad Sci U S A,* 91**,** 3438-42.

WATERS, M. G., SERAFINI, T. & ROTHMAN, J. E. 1991. 'Coatomer': a cytosolic protein complex containing subunits of non-clathrin-coated Golgi transport vesicles. *Nature,* 349**,** 248-51.

WEERAPURA, M., NATTEL, S., CHARTIER, D., CABALLERO, R. & HEBERT, T. E. 2002. A comparison of currents carried by HERG, with and without coexpression of MiRP1, and the native rapid delayed rectifier current. Is MiRP1 the missing link? *J Physiol,* 540**,** 15-27.

WEGENER, F. T., EHRLICH, J. R. & HOHNLOSER, S. H. 2008. Amiodarone-associated macroscopic T-wave alternans and torsade de pointes unmasking the inherited long QT syndrome. *Europace,* 10**,** 112-3.

WEIGERT, R., YEUNG, A. C., LI, J. & DONALDSON, J. G. 2004. Rab22a regulates the recycling of membrane proteins internalized independently of clathrin. *Mol Biol Cell,* 15**,** 3758-70.

WIBLE, B. A., HAWRYLUK, P., FICKER, E., KURYSHEV, Y. A., KIRSCH, G. & BROWN, A. M. 2005. HERG-Lite®: A novel comprehensive high-throughput screen for drug-induced hERG risk. *Journal of Pharmacological and Toxicological Methods,* 52**,** 136-145.

WILDENTHAL, K., WAKELAND, J. R., ORD, J. M. & STULL, J. T. 1980. Interference with lysosomal proteolysis fails to reduce cardiac myosin degradation. *Biochemical and Biophysical Research Communications,* 96**,** 793-798.

WITCHEL, H. J. 2007. The hERG potassium channel as a therapeutic target. *Expert Opin Ther Targets,* 11**,** 321-36.

WITCHEL, H. J. 2010. Drug-induced hERG Block and Long QT Syndrome. *Cardiovascular Therapeutics***,** no-no.

XIA, F., GAO, X., KWAN, E., LAM, P. P., CHAN, L., SY, K., SHEU, L., WHEELER, M. B., GAISANO, H. Y. & TSUSHIMA, R. G. 2004. Disruption of pancreatic beta-cell lipid rafts modifies Kv2.1 channel gating and insulin exocytosis. *J Biol Chem,* 279**,** 24685-91.

XIAO, J., LUO, X., LIN, H., ZHANG, Y., LU, Y., WANG, N., YANG, B. & WANG, Z. 2007. MicroRNA miR-133 represses HERG K+ channel expression contributing to QT prolongation in diabetic hearts. *J Biol Chem,* 282**,** 12363-7.

YAMAMOTO, H., SAKANE, H., MICHIUE, T. & KIKUCHI, A. 2008. Wnt3a and Dkk1 regulate distinct internalization pathways of LRP6 to tune the activation of beta-catenin signaling. *Dev Cell,* 15**,** 37-48.

YAN, F. F., LIN, Y. W., MACMULLEN, C., GANGULY, A., STANLEY, C. A. & SHYNG, S. L. 2007. Congenital hyperinsulinism associated ABCC8 mutations that cause defective trafficking of ATP-sensitive K+ channels: identification and rescue. *Diabetes,* 56**,** 2339-48.

YANG, C. & KAZANIETZ, M. G. 2003. Divergence and complexities in DAG signaling: looking beyond PKC. *Trends in Pharmacological Sciences,* 24**,** 602-608.

YANG, J. S., LEE, S. Y., GAO, M., BOURGOIN, S., RANDAZZO, P. A., PREMONT, R. T. & HSU, V. W. 2002. ARFGAP1 promotes the formation of COPI vesicles, suggesting function as a component of the coat. *J Cell Biol,* 159, 69-78.

YELLEN, G. 1984. Ionic permeation and blockade in Ca2+-activated K+ channels of bovine chromaffin cells. *J Gen Physiol,* 84**,** 157-86.

YU, F. H. & CATTERALL, W. A. 2004. The VGL-chanome: a protein superfamily specialized for electrical signaling and ionic homeostasis. *Sci STKE,* 2004**,** re15.

ZACHARIAS, D. A., VIOLIN, J. D., NEWTON, A. C. & TSIEN, R. Y. 2002. Partitioning of lipid-modified monomeric GFPs into membrane microdomains of live cells. *Science,* 296**,** 913-6.

ZERANGUE, N., SCHWAPPACH, B., JAN, Y. N. & JAN, L. Y. 1999. A new ER trafficking signal regulates the subunit stoichiometry of plasma membrane K(ATP) channels. *Neuron,* 22**,** 537-48.

ZERIAL, M. & MCBRIDE, H. 2001. Rab proteins as membrane organizers. *Nat Rev Mol Cell Biol,* 2**,** 107-17.

ZHANG, C., MIKI, T., SHIBASAKI, T., YOKOKURA, M., SARAYA, A. & SEINO, S. 2006. Identification and characterization of a novel member of the ATP-sensitive K+ channel subunit family, Kir6.3, in zebrafish. *Physiol Genomics,* 24**,** 290-7.

ZHOU, Z., GONG, Q. & JANUARY, C. T. 1999. Correction of defective protein trafficking of a mutant HERG potassium channel in human long QT syndrome. Pharmacological and temperature effects. *J Biol Chem,* 274**,** 31123-6.

ZINGMAN, L. V., HODGSON, D. M., BAST, P. H., KANE, G. C., PEREZ-TERZIC, C., GUMINA, R. J., PUCAR, D., BIENENGRAEBER, M., DZEJA, P. P., MIKI, T., SEINO, S., ALEKSEEV, A. E. & TERZIC, A. 2002. Kir6.2 is required for adaptation to stress. *Proc Natl Acad Sci U S A,* 99**,** 13278-83.

ZUK, P. A. & ELFERINK, L. A. 1999. Rab15 mediates an early endocytic event in Chinese hamster ovary cells. *J Biol Chem,* 274**,** 22303-12.

ZUK, P. A. & ELFERINK, L. A. 2000. Rab15 differentially regulates early endocytic trafficking. *J Biol Chem,* 275**,** 26754-64.

ZUZARTE, M., HEUSSER, K., RENIGUNTA, V., SCHLICHTHORL, G., RINNE, S., WISCHMEYER, E., DAUT, J., SCHWAPPACH, B. & PREISIG-MULLER, R. 2009. Intracellular traffic of the K+ channels TASK-1 and TASK-3: role of N- and C-terminal sorting signals and interaction with 14-3-3 proteins. *J Physiol,* 587**,** 929-52.

ZUZARTE, M., RINNE, S., SCHLICHTHORL, G., SCHUBERT, A., DAUT, J. & PREISIG-MULLER, R. 2007. A di-acidic sequence motif enhances the surface expression of the potassium channel TASK-3. *Traffic,* 8**,** 1093-100.